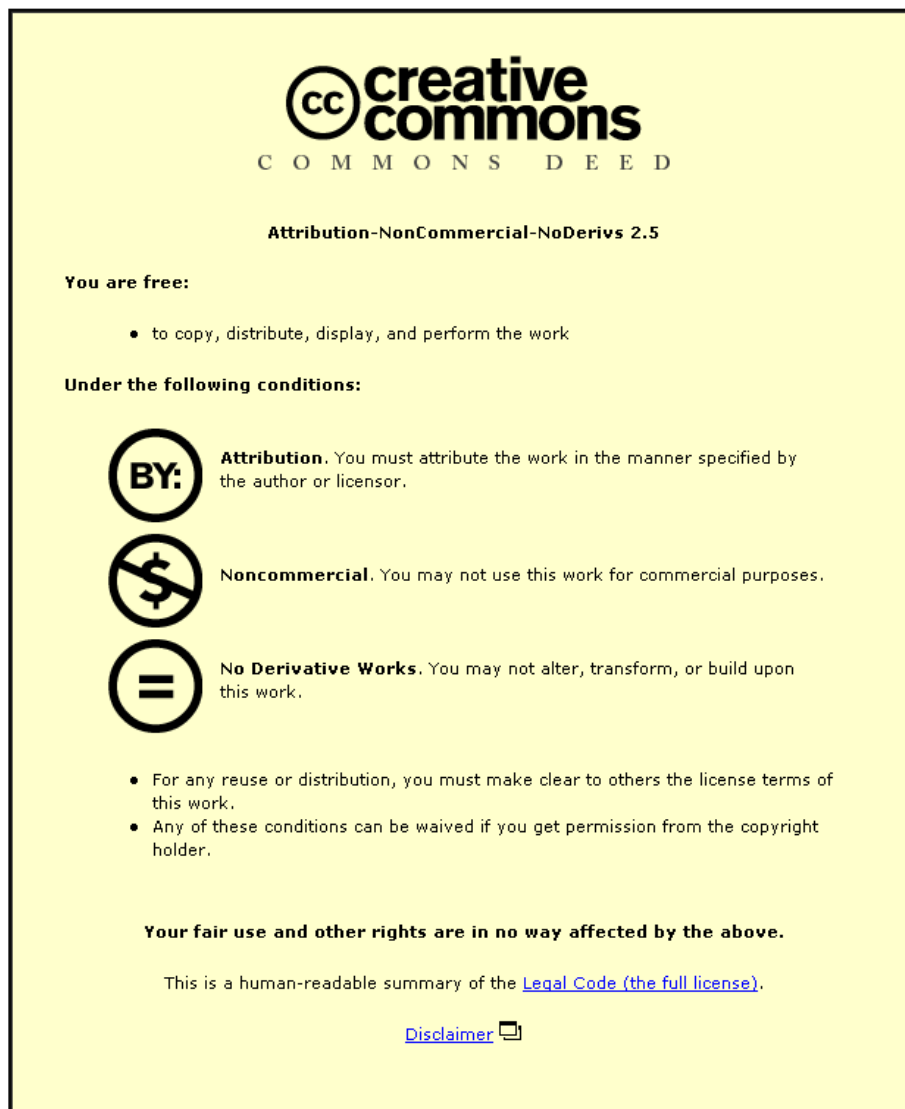


This item was submitted to Loughborough University as a PhD thesis by the author and is made available in the Institutional Repository (<https://dspace.lboro.ac.uk/>) under the following Creative Commons Licence conditions.



For the full text of this licence, please go to:
<http://creativecommons.org/licenses/by-nc-nd/2.5/>

BLDSC no :- DX 176072

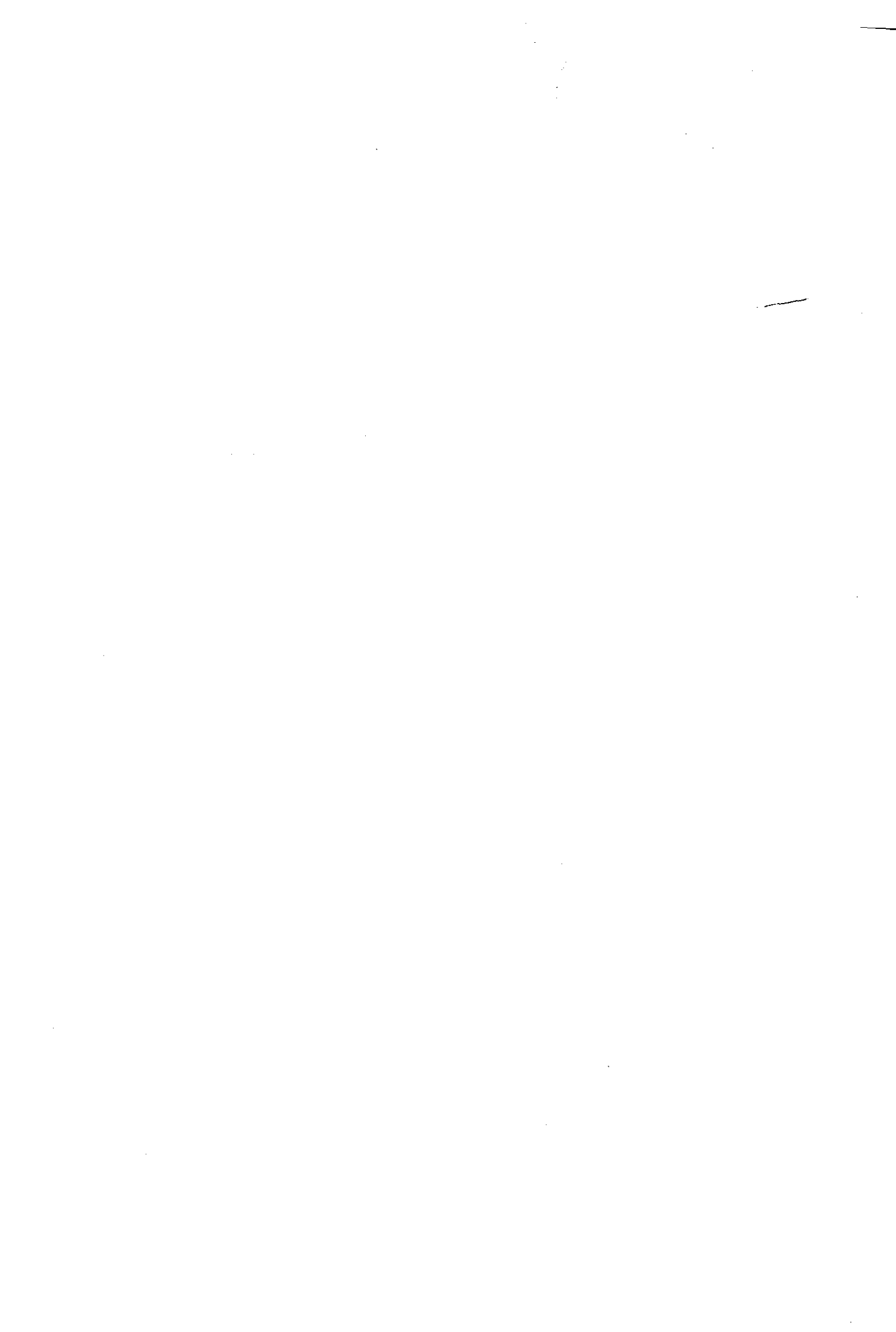
LOUGHBOROUGH
UNIVERSITY OF TECHNOLOGY
LIBRARY

AUTHOR/FILING TITLE	
MURRAY-JONES, P. J.	
ACCESSION/COPY NO.	
0400 73889	
VOL. NO.	CLASS MARK
	LOAN COPY

0400738899



BADMINTON PRESS
18 THE HALFCROFT
SYSTON
LEICESTER LE7 8LD
ENGLAND
TEL: 0533 602917
FAX: 0533 696636



ASPECTS
OF THE
LEAD ACID BATTERY.

By
Peter Murray-Jones.

A Doctoral Thesis Submitted in Partial Fulfilment of the Requirements for the Award of
Doctor of Philosophy of Loughborough University of Technology.

September, 1992

© By Peter James Murray-Jones (1992).

ERRATA:

1. There is no figure 6.
2. Photo. 21 has been reproduced incorrectly, however photo. 18 is identical— please refer to this photograph.

040073889

Aug 93

W992889

The work in this thesis has not been submitted, in full or in part, to this or any other institution for a higher degree.

ACKNOWLEDGMENTS

I wish to thank my supervisors Professor N. A. Hampson and Drs. M. Ball and P. Mitchell for their support and direction throughout the project. I am also particularly grateful to Dr. S. R. Ellis for his guidance in electrochemical techniques, his assistance in interpreting the results and for his helpful comments throughout the work.

My sincere thanks goes to the Chemistry Department's technical staff who helped with the provisioning of various pieces of laboratory equipment, to John Brennan who helped by printing the SEM photographs and to the University's computer centre staff who never failed to keep things running smoothly.

My gratitude also goes to Dr. B. Culpin of *Chloride plc.* for his interest & assistance and I would like to acknowledge the financial support of *Australian Associated Smelters Pty Ltd.*

Finally to the department's tea-room bridge club and all my fellow students go my best wishes for the future.

To my parents....

SUMMARY

Two aspects of the lead acid battery have been researched in this work. The first investigates some of the complex questions concerning the nature, composition and chemistry of lead sulphate membranes using scanning electron microscopy (SEM), impedance spectroscopy (IS) and inorganic chemistry techniques. A review of the literature on lead sulphate and precipitate impregnated membranes together with their role in the lead acid battery is presented.

The second area of study involved the novel idea of applying macro defect free (MDF) cement technology to the manufacture of lead acid battery paste. The MDF strategy increased the strength of Portland cement pastes ten fold by a reduction of their macro voids, a comparable increase in battery plate strength—with a subsequent increase in cycle life and/or capacity—being the aim. Two polymers polyvinyl alcohol (PVA) and polyacrylic acid (PAA), associated with the technology, were chosen as plate additives. BET, mercury porosimetry and X-ray powder diffraction (XPD) evaluated changes in plate characteristics, during electrical cycling, of prepared lead acid battery plates.

SEM results showed that lead sulphate crystals formed a tighter more compact layer around 7 mol dm^{-3} and established their osmotic behaviour and water susceptibility. However impedance spectroscopy and inorganic analysis provided little further evidence as to the properties, or nature, of lead sulphate membrane.

MDF results showed that the that addition of between 0.6 and 0.9% PAA provided a beneficial effect. A theory is presented to explain this.

LIST OF ABBREVIATIONS USED:

a.c.	Alternating Current
A	Area (of electrode)
C_{dl}	Double layer capacitance
C_o^b	Bulk concentration of Oxidised species
C_R^b	Bulk concentration of Reduced species
C_o^s	Surface concentration of Oxidised species
C_R^s	Surface concentration of Reduced species
d.c.	Direct Current
D_o	Fick's diffusion coefficient (for species O)
e	The voltage at a distance x along one idealised pore axis
e_0	The voltage at the mouth of a pore (distance x=0)
E	i) The potential of the electrode measured against a suitable reference electrode ii) The total voltage iii) The open terminal voltage of a battery
E^0	The formal potential of a cell at standard conditions
F	Faraday's constant
i_o	The exchange current density
i_t	The instantaneous current (at time t)
I_{max}	The maximum current
k_f	The forward (cathodic) rate constant
k_b	The backwards (anodic) rate constant
k_o	The rate constant for species O
k^o	The potential independent rate constant
k^0	The potential independent rate constant, at standard conditions
j	$\sqrt{(-1)}$
l	The length of a pore
N	The amount of substance diffusing across an area
N_o	Avogadro's number.
q	The flux (of material)
r^p	The radius of a pore
r_1	The radius of curvature of a liquid's meniscus
R	The universal gas constant
R_d	The resistance of a solution <i>per unit length</i>
R_d	The charge transfer resistance of the solution <i>per unit length</i>
R_{sol}	The resistance of connection leads and electrolyte
R_{ct}	The charge transfer resistance

STP	Standard Temperature and Pressure
t	Time
T	Temperature
TFD	Time For Discharge
TOC	Top Of Charge
V_{\max}	The maximum voltage
x	i) The distance from the electrode surface to the bulk of the solution ii) The distance along an idealised pore axis
\bar{x}	The <i>mean</i> distance from the electrode
z	The number of electrons involved in an electrochemical reaction
Z	An impedance
Z_w	The Warburg impedance
α	i) The <i>cathodic</i> charge transfer coefficient ii) A phase identifier of either PbO or PbO ₂
β	i) The <i>anodic</i> charge transfer coefficient ii) A phase identifier of either PbO or PbO ₂
γ	A surface tension
Γ	Surface coverage (surface excess)
η	The overpotential
θ	i) Diffraction ('reflection') angle of an X-ray beam ii) The contact angle, between a liquid and a solid
κ	Conductance (per unit length)
ρ	i) (Pore) penetration depth ii) Electrolyte resistivity
σ	The warburg coefficient
σ°	The surface area of a site (usually taken as an the area of the adsorbate molecule)
Σ	The specific surface area of the solid
ϕ	Phase angle
ω	Angular frequency = $2\pi f$

CONTENTS

SUMMARY	1
LIST OF ABBREVIATIONS USED	2
CHAPTER ONE	
INTRODUCTION	6
CHAPTER TWO	
THEORETICAL PRINCIPLES	16
CHAPTER THREE	
A REVIEW OF THE LITERATURE ON LEAD SULPHATE MEMBRANES	38
CHAPTER FOUR	
EXPERIMENTAL	42
CHAPTER FIVE	
MEMBRANE STUDIES	48
CHAPTER SIX	
FARADAIC IMPEDANCE MEASUREMENTS	55
CHAPTER SEVEN	
X-RAY POWDER DIFFRACTION STUDIES	59
CHAPTER EIGHT	
MACRO DEFECT FREE PASTE STUDIES	63
CHAPTER NINE	
FINAL DISCUSSION	71
APPENDIX ONE: Program to Control X Ray Diffractometer & Display Results.	74
APPENDIX TWO: Program to Find The Main Peaks in an XPD Pattern.	78

APPENDIX THREE: Program to Form a Cured Plate. 80

APPENDIX FOUR: Program to Cycle & Record Readings from a Plate. 82

CHAPTER ONE.

INTRODUCTION.

1.1 Brief History.

Volta, in 1800, was the first to discover the secondary (*storage*) battery principle. However, it wasn't until 1859, when Gaston Planté constructed the "lead-lead oxide" battery (commonly called the lead acid battery), that the first practical rechargeable cell was built. It consisted of lead sheets, separated by strips of flannel, rolled together and immersed in sulphuric acid. Planté discovered that by passing a current through this arrangement he was able to convert the surface of one plate to lead dioxide and the other surface to porous lead, which provided an electrical current when connected to an external circuit. It was the culmination of years of research into common metal-metal couples and provided him with his only successful metal¹.

In 1881 Sellon², working on an idea by Faure and Volckmar, developed pocketed, pasted plates for electrodes. These electrodes were made of lead and powdered lead oxides mixed with sulphuric acid and placed into a supporting grid (which also acted as a current collector). It greatly increased the surface area available and significantly improved the capacity of the new battery—it heralded a new era; the lead acid battery had come of age. With this increased capacity new applications were found, the most important of these being the SLI (Starter, Lighting, Ignition) battery for automobiles. Today this still uses the pocketed, pasted plate design and accounts for almost 45%³ of lead acid batteries sales. Other major improvements have occurred: first with *antimonial grid alloys*—which prevented grid isolation, then with *negative expanders*—which greatly increased the surface area (and subsequently the capacity) of the negative plate and with *synthetic separators*—which prevented conductive extensions 'shorting' on adjacent plates. Recent developments have been in the area of *recombination* ("*maintenance free*") *batteries*, where a gaseous pathway leads oxygen, evolved at the positive during charging, to the negative plate where it is reduced back to water.

1.2 Manufacture of the SLI Lead Acid Battery Plates.

The design of the modern lead-acid battery varies considerably with the application, but the basic principles remain the same. The battery consists of an electrolyte of aqueous sulphuric acid (usually around 5 mol dm⁻³), a positive electrode of *porous lead dioxide*, a negative electrode of porous lead (known as '*spongy lead*') and a lead *alloy grid* framework structure to support the two active masses. This framework usually consists of either lead-antimony, lead-calcium or lead-calcium-tin; first to improve the inherent weakness of the lead and second to change the grid corrosion properties (one of the main

contributions to battery failure). The grid also serves as a current collector, maintaining a uniform distribution throughout the active mass—and so minimising the resistance of the battery.

The active material is derived from a mixture of lead oxide and lead powder which is manufactured in several steps, figure 1. First lead monoxide is obtained either by passing air over large lead blocks which are rolled in 'churns'— known as Ball Mills — or by means of 'Barton Pots' in which air is passed through molten lead. In either case a '*leady oxide*' mixture, consisting of 60% lead monoxide and 40% lead, is produced which is then used in the manufacture of both plates.

If positive plates are being produced, sodium carboxymethyl cellulose (CMC) or silica may be added. CMC is used to prevent 'buckling' of the positive electrode as it expands during *forming* (see below). While silica allows the production of a paste with a very high liquor content. If the *leady oxide* mixture is required for the production of the negative electrode, then 'expanders' such as lampblack, barium sulphate or 'organics' (e.g. stearic acid and CMC), are added⁴. The term '*expander*' is nowadays used loosely and normally refers to any material added to the negative electrode, not necessarily one which will increase its porosity. Barium sulphate, the only true expander mentioned above, is added, in concentrations of up to 1.25%, to act as a nucleation centre for the formation of lead sulphate crystals. This inhibits the formation of lead sulphate on the electrode's active material, thereby improving the battery's capacity and cycle life. Lampblack, added in amount up to 0.25%, increases the electrical conductivity and also enhances the capacity of the negative electrode at low temperatures. Organics, present in concentration of up to 0.33%, serve several functions. Stearic acid, a water repellent, is for instance added as an 'antioxidant' agent so that 'dry-charged' batteries are capable of keeping their charge over a long period of time. Other organics reduce polarisation in the cell and so increase the capacity of the battery. Finally, in order to strengthen the active material, both electrodes often have polyester fibres added. These also serve to reduce shedding of the active material, especially during formation.

The positive and negative plates, including their additives, are then mixed with a small, but significant, amount of sulphuric acid. The quantity of sulphuric acid to lead oxide paste (regardless of the actual concentration) determines the amount of basic sulphates formed and therefore the density of the paste. With moderate quantities of acid, the capacity of the positive plate increases with expansion and the consequent lowering of density. Over-expansion, however, results in the shedding of active material and a shortened battery life⁵. It is normal, therefore, to control the expansion of the paste by ensuring that its specific gravity is held within defined limits.

After the material has been pasted on to the grids, the plates are left for some hours to '*cure*'. This process varies from company to company, but is essentially the conversion of lead and lead monoxide to the sulphate or basic sulphates. The high-metallic, uncalcined oxide plates in present-day use give a

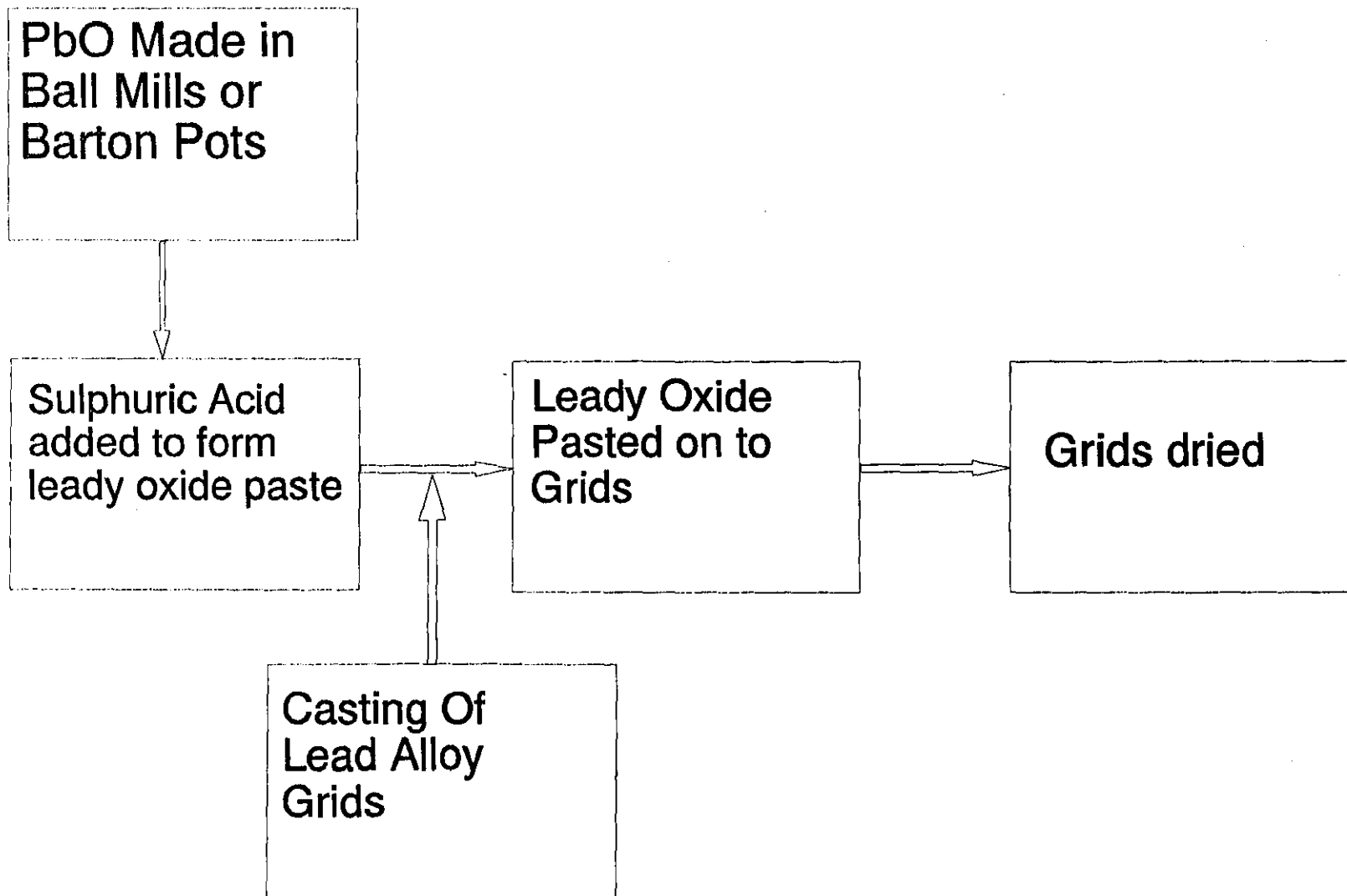


Figure 1

highly reactive product which readily oxidises if the moisture content in the paste falls to around 5 or 6%. The curing process is, therefore, the reduction of the water content to a catalytic level of about 5%, which is usually achieved by one of two methods:

- 'Flash drying' the plates and storing at ambient temperature for 3 to 4 days.
- 'Oven drying', between 38 and 65°C, at high humidity for 12 to 15 hours.

During this period the amount of free metallic lead falls from 40% to near 5%. This is desirable as it improves the strength of the dried plates and also reduces the possibility of the plates crumbling ('washing') or flaking ('scaling') during formation or later service.

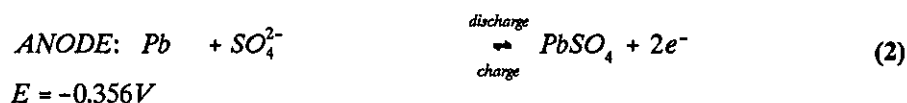
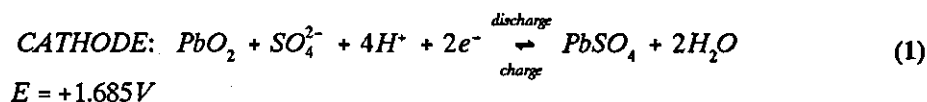
The industrially favoured positive-plate material, after curing, is tri-basic lead sulphate ($3\text{PbO}\cdot\text{PbSO}_4\cdot\text{H}_2\text{O}$), as this increases the capacity of the battery on forming. Since tri-basic lead sulphate is the low temperature stable product^{6,7}, battery plates are usually cured below 70°C (50 to 60°C being typical).

When cured the positive plates are immersed in dilute sulphuric acid (usually $< 2 \text{ mol dm}^{-3}$), connected to an external current supply and electrochemically oxidised (as the anode of a large Faradaic cell) from lead sulphate or basic sulphates to lead dioxide; while the negative plates (forming the cathode of the Faradaic cell) are correspondingly reduced to porous lead. This process is known as 'forming' and the time required for completion is dependent on a number of factors:

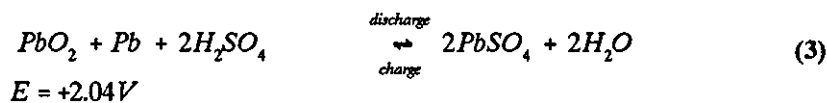
1. The forming current; it is generally better to use a low forming current in order to avoid 'gassing' and/or the formation of pellets of unreactive material, surrounded by a PbO_2 sheath.
2. Acid concentration; the optimum acid concentration lies in the range 1.050 to 1.150 SG (if the acid density is decreased more $\alpha\text{-PbO}_2$ is formed)⁸.
3. Temperature; the ideal temperature for the forming solution differs sharply between the positive and negative electrodes. The positive electrode gives a better capacity when formed at 46°C (as the temperature increases more $\alpha\text{-PbO}_2$ forms), whereas the negative electrode shows a better performance when formed between 10 and 32°C^{9,10,11}.
4. Plate thickness.
5. Type of plate used (for example: *Planté, pasted plate, tubular etc.*).

1.3 Chemistry.

The chemistry of the lead acid battery is based upon the *double sulphate theory* which was proposed by Gladstone and Tribe in 1883¹². This theory was fiercely disputed when it was first introduced and it was not until the advent of X-ray crystallography that final acceptance occurred and opposing theories were rejected. The double sulphate theory can be broken down into the processes which occur at each electrode:

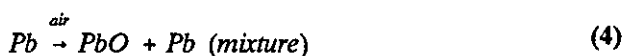


With the overall reaction being:

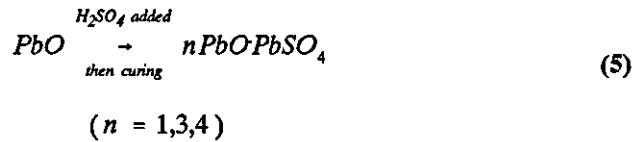


Today the proof of the double sulphate theory lies in the identification of the materials, their thermodynamic properties and, ultimately, in crystallographic measurements^{8,13,14}.

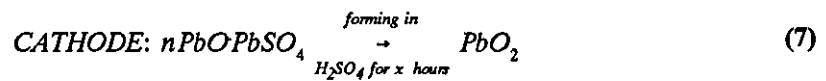
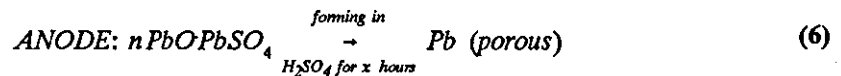
During manufacture the following reactions occur. First, inside a Ball Mill or Barton Pot air is passed over heated lead:



Additives (section 1.2), particular to each plate, are then added before treatment with sulphuric acid. After this the mix is pasted on to lead alloy grids and allowed to cure. A variety of basic lead sulphates are formed:



Finally, the cured plates are electrochemically formed— either reducing the basic sulphates to spongy lead, or oxidising them to lead dioxide:



1.4 The Place of the Lead Acid Battery Today.

Of the many scientific discoveries of the 19th Century few would have believed that the lead acid battery would achieve the importance and popularity that it has today. The lead acid battery is now fully integrated into modern life and regarded as an essential component for systems as diverse as: motor vehicles, uninterrupted power supplies (UPS systems), portable electronic equipment, emergency lighting or standby power sources (in places like hospitals, telephone exchanges and power stations).

Table 1^{3,15} compares the lead acid battery with some rival secondary battery systems. One can summarise the advantages of the lead acid battery as follows:

1. Inexpensive raw materials— the base materials are lead and sulphuric acid, both of which are readily available and cheap.
2. Easy to manufacture— the production process is straightforward and eliminates the need for expensive, specialised machinery.
3. Relatively high open circuit voltage (OCV) per cell— means fewer cells are required to meet a particular voltage specification.
4. Highly versatile— the battery can be manufactured to meet specific applications for high current, high power capacity or long life.
5. Has a good 'shelf-life'— making bulk purchases, of produced battery, commercially viable.

The system does have disadvantages— notably a low power to weight ratio (energy density), capacity utilization and toxicity problems— however these have proved little deterrent for consumers who

Battery Type	open circuit voltage /V	Energy Density / W hours kg ⁻¹		Practical Volume /W hours l ⁻¹	Cycle Life	Relative Cost per kW hour
		Theory:	Actual:			
Lead Acid	2.10	161	20-30	40-60	1200-1500	1-7
Nickel Cadmium	1.30	236	15-25	25-50	1000-2000	14-20
Nickel Iron	1.41	267	25-45	40-70	2000	20
silver Zinc	1.59	460	55-120	90-250	10-200	23

Table 1: Comparisons of some Secondary Battery Systems.

consider the lead acid battery's cheapness, versatility and simple maintenance preferable to that of other battery systems.

Research is continuing into: *the charge/discharge mechanism* (gas recombination), *alloying performance* (passivation) and *'membrane' properties*. Current research¹⁶ has shown that lead can be reclaimed from old batteries— giving the lead acid battery a 'greener' image not enjoyed by other secondary battery systems.

1.5 The Basis Of This Research: New Ideas In Lead Acid Battery Technology.

There is a belief in the battery industry that making lead acid battery paste is analogous to making cement! However, this idea is not new— Schallenberg¹ in his history on storage battery makes the following remarks:

●*"In modern (lead acid battery) manufacturing practice the paste for battery plates is made from a mixture of dilute sulphuric acid and litharge.... When mixed with sulphuric acid (it) behaves like cement: the mass hardens & releases heat.... It is important that the rate of drying is slow— if this is done the setting process will produce long, fibrous, needle like crystals of lead sulphate throughout the active material— giving the formed material good coherence.*

●*"Also analogous to cement technology is the mixing of the lead paste: it should have a damp, greasy crunchy feel, (should) shear well but must not flow or be sticky... Otherwise durability is lost.*

●*"Moreover... if the mix is too wet, too dry or allowed to set too rapidly then the durability of the plate will suffer.*

●*"Oversulphation is a further problem... an enamel like deposit of sulphate is analogous to the freeze-thaw ice effect on cracks in rocks & roads."*

Clearly these points, if read out of context, could equally have applied to lead acid battery or cement manufacture— and it is similarities such as these that have lead workers to believe that the two processes were analogous. The rest of this chapter briefly explains how recent discoveries in the cement industry might be used as an important innovation to the preparation and production of lead acid battery pastes.

1.5.1 The Hydration of Portland Cement.

Portland cement contains a number of rather impure chemical constituents, the most important being tricalcium silicate (C_3S), dicalcium silicate (β - C_2S), tricalcium aluminate (C_3A) and an alumino-ferrite

phase (usually designated C_4AF)^{*}. When preparing cement mixes these compounds are used in a powdered form, reacting readily with the water to form insoluble hydration products which, in cement paste (a mixture of cement and water) or *concrete* (a mixture of cement paste, sand and aggregate filler), gradually replaces the water between the cement grains, eventually binding the composite material together¹⁷.

The hardening in a cement paste is mainly due to the hydration of the two calcium silicate compounds C_3S and C_2S , the product being an ill-defined, colloidal calcium-silicate-hydrate gel (C-S-H). In this hardened cement paste the C-S-H gel forms a finely divided and amorphous matrix, occupying about 70% of the mass and providing the main bonding agent (the various constituents of Portland cement do not react with water independently of one another, however, cross reaction and synergistic effects probably occur). The remaining constituents of the paste are calcium hydroxide (a by-product of the cement hydration process) and various complex aluminate hydrates. It has been identified that the aluminate components of the mix do not significantly contribute to the overall, long-term, strength; the long term strength coming from, initially, C_3S during the first few weeks and subsequently, because of the slower reaction time, C_2S over a period of many months, or years. The hydration of this silicate material has been, therefore, central in the study of Portland cement but, although X-ray diffraction, chemical analysis and electron microscopy have answered many questions, much about the structure, physical nature and chemical reactions were, until recently, unresolved.

An important question in cement technology has been how to explain the cement hydration and set phenomena. One could observe an initial heat release, as water was added to the mix, then a quiescent period (which lasted several hours) followed by a further exothermic reaction with the onset of hardening. Two hypotheses had been suggested to explain this. The first viewed the mix-heat-wait-heat phenomena as a solubility product problem—it said that the quiescent phase was due to the silicates in the cement taking time to attain a solubility product high enough to react. The second theory was based on an impermeable coat being formed around the silicates which acted as a barrier to further reaction until a sufficient amount of silicate in solution caused the exothermic reaction to occur. Of the two theories the former probably had greater support until studies by Double *et al.*¹⁸ and Birchall *et al.*¹⁹ showed that the cement hydration problem could be explained by a *silicate garden* mechanism.

Silicate gardens have been known for many years²⁰, they are tubiform excrescences which emerge from the surface of a soluble di- or tri-valent metal salt crystal when immersed in a solution of sodium silicate (or other similar solutions—zincates, stannates, aluminates and borates, for example) where a gelatinous,

* In cement technology a shortened notation is used to denote cement compounds: C = CaO, S = SiO₂, A = Al₂O₃, F = Fe₂O₃ and H = H₂O. For example C_3S is, therefore, $3(CaO) \cdot SiO_2$

sheath is formed around the crystal preventing further hydration of material beneath this layer—a *semi-permeable membrane*. The membrane, due to osmosis, continues to allow water to pass but then suddenly ruptures—releasing the material inside—to form ‘outgrowths’, or *fibrils*, which extend from the crystal centres into the body of the material.

Double and Birchall suggested that the quiescent phase, in the cement hydration, was due to a semi-permeable membrane formation which initiates a dormant period during which time only water (because of the semi-permeability) passes through the membrane to continue the attack on the inner, anhydrous material. The quiescent phase terminates when the intra-membrane pressure causes membrane rupture, releasing the hydrosilicate, from within the membrane, into the external solution and causing the fibrils of hydrosilicate to extend and interweave from grain centre to grain centre forming an interlocking matrix and a consequent setting of the cement.

1.5.2 Macro Defect Free (MDF) Cement.

One goal of inorganic chemists has been the development of an *inorganic* thermosetting resin with the properties and advantages of an inorganic material—non-combustibility, resistance to chemical attack and high temperature workability, for example. Birchall²¹ considered that cement would be such a material, if its inherent weakness could be overcome. This inherent weakness of cement materials has been shown to be due to the presence of unlinked *voids*²² (of up to 1 mm in size) which can not be assessed by porosity measurement techniques (they are non open pores). If, therefore, a reduction in these unlinked pores can be achieved then a consequent increase in the material strength should occur²³.

MDF strategy reduced the macro voids in cement pastes by reducing the amount of water used, this subsequently meant voids, caused by the evaporation of water, were reduced and the cement strength increased. However reducing the amount of water to such an extent would normally have been impossible because water - cement ratios of less than 0.22 are a crumbly, sand like mixture. To overcome this problem Birchall²⁴ added a hydrophillic polymer (polyvinyl alcohol), which increased the workability of the mix to that of a gel. Then by passing the cement paste between large rollers trapped air was squeezed out, removing the larger voids and producing a denser paste.

The polymer, added to the paste, was found to perform a number of other functions:

- First, the polymer coats the cement particles preventing agglomeration,
- Second, the polymer reduces the friction between grains allowing a workable material to form,

- Thirdly, shear is now transmitted *throughout* the structure (whereas previously water cavities would form)— allowing aggregated particles to be broken down and homogeneity to occur more easily and,
- Lastly, the polymer joins in the setting reaction— producing a molecular inorganic - organic composite, with a 1% total porosity, a maximum defect size of 100 μm and a tensile strength of 150 MPa.

1.5.3 The Lead Acid Battery, Silicate Gardens and MDF cement.

In 1984 Julian²⁵ reviewed the history and development of the lead acid battery, remarked on the bewildering amount of information generated and drew attention to the need for further investigation into the following aspects:

- shelf life,
- recovery after discharge stand,
- loss of capacity— especially with Ca grids,
- charge acceptance efficiency and
- faradaic efficiency.

Also the following scientific problems, which were current at that time:

- What effects does PbO_2 atomic changes have on softening and shedding,
- What role does H^+ , OH^- and H_2O play?
- What relationship is there between crystal structures and plate microstructure?
- How do changes in PbO_2 atomic structure affect plate structure and cycle life?

This led Julian to propose a novel way to research the lead acid battery. He suggested that progress might be made by looking at developments and improvements in *other* branches of chemistry which could be applied to solve similar problems in the lead acid battery industry. In particular further research into the following two areas was suggested:

1. *Hunt the proton:* Briefly put, this states that rather than doing experiments that look at one feature of the lead-acid battery at a time, one should look at what one really wants— *the proton*. For example Caulder²⁶ had shown that *active* PbO_2 has two different hydrogen species, whereas *inactive* PbO_2 has hydrogen present in only one; Hill²⁷ agreed that the oxygen lattice was complete and that the charge balance comes from hydrogen or hydroxyl groups. Thus hydrogen— a very mobile species in *defect oxides*— must be investigated to elucidate the reactions in the lead-acid electrode and, Julian argues, papers that do not mention hydrogen must now explain why*.

* Chapter 9, page 71, discusses recent developments in the lead acid battery, in particular the two different hydrogen species, associated with *active* and *inactive* PbO_2 , are now considered not to exist— hydrogen probably does not play any part in the changes between the two states.

2. *Membrane Technology, 'Silicate gardens' and Macro Defect Free Cement.* The point Julian wanted to make was that the similarities between cement hydration and lead acid battery paste product may indicate another potential area of research in battery technology. For example—the setting of cement and the setting of battery paste (curing) are both dependent upon the water content, are influenced by sulphates (CaSO_4 for cement, BaSO_4 in battery pastes, while lignosulphonates control the rheology), exhibit an exothermic reaction as setting occurs and, more particularly, both structures are *porous*. What is suggested is that there are sufficient similarities between the silicate gardens, cement hydration and the formation of amorphous material in lead acid battery plates that an examination of the physical chemistry of the former may throw light on various ill-understood processes/mechanisms of the latter.

This research looks into the second aspects of Julian's paper:

● *Does osmotic behaviour cause the amorphous structures seen in a lead acid battery?*

—can the silicate gardens explanation be used to explain the large amount of amorphous material present in battery plates²⁸?

● *What chemical conditions lie behind a semi-permeable PbSO_4 membrane?*

—Can Ruetschi's²⁹ work on semi permeable membranes be extended to look at actual battery systems?

● *Should not the osmotic and semi-permeable behaviour of a PbSO_4 film be considered as well as the recrystallization phenomena invoked to explain the formation of a non-recharge PbSO_4 layer after many cycles?*

—Ruetschi proposed that alkaline stable basic lead sulphates occur⁻ at the lead acid battery electrodes because of the semi permeable behaviour of lead sulphate membranes; could the microstructural changes, within the electrode's surface layer, be an explanation of the capacity loss?

To answer these questions one must re-evaluate the work of Ruetschi^{29,30}, make an electron microscopical investigation of lead sulphate membranes and apply modern electrochemical techniques to examine its properties. In the experiments which follow the new ideas of Julian and those of traditional electrochemical technology are combined.

CHAPTER TWO.

THEORETICAL PRINCIPLES.

2.1 The Electrode-Electrolyte Interphase.

In contrast to an interface— an abrupt, sharp change between two phases— an interphase is a region between two phases where properties of one phase slowly change into that of the other. It is a region in which the properties have not yet reached the bulk of either phase. This region is of fundamental importance in determining the electrode kinetics, the equilibrium conditions and the resulting reactions and products.

The simplest model of the interphase was that proposed by Helmholtz³¹. Consider an electrode placed in an electrolyte, there is a break-down of electrical neutrality at the phase boundary; an *electrical* double layer is created, figure 2. Here the interphase may be regarded as two planes of equal, but opposite, charge held rigid by a fixed electrostatic force. Ions in solution align up (at a fixed distance) with charges at the electrode surface, balancing out the charge. Three assumptions have to be made for a valid model:

1. no transfer of charge occurs across the interphase,
2. the separated charges are in electrostatic equilibrium,
3. the charged layer, in solution, changes with the electrode potential.

When these conditions hold the interphase behaves, electrically, like an ideal capacitor— there is no resistive component. An electrode which obeys these conditions is termed "*ideally polarisable*". The classical, and indeed only practical example is the mercury electrode, in 1 mol dm⁻³ KCl.

Gouy³² and Chapman³³ further developed the model of the electrochemical interphase. Working independently, they both realised that, in an electrolyte, ions would not be stationary but free to move and subject to thermal agitation. The greatest concentration of excess charges, however, would occur adjacent to the electrode— where the electrostatic forces are able to overcome the thermal agitation. Further away from the electrode electrostatic forces would be weaker, resulting in a diffuse layer around the electrode, figure 3.

The model used to predict the diffuse layer was obtained by envisaging the electrolyte's ions as point charges, which can approach to within a very small distance of the electrode surface. This leads to surprisingly high concentrations at the interphase and 'double layer' capacitances lower than that observed experimentally. This seriously limits the use of the Gouy-Chapman model and has led to a further modification— the Stern model.

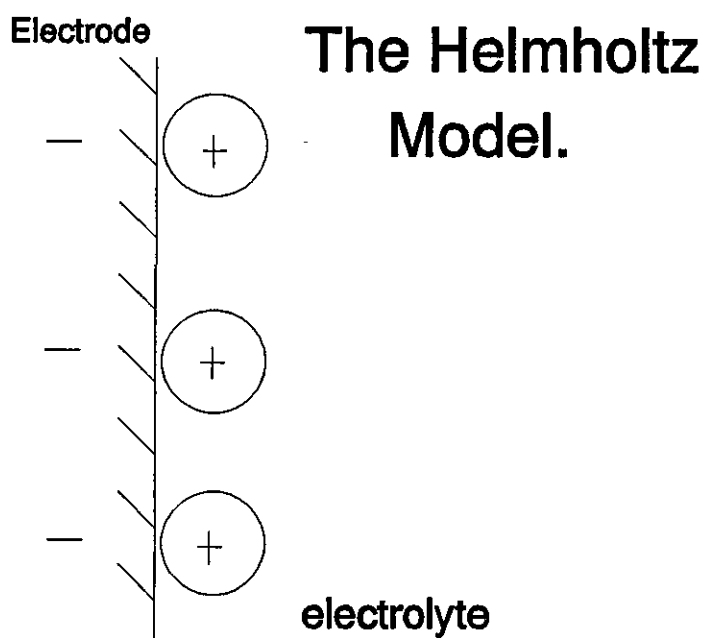


Figure 2

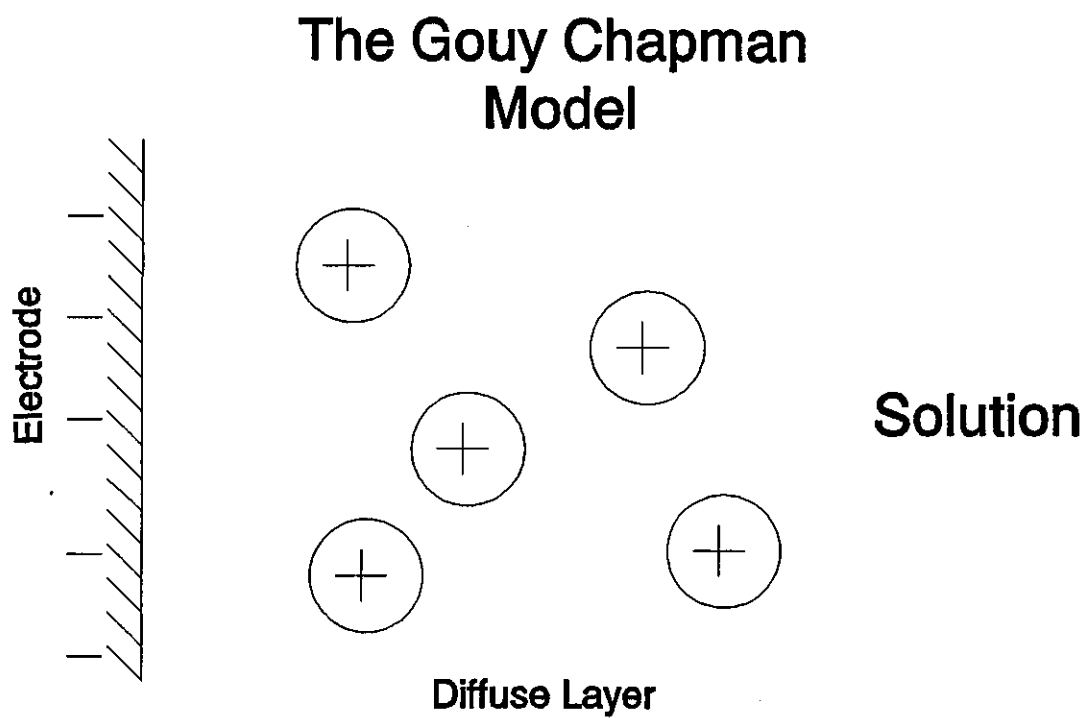


Figure 3

In the Stern model³⁴ the two previous models are combined. This takes into account the idea of a diffuse layer— an interphase— as well as the size of the ions. A monolayer of ions, according to this model, approach to within a certain critical distance of the electrode surface, the Helmholtz layer. Further away from the electrode other ions are distributed diffusely in a layer which extends to the bulk of the solution; the *diffuse layer*, figure 4. Stern assumed, for the model, that anions and cations approach would be the same, although he believed that this may not always be valid. Stern also postulated that some ions may undergo an adsorption to the electrode by a non-electrostatic mechanism, which would also limit the model's application.

In 1947 a further modification was developed by Grahame³⁵, who suggested that the presence of dipoles due to water molecules, at the electrode surface, should be taken into consideration. At least three layers, it was suggested, should be considered when describing the interface: the inner Helmholtz plane, the outer Helmholtz plane and the diffuse layer. By splitting the Helmholtz plane, in this way, Grahame was able to separate specifically adsorbed ions that had lost their hydration layer— the inner Helmholtz plane— from normally hydrated ions which are still held by electrostatic forces at their distance of closest approach to the electrode surface— the outer Helmholtz plane— figure 5. Grahame was then able to show that the total capacitance of the 'double layer' was the sum of two capacitors in series:

$$\frac{1}{C_d} = \frac{1}{C_F} + \frac{1}{C_D} \quad (8)$$

Where: C_d = Capacitance of the Double Layer

C_F = Capacitance of the Fixed (Inner Helmholtz) layer

C_D = Capacitance of the Diffuse (Outer Helmholtz) layer

Equation (8) shows that if the electrolyte is diluted, the value of the diffuse layer will become more significant; the small capacitance will determine the overall total capacitance C_d — C_d will become independent of C_F . As the concentration falls still further it can be shown, experimentally, that a sharp minimum is obtained in a plot of C_d Vs. potential. This corresponds to a point of zero charge at the electrode. Frumkin³⁶ discussed the importance of the point of zero charge, indicating that it is not affected by the addition of 'potential-determining' ions. Pointing out, therefore, that this determination can be used when considering charge adsorption at a polarisable electrode.

Further improvements to this model were developed by Devanathan, Bockris and Müller³⁷. It was suggested that the preponderance of solvent ions at the interphase would affect the dielectric properties of the inner Helmholtz plane. They proposed that a layer of orientated dipoles of water covered the surface of the electrode and only specifically adsorbed ions, with no hydration shell, could displace the orientated water dipoles. It was stated that the specific adsorption of a species was due, not to covalent bonding, as Grahame had thought, but to the lack of the primary hydration shell. The water molecules

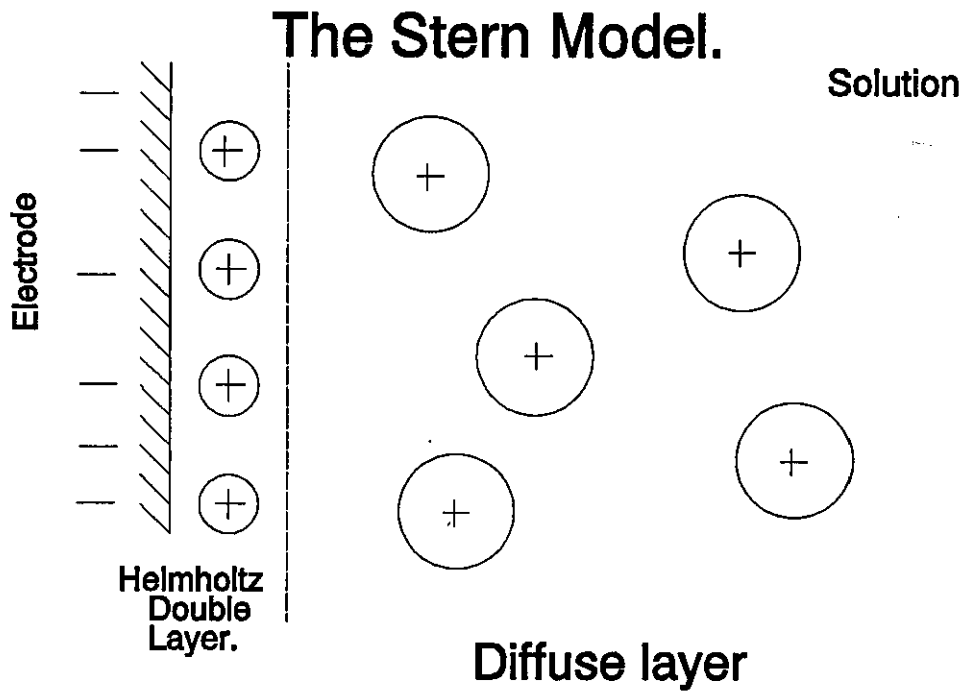


Figure 4

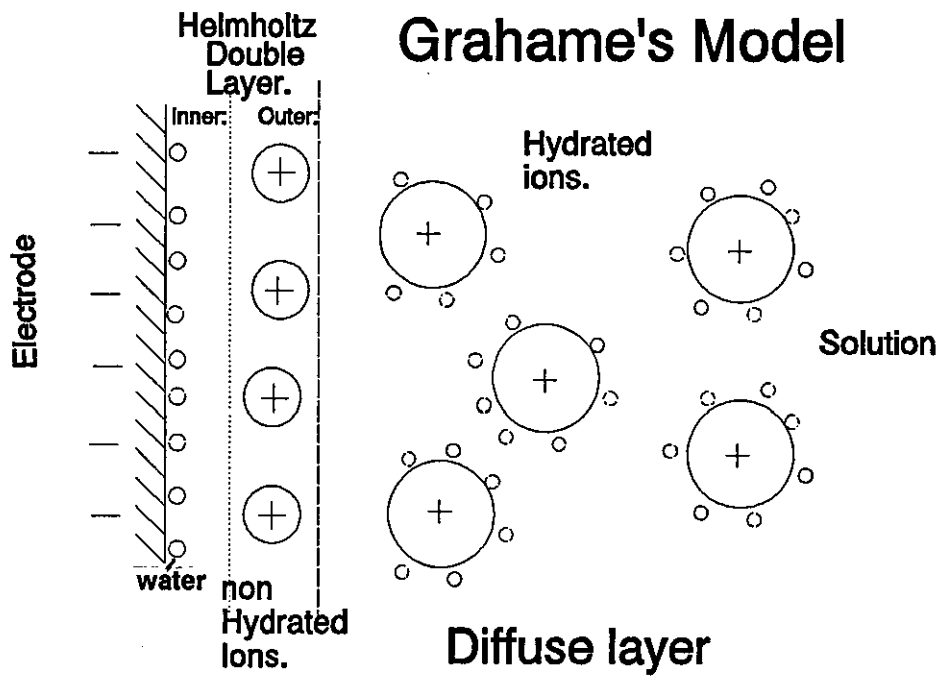


Figure 5

were thought to adsorb with their negative dipoles pointing either towards, or away from, the electrode surface depending on the potential.

Although this model has received general acceptance as a fair description of the 'double layer', studies by Cooper and Harrison³⁸ have argued that the structure of the interphase arises from the differences between aqueous anions and cations causing a net distributed charge to act at a mean distance from the electrode, \bar{x} . A dielectric constant is therefore set up which varies with the mean distance (\bar{x}), surface excess of charged particles (Γ), concentration and the cation/anion size. However this statistical model of the double layer has yet to find general acceptance.

2.2 The Charge Transfer Process.

Consider the cathodic reduction of an ion at an electrode surface. This can be represented by:



where: k_f is the forward (cathodic) rate constant,

k_b is the reverse (anodic) rate constant.

z is the number of electrons

The current for the forward, cathodic reaction is given by*:

$$i_f = zFAk_f C_o^s \quad (10)$$

while the current for the reverse, anodic reaction is given by:

$$i_b = zFAk_b C_R^s \quad (11)$$

Where: C_o^s is the concentration at the electrode surface of the oxidised species O.

C_R^s is the concentration at the electrode surface of the reduced species R.

A is the reaction area.

* The convention adopted here is that the reaction proceeds from left to right and the overall current for this process is positive.

The current flowing through an external circuit is the difference between the forward and reverse processes:

$$\begin{aligned} i_{total} &= i_f - i_b \\ &= zFA(k_f C_o^s - k_b C_R^s) \end{aligned} \quad (12)$$

The rate constants k_f and k_b are given by:

$$\begin{aligned} k_f &= k_f^o \exp\left(\frac{-\alpha zFE}{RT}\right) \\ k_b &= k_b^o \exp\left(\frac{(1-\alpha) zFE}{RT}\right) \end{aligned} \quad (13)$$

where: α is the charge transfer coefficient (usually close to 0.5)

E is the potential of the electrode (as measured against a suitable reference electrode)— that is $(E-E^{\theta})$.

k_f^o, k_b^o are the potential independent values of k_f and k_b .

By substituting (13) into (12) one can obtain:

$$i = zF A \left[k_f^o C_o^s \exp\left(\frac{-\alpha zFE}{RT}\right) - k_b^o C_R^s \exp\left(\frac{(1-\alpha)zFE}{RT}\right) \right] \quad (14)$$

But at equilibrium the total current is zero. Hence no concentration gradients exist at the surface and if one assumes unity surface area, one has:

$$\begin{aligned} i_f &= i_b = i_o \\ i_o &= zF k_f^o C_o^s \exp\left(\frac{-\alpha zFE_r}{RT}\right) \\ &= zF k_b^o C_R^s \exp\left(\frac{(1-\alpha)zFE_r}{RT}\right) \end{aligned} \quad (15)$$

where: E_r is the reversible potential

i_o is the *exchange current density* the current which flows at equilibrium.

By eliminating k_f, k_b from (14), using (15) gives:

$$i = i_o \left[\exp\left(\frac{-\alpha z F (E - E_r)}{RT}\right) - \exp\left(\frac{(1-\alpha) z F (E - E_r)}{RT}\right) \right] \quad (16)$$

where $(E - E_r)$ is defined as the charge transfer (or activation) *overpotential*³⁹, η^* . This equation has become known as the *Erdey-Gruz and Volmer equation*⁴⁰ and holds for any solution when the surface concentrations do not differ significantly from the bulk. If, however, this is not the case— for example, when the currents are not low— then equation (16) becomes the *Butler-Volmer equation*:

$$i = i_o \left[\frac{C_o^s}{C_o^b} \exp\left(\frac{-\alpha z F \eta}{RT}\right) - \frac{C_R^s}{C_R^b} \exp\left(\frac{(1-\alpha) z F \eta}{RT}\right) \right] \quad (17)$$

Butler⁴¹ was the first to introduce the concept of an exchange current, its dependence on reactant concentration is given by⁴²:

$$i_o = z F k^o C_o^{(1-\alpha)} C_R^{\alpha} \quad (18)$$

Where k^o is the *apparent* rate constant⁴³.

* The advantage of working with i_o rather than k^o is that the current can be described in terms of the deviation from the equilibrium potential, η (rather than the formal potential E^0).

Two special cases of the Erdey-Gruz and Volmer equation are important:

1. At Low Overpotentials.

$$\begin{aligned} \text{WHEN: } |\eta| &< \frac{RT}{\alpha zF} \\ \text{or, } |\eta| &< \frac{RT}{(1-\alpha)zF} \end{aligned} \quad (19)$$

The plot of overpotential against current is linear, with the coefficient of regression corresponding to an electrical resistance—the *charge transfer resistance*, R_{α} :

$$R_{\alpha} = - \left(\frac{\partial \eta}{\partial i} \right)_{i=0} \quad (20)$$

By differentiating (16), at $\eta=0$, one obtains:

$$\left(\frac{\partial i}{\partial \eta} \right)_{\eta=0} = \frac{-zFi_o}{RT} \quad (21)$$

and:

$$R_{\alpha} = \frac{RT}{zFi_o} \quad (22)$$

Thus, the exchange current density can be obtained from the charge transfer resistance at the reversible potential. Equation (22) serves to define R_{α} ⁴⁴.

2. At High Overpotentials.

$$\begin{aligned} \text{When } |\eta| &> \frac{RT}{\alpha zF} \\ \text{or, } |\eta| &> \frac{RT}{(1-\alpha)zF} \end{aligned} \quad (23)$$

One of the exponents from (16) can be neglected. For a high *cathodic* overpotential, one has:

$$\eta = \frac{RT}{\alpha zF} \log_e i_o - \frac{RT}{\alpha zF} \log_e i \quad (24)$$

while for a high *anodic* overpotential:

$$\eta = \frac{RT}{(1-\alpha)zF} \log_e i_o - \frac{RT}{(1-\alpha)zF} \log_e i \quad (25)$$

Equations (24) and (25) are known as the *Tafel* relationships⁴⁵.

The exchange current density can therefore be obtained from values of the charge transfer resistance at low potentials by extrapolating $\log i$ Vs. η plots back to the equilibrium potential (measured at high overpotential).

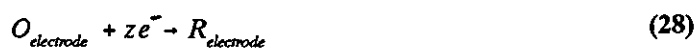
The theory of the charge transfer process, summarised above, applies *only* to the simple electrode reaction in which all the electrons are transferred simultaneously. Losev⁴⁶ has extended the treatment to successive electron transfer processes with a single rate-determining step. Levich⁴⁷, Marcus⁴⁸ and Dogonadse⁴⁹ have derived charge transfer equations using a quantum mechanical approach. Here the reaction does not occur in one *smooth* step, over a single energy barrier, but proceeds by a number of steps. First, the reactant diffuses to the electrode then the ionic shell rearranges itself and finally the electron is transferred (the earlier stages are all in equilibrium and can be treated by thermodynamics, the final stage, however, must be treated kinetically). After charge transfer has been completed, the ligand bond distances are altered and so the solvent dipoles and ionic atmosphere reorientates. A principal feature of these models is that electron transfer involves no change in energy.

2.3 Mass Transport and Charge Transfer Processes.

If one again considers the reaction:



this process may be considered to be composed of three individual processes:



The overall flow of electrons, or current, can be limited by either process (27) or (28). *Mass transport control* occurs when the reaction is limited by the rate at which the bulk material flows into the electrode; that is when equation (27) is the slowest process. If equation (28) is the slowest process, then the overall reaction is limited by the rate of electron transfer and the reaction is known as *charge transfer controlled*. Sometimes neither process step is *slow* compared with the chemical transformation which the electroactive species is undergoing. In this case the chemical transformation is the rate determining step.

There are *three* modes of mass transfer typically encountered, these will now be summarised.

2.3.1 Migration.

Mass transfer by migration is the result of forces exerted on charged particles by an electric field. In the presence of a large excess of a suitable support electrolyte the migration of electroactive species is minimised to such an degree that it can be neglected.

2.3.2 Convection.

Natural, or free, convection always develops spontaneously in any solution undergoing electrolysis. This occurs because of density fluctuations near the electrode, although thermal or mechanical disturbances can also contribute to the effect.

Forced convection may also be present due to other, external, turbulence—such as stirring the solution, rotating the electrode or gaseous bubbling.

2.3.3 Diffusion.

A concentration gradient develops whenever an electrode is operated and electrolysis begins. Moreover as diffusion occurs to some extent in *every* electrode system, it is a very important concept which will be developed further.

2.3.3.1 Fick's First Law.

Consider a planar electrode immersed in an electrolyte solution containing O, a species which reacts according to equation (26). Then the amount of moles N, of O, which diffuse past a given area A, in a time dt is given by *Fick's First Law* of diffusion:

$$\frac{dN}{A dt} = -D_o \frac{\partial C_o}{\partial x} \quad (30)$$

Where: C_o is the concentration of species O,

x is the distance from the given area, A.

The left-hand side of equation (30) is known as the *flux* q and is the amount of moles of species O diffusing through a unit area in unit time. D_o is *Fick's Diffusion coefficient* for O, and is defined as the amount of species O crossing a unit area, per unit time, under unit concentration gradient conditions.

2.3.3.2 Fick's Second law.

As the extent of the reaction continues, the amount of species O decreases and both C_o and $(\partial C_o/\partial x)$ decrease with time. This is the basis of *Fick's Second Law* of diffusion, which states*:

$$\frac{\partial C_o}{\partial t} = D_o \frac{\partial^2 C_o}{\partial x^2} \quad (31)$$

The current at any time t, is proportional to the flux per unit area at the electrode surface (i.e. $x=0$):

$$\begin{aligned} i_t &= zFAq(o,t) \\ &= -zFAD_o \left(\frac{\partial C_o}{\partial x} \right)_{o,t} \end{aligned} \quad (32)$$

The value $\left(\frac{\partial C_o}{\partial x} \right)_{o,t}$ can be obtained by solving the differential equation (31), using appropriate

boundary conditions:

1. At $t=0$, $C_o^a = C_o^b$
2. At $t>0$, $C_o^a = 0$
3. $C_o \rightarrow C_o^b$ as $x \rightarrow \infty$.

The solution of the differential equation (31)— at any distance, x from the electrode or time, t, since the start of electrolysis is:

$$C_o(x,t) = C_o^b \frac{2}{\pi^{1/2}} \int_0^{x/2} D^{1/2} t^{1/2} \exp(-y^2) dy \quad (33)$$

(where y is the dummy argument for x). On rearrangement the final expression for the instantaneous current, at a *planar electrode*, under *diffusion control* becomes:

$$i = \frac{zFAD_o^{1/2} C_o^b}{\pi^{1/2} t^{1/2}} \quad (34)$$

This is known as the *Cottrell equation*.

* D_o usually depends on concentration too, therefore equation (31) is actually only valid for *small* concentration ranges.

2.4 Linear Potential Sweep and Cyclic Voltammetry.

In this technique a potential, applied to an electrode, is changed linearly with time in a repetitive manner. The current produced from this procedure is then measured— either as function of the potential or of time. If only a single sweep (anodic or cathodic) is performed then the technique is known as linear sweep voltammetry (*L.S.V.*).

Theoretical analysis has been carried out by a number of workers including Randles⁵⁰ and Sevcik⁵¹. The fundamental feature of a voltammogram is that current peaks occur at precise potentials— *characteristic* of the reactions taking place at the electrodes. The shape and position of the current peaks are dependant upon several factors— including: sweep rate, electrolyte-electrode composition and concentration of the reactants involved.

Whereas LSV is usually used for accurate kinetic measurements (because no concentration gradients exist at the beginning of sweep and only one sweep is performed) in *cyclic voltammetry* complex concentration gradients make quantitative work impossible— this method is usually employed to identify steps in the overall reaction, or to identify changes which occur, at the electrode's surface, with time— porosity development, chemical changes or grain boundary effects for example. The mechanisms being proposed by cyclic voltammetry, are only relevant to the specific experimental conditions chosen; kinetic parameters can only be evaluated if the reaction mechanism is qualitatively known by some other means. In this study LSV was used to determine the rest potential of PbSO₄ couples and the stability of PVA and PAA at lead acid battery potentials.

2.5 Surface Area Measurements.

2.5.1 BET Measurements.

The BET treatment is based on a kinetic model of the adsorption process put forward by Langmuir⁵², where the surface of the solid was regarded as an array of adsorption sites. A state of *dynamic* equilibrium was postulated in which the rate at which molecules arrive from the gaseous phase, and condense on to bare sites, is equal to the rate at which molecules evaporate from occupied sites.

Langmuir also proposed equation-isotherms for subsequent molecular layers, however these equations proved too complex to be of practical value and it was to simplify them that Brunauer, Emmett and Teller⁵³ put forward three (simplifying) assumptions:

1. For all layers, except the first, the heat of adsorption is equal to the molar heat of condensation.
2. For all layers, except the first, the evaporation-condensation conditions are identical.

3. When the saturated vapour pressure is attained, the adsorptive condenses to a bulk liquid on the surface of the solid being measured (i.e. the number of layers becomes infinite).

When these assumptions are made to the Langmuir isotherm, the BET equation naturally follows:

$$\frac{n}{n_m} = \frac{1}{1 - \frac{P}{P^\circ}} - \frac{1}{1 + (c-1) \frac{P}{P^\circ}} \quad (35)$$

Where: n/n_m is the fractional amount of substance adsorbed at p compared with that adsorbed at STP,
 c is proportional to the molar heat of condensation,
 p/p° is the fractional present pressure compared with the saturated vapour pressure, p° .

The slope and intercept give two simultaneous equations:

$$\begin{aligned} \text{slope} &= \frac{(c-1)}{n_m c} \\ \text{intercept} &= \frac{1}{n_m c} \end{aligned} \quad (36)$$

From which the surface area of a material can be obtained through the relationship:

$$n_m = \frac{\Sigma}{N_o \sigma^\circ} \quad (37)$$

where: Σ is the specific surface area of the solid,
 σ° is the surface area of a site (usually taken as an the area of the adsorbate⁵⁴),
 N_o is Avogadro's number.

Both practical and theoretical requirements limit the number of substances which can be used as adsorptives. McClellan and Harnsberger⁵⁴ found that they could only recommend five (out of 128 substances investigated)—Nitrogen, Argon, Krypton, benzene and *n*-butane.

2.5.2 Mercury Porosimetry

Mercury porosimetry is used to determine the pore size distribution—and subsequently the surface area of a porous material. It was originally developed to determine pore sizes in the ‘macropore’ range, where gaseous pore sizing methods break down for practical reasons. The full scope of the technique became apparent when Ritter and Drake^{55,56} developed a procedure for making measurements at high pressure.

The technique uses the fact that mercury has a contact angle greater than 90° and an excess pressure, Δp , is required to *force* liquid mercury into the pores. The idea of using mercury intrusion to measure pore size was first suggested by Washburn⁵⁷ who derived the basic porosimetry equation (often known as the *Washburn equation*):

$$r^p = -\frac{2\gamma \cos \theta}{\Delta p} \quad (38)$$

where: r^p is the radius of the pore

γ is the surface tension of the mercury (usually taken as 480 mN m⁻²)

θ is the contact angle of the mercury (usually taken as 140°).

To derive this equation, first note that the Laplace-Young^{58,59} equation (which describes the pressure of a small amount of liquid in a capillary) is:

$$p^{Hg} - p^g = -\gamma \left(\frac{1}{r_1} + \frac{1}{r_2} \right) \quad (39)$$

where: p^{Hg} is the pressure in the liquid mercury phase.

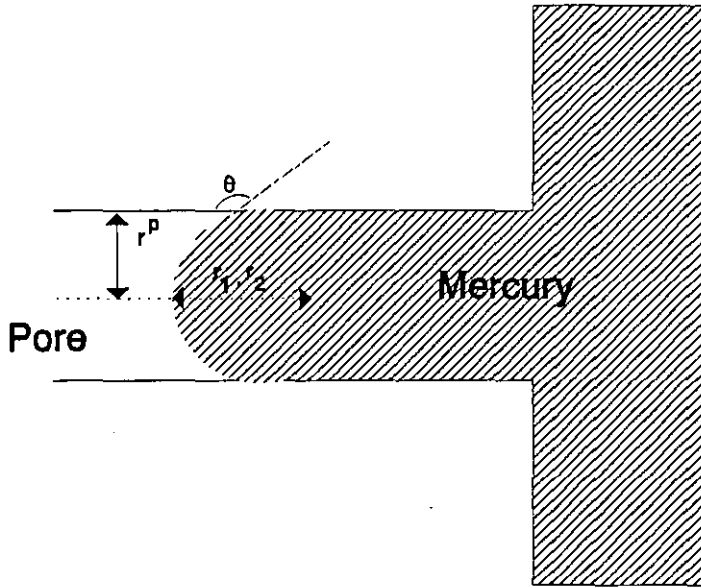
p^g is the pressure in the gaseous phase.

r_1 and r_2 are the inner and outer radii of curvature of the meniscus.

Then, by considering that mercury’s meniscus approximates to a segment of a sphere (figure 7) the following simplifications can be made:

$$r_1 = r_2 = \frac{r^p}{\cos \theta} \quad (40)$$

Combining equations (39) and (40) then gives the Washburn equation, when rearranged.



Mercury Penetrating a Cylindrical Pore.

Figure 7

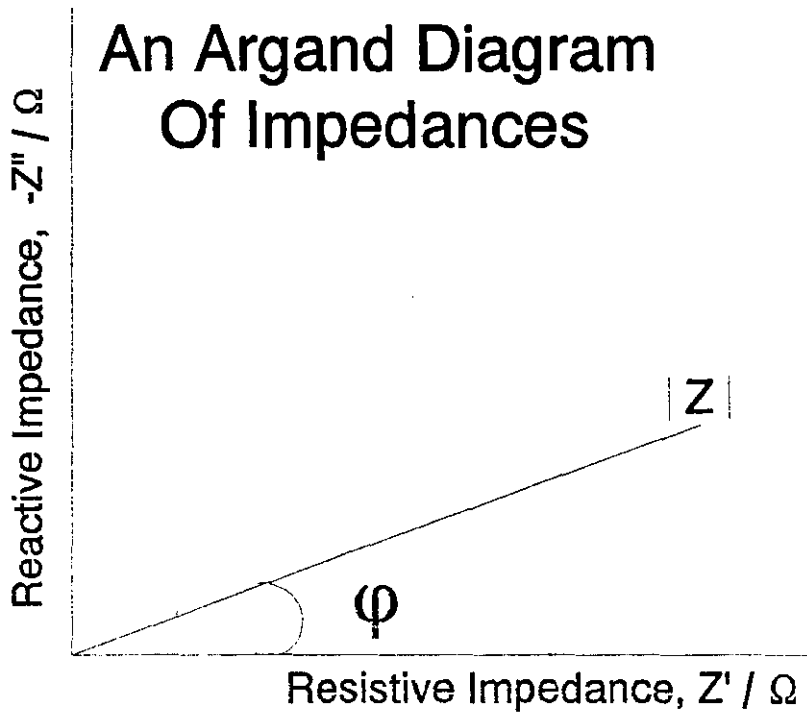


Figure 8

Basically the mercury porosimetry technique consists of measuring the amount of mercury which penetrates into an evacuated solid as a function of an applied hydrostatic pressure. Nowadays automated porosimetry machines are routinely employed for this type of work.

2.6 Theory of Faradaic Impedance Spectroscopy.

2.6.1 Introduction.

Impedance spectroscopy (IS) is usually used to study the kinetic parameters of an electrochemical system. The kinetic parameters, of the electrode being considered, are then evaluated to give a better understanding of the type of reaction occurring and the transport mechanism involved. Transfer coefficients, exchange current densities and charge transfer investigations involving adsorption of reactant or product are normal areas where IS has been used with success. New areas are also coming to light: direct IS of batteries, electroplating, fuel cells and of solid state systems are revealing such things as 2/3 dimensional crystallisation & growth mechanisms and state of charge. In this work IS was employed to determine whether a membrane was present and, if so, its possible structure.

The IS technique proceeds as follows. A small, alternating voltage v , is applied to the electrodes of a cell which, in turn, are usually held at a required potential (normally the rest potential of the system under consideration, thus limiting the current flow and maintaining reversible conditions). The amplitude of the applied voltage varies sinusoidally with time, t , along with a corresponding current, i . If a sinusoidal wave has a frequency, f , then one has:

$$\begin{aligned}\omega &= 2\pi f \\ v &= V_{\max} \sin \omega t \\ i &= I_{\max} \sin(\omega t - \phi) \\ Z &= \frac{V_{\max}}{I_{\max}} \arg \phi \\ Z &= |Z| \arg \phi\end{aligned}$$

Where: Z is the impedance of the cell,

ϕ is the phase angle between the current and the voltage (figure 8).

It has been found that when a voltage is applied to a capacitor, or inductor, a phase change is noticed in the current. For a capacitor the current leads the voltage by 90° , for an inductor the voltage leads the current by 90° . Argand diagrams have been used to denote real and imaginary impedances (90° out of

phase) in electrical engineering practice and are invaluable in electrochemistry—in the form of "complex plane" (*Sluyter*) plots (section 2.6.2)—where a great deal of information can readily be obtained. By convention capacitive reactance is plotted negatively (in the fourth quadrant), however, this is inconvenient in electrochemistry where reactances are mostly capacitive, it is therefore customary to use the first quadrant (by multiplying the reactance value by -1), this practice is adopted here.

Complex numbers have also been used to represent impedances, using the *j* notation to represent 90° phase shifts, this greatly facilitates the manipulation of equations involving disparate entities:

$$Z = R + jX \quad (41)$$

where: *R* is the resistance,
 X the reactance and
 j is the $\sqrt{-1}$.

2.6.2 The Cell Impedance.

Consider a cell which is made up of the Helmholtz double layer (section 2.1). One can envisage an equivalent electrical circuit would be made up of a capacitance and resistance in parallel⁶⁰, figure 9 (where C_{dl} represents the capacitance of the double layer and *R* the resistance associated with it). This equivalent circuit would give an impedance plot, in the complex plane, like that shown in figure 10^{61,62}.

Warburg^{63,64} was the first to calculate the faradaic impedance of a cell, assuming no double layer capacitance, and combining the model for the double layer capacitance with this model for the faradaic impedance one obtains a working model of the whole electrochemical interface, as proposed by Randles⁶⁵. Randles' model gives a good approximation for fast electrode reactions, in galvanic cells, involving a one step redox reaction—and is shown in figure 11, with a typical impedance plane diagram shown in figure 12.

Simple Double Layer Model

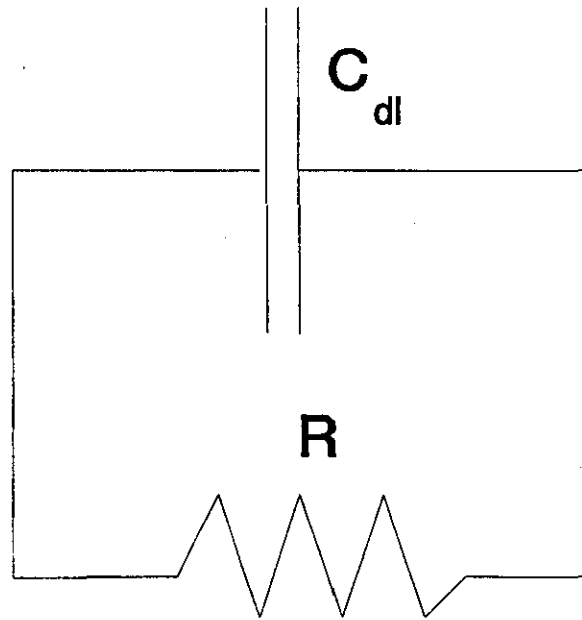


Figure 9

Graph of Reactive Impedance against Resistive Impedance for a Simple Double Layer System.

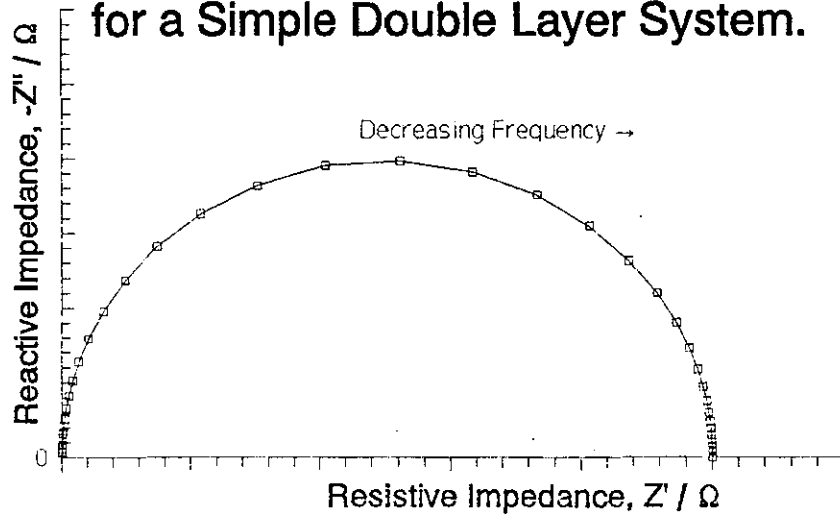
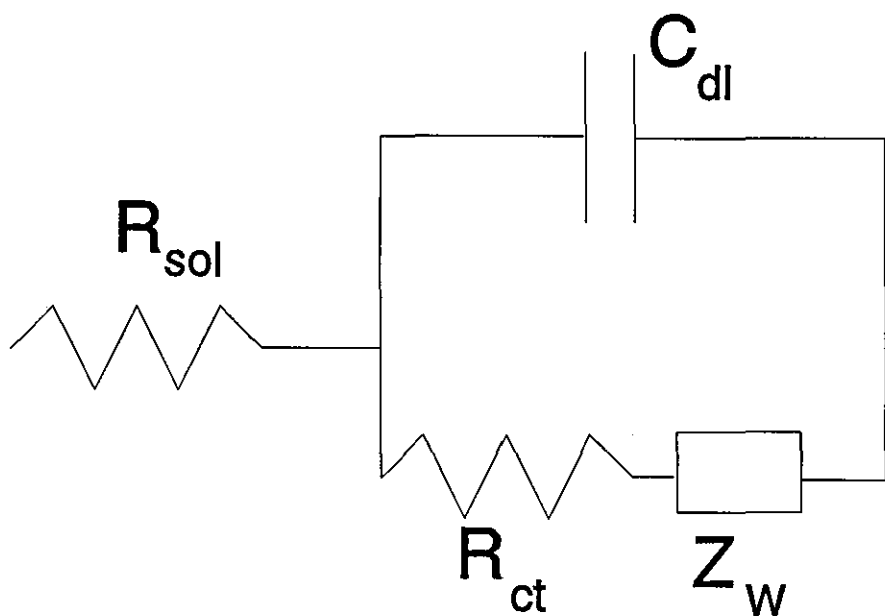


Figure 10



The Simple Randles' Circuit

Figure 11

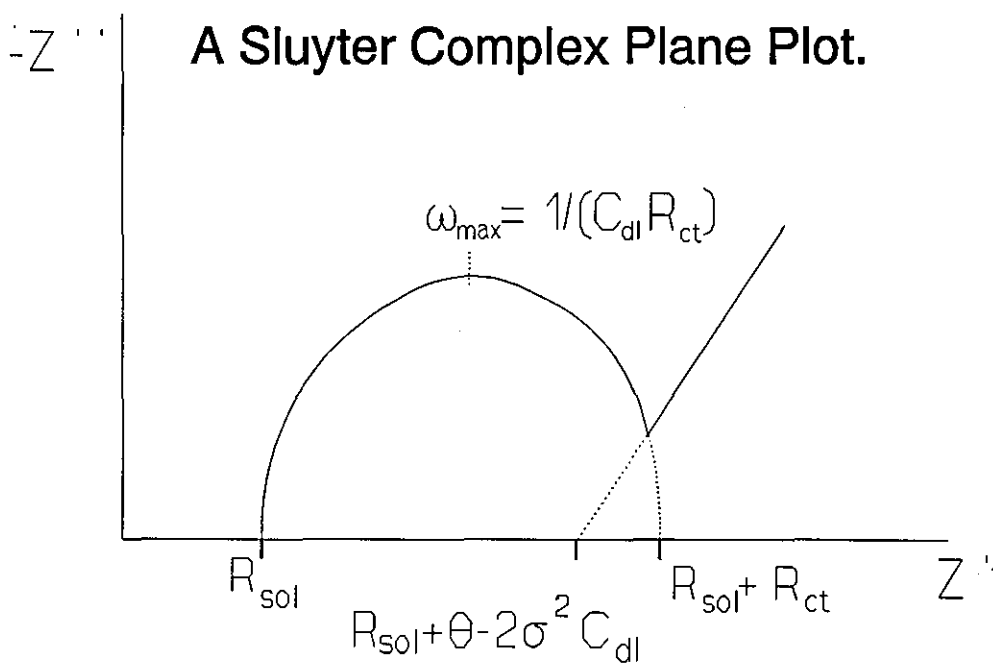


Figure 12

In the Randles' model one also sees the addition of a resistance, R_{s0} , which is added outside the electrode-electrolyte equivalent circuit to account for the solution resistance (and any resistance associated with leads to the electrode). R_{ct} is the charge transfer resistance, this represents the activation polarisation of the electrode reaction, and is also related to the rate of reaction. Z_w is the Warburg impedance, it represents the impedance to a.c. due to charged species diffusing to and from the electrode. Warburg, using Fick's second law of diffusion with appropriate boundary conditions (section 2.3), showed:

$$Z = \sigma\omega^{-1/2} - j\sigma\omega^{-1/2} \quad (42)$$

Where σ is the Warburg coefficient, at equilibrium:-

$$\sigma = \frac{RT}{z^2 F^2 2^{-1/2}} \left(\frac{1}{C_o^b D_o^{-1/2}} + \frac{1}{C_R^b D_R^{-1/2}} \right) \quad (43)$$

and R_{ct} is the charge transfer resistance at equilibrium, which is given by:

$$R_{ct} = \frac{RT}{z^2 F^2 k_o^0 (C_o^b)^{\alpha} (C_R^b)^{1-\alpha}} \quad (44)$$

It is important to note that these equations only hold at equilibrium potentials. Away from this value, equations (43) and (44) must be suitably modified before one can continue to express them in terms of bulk concentrations^{66,67}.

Sluyters¹¹⁶ suggested a method for measuring R_{sol} , C_{dl} , R_{ct} and σ by using a novel method of presentation. In this method, the imaginary component, Z'' , of the total cell impedance is plotted against the real component Z' , as a function frequency*. One has:

$$Z = R_{sol} + \frac{1}{j\omega C_{dl} + \left(\frac{1}{R_{ct} + \sigma\omega^{-1/2} - j\sigma\omega^{-1/2}} \right)} \quad (45)$$

after separation of real and imaginary parts:

$$Z' = \frac{R_{sol} + R_{ct} + \sigma\omega^{-1/2}}{(\sigma\omega^{-1/2}C_{dl} + 1)^2 + \omega^2 C_{dl}^2 (R_{ct} + \sigma\omega^{-1/2})^2} \quad (46)$$

$$Z'' = \frac{\omega C_{dl}(R_{ct} + \sigma\omega^{-1/2}) + \sigma\omega^{-1/2}(\sigma\omega^{-1/2}C_{dl} + 1)}{(\sigma\omega^{-1/2}C_{dl} + 1)^2 + \omega^2 C_{dl}^2 (R_{ct} + \sigma\omega^{-1/2})^2} \quad (47)$$

But, at low frequencies the effects of the double layer capacitance may be neglected and the impedance reduces to Z_w , the Warburg impedance due to diffusion:-

$$Z = R_{sol} + R_{ct} + \sigma\omega^{-1/2} - j(\sigma\omega^{-1/2} + 2\sigma^2 C_{dl}) \quad (48)$$

This is a plot of a straight line, with a 45° slope and an intercept on the Z' axis of R_{sol} , figure 13.

At high frequencies, the concentration polarisation can be neglected and equation (45) reduces to:

$$Z = R_{sol} + \frac{R_{ct}}{1 + \omega^2 C_{dl}^2 R_{ct}^2} - j \frac{\omega C_{dl} R_{ct}}{1 + \omega^2 C_{dl}^2 R_{ct}^2} \quad (49)$$

Which is a plot of a semicircle; R_{ct} and C_{dl} are acting as a parallel resistance and capacitance (cf. figure 10). In a sluyters' plot one usually observes the diffusion limiting case taking over from the high frequency semicircle as the frequency decreases; at low frequencies a "Warburg tail" rises at 45° from the real axis (figure 12).

* As previously noted it is customary to multiply the imaginary impedance by -1, so that a plot in the first quadrant is obtained. This means that a Sluyters plot is normally a plot of $-Z''$ against Z' .

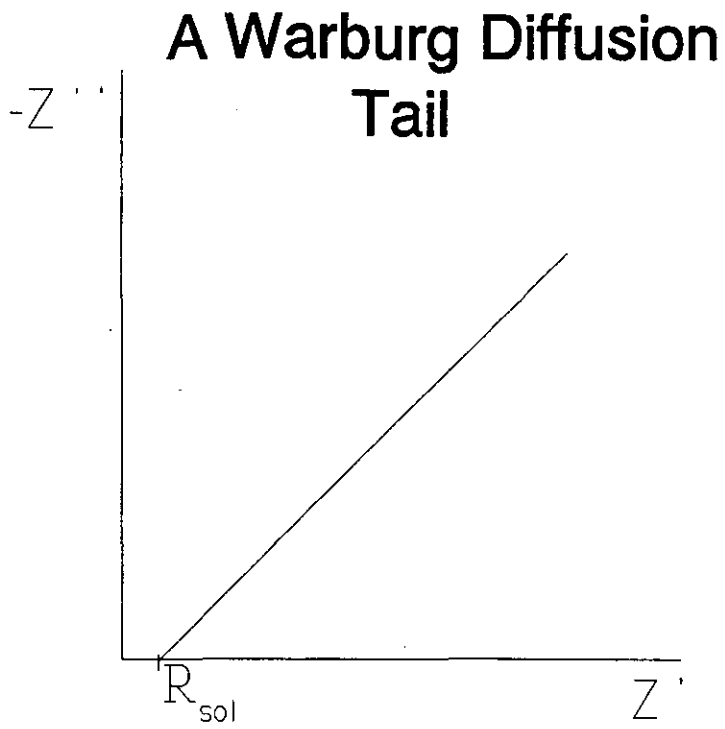


Figure 13

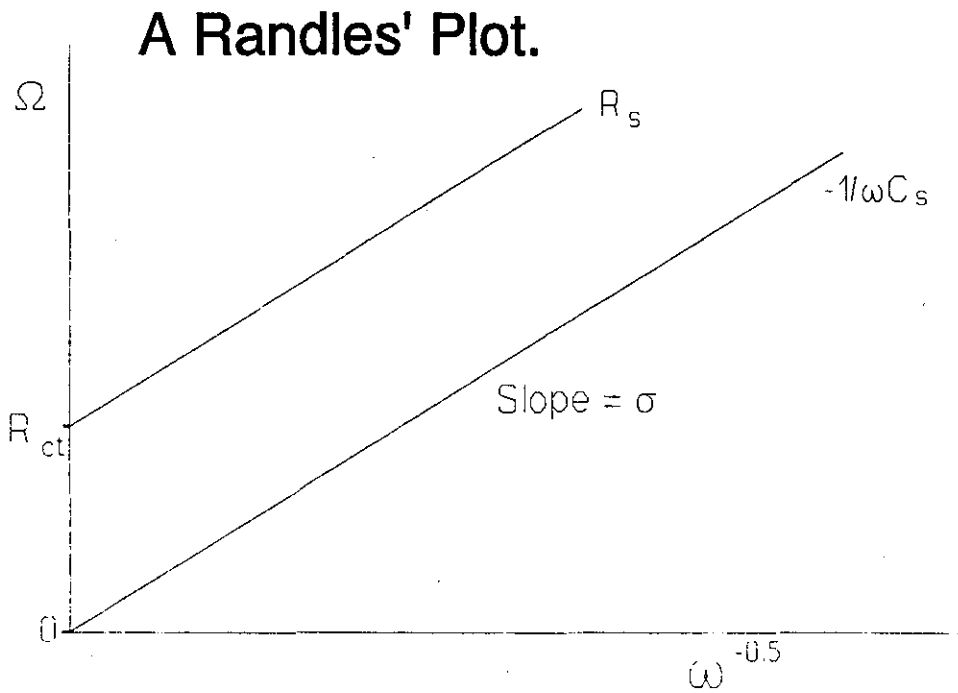


Figure 14

If one considers, as Sluyters did, the special points on the impedance plane plot (figure 12) one can see that it is relatively simple to obtain useful information. R_{tot} and R_{ct} can be read off immediately and if the frequency at the top of the semicircle is known, then:

$$\omega_{\text{max}} = \frac{1}{(R_{\text{ct}} C_{\text{dl}})} \quad (50)$$

and so C_{dl} can be obtained.

Another established method of depicting impedance spectra was described by Randles⁶⁵. Randles, assuming a diffusion controlled, one electron reaction (often at low concentrations of reactants and products) showed that if the real and imaginary components, after the double layer capacitance has been subtracted (i.e. the series resistance R_s and the reactance of the series capacitance C_s), are plotted against $\omega^{-1/2}$. Two parallel lines are obtained, with a slope equivalent to σ and a y-intercept, for the R_s line, of R_{ct} — figure 14.

2.6.3 Practical Considerations.

It is usual in IS to consider *smooth, planar* electrodes at equilibrium*, this simplifies the equations and processes involved and makes an analytical interpretation of the results possible⁶⁶. However *three* important modifications should be mentioned here:

* One consequence of equilibrium conditions is that no net (d.c.) current must flow. If a current does flow the equations above would no longer be valid and other equations involving surface concentrations and rate constants would have to be substituted. This leads to more complex equations and unfortunately to a situation where less data is able to be extracted. Other workers, to overcome the constraint of working at equilibrium conditions, have used the *rotating disc electrode*. This method enables the boundary conditions for Fick's second law of diffusion to be set— and the corresponding impedance equations established.

2.6.3.1 Porous electrodes.

De Levie⁶⁸ reviewed the literature of porous electrodes and presented a theoretical treatment of it. A model, known as the 'Pore Model', was then described. This is a one dimensional model (valid when the distance over which the concentration and potential change is large compared with the dimensions of the pore) where the electrode is represented by an array of parallel cylindrical pores, with a radius perpendicular to the outer surface. The pores are considered to be completely filled with electrolyte and their matrix of negligible resistance (figure 15 shows a model electrical circuit). If Z is the general impedance of the electrical interphase *per* unit pore length then:

$$\begin{aligned} de &= -iRdx, \quad \frac{de}{dx} + iR = 0 \\ di &= -\frac{e}{Z}dx, \quad \frac{di}{dx} + \frac{e}{Z} = 0 \end{aligned} \quad (51)$$

where: x is the distance along the axis of the pore and

e is the voltage at distance x .

Assuming that both R and Z are independent of x (not strictly true in batteries because of concentration polarisation) one obtains:

$$\begin{aligned} \frac{d^2e}{dx^2} - \frac{R}{Z}e &= 0 \\ \frac{d^2i}{dx^2} - \frac{R}{Z}i &= 0 \end{aligned} \quad (52)$$

In the case of a pore of length l :

$$\begin{aligned} \text{at : } x &= 0 \quad e = E \\ \text{and : } x &= l \quad \frac{de}{dx} = 0 \\ \therefore e &= e_0 \frac{\cosh \{(ZR)^{1/2}l - (ZR)^{1/2}l\}}{\cosh \{(ZR)^{1/2}l\}} \end{aligned} \quad (53)$$

The current, i_0 , entering the pore (i.e. at $x=0$) is given by:

$$\begin{aligned} i_0 &= -\frac{1}{R} \left(\frac{de}{dx} \right)_{x=0} \\ &= \frac{(ZR)^{1/2}E}{R} \tanh \{(ZR)^{1/2}l\} \end{aligned} \quad (54)$$

Line transmission for a pore

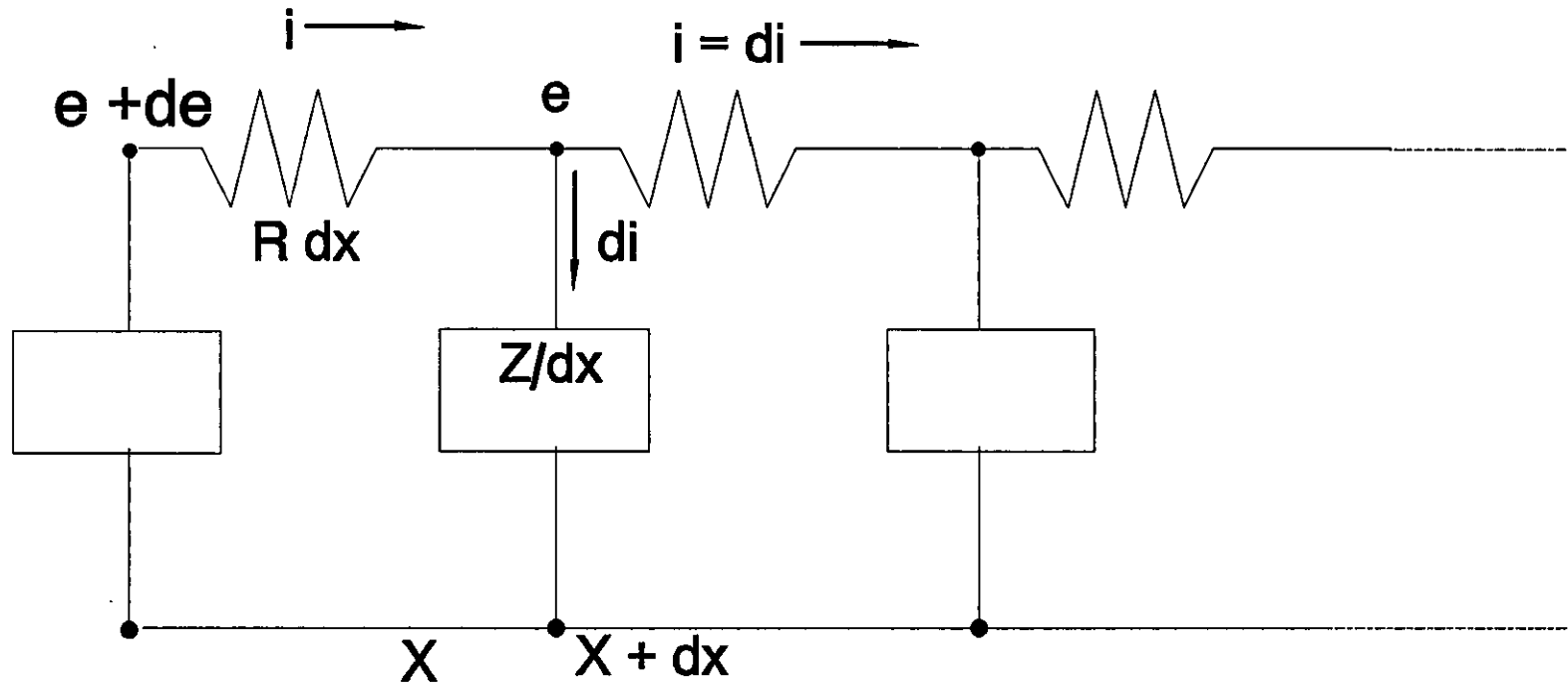


Figure 15

So the pore behaves as an impedance:

$$\begin{aligned} Z_o &= \frac{E}{i_o} \\ &= (RZ)^{1/2} \operatorname{cotanh} \{(ZR)^{1/2}l\} \end{aligned} \quad (55)$$

An important characteristic was defined by De Levie, ρ . This is known as the *penetration depth* and indicates an optimum thickness for a porous electrode. Any electrode which is thinner than this penetration depth tends to behave like a planar electrode, while any electrode thicker is inefficient. ρ is defined as:

$$\rho = \left(\frac{R_o}{R_d} \right)^{1/2} \quad (56)$$

where R_o is the solution resistance per unit length and R_d is the charge transfer resistance of the solution per unit length:

$$\begin{aligned} R_o &= \pi r^2 \kappa \\ R_d &= \frac{RT}{2zF\pi r i_o} \end{aligned} \quad (57)$$

κ is the conductance per unit length.

Further, ρ may also be defined as:

$$\rho = \frac{\sqrt{|Z|R}}{R \cos(\phi/2)} \quad (58)$$

De Levie showed that if l is more than 3ρ then the *cotanh* term in equation (55) may be neglected and the pore will behave like a semi-infinite one:

$$\frac{1}{\rho} = \left(\frac{RT\kappa}{2zFi_o} \right)^{1/2} \quad (59)$$

It can now be seen (equation (58)) that the apparent pore impedance will be equal to \sqrt{ZR} and (since $\sqrt{Z} = r^{1/2} \cos \frac{1}{2}\theta + j r^{1/2} \sin \frac{1}{2}\theta$) it follows that the phase angle of a porous electrode impedance is *half* that of the equivalent flat electrode. Every aspect of a complex plane plot is reduced and a flatter, smaller curve is created when a porous electrode is used. Consider, for example, the case of an ideal, polarised electrode where $Z = -1/j\omega C_{dl}$, in the complex plane a straight line at 45° to the real axis (compared with

90° for a planar electrode) is obtained. Moreover, for a system consisting of a Warburg impedance then a *dihedral angle* of 22.5° to the real axis (compared to a 45° line for planar electrode) is obtained.

Theoretically it has been suggested⁶⁹ that a more suitable method of plotting in the complex plane, for porous electrodes, is to use the *squares* of the imaginary and real impedances. The arc would then give a radius inversely proportional to the reactants' concentration and, if the mean pore radius was known, the charge transfer resistance and rate constants could also be obtained.

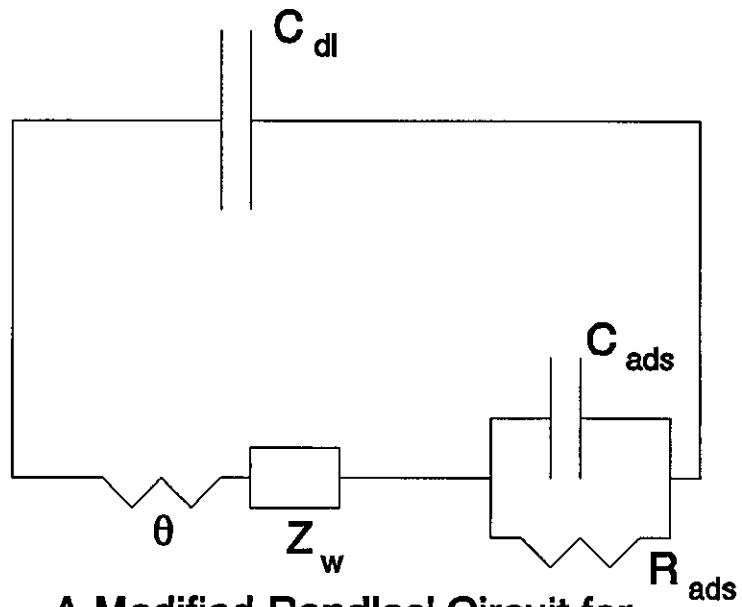
2.6.3.2 Adsorbed Surface.

The Randles' circuit (figure 11) has been extended by Grahame⁷⁰ and Sluyters⁶⁶ to include the effects from surface adsorption. It was shown that while non-electroactive species simply add to the double layer capacitance, adsorption of an electroactive species on to the electrode surface was equivalent to having a further active capacitance in the Faradaic section of the equivalent circuit—the modified equivalent circuit is shown in figure 16⁷¹, and a typical complex plane plot in figure 17.

2.6.3.3 Membrane Effects.

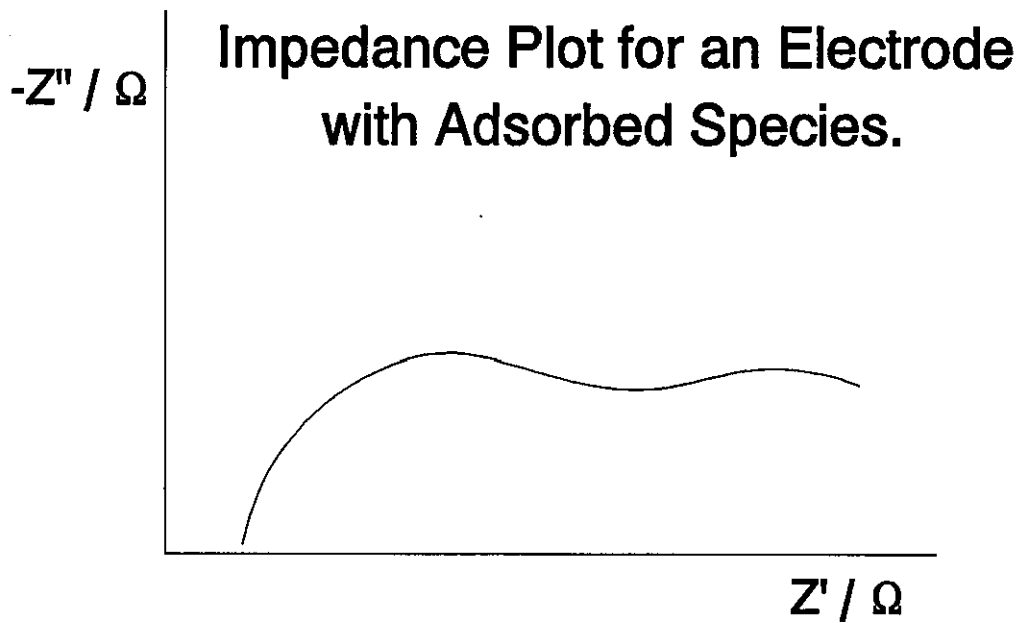
Section 2.6.2 dealt with general impedance plane plots, particularly low concentration (typically 10⁻⁶ to 10⁻¹ mol dm⁻³), aqueous solutions at or near the equilibrium of the system. In these situations the Randles' circuit gives a good approximation of a reaction which is controlled solely by charge and mass transfer processes. However, when a membrane, or film, is placed across the impedance pathway new conditions and boundary equations apply. Furthermore, the form of these equations is also altered depending upon the extent that the *film* interacts with the alternating current. Present day theories, which deal with membranes and films^{72,73}, usually limit their discussion to redox membranes of the type Fe(CN)₆ⁿ⁻, FeCl₃ or polymer films on corrodible metals like iron or copper; workers have yet to investigate membrane properties associated with lead sulphate corrosion films.

Impedance plane plots of membranes or films show a typical Randles' behaviour at high frequencies—where the size of the semi circle is modified by the membrane/film resistance, R_F—and with a Warburg tail which changes to a *capacitive* behaviour at a *transition frequency* (which corresponds to the alternating current, or *concentration wave*, becoming comparable with the membrane/film thickness), figure 18⁷².



A Modified Randles' Circuit for Adsorbed Species.

Figure 16



Impedance Plot for an Electrode with Adsorbed Species.

Figure 17

Impedance Plane for a Membrane Modified Electrode.

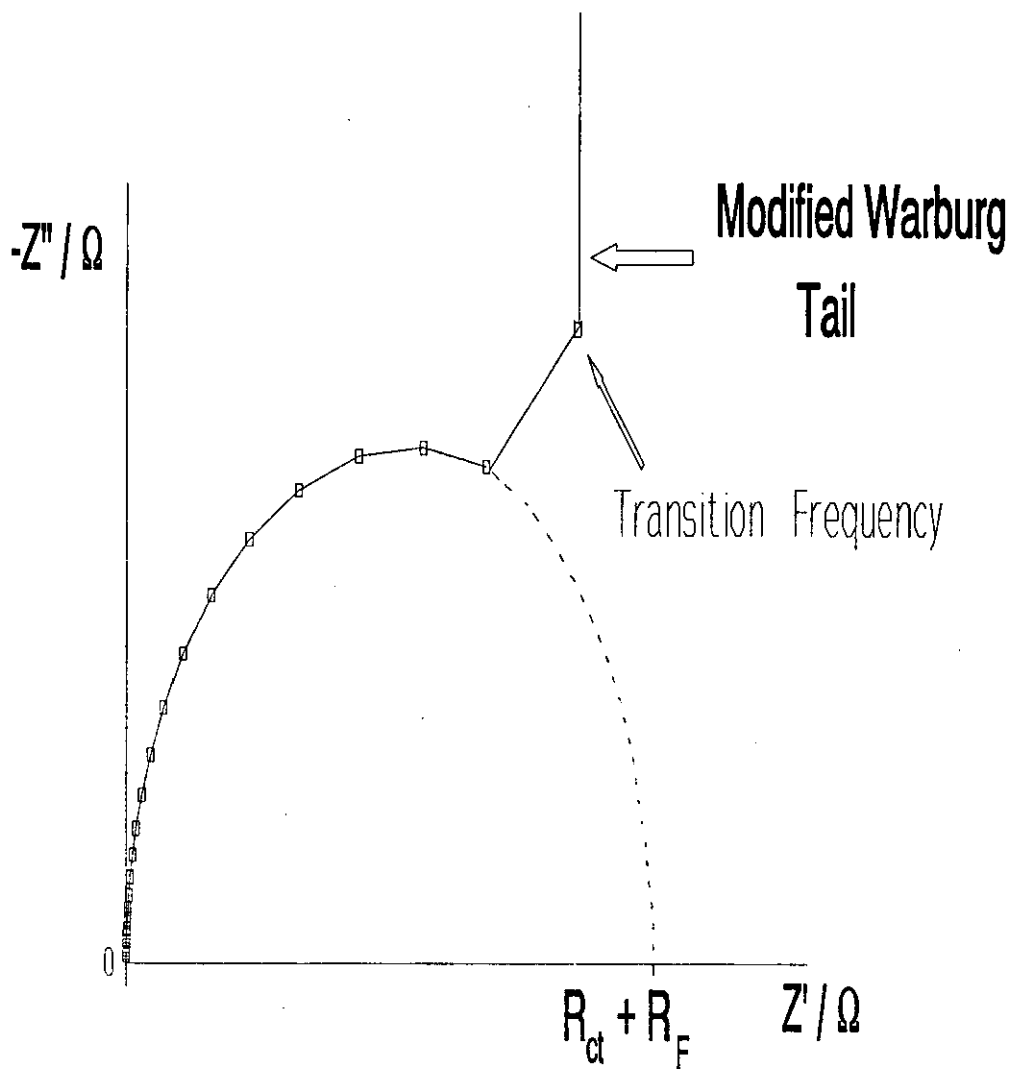


Figure 18

2.7. X-Ray Powder Diffraction (XPD).

2.7.1 Introduction.

The electric fields surrounding atoms interfere with and diffract X-rays. If one considers the case when an X-ray beam hits a simple arrangement of atoms at an angle θ most of the X-rays pass straight through, but a small proportion are *scattered* by the electrons, figure 19. However only in the plane that contains the normal, incident and scattered X-ray beam, will the radiation be *in phase*— and hence produces a diffracted beam. This holds no matter what direction the incident radiation comes from; the X-ray beam actually behaves as if it was being *reflected* from the electron layer (and so are often referred to as reflections). Moreover, as all the crystals in the sample are randomly orientated the diffracted beam actually lies anywhere on a cone of *angle* 2θ . It is usual to refer to the ‘reflections’ in terms of these 2θ values.

If one now considers an X-ray beam striking several layers of atoms, figure 20, each layer will produce a diffraction beam. But only if *all* the diffractions from these layers are in phase will there be a ‘reflection’ at this angle and this will only occur when the distance travelled by the X-rays from the different layers is a whole number of wavelengths. This condition is known as *Braggs Law*:

$$2d \sin \theta = n \lambda \quad (60)$$

where: d is the interplanar spacing,

λ is the wavelength of the X-ray

Monochromatic X-rays are required for Braggs law to hold.

2.7.2 Practical Considerations.

In XPD (unlike single crystal spectroscopy) no three dimensional information can be obtained, as only the interplanar spacing (that is, d values) can be measured. It is therefore impossible to determine an unknown unit cell from this method. The XPD strength lies in its ability to ‘*fingerprint*’ unknown compounds— or different phases of the *same* compound— quickly and reliably. Two ‘problems’ must be overcome when using the technique. These are described below.

2.7.2.1. Preferred Orientation.

It is difficult to ensure that the orientation of the sample’s crystals are completely random when preparing an XPD sample. Alignment of the crystals occur and the intensity in certain directions is enhanced (i.e. *preferred orientation* occurs). This means the XPD pattern is harder to identify, because

Path of an X ray beam through an array of atoms (or electron point charges)

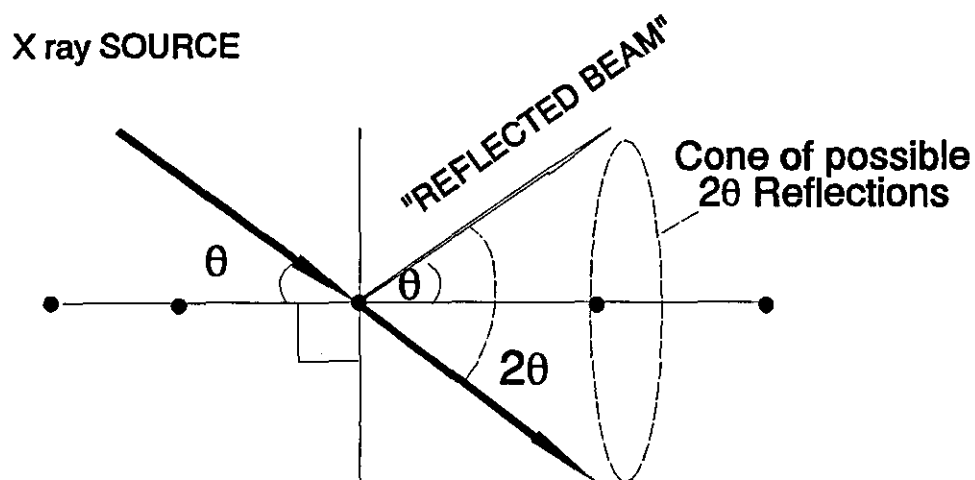


Figure 19

Bragg's Law.

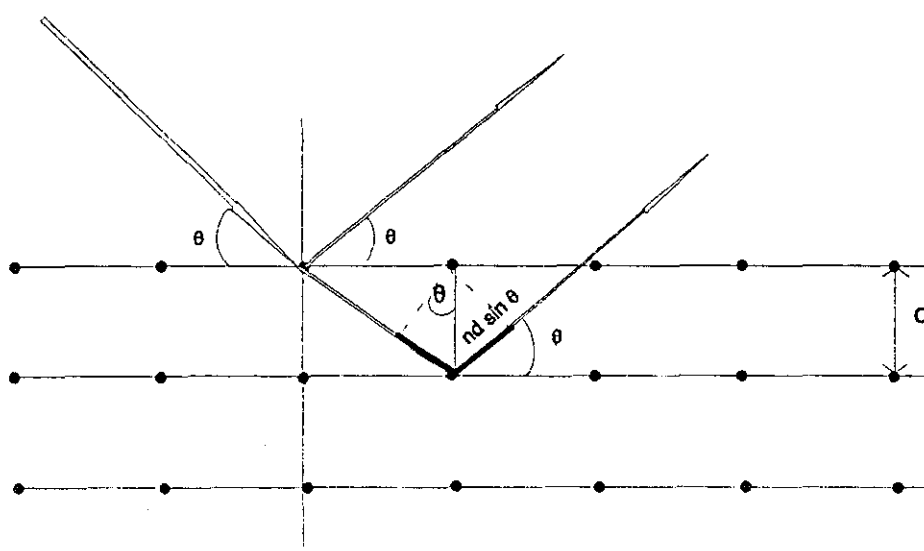


Figure 20

the relative intensities of the peaks do not accurately correspond to the proportions of the unknowns in the sample. Elimination of preferred orientation is difficult, however one of the best methods for achieving this is to mix the material thoroughly (often using a pestle and mortar) and then sprinkle the powder on to a slide coated with petroleum jelly. This results in a random orientation of the crystals in the sample and ensures no preferred orientation occurs, but unfortunately means that the crystals are subjected to great pressure changes while being mixed and so *phase changes* of the crystals can occur.

2.7.2.2. Inaccuracy in Measuring 2θ Values.

Although one of the best methods for eliminating preferred orientation is to use a slide coated with petroleum jelly this method also tends to cause the specimen not to be flush with the surface of the holder, so that it will not be correctly centred and slight inaccuracies in the measured 2θ values occur⁷⁴.

To eliminate this error, an XPD of standard substance— usually silicon— is performed. This has a known diffraction pattern and is used to calibrate the diffractometer.

CHAPTER THREE.

A REVIEW OF THE LITERATURE ON LEAD SULPHATE MEMBRANES IN THE LEAD-ACID BATTERY.

3.1 Introduction.

Although for more than a century the lead-acid battery has been researched, developed, and improved, there are still chemical processes which have not been fully elucidated. As a paper by Julian²⁵ has pointed out, not only are there scientific problems (relating to the chemical role of water, H⁺ and OH⁻ species), but also production-performance problems (relating to shelf life and capacity) still associated with the lead-acid battery. In this chapter just one section of the vast literature on the lead-acid battery, is reviewed.

3.2 Precipitate Impregnated Membranes.

Hirsch-Ayalon first reported that a high membrane potential (224-240 mV) occurred at cellophane and parchment paper membranes with limewater on one side and calcium hydrogencarbonate/ CO₂ solution on the other side⁷⁵. The effect proved more general, and was observed with H₂SO₄// Ba(OH)₂, Ca(OH)₂// H₃PO₄ or (COOH)₂. To explain these effects he introduced the idea of a Donnan equilibrium^{76,77} between the two solutions, due to a precipitation *inside* the partitioning membrane, preventing the passage of precipitating ions, but allowing smaller ions (such as H⁺ and OH⁻) and water to pass freely. A membrane potential of 57.7 mV per pH unit was observed with 0.025 M Ba(OH)₂ and H₂SO₄ solutions. This was subsequently shown to be in agreement with the Donnan equilibrium equation:

$$M.P. = 2.3026 \frac{RT}{F} (pH_1 - pH_2) \quad (61)$$

where: M.P. is the membrane potential

pH₁ and pH₂ signify the pH in solutions 1 and 2 respectively.

In another paper Hirsch-Ayalon⁷⁸ compares the difference between precipitate impregnated membranes and those of the more classical 'semi-permeable membranes', such as copper ferrocyanide (Cu₂Fe(CN)₆), and underlines that the latter membranes are self supporting and so do not require a 'holding' matrix.

Later experiments showed:

a) that concentrations below 0.001 M caused the membrane to become 'deconditioned' (that is, to lose its perm-selectivity)⁷⁹

b) that the addition of further ions to one solution would have a characteristic Donnan-equilibrium-effect on the membrane potential⁸⁰. In later papers, Hirsch-Ayalon changed his term 'Precipitate impregnated membrane' (or simply 'Precipitate Membrane') to the more expressive '*Precipitation membrane*'⁸¹.

Further work on precipitate membranes has been carried out by Honig and Hengst^{82,83,84}. In a paper with Hirsch-Ayalon⁸², they extended the diffusion path, which was only 0.02 cm long in cellophane films, to 4 cm in agar, by the use of a specially designed glass block. This led to considerable broadening of the precipitation zone, but with a potential difference across it similar in magnitude to that of the BaSO₄-cellophane membrane; showing that the precipitation zone had the same characteristics as that of a BaSO₄ precipitate membrane. Using microprobes the potential along the precipitation zone was measured, and it was found to rise steeply over a short distance, near to the precipitation front. A theory of the function of precipitate membranes was given, in which they stated that the cause of the semi-permeability was:

1. a charge of like ions being adsorbed on to the precipitate which subsequently repel similarly charged ions approaching the membrane front, and

2. a change in the solubility product due to the movement of solute from water to cellophane (or agar) medium, which was thought to help decrease the permeability of the membrane towards SO₄²⁻ and Ba²⁺.

In a later paper⁸³ Honig and Hengst used current-voltage (I/V) curves to obtain more information about the mechanism of electrical transport through BaSO₄ membranes. They showed that all I/V curves had a decrease in current with the voltage rise, to the membrane potential, then no current at the membrane potential and finally a small negative current at higher potentials. The positive current was explained by assuming a mechanism of decomposition of water, coupled with ionic mobility across the membrane. When K⁺ or Cl⁻ was added, a different I/V curve was found corresponding to a change in the Donnan potential due to the addition of another non-permeating ion. In a final paper⁸⁴ various mechanisms of flow between two separated solutions were considered. *Electro-migration* (or the movement of ions under an electrical field) was judged to be the major component when the membrane is in the 'conditioned' state.

For a detailed review of the theoretical considerations of transport in artificial membranes a Chemical Review by Lakshminarayanaiah⁸⁵ is admirable. This review also presents information on the manufacture of artificial membranes in 1965.

These papers can be summarised to show four main points associated with the precipitate impregnated membranes:

- 1. A *minimum* concentration (0.001 M for cellulose membranes) must exist on either side of the support membrane before Donnan equilibrium can occur, this is related to the *solubility product* of precipitate in the support membrane.
- 2. The support membrane contains a band of charged precipitate. It is this that repels similarly charged species, thereby causing the semi-permeability.
- 3. The semi-permeable behaviour of the precipitate impregnated membrane, in turn, causes a Donnan equilibrium potential to be established between the two ionic solutions, on either side of the membrane.
- 4. Other ionic species dissolved in one solution will affect the Donnan equilibrium potential due to the further ionic charge carriers being unevenly distributed on one side of the membrane²⁹.

It is interesting to note that it was this last aspect of precipitate membranes which Ruetschi used to characterise a lead sulphate film as a semi-permeable membrane

3.3 Lead Sulphate Membranes in the Lead-Acid Battery.

Ever since the discovery of α -PbO₂, PbO and basic lead sulphates in the positive active mass^{86,87,88}, of the lead-acid battery, any theory of the reactions involved has had to account for these alkaline stable products in an ostensibly acidic environment. While early explanations simply accepted formation of the corrosion products in an acidic media, a paper by Ruetschi and Angstadt³⁰ gave experimental evidence to show that a lead sulphate barrier, or membrane, could exist on the *outside* of the positive active mass. This membrane, Ruetschi stated, was impermeable to H⁺ (H₃O⁺), SO₄²⁻ and water, but permeable to OH⁻ ions. The result was an alkalisation of the interior active mass; accounting not only for the stability of the *alkaline-stable* products, but also for the high corrosion rate which occurs at the positive electrode.

Pavlov *et al.* working on similar lines, discussed an '*alkalizing mechanism*' where compounds such as Pb(OH)₂, PbOH⁺ or PbOH⁻ were formed as intermediates in the production of α -PbO₂ and basic sulphates. Pavlov⁸⁹ correlated the composition of the anodic layer by X-ray Powder Diffraction and analytical determinations. In later experiments⁹⁰ the case of a perm-selective membrane was considered. Small ions, such as H⁺ and OH⁻ were thought to arrive at the metal grid surface, while larger ions, like SO₄²⁻, would be strongly hindered, due to the small pore diameters between the lead sulphate crystals. Pavlov^{91,92} went on to describe how a Donnan equilibrium mechanism^{76,77} would produce an internally alkaline medium, due to the diffusion of OH⁻ species through the semi-permeable membrane, figure 21⁹³.

Lead Electrode Alkalisiation Mechanism

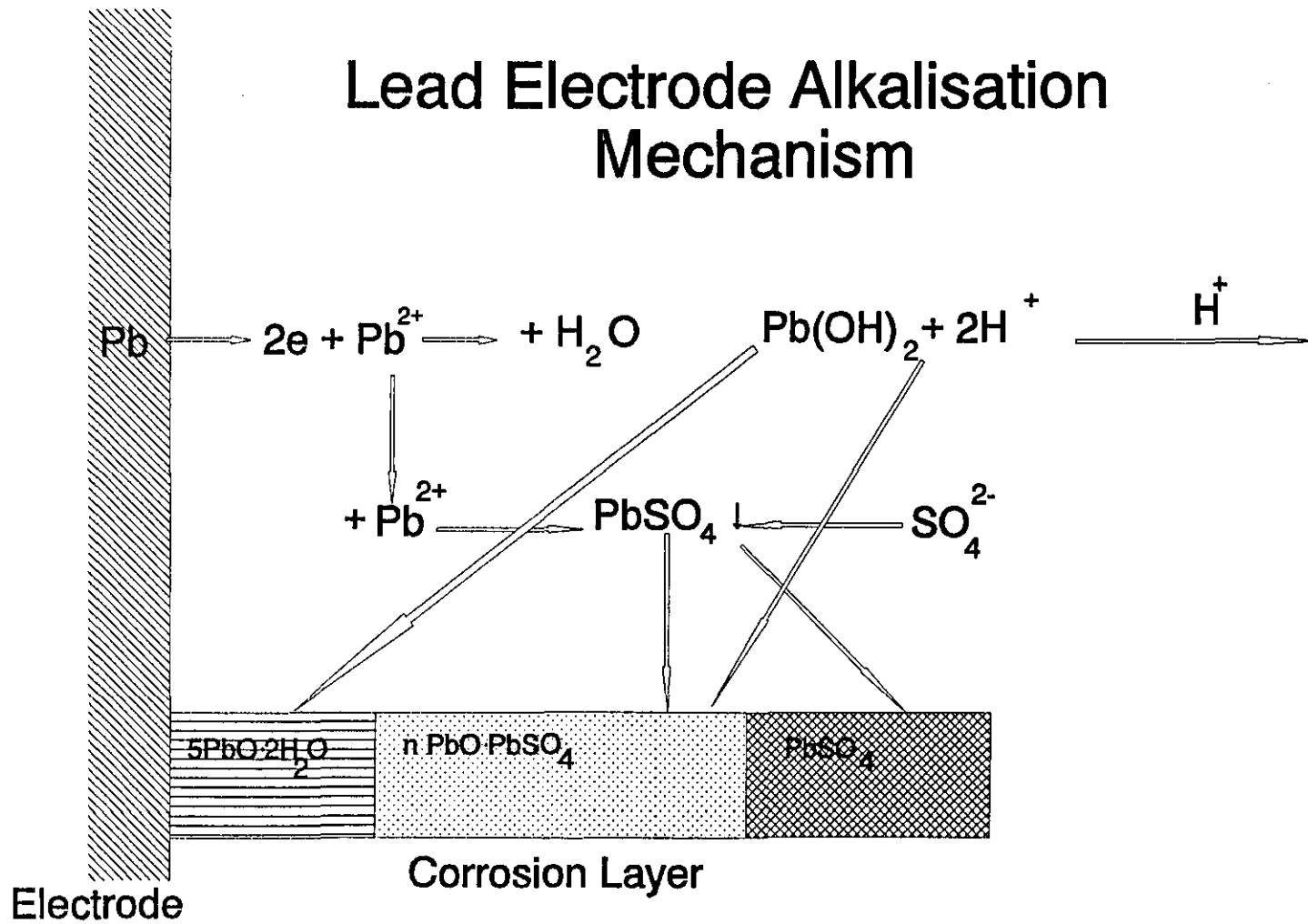


Figure 21

With the new evidence for perm-selective lead sulphate membranes a later paper by Ruetschi²⁹ reconsidered his earlier work³⁰. Using a special cell, a barium sulphate layer, previously precipitated into a cellophane film, was positioned between the two compartments, and the Donnan equilibrium potential, (due to the non-permeability of Ba^{2+} , SO_4^{2-} and HSO_4^- ions and the permeability of H^+ , OH^- and H_2O), measured. The high resistance of precipitate impregnated membranes required the use of a voltmeter with a very high input impedance ($>10 \text{ T}\Omega$). Two reference electrodes were used to measure the potential across the film: $\text{Hg}/\text{Hg}_2\text{SO}_4$ for H_2SO_4 solutions, Hg/HgO (*sat.*) for $\text{Ba}(\text{OH})_2$ solutions and H^+/H_2 when the pH of the solution was varied. A maximum concentration of 0.1 M was invariably used. Ruetschi continued by discussing the use of the perm-selective membrane potentials, within a corrosion layer, and found that by reassigning the plateau potentials between Pb or PbO_2 and PbO , PbSO_4 or basic sulphates it was possible to account for the diffusion potentials in the corrosion layer, Table 2²⁹ (a recent re-evaluation of anodic films at different pH's and potentials, reported by Guo⁹⁴, supports this construction). To do this an assumption about the equilibrium conditions behind the lead sulphate membrane had to be made, either:

i) an equilibrium condition corresponding to the co-existence of PbSO_4 and $\text{PbO}\cdot\text{PbSO}_4$ which gives rise to an internal pH of 6.35, or

ii) an equilibrium corresponding to solubility of PbO , which gives an internal pH of 9.34

was proposed. The latter assumption showed the weakest correlation and has the least support from experimental evidence. By reassigning these plateau potentials, however, Ruetschi was able to show that, by taking into account diffusion potentials, definite electrochemical couples could be demonstrated in the corrosion film of lead. Ruetschi concluded by illustrating the structure of a multi-phase film which can build up on a lead electrode, figure 22²⁹.

The validity of some of Ruetschi's arguments should also be considered. For example the use of such low concentrations to form a *true* membrane has to be questioned, although precipitate impregnated membranes have been conditioned with much lower concentrations^{75,80,95}. Moreover, upon reading the paper one finds no control experiments, no results using lead sulphate membranes (barium sulphate was presented) and no reason why a precipitate impregnated membrane should behave like an actual *amorphous surface* covering of lead sulphate was given— even though answers to these questions are fundamental to believing in a lead sulphate-semi-permeable membrane theory. Further work would, obviously, clarify these points and possibly provide a very convincing argument for a Ruetschi-Pavlov semi-permeable model.

Recent developments have seen improvements in the reaction schemes outlined above^{96,97,98}, however no more work has been carried out on lead sulphate membranes and the foregoing points still remain.

Expt. plateau potential (Vs. Hg/Hg ₂ SO ₄) / V	Electrode Reaction	pH (at potential determining site)	Film diffusion Potential / V	Calculated plateau potential (Vs. Hg/Hg ₂ SO ₄) / V
1.12	PbO ₂ + SO ₄ ²⁻ + 4H ⁺ + 2e ⁻ ↔ PbSO ₄ + 2H ₂ O E=1.685 - 0.1182 pH + 0.0295 log A(SO ₄ ²⁻)	-0.48 (4.2 M H ₂ SO ₄)	0	1.120
0.50	2PbO ₂ + SO ₄ ²⁻ + 6H ⁺ + 4e ⁻ ↔ PbO·PbSO ₄ + 3H ₂ O E=1.422 - 0.0886 pH + 0.0147 log A(SO ₄ ²⁻) 5PbO ₂ + 10H ⁺ + 10e ⁻ ↔ 5PbO·2H ₂ O + 3H ₂ O E=1.070 - 0.0591 pH	6.35* (log A(SO ₄ ²⁻) = -3.9) 9.34**	0.405 0.586	0.588 0.470
-0.38	5PbO·2H ₂ O + 10H ⁺ + 10e ⁻ ↔ 5Pb + 7H ₂ O E=0.260 - 0.0591 pH PbO·PbSO ₄ + 2H ⁺ + 4e ⁻ ↔ 2Pb + SO ₄ ²⁻ + H ₂ O E=-0.099 - 0.0295pH - 0.0148 log A(SO ₄ ²⁻)	9.34** 6.35*	0.586 0.405	-0.332 -0.443
-0.96	PbSO ₄ + 2e ⁻ ↔ Pb + SO ₄ ²⁻ E=-0.356 -0.0295 log A(SO ₄ ²⁻)	-0.48	0	-0.970

Table 2: Electrochemical Couples in the lead Corrosion layer²⁷.

* Equilibrium value for coexistence of PbSO₄ and PbO·PbSO₄

** Equilibrium value for PbO

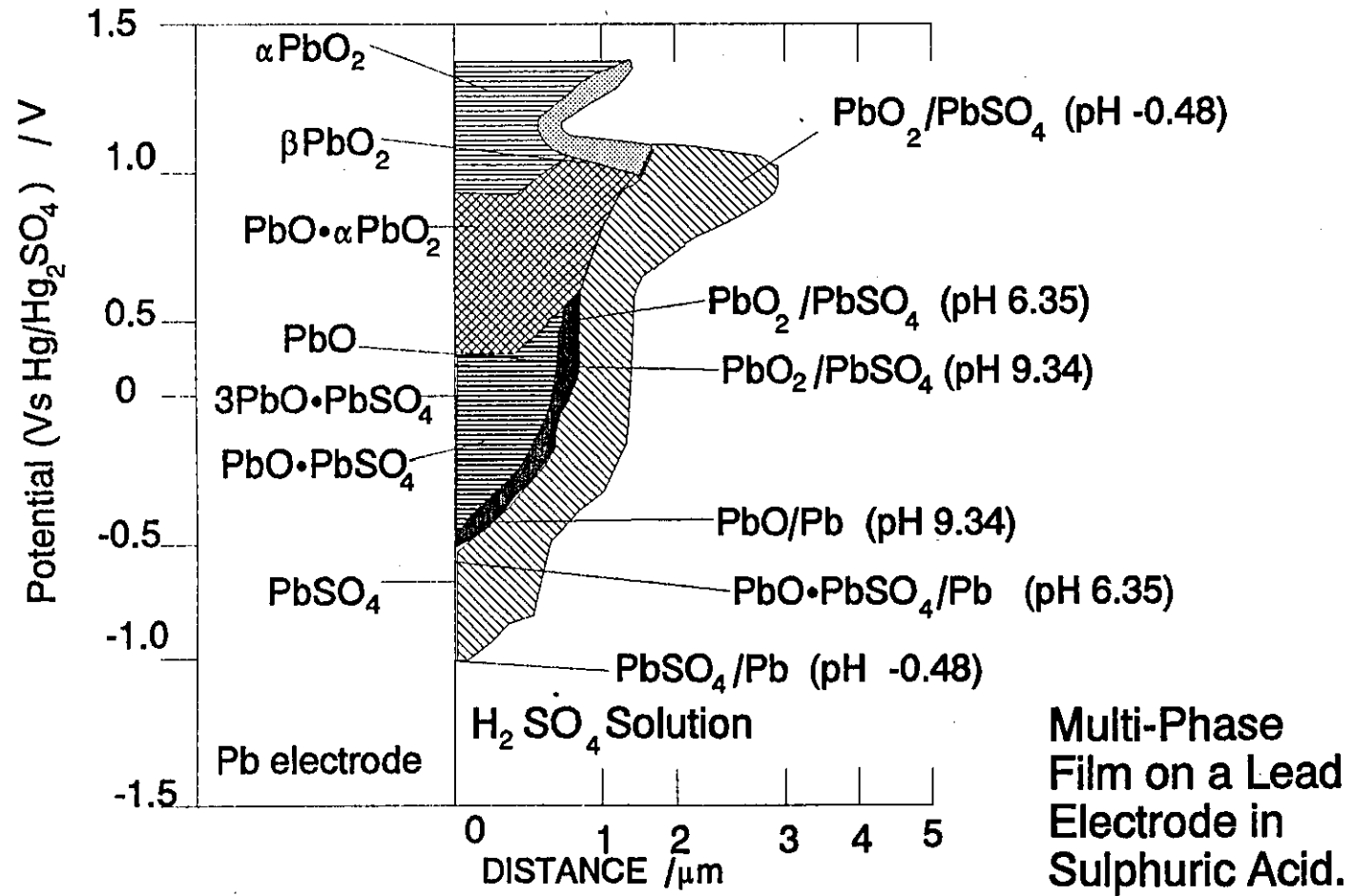


Figure 22

CHAPTER FOUR.

EXPERIMENTAL.

4.1. General.

4.1.1 Materials and Solutions.

1. Sulphuric Acid Solutions.

Sulphuric acid solutions, used in the experiments, were made from 'AnalaR' grade (1.84 SG, 98% H₂SO₄) and triply distilled water (distilled water for non-electrochemical experiments), obtained from stock. The electrolyte used in all electrochemical experiments, apart from plate cycling, was deoxygenated for at least 30 minutes, by the passage of oxygen free nitrogen through the solution, before the start of each experiment. Repeats of any experiment had subsequent deoxygenation for at least 10 minutes.

2. 10% (v/v) Nitric Acid Etch Solution.

A stock solution of 1 mol dm⁻³ was prepared with SLR grade Nitric acid and singly distilled water whenever required.

3. Tetrabutylammonium Tetrafluoroborate, (Bu)₄N⁺BF₄, Support Electrolyte.

This was prepared by the addition of a sodium tetrafluoroborate solution to a tetrabutylammonium sulphate solution. Each solution was heated to 60°C and filtered before mixing. The immediate precipitate (of (Bu)₄N⁺BF₄) was then filtered and washed with water and ether, then dried in an oven (90°C) for 24 hours.

4. PbO₂ Electroplating.

The PbO₂ electroplating solution was prepared by adding 125.54 g Analar PbO slowly to 121 cm³ Analar HClO₄ (62%) in a graduated flask. The mixture was cooled using an ice bath. Once all the PbO had been added the solution was made up to 250 cm³ with distilled water.

The resulting solution of lead perchlorate (2.25 mol dm⁻³) should have been colourless, however it was noticed that on occasion a slight brown suspension was present. This was removed by filtration of the perchlorate solution via a Büchner flask.

5. Lead Oxide ('Grey Oxide') Powder.

The oxide used in this work was commercially made material from *Chloride plc*^{*}, and is a mixture of approximately 40% Pb and 60% PbO, produced in a Ball Mill (chapter 1, page 7). The grey oxide was sent freshly prepared in a *sealed* plastic bag and on arrival was stored in a desiccator until required.

6. Lead Oxide Paste (P10).

The leady oxide paste (P10), from *Chloride plc*, used in this work is commercially prepared leady oxide powder with added sulphuric acid. The leady oxide paste was always sent freshly prepared, wrapped in several plastic bags and on arrival was stored in a desiccator until required.

Tests carried out on P10 showed that the liquor content was approximately 10%.

7. Silica Gel.

In all experiments where a desiccator was used, dried self indicating (SLR grade) silica gel was used as the desiccant.

8. Preparation of Polyvinyl Alcohol (PVA) Solutions.

SLR grade PVA, $[\text{CH}_2\text{CH}(\text{OH})]_n$, (molecular weight: 77000-79000, 98% hydrolysed) pellets were added to a round bottomed flask (RBF) distilled water was then added to make either a 5 or 10 wt% solution when the polymer was fully dissolved. A magnetic follower was added and the mixture refluxed (with magnetic stirring) at 80°C for 6-8 hours and then stored in a sealed, plastic bottle.

9. Preparation of Polyacrylic Acid (PAA) Solution.

A 50 wt% water solution of SLR grade PAA, $[\text{CH}_2\text{CH}(\text{CO}_2\text{H})]_n$, (molecular weight: 5000) was diluted to 5 or 10% (wt/wt) before use as a surfactant (chapter 8, page 64).

^{*} *Chloride Technical*, who actually supplied the materials, are a subsidiary of *Chloride plc* and for simplicity the parent company is referred to in this work.

4.1.2 Cleaning Of Glassware.

All glassware was cleaned with a 50:50 mixture of concentrated nitric and sulphuric acid for at least 48 hours, followed by a thorough wash using distilled water. Finally the glassware was soaked in triply distilled water for 24 hours before use.

4.1.3 The Three Limbed Electrolytic Cell.

The electrolytic cell used in impedance measurements was a standard three limb cell formed from borosilicate glass with ground glass fittings figure 23. In impedance studies the secondary electrode was made very large (with respect to the working electrode), to reduce the capacitance, and so was situated around the working electrode compartment. Contact was made via a small hole situated in the top portion of the cell. As the secondary electrode compartment of the standard three limb cell was not used it was stoppered off. Nitrogen could be bubbled through the working electrode compartment, without the necessity of any dismantling, by using the nitrogen inlet tube. A luggin capillary of 1 mm diameter was used in conjunction with the reference electrode; the tip being located 4 mm from the working electrode (this kept the IR voltage drop to a minimum, by preventing obstruction of the current pathway between the working and secondary electrode).

4.1.4 The Lead Working Electrode.

Pure metallic lead rods (99.999% Pb) were fitted into a shroud of PTFE, which had one end threaded so that it could be screwed into a PTFE holder, figure 24. A stout spring was soldered to the back of the electrode in order to make good electrical contact with a metallic rod, which was used to form the electrical contact with the working electrode. A liquid-tight seal was achieved by the use of PTFE tape around the screw thread and the join between the working electrode and holder. The rods used formed an exposed disc of 3 mm diameter (cross-sectional area = 0.071 cm^2).

The lead discs were polished to a smooth finish using 600 and 1200 grit silicon carbide paper, followed by roughened glass, then washed with distilled water. The electrode was placed into its holder before being etched with 10% nitric acid for 30 seconds (to remove the cold worked surface) and washed with distilled water. The electrode was then placed into the cell and connected to a potentiostat before being immersed in the electrolyte.

Three limb electrode cell.

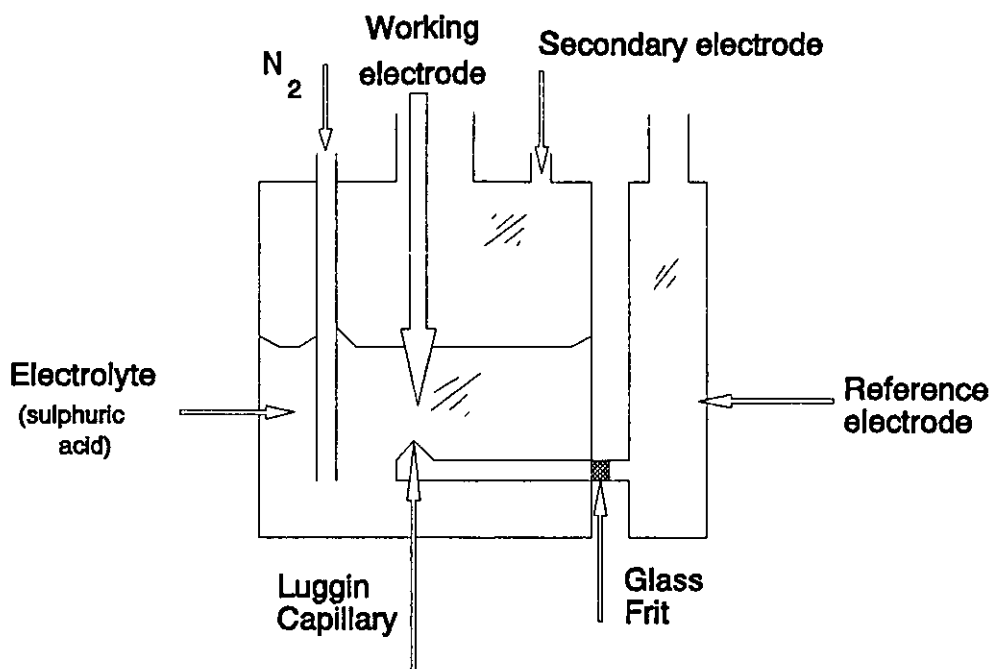


Figure 23

PTFE ELECTRODE

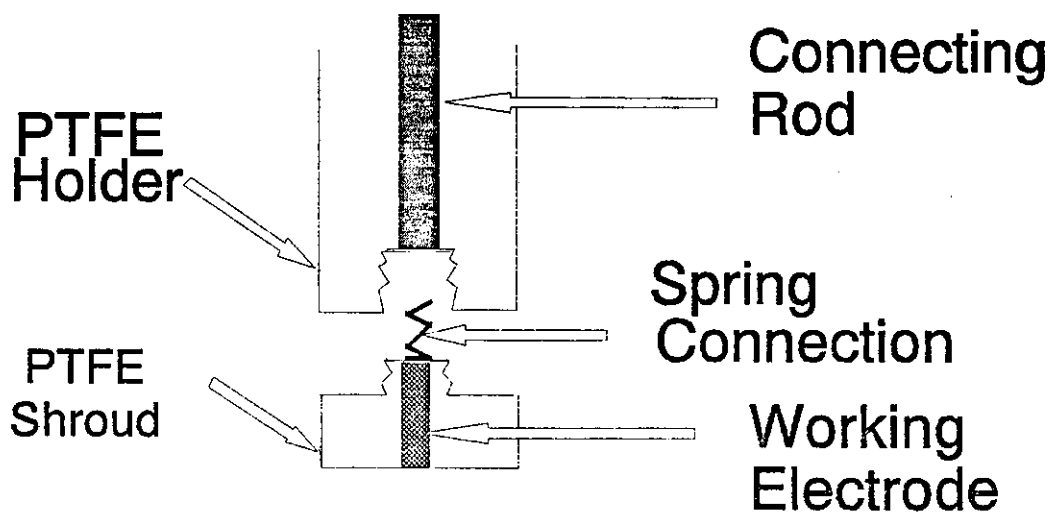


Figure 24

4.1.5 The Lead Dioxide Working Electrode.

A platinum rod working electrode was fitted into a PTFE shroud, in a similar manner to that described for lead (figure 24). The platinum disc (5 mm diameter) was then cleaned with a 1:1:1 solution of glacial acetic acid, hydrogen peroxide (40 vol) and distilled water for 30 seconds, then washed before being placed in a lead perchlorate deposition bath (see above). The bath was heated to 60°C and constantly stirred using a magnetic hotplate stirrer. A current of 1 mA cm⁻² was passed, galvanostatically, using a platinised platinum secondary electrode for 5 hours*. The liquid level of the deposition bath was maintained by the addition of distilled water, as required. A layer of lead dioxide about 0.2 mm thick had then been deposited. The porous PbO₂ layer was then washed with tridistilled water and stored in a sealed plastic bag until required.

4.1.6 Reference Electrodes.

4.1.6.1 The Mercury/ Mercury (I) Sulphate Reference Electrode.

The reference electrode used in all experiments was the mercury(I) sulphate reference electrode: Hg/Hg₂SO₄. The construction, shown in figure 25, involved a platinum 'wick', soldered to a copper wire and encased in a glass sheath. The platinum wick was immersed into a pool of mercury which then had a thin paste of mercury(I) sulphate and sulphuric acid (of an appropriate concentration) poured over it.

The Hg/Hg₂SO₄ couple lies at +0.6158 mV against the standard hydrogen electrode (S.H.E).

4.1.6.2 The Lead Dioxide Reference Electrode.

A 10 cm² sheet of Platinum foil was electrochemically plated with lead dioxide, using the method described in section 4.1.5, except that a forming current of 10 mA cm⁻² for 3.5 hours was employed.

PbO₂/Pb couple lies at +1.685 V against S.H.E.

* It was found that if a current of 10 mA cm⁻² was used (commonly used for the preparation of a lead dioxide reference electrode— section 4.1.6.2) the PbO₂ disc would fall off during impedance work.

Hg/Hg₂SO₄ Reference Electrode

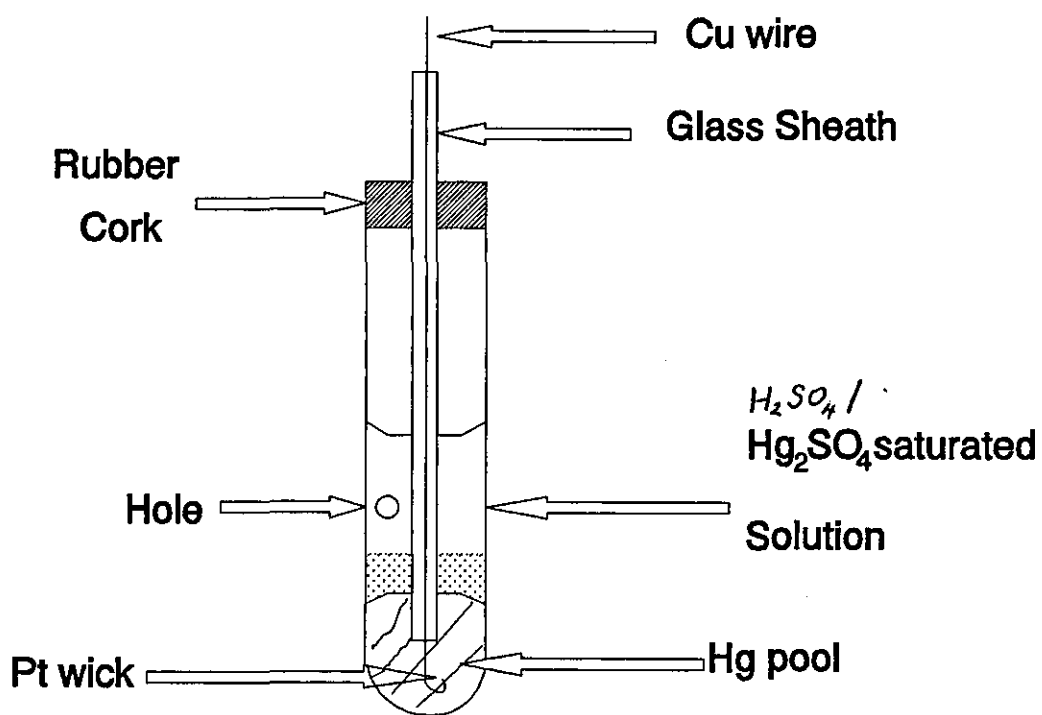


Figure 25

4.2 Electrical Circuits.

4.2.1 Linear Sweep Voltammetry (LSV).

A schematic electrical circuit is shown in figure 26. Potentiostatic control was obtained using a Thompson 'mini' potentiostat in conjunction with a Thompson electrochemical sweep generator. The working electrode (WE), secondary electrode (SE) and reference electrode (RE) were selected separately for each of the following experiment. A potentiostatic sweep rate of 4 mV s^{-1} was applied (using a Thompson ramp generator). The resulting current (observed as a voltage across an appropriate 'sense' resistor in the working electrode lead) was recorded, versus potential, on an X-Y recorder. Remote sensing (RS) was also employed to remove all uncompensated resistances in the working electrode lead.

4.2.1.1. Lead - Lead Sulphate Voltammetry.

The working electrode was a 3 mm diameter lead disc (figure 24) which was prepared as outlined in section 4.1.4. The secondary electrode was a carbon rod and reference electrode a standard $\text{Hg}/\text{Hg}_2\text{SO}_4$ reference electrode. The potentiostat was set at -1200 mV and the lead disc was swept between -1200 to +800 mV. A water bath was used to thermostatically control the electrolyte temperature at 22°C .

4.2.1.2. Lead Dioxide - Lead Sulphate Voltammetry.

An electro-deposited PbO_2 disc on platinum (from Pourbaix diagrams it should be noted that it is *not* thermodynamically possible to form PbO_2 on Pb under acidic conditions⁹⁹) was used— section 4.1.5. The disc was swept between +1200 and +800 mV, otherwise there was no change in the conditions from those mentioned for $\text{Pb} \rightarrow \text{PbSO}_4$ sulphate voltammetry.

4.2.1.3. Voltage Stability of PVA and PAA.

To measure the suitability of PVA and PAA under high voltage conditions (i.e. at hydrogen & oxygen evolution on lead or lead dioxide) a linear sweep voltammogram from -2 to +2 V was performed. This meant a non-aqueous medium had to be used and experiments showed that although dimethylformaldehyde (DMF) and dimethylsulphoxide (DMSO) could be used as solvents, the former (DMF) provided poor resolution and started to break-down too early— giving too narrow a window. DMSO was therefore selected as the solvent. A support electrolyte of tetrabutylammonium tetrafluoroborate (see 4.1.1) was added to increase the conductivity of the DMSO solution. The schematic

LSV Schematic Diagram

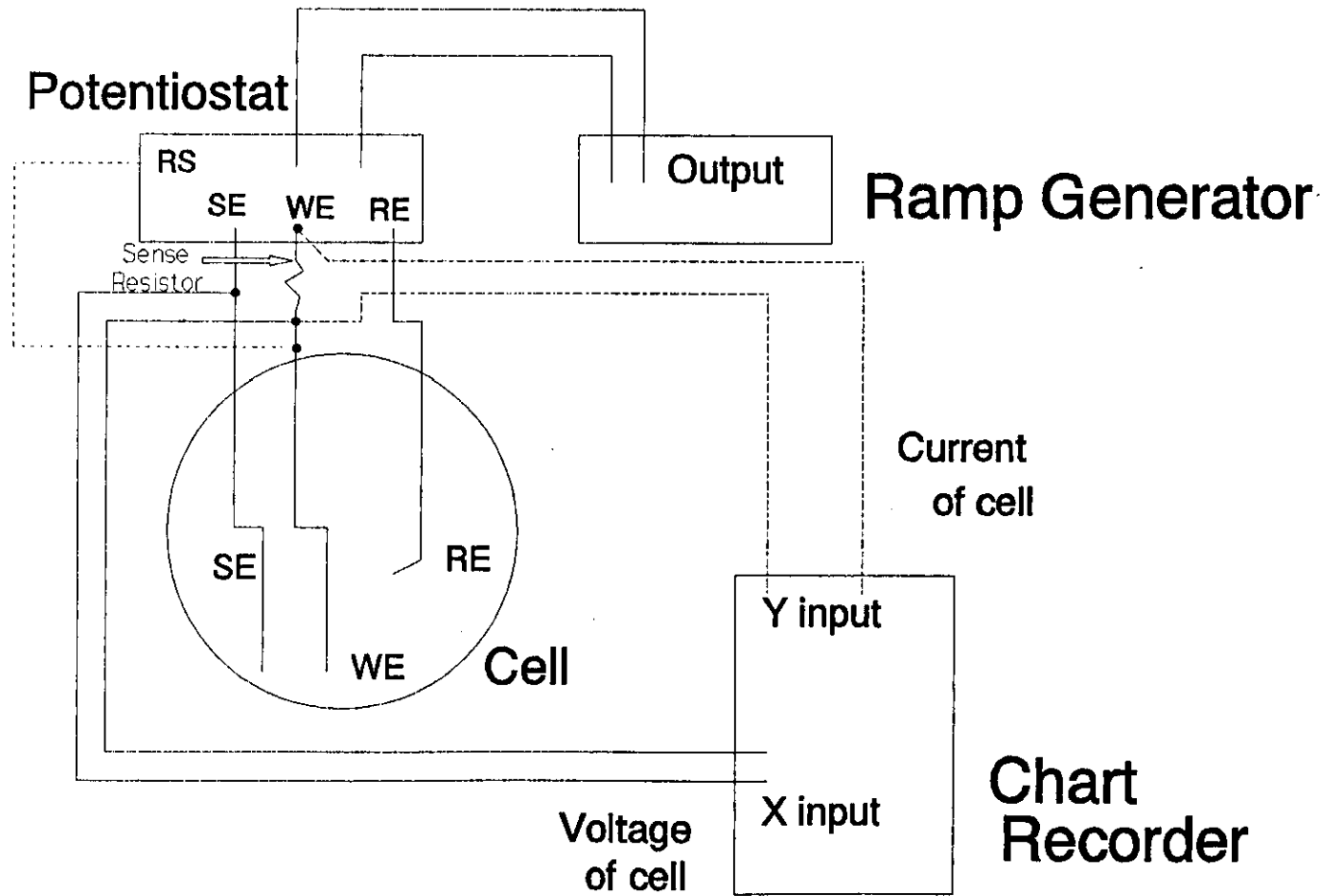


Figure 26

diagram (figure 26) again shows the basic lay out, this time the working electrode was a platinum wire, secondary electrode a carbon rod and the reference electrode mercury-mercury (I) sulphate.

4.2.2 Impedance Measurements.

This is discussed in chapter 6.

4.2.3 Positive Plate Cycling.

This is discussed in chapter 8.

4.3 X-Ray Powder Diffraction (XPD).

A small amount of the sample to be analyzed was ground into a fine powder (so that X-ray scatter was lowered and intensity increased) and mounted on to a microscope slide which had a very thin layer of petroleum grease smeared on to the middle of the slide. The slide was then mounted into a Philips PW 1050 diffractometer set to the required starting angle and the X-ray source switched on. The X-rays were from the $K\alpha$ Cu band having a wavelength of 0.1542 nm. A Hiltonbrookes stepper motor, used to change the diffraction angle, was controlled by an Apple 2e microcomputer. This enabled the step size and integration time at each step to be controlled. The BASIC programme (Appendix 1, page 74), allowed quick, 'low noise' XPD patterns to be obtained in approximately 2.5 hours (all XPD runs were from two-theta values of 6° to 60° with steps of 0.1° and an integration time of 10 seconds) via an 8 bit Analog to Digital Converter (ADC) add-on board. Results were then stored on disc for later analysis (Appendix 2, page 78), or 'file transferred' to a Honeywell DPS8 'Multics' mainframe computer via 'Kermit', for storage.

4.4 Freeze Drying, Gold Sputtering and Scanning Electron Microscopy.

On site liquid nitrogen was used to freeze any sample requiring freeze drying. The sample would then be transferred to a Chemlab SB6 freeze drier, and pumped down to 0.13 Pa, over several hours, before being stored in a desiccator.

If a sample was to be examined under the Scanning Electron Microscopy (SEM) it was first covered in a gold coating to prevent electrostatic build up. This was achieved using a Polaron Ltd E5150 gold sputter with an automatic gold coating attachment. The SEM used was an ISI-SS40.

* Kermit is a file transfer 'protocol' developed at Columbia University.

CHAPTER FIVE.

MEMBRANE STUDIES.

5.1 Introduction.

Ruetschi investigated the properties of perm-selective membranes by precipitating lead sulphate *into* a cellophane support membrane²⁹ and found that a potential difference was set up between the solutions on either side of this membrane.

From a theoretical standpoint he then said that this would account for the difference in potential seen between lead acid battery and theoretical predicted values. However, these experiments were performed with an internally precipitated 'film', at low concentrations— neither of which is comparable with the situation inside a lead acid battery. Moreover, it was also possible that his results could have been due to the cellophane support material, rather than the internally precipitated lead sulphate membrane, as Ruetschi's work did include any control experiments. Similarly, no link between a precipitated impregnated membrane and a true surface covering was established. The experiments presented here endeavour to discover more about lead sulphate membranes.

5.2 Experimental Techniques.

A series of experiments, to form sulphate membranes, were undertaken, and for clarity these are outlined separately.

5.2.1. Leady Oxide discs.

Leady oxide powder (60% PbO, 40% Pb) from *Chloride plc* was pressed into discs using a KBr press at 10 tons per square inch for 30 minutes. The discs were then reacted with sulphuric acid in the following ways:

- i) Placed in 1-18 mol dm⁻³ sulphuric acid for 30 minutes, at ambient temperature (20°C).
- ii) Placed in 10 mol dm⁻³ sulphuric acid* and the reaction times varied from 5 minutes to 24 hours, at ambient temperature (20°C).
- iii) Placed in 10 mol dm⁻³ sulphuric acid, for half an hour, and the temperature varied, by the use of a thermostatically controlled water bath, from 25 to 75°C.

* The concentration of 10 mol dm⁻³ for sulphuric acid was chosen in later work because earlier experiments indicated that this was the most likely concentration to form an amorphous sulphate layer.

After the reaction in the sulphuric acid the discs were removed with the aid of a pair of tweezers and washed with either:

- i) distilled water, or
- ii) industrial alcohol (98% ethanol)*

for 30 seconds before immersing in liquid nitrogen and freeze dried. A portion of the disc was then cut, using a scalpel and mounted for examination under the SEM.

5.2.2. Metallic lead discs.

Pure metallic lead rods (99.999% Pb) were fitted into a sheath of PTFE, figure 24. The exposed end of the lead rod (a disc) was then polished to a smooth finish using 600 and 1200 grit silicon carbide paper, followed by alumina (grade 100-200 mesh) and roughened glass. The lead discs were etched in 10% nitric acid for 30 seconds and then washed with distilled water.

One of The following methods was used to form a film of lead sulphate on the lead discs:

- i) The lead discs were immersed in 7 mol dm⁻³ sulphuric acid for 30 minutes, at ambient temperature (20°C).
- ii) The discs were left for approximately 17 hours in a warm oven (85°C), before being immersed in 7 mol dm⁻³ sulphuric acid for 30 minutes (this was to enable a lead oxide layer to form over the polished lead).

5.2.3 Lead sulphate membrane formation on various support materials.

A number of support materials were examined—and used to either to recreate Ruetschi's original experimental conditions²⁹, or to attempt to *create* a homogeneous *surface layer* of lead sulphate crystals.

5.2.4. Dialysis Tubing as the Support Material.

In experiments similar to Ruetschi's (chapter 3, page 40), dry dialysis tubing ("Visking tubing"—a regenerated cellulose strip with a pore size of 2.4 nm), was used as a matrix for lead sulphate precipitation. Various concentrations of analar lead nitrate solution and analar sulphuric acid were used on either side of the dialysis tubing, which was firstly conditioned—i.e. wetted—before use. This was

* Because of osmotic pressure build-up with water, ethanol was employed to prevent any possible membrane rupture.

achieved in a variety of ways:

- i) Conditioned in distilled water for 24 hours,
- ii) Conditioned in the Pb^{2+} membrane forming solution for 12-24 hours,
- iii) Conditioned in the SO_4^{2-} membrane forming solution for 12-24 hours.

After this conditioning period, the dialysis tubing was sealed at one end, filled with either the acid or lead solution, and sealed at the other end. It was then placed in a conical flask containing the other solution (lead or acid, respectively) and covered with plastic film to prevent evaporation.

The dialysis tubing was left for various lengths of time, ranging from a few hours up to one month. Once the conditioning process was complete one end of the tubing was cut and the internal solution drained out. A section was then removed, using dissecting scissors, immediately immersed in liquid nitrogen and freeze dried ready for examination under the Scanning Electron Microscope (SEM).

5.2.5. PTFE-membrane filters as the support material.

The high resistance to attack by sulphuric acid, which Polytetrafluoroethylene (PTFE) possesses made this material worthy of consideration as a replacement for the dialysis tubing as the support medium. The apparatus for this experiment is shown in figure 27. A high molarity of sulphuric acid (7 mol dm^{-3})* and lead nitrate solution (1 mol dm^{-3}) was employed so that a high rate of nucleation would occur and, therefore, a low crystal growth rate. Circular PTFE membrane filters used were from Sartorius (type SM 11807), having a diameter of 13 mm and a pore size of $0.2 \mu\text{m}$. The membrane, once assembled in the apparatus, was left for times ranging between 24 and 60 hours. After this time, the PTFE filter was immersed in liquid nitrogen and freeze dried. A SEM study was then performed.

Glass microfibre, Celgard (a popular battery separator made from polypropylene and cellulose) and Porvic 1 (a non-sintered PVC battery separator) and 2 (a sintered, unplasticised PVC battery separator) were used as replacements for PTFE in the experiments above.

* $7 \text{ mol dm}^{-3} \text{H}_2\text{SO}_4$ was chosen because previous experiments had shown that this was the point at which the onset of *micro* PbSO_4 crystals occurred— that is where a lead sulphate membrane might develop due to a large array of crystal sites forming.

Membrane forming unit

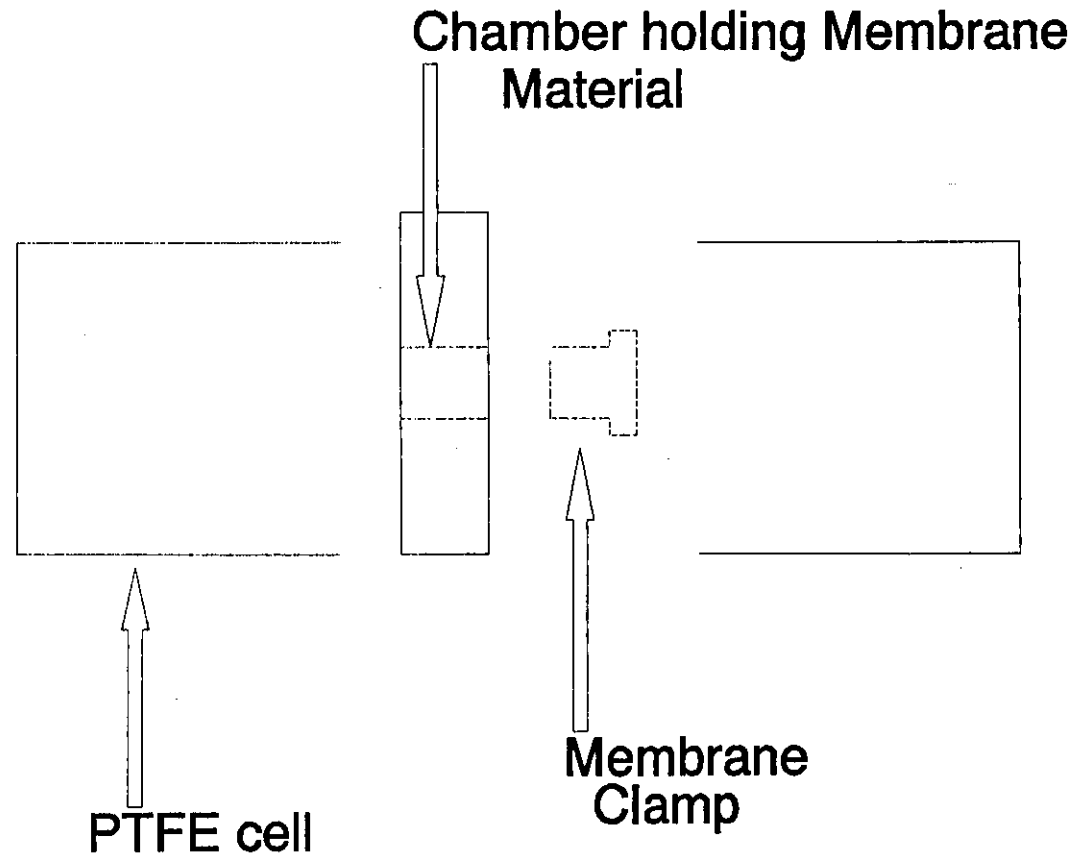


Figure 27

5.2.6 Production of Lead Sulphate Membranes by forming Lead Amalgamation.

A lead sheet (99.99% Pb) was placed in 10 mol dm⁻³ H₂SO₄, for eight hours, in such a way as to immerse only *one* side. After which time the lead sheet was removed, washed with industrial alcohol and dried in air for 5 minutes. The reacted side was then covered with sellotape^{*} to support the lead sulphate film. The lead was then removed by amalgamation—— by placing the unreacted side of the lead sheet into a dish of mercury and stirring the mercury with a magnetic follower^{**}.

5.2.7 Electrochemical Techniques.

The Cell Impedance Measurement System is outlined in Chapter 6, page 55. This method was used to investigate the presence of lead sulphate membranes in the system Pb/PbSO₄/H₂SO₄ using a lead rod (99.999% Pb) fitted into a PTFE shroud to form a 3 mm diameter lead disc (figure 24) and immersed into sulphuric acid.

5.3 Results and Discussion.

5.3.1 Visking Tubing as the support membrane.

When using sulphuric acid or lead nitrate solutions of 0.001, 0.01 and 0.1 mol dm⁻³, the SEM revealed that crystals were precipitating *inside* the dialysis tubing (photo.'s^{***} 1 & 2)—— no uniform surface film ever being produced. This precipitation could be seen almost immediately the dialysis tubing was placed into the acid or lead solution, by the translucent cellulose membrane clouding and becoming opaque. The clouding was reduced when using concentrations of about 0.001 mol dm⁻³.

* Later experiments were going to use polymethyl methacrylate as the support matrix.

** After the lead had amalgamated it was intended to remove the lead sulphate layer from the sellotape with the aid of acetone, then place the lead sulphate film between two cellophane films and measure the diffusion of ions across two different solutions. However, although several attempts were made, it finally proved to be an impossible task to separate the lead sulphate film.

*** SEM photographs show magnification (per thousands) as the first number on the bottom, left hand side.

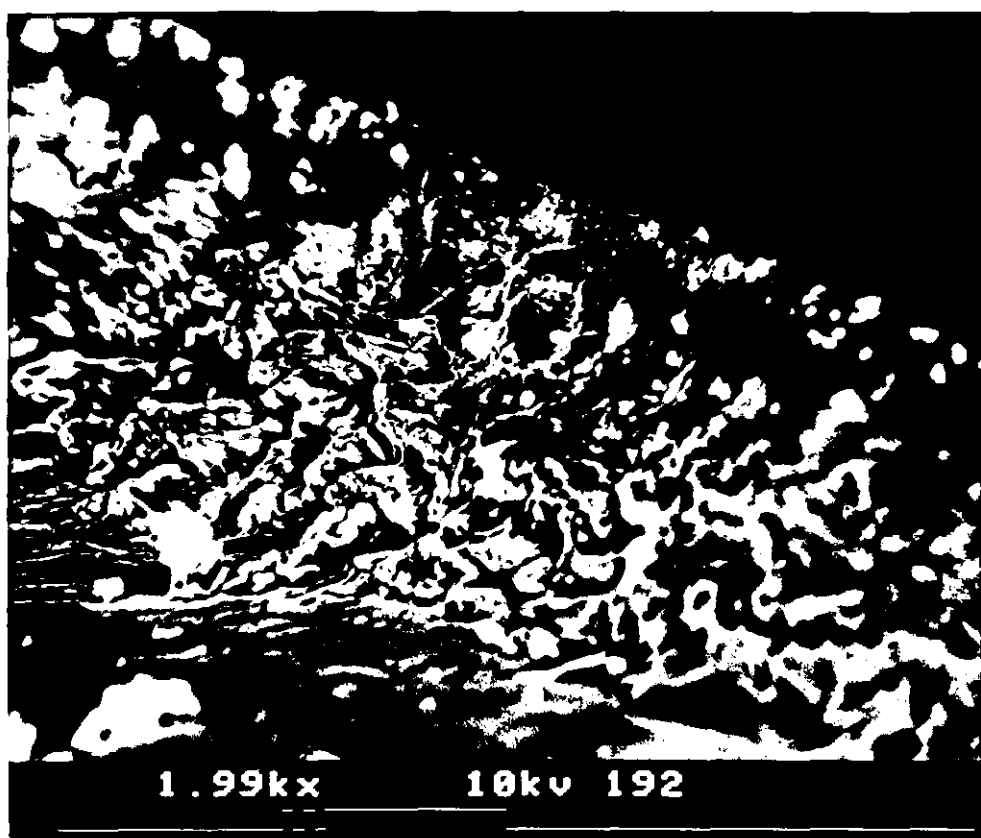
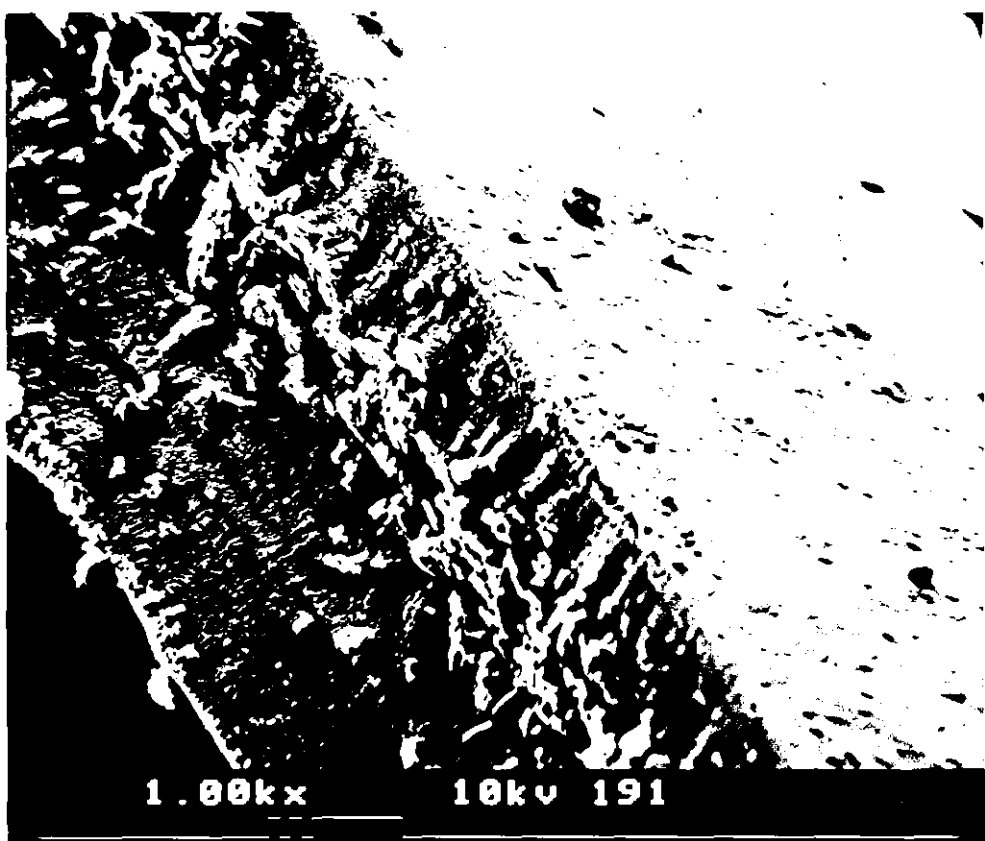
SEM picture of internal precipitation in visking tubing [using H_2SO_4 (0.1 mol dm^{-3}) and $\text{Pb}(\text{NO}_3)_2$ (0.1 mol dm^{-3}) solution for 24 hours at ambient temperature (20°C)].

PHOTO. 1:

—Magnification x 1,000

PHOTO. 2:

—Magnification x 1,990



Conditioning of the cellulose membrane by either—

i) immersing the dry dialysis tubing in the corresponding acid, or lead, solution before commencing the experiment, or

ii) allowing a 'start-up' period, where a solution was left inside the support membrane which was subsequently suspended in a flask of distilled water, or

iii) performing both i) and ii)—

before immersion into the respective flask of acid, or lead, solution did not alter the result (i.e. no uniform lead sulphate film was ever achieved). The SEM showed only some large crystals (40 μm) on the surface of the membrane (photo.'s 3 & 4).

When the molarity of acid and lead solutions were increased to 1 mol dm⁻³, the cellulose tubing turned brown and often became brittle. The scanning electron micrograph of this material revealed that an amorphous layer was *starting* to form on the surface (photo.'s 5 & 6), presumably due to the higher concentrations of lead and acid solutions used.

These experiments are similar, in many ways, to Hirsch-Ayalon's earlier work in this field⁷⁵, in which he precipitated barium sulphate *into* a cellulose membrane, he called this type of membrane a "*precipitate impregnated membrane*". Hirsch-Ayalon also found that a concentration of at least 0.001 M of Ba²⁺ and SO₄²⁻ ions was required to 'condition' the membrane, i.e. a Donnan equilibrium potential^{76,77} did not occur when the concentrations of Ba²⁺ and SO₄²⁻ were lowered below 0.001 M. The reduced opaqueness, when using concentrations 0.001 mol dm⁻³, in the above experiments, can now be seen as due to a near 'de-conditioning', or low internal precipitation, in the membrane.

5.3.2 Other Support Membranes.

The PTFE membrane filters allowed the movement of liquid from the least concentrated lead nitrate solution (1 mol dm⁻³) to the more concentrated sulphuric acid solution (7 mol dm⁻³). This movement was slow and although a precipitate was produced, there was no lead sulphate surface film. The well known "non-stick" nature of PTFE probably caused a collapse of any surface film during its removal. The scanning electron micrographs, however, have not revealed any internally precipitated lead sulphate.

With glass-microfibre the scanning electron micrographs, showed that although crystals had formed no amorphous structures were produced. Celgard, Porvic 1 and 2, on the other hand, had only a few discernable lead sulphate crystals on the surface.

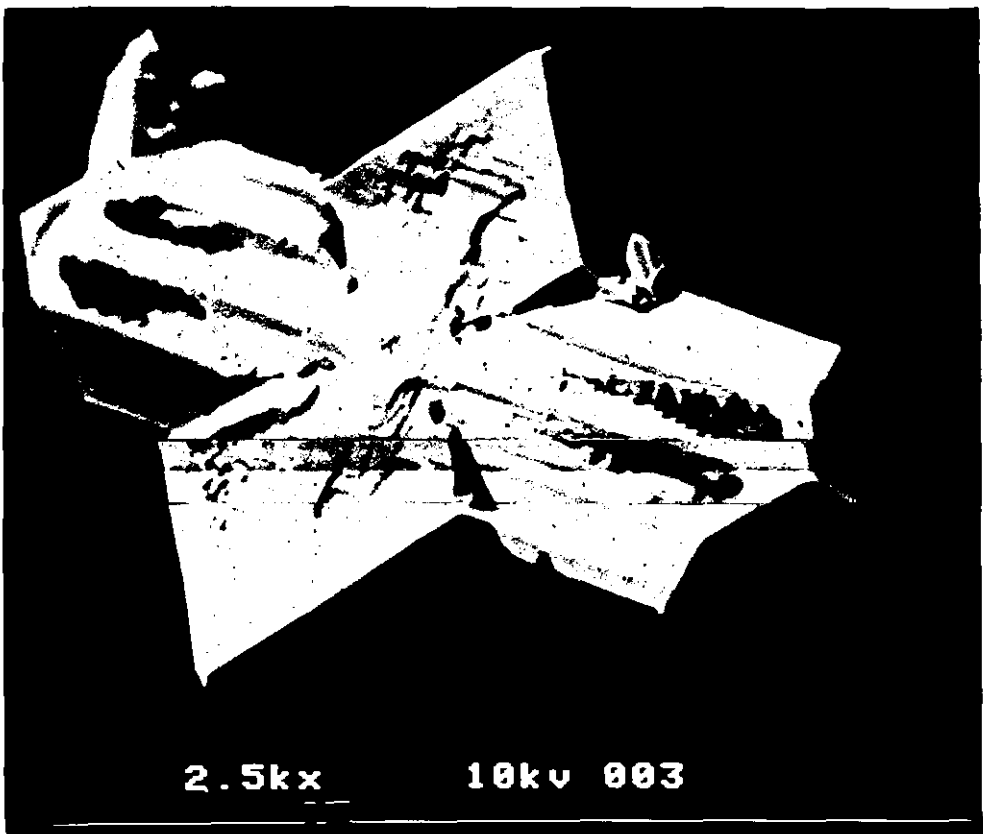
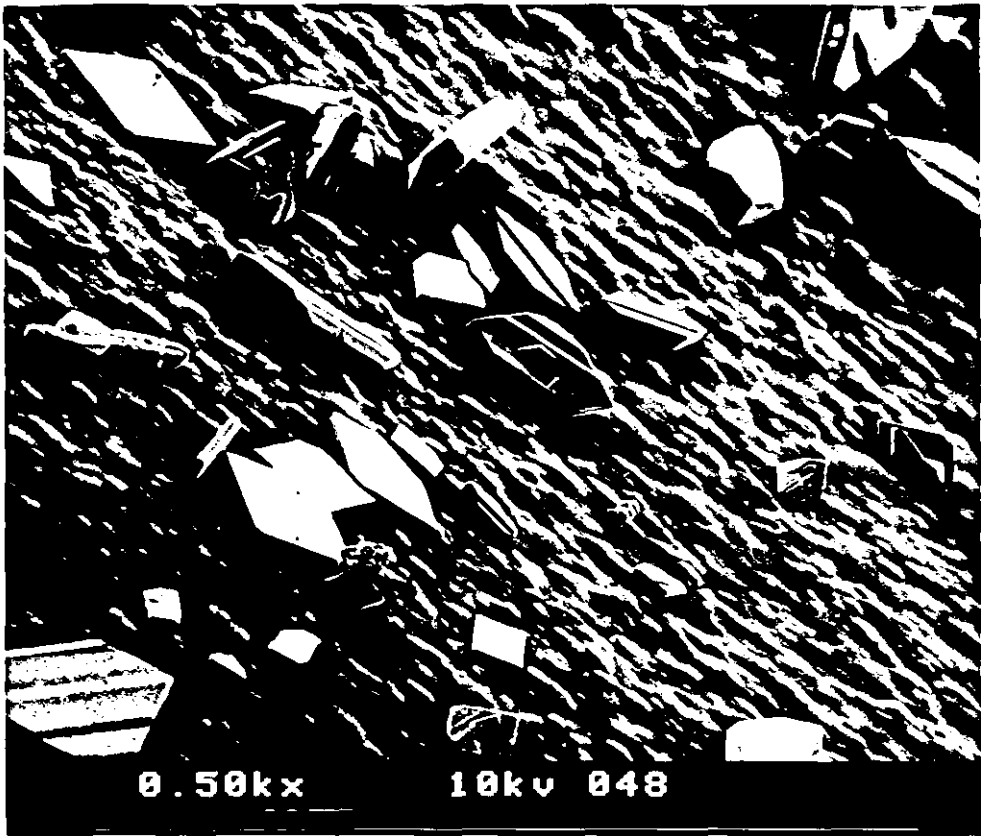
SEM picture showing large crystal formations on 'conditioned' membrane [using H_2SO_4 (0.1 mol dm^{-3}) and $Pb(NO_3)_2$ (0.1 mol dm^{-3}) solution for 24 hours at ambient temperature (20°C)].

PHOTO. 3:

—Visking tubing conditioned in H_2SO_4 (0.1 mol dm^{-3}) solution for 24 hours.

PHOTO. 4:

—Visking Tubing conditioned in $Pb(NO_3)_2$ (0.1 mol dm^{-3}) solution for 24 hours.



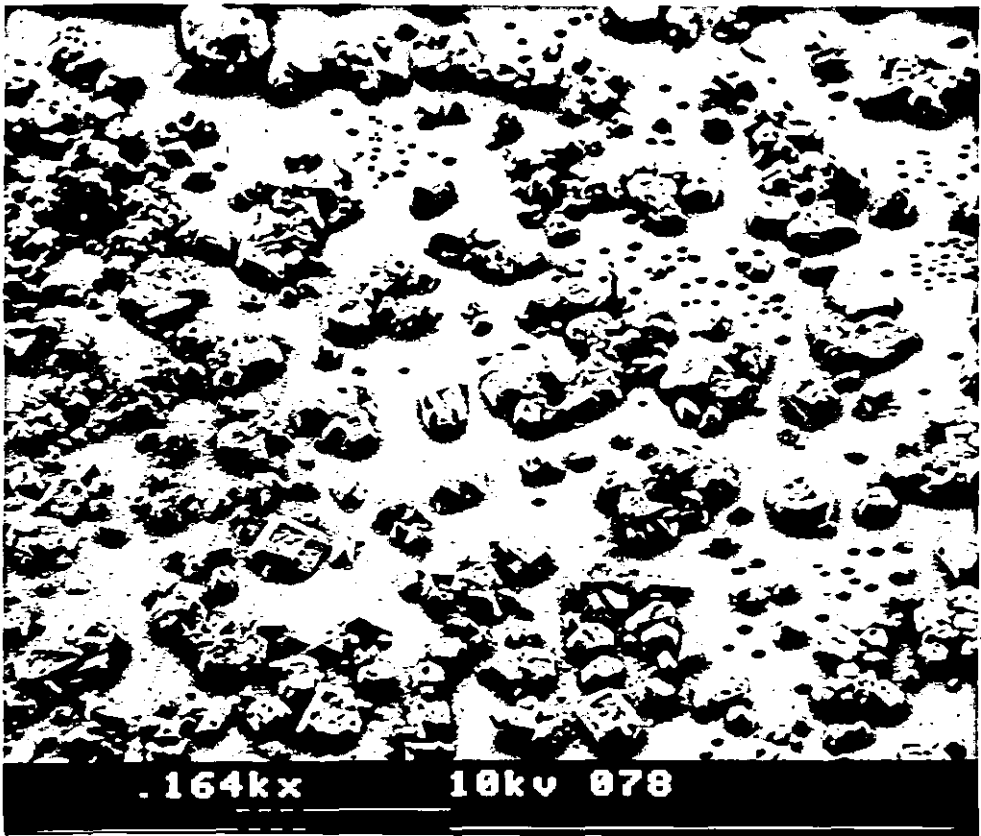
SEM showing increased surface coverage with concentrated solutions [using H₂SO₄ (1 mol dm⁻³) and Pb(NO₃)₂ (1 mol dm⁻³) solution for 24 hours at ambient temperature (20°C)].

PHOTO. 5:

—Magnification x 164

PHOTO. 6:

—Magnification x 900



5.3.3. Formation of a Membrane on PbO discs.

Photo.'s 7 to 28 show the effect of a change in acid concentration, reaction time, temperature or sample preparation on the surface structure of the leady oxide discs. Several important features are shown by these scanning electron micrographs:

1. When the leady oxide disc was immersed in sulphuric acid, a crystalline deposit was observed on the surface. As the concentration was increased the crystalline deposit became smaller and less uniform. At a concentration of about 7 mol dm^{-3} a distinct change in the deposit could be seen— *an amorphous layer was starting to form.*
2. If the discs, having this amorphous surface structure, were washed with distilled water, rather than industrial alcohol, the water was able to permeate the surface film and cause *buckling*, or rupture. The selectivity of the surface film to small molecules was demonstrated by this buckling.
3. When the reaction time was varied, it was discovered that a surface film started to appear within 15 minutes and became progressively more amorphous in structure. The surface layer on the leady oxide discs increased continuously during the reaction time, becoming quite deep if the reaction time was more than an hour.
4. When the temperature of the sulphuric acid was raised, the surface film became more amorphous, as finer particles started to develop on the surface of the leady oxide disc.

Infra red spectroscopy showed that although lead sulphate was a probable product from the reaction between sulphuric acid and the leady oxide discs, the absorptions bands were too broad to distinguish the compound uniquely. Raman spectroscopy, like infra-red spectroscopy, did not distinguish the compound uniquely, but was able to show that lead sulphate was a probable product.

5.3.4 Amalgamation of Lead Sulphate Membranes

The idea behind this approach was to sandwich a lead sulphate layer between two cellophane films (in a similar approach as Huber¹⁰⁰) and measure the diffusion of ions across two different solutions—repeating and expanding Ruetschi's experiments. This would have given a more realistic appraisal of the effects of a lead sulphate film. However, attempts made to isolate layers of lead sulphate formed on lead, by removing the support lead by amalgamation with mercury unfortunately met problems: the removal of the lead sulphate layer was difficult— as it entailed several steps— and disruption, during any stage

of preparation, destroyed the film. Moreover, the only available lead sheet was fairly thick and removal of the lead required so much mercury that turbulence broke the layer.

5.4 Further Work

The difficulties encountered with the amalgamation experiments meant that an interesting section of work could not be completed. Repeating this work with thinner lead sheets may provide interesting results.

Summary.

Experiments with sulphuric acid on leady oxide discs showed that the point at which *onset of micro* PbSO_4 crystals occurred was at 7 mol dm^{-3} and consequently implies that a lead sulphate membrane formation would be more likely above this concentration. Bialacki¹⁰¹ studying a PbSO_4 layer on PbO_2 showed that with sulphuric acid concentrations of 7 mol dm^{-3} , and above, a more compacted layer of lead sulphate crystals started to form.

Evidence for lead sulphate membranes was indicated by the buckling of the surface layer of leady oxide discs which had been reacted with sulphuric acid and subsequently washed with water (this effect was not observed if industrial alcohol was used) and implies that the lead sulphate layer must be susceptible to osmosis.

SEM's (Photos 7 to 12) showing the effect of increasing the H_2SO_4 concentration on the surface of a leady oxide disc [reaction time 30 minutes, ambient temperature (20°C), then washed with *industrial alcohol*].

PHOTO. 7:

—concentration $1 \text{ mol dm}^{-3} \text{ H}_2\text{SO}_4$

PHOTO. 8:

—concentration $3 \text{ mol dm}^{-3} \text{ H}_2\text{SO}_4$

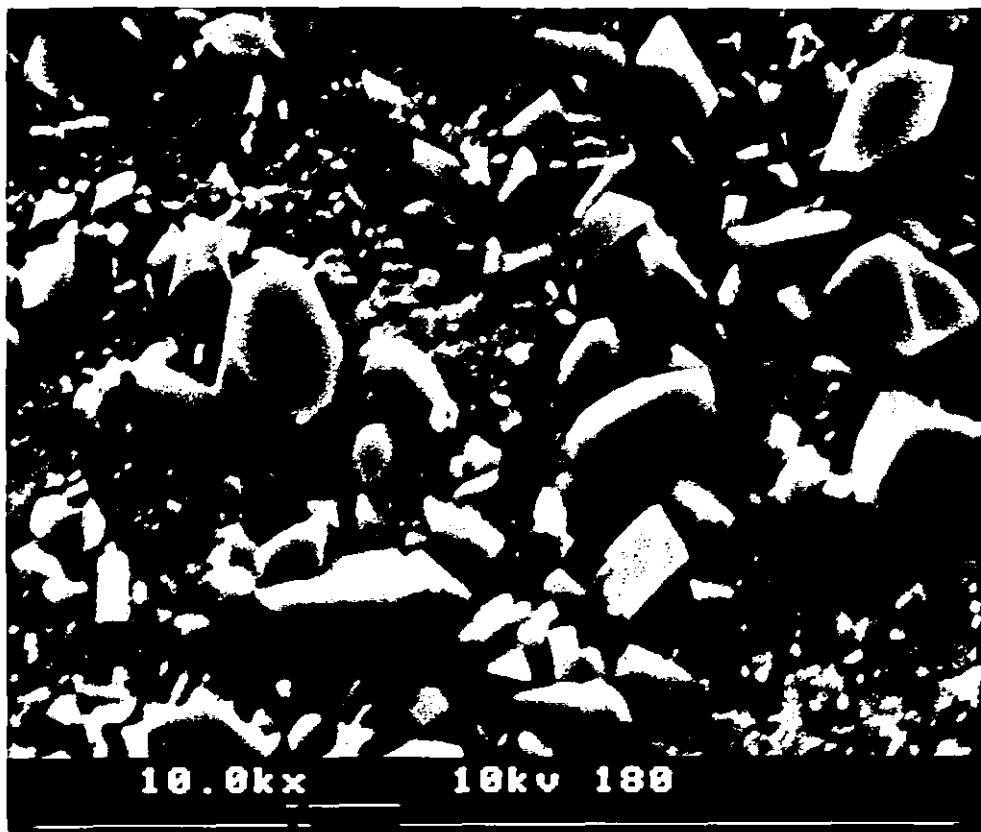
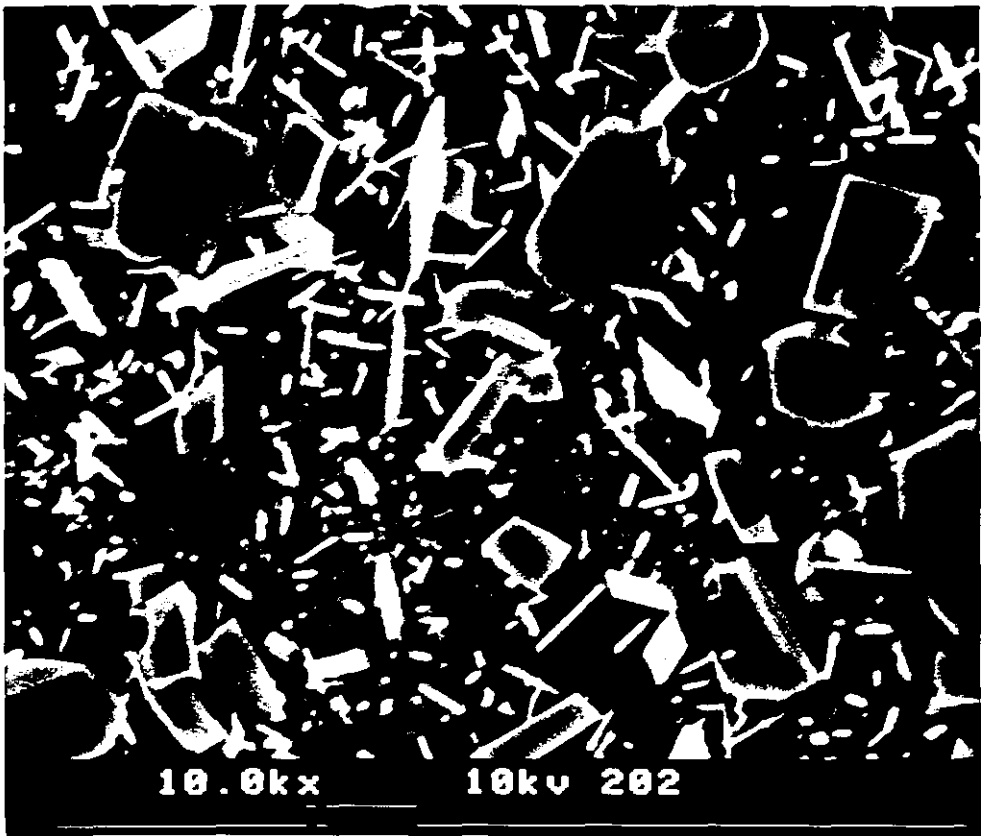


PHOTO. 9:

—Text as for PHOTO. 7,

but concentration

$5 \text{ mol dm}^{-3} \text{ H}_2\text{SO}_4$

PHOTO. 10:

—Text as for PHOTO. 7,

but concentration

$7 \text{ mol dm}^{-3} \text{ H}_2\text{SO}_4$

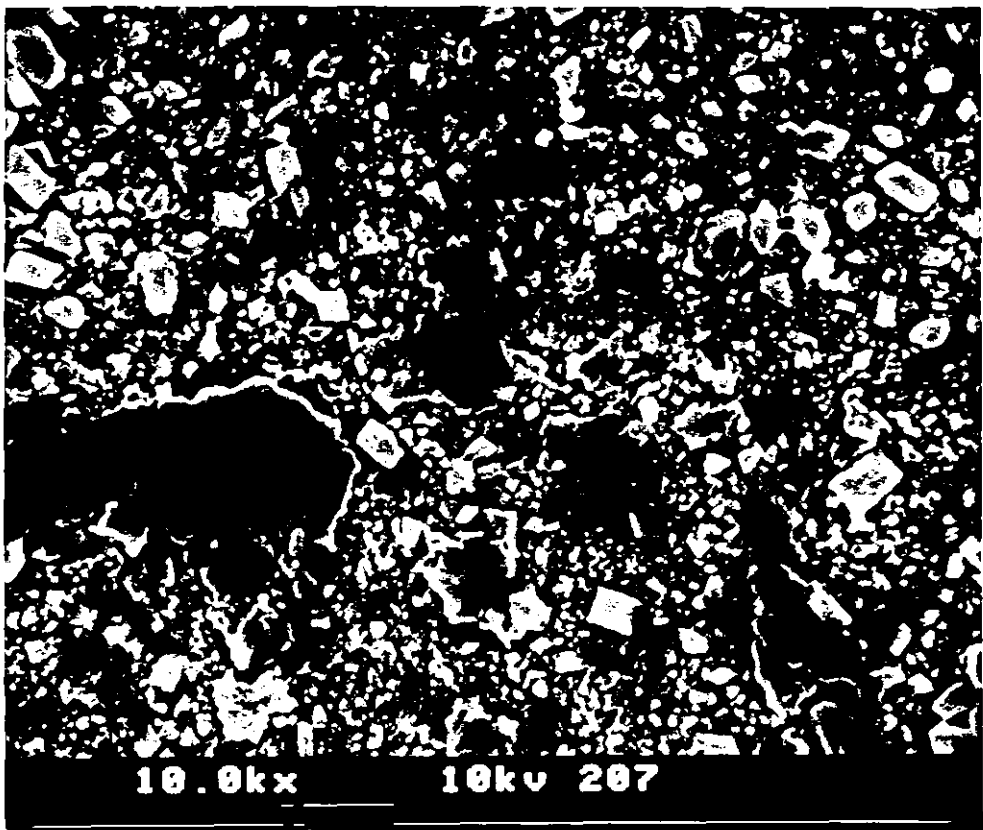
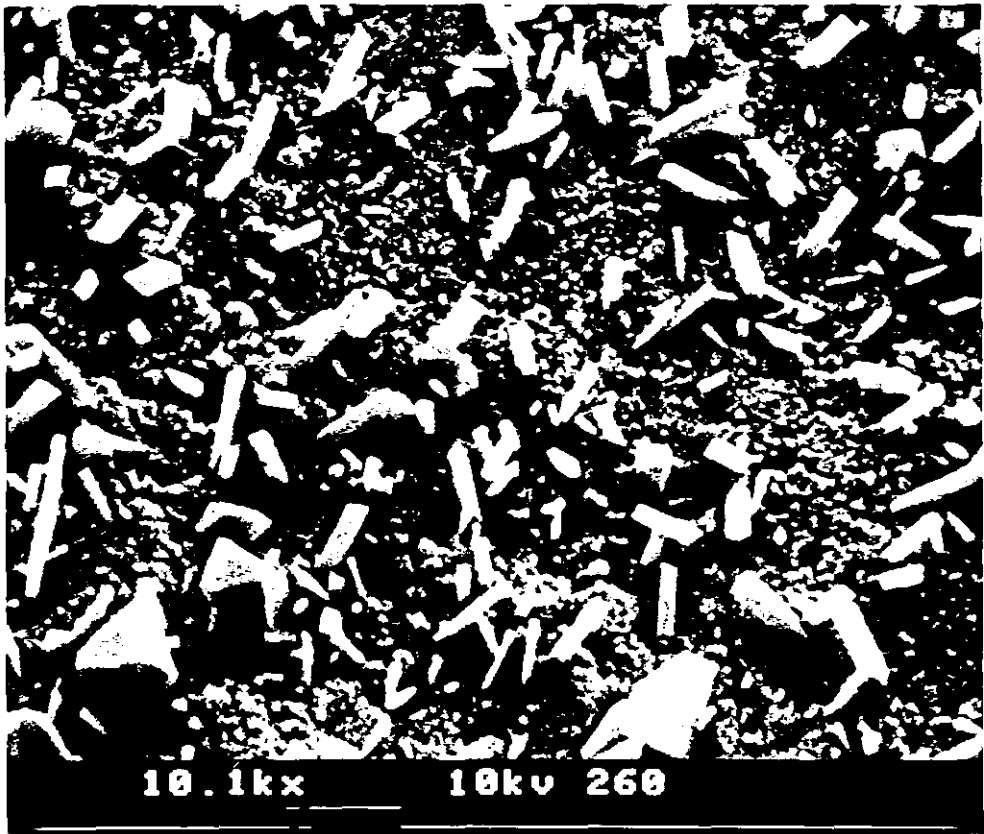


PHOTO. 11:

—Text as for PHOTO. 7,

but concentration

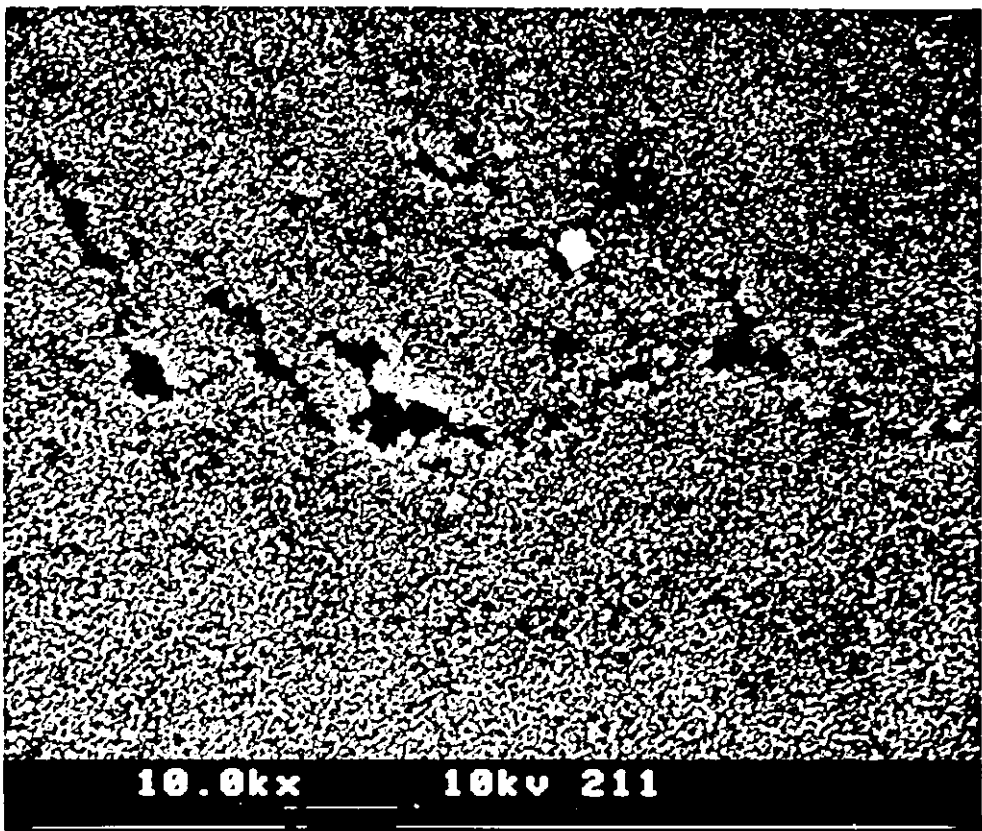
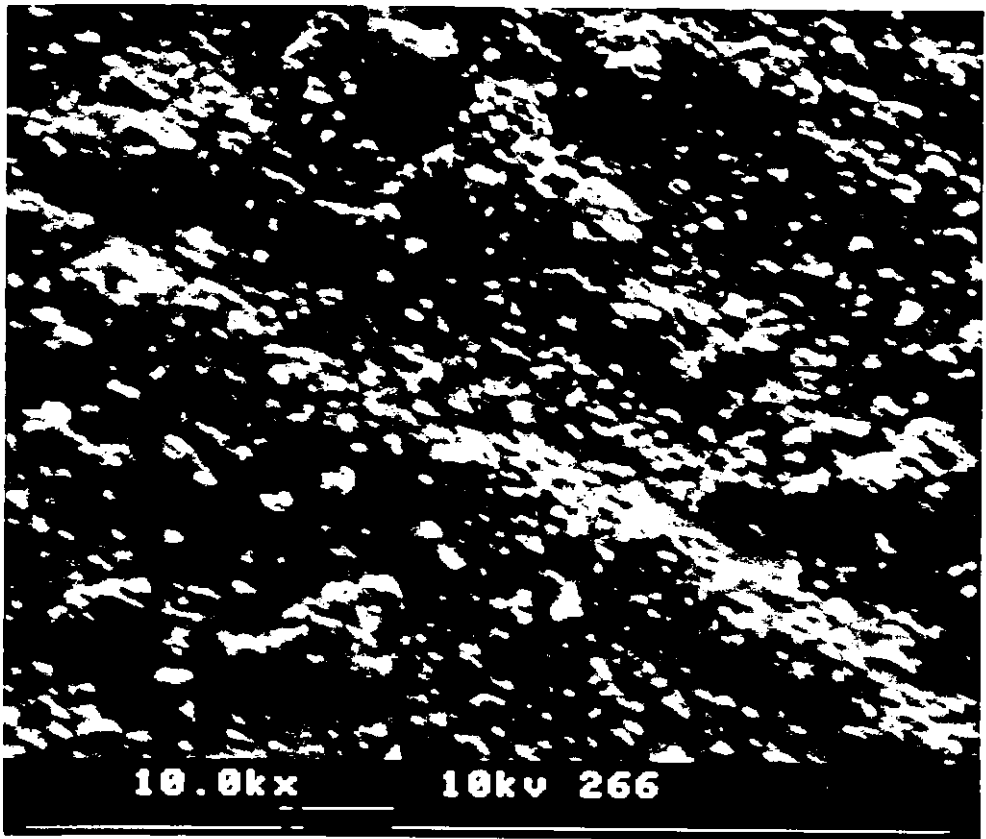
$8 \text{ mol dm}^{-3} \text{ H}_2\text{SO}_4$

PHOTO. 12:

—Text for PHOTO. 7,

but concentration

$10 \text{ mol dm}^{-3} \text{ H}_2\text{SO}_4$



SEM's (Photos 13 to 18) showing the effect of increasing the H_2SO_4 concentration on the surface of a leady oxide disc [reaction time 30 minutes, ambient temperature (20°C), then washed with *distilled water*].

PHOTO. 13:

—concentration

$1 \text{ mol dm}^{-3} \text{H}_2\text{SO}_4$

PHOTO. 14:

—concentration

$3 \text{ mol dm}^{-3} \text{H}_2\text{SO}_4$

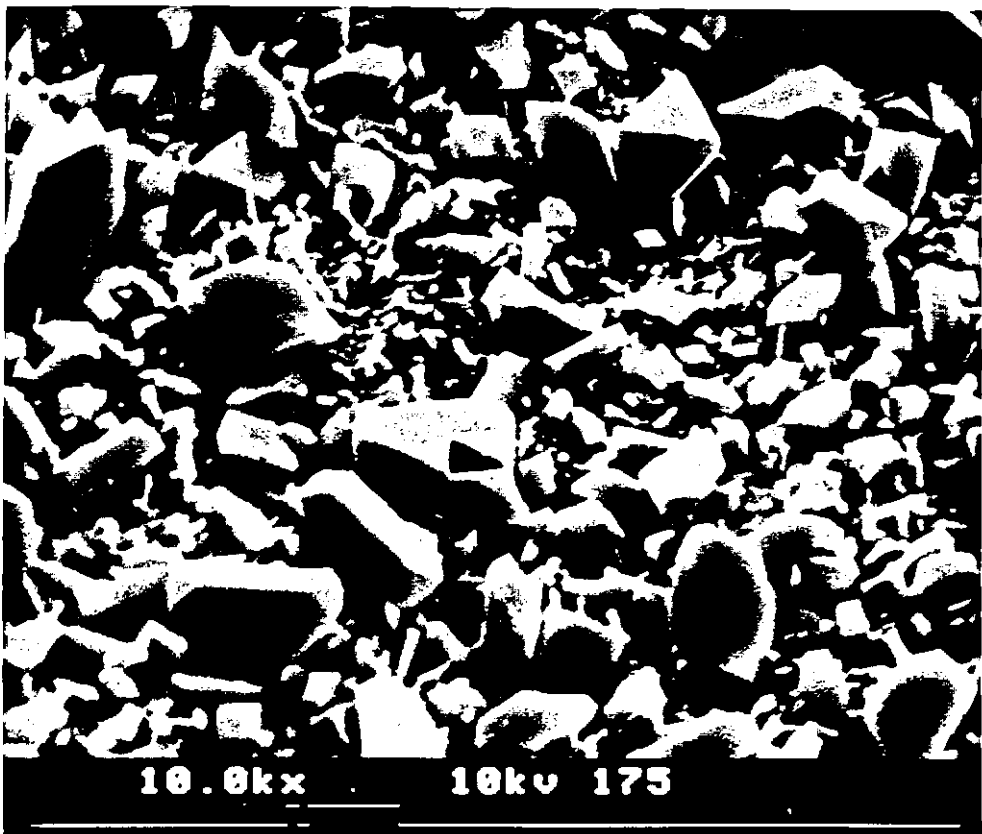
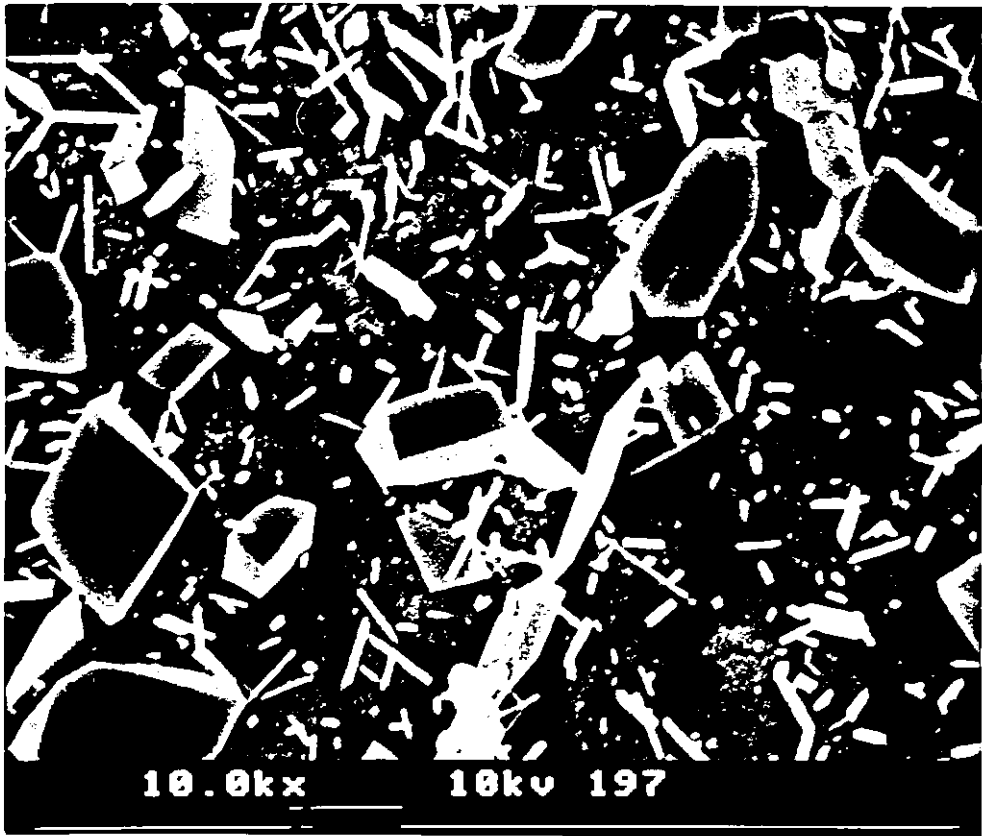


PHOTO. 15:

—Text as for PHOTO. 13,

but concentration

$5 \text{ mol dm}^{-3} \text{ H}_2\text{SO}_4$

PHOTO. 16:

—Text as for PHOTO. 13,

but concentration

$7 \text{ mol dm}^{-3} \text{ H}_2\text{SO}_4$

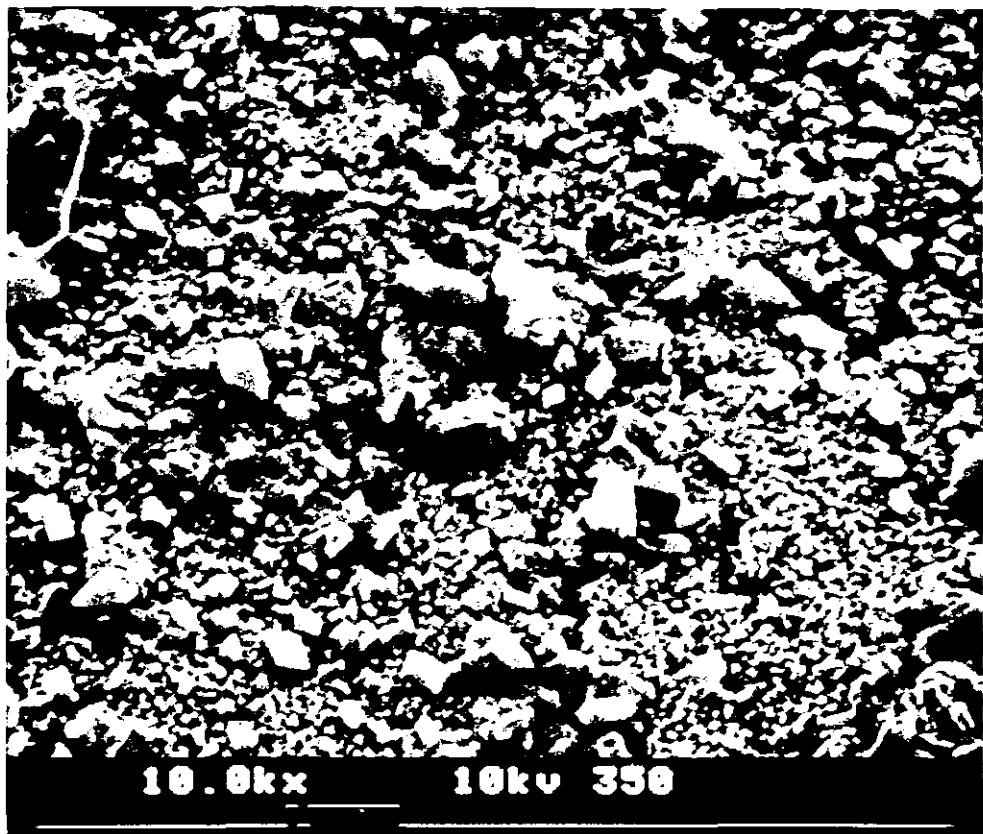
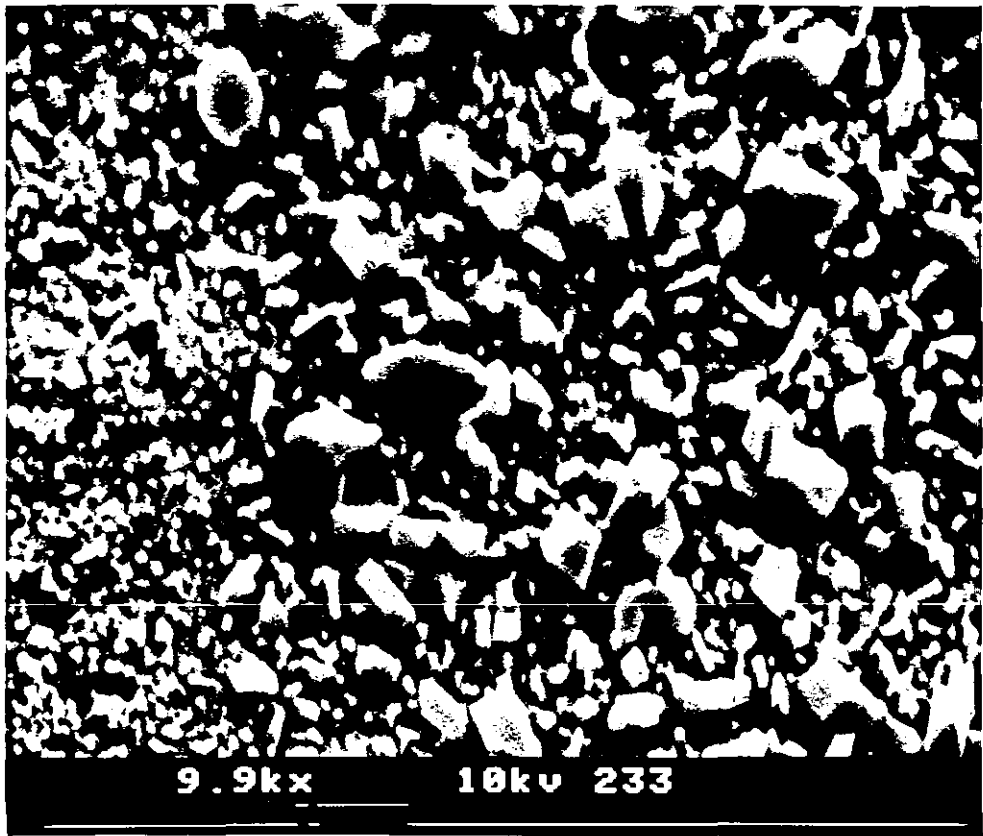


PHOTO. 17:

—Text as for PHOTO. 13,

but concentration

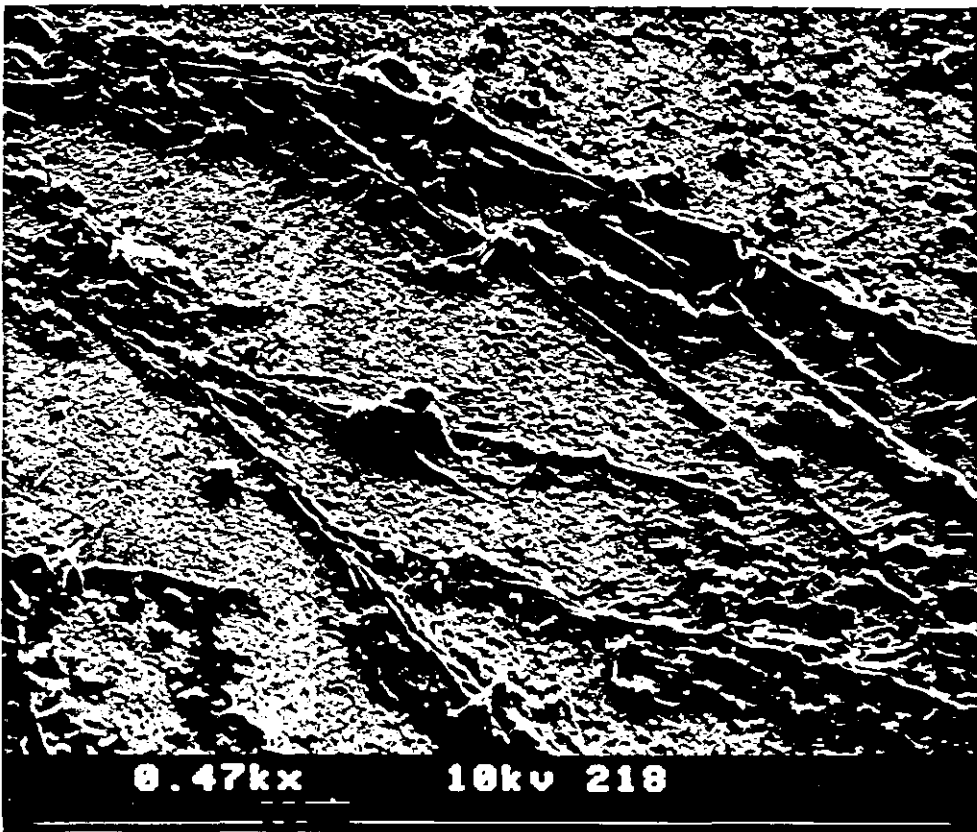
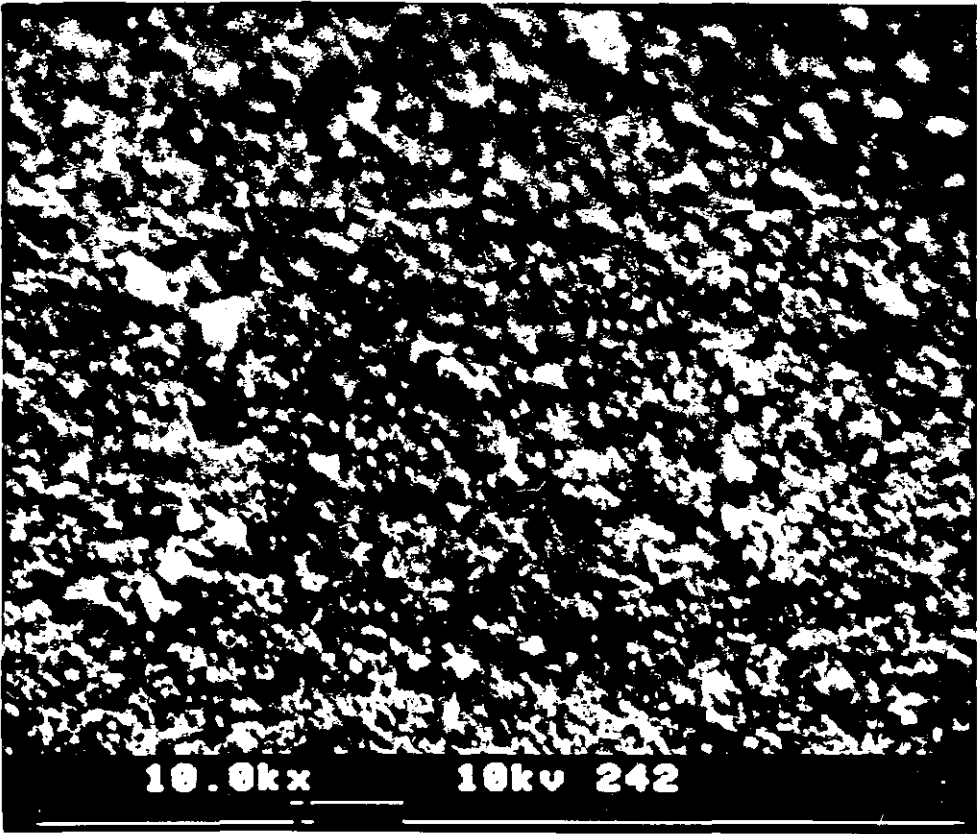
8 mol dm⁻³ H₂SO₄

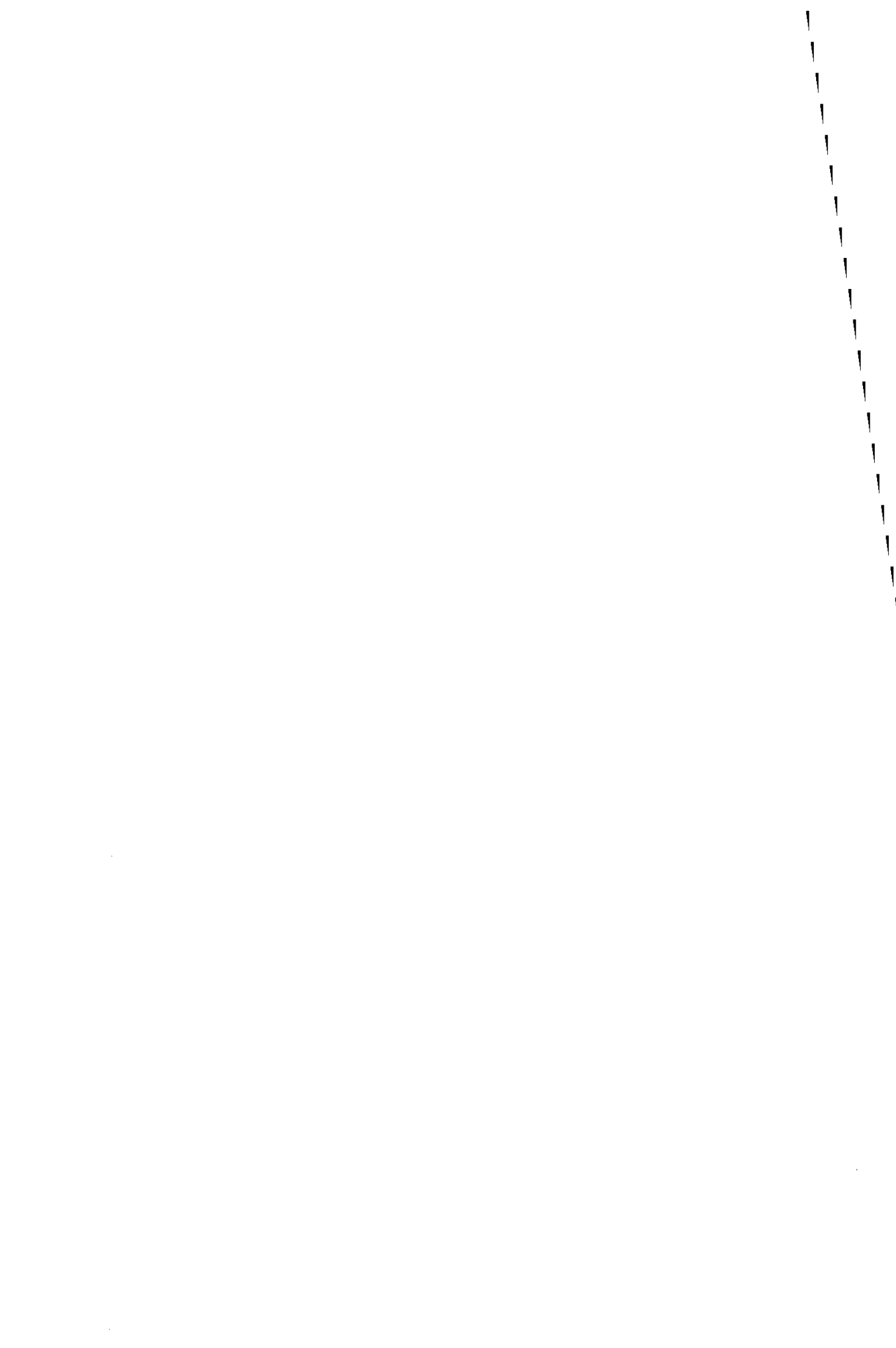
PHOTO. 18:

—Text as for PHOTO. 13,

but concentration

10 mol dm⁻³ H₂SO₄





SEM's (Photos 19 to 25) showing the effect of increasing the reaction time on the surface of a leady oxide disc [H_2SO_4 (10 mol dm^{-3}), ambient temperature (20°C), then washed with *distilled water*].

PHOTO. 19:

—reaction time

5 minutes

PHOTO. 20:

—reaction time

15 minutes

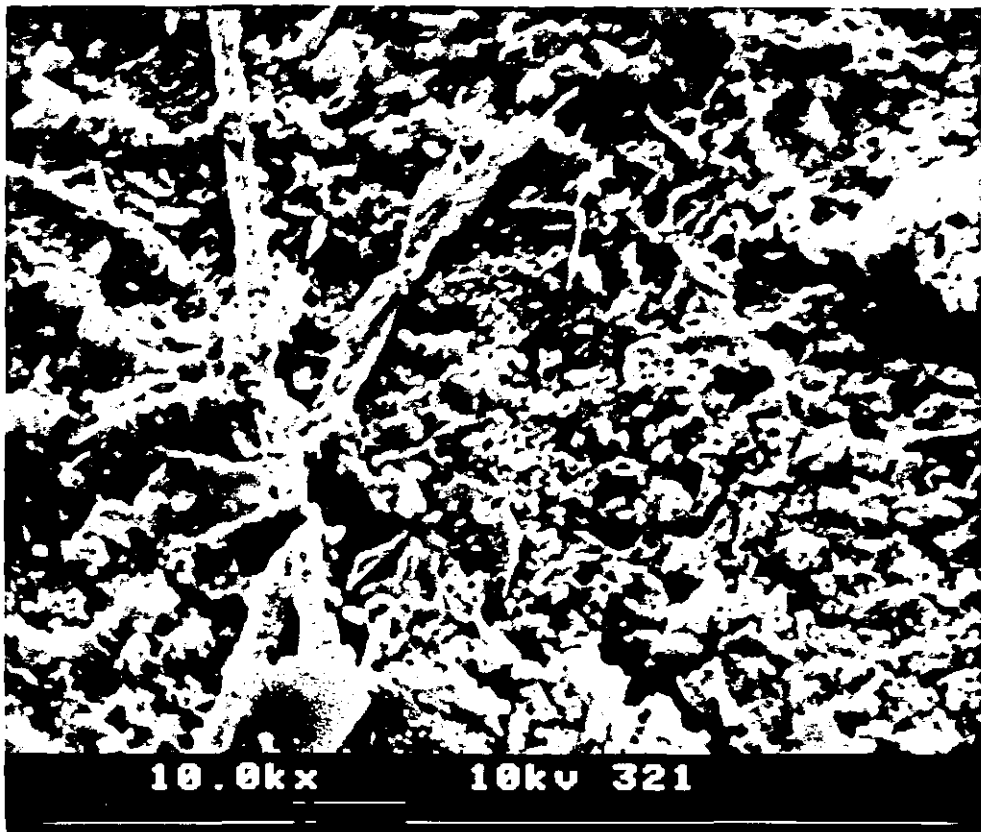
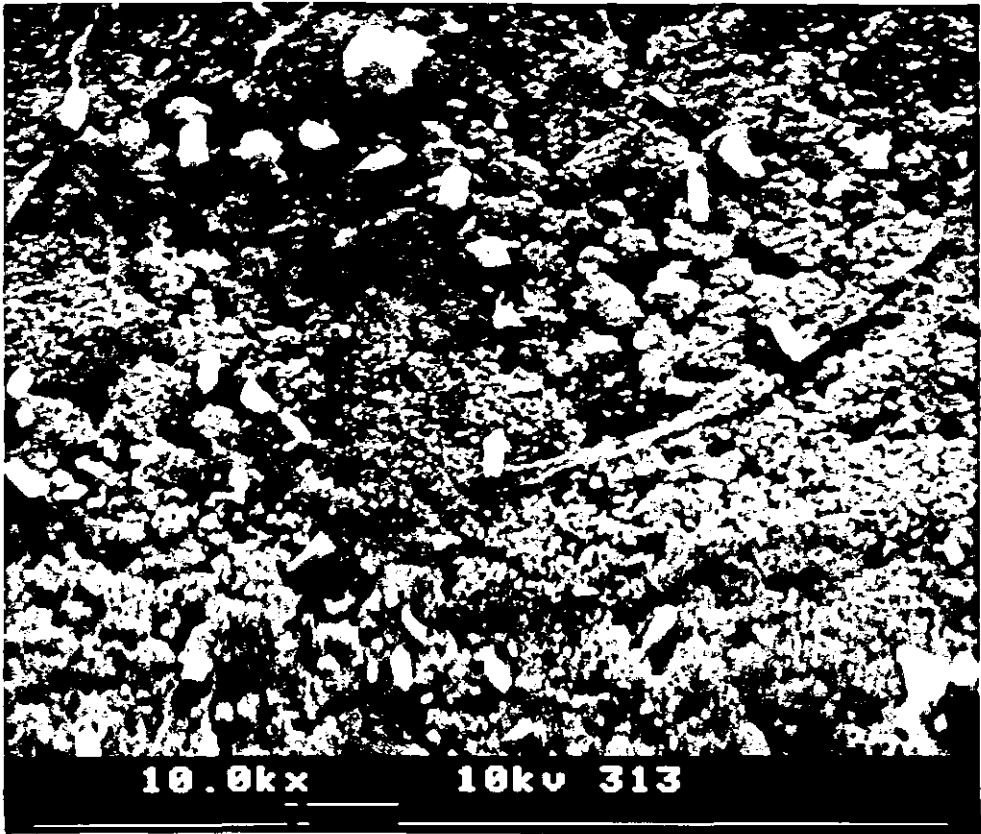


PHOTO. 21*:

—Text as for PHOTO. 19,

but reaction time

30 minutes

PHOTO. 22:

—Text as for PHOTO. 19,

but reaction time

1 hour

* ERRATA: For PHOTO. 21, please see PHOTO. 18 (photo.'s 18 and 21 are identical).

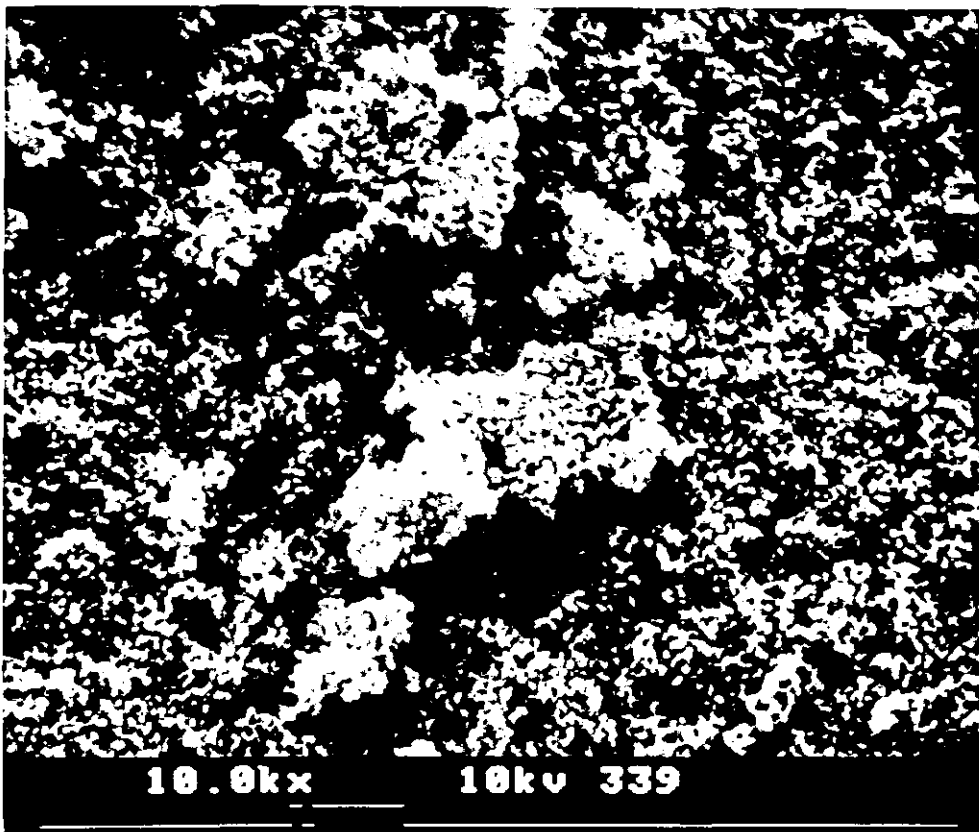
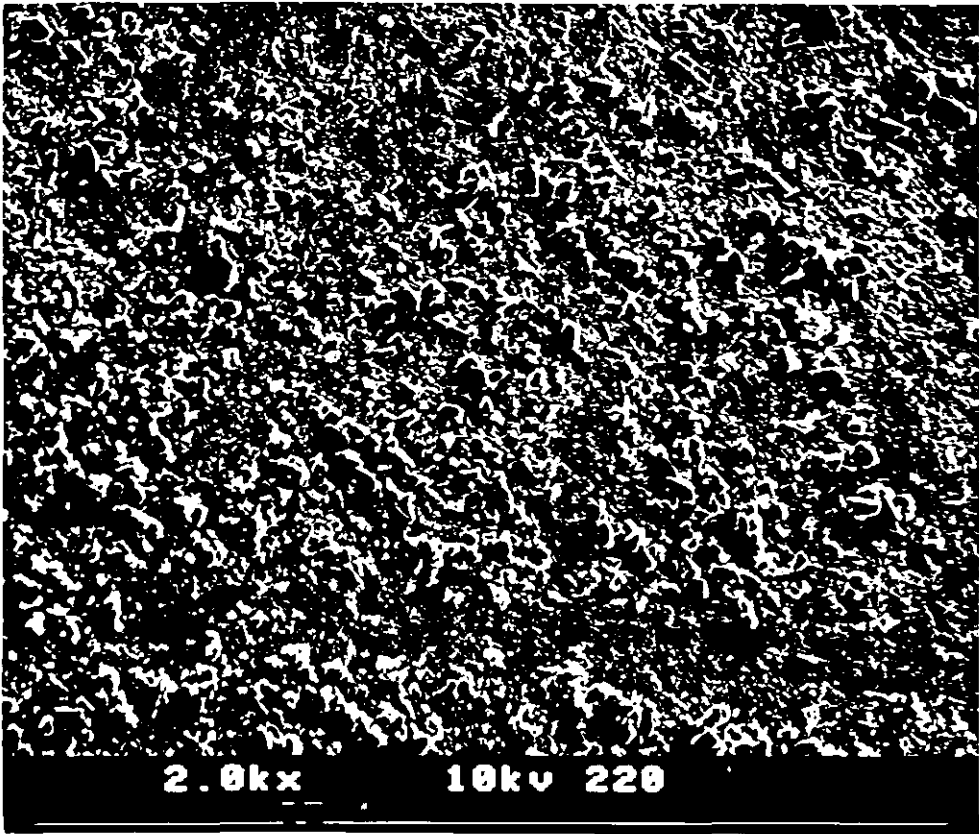


PHOTO. 23:

—Text as for PHOTO. 19,

but reaction time

6 hour

PHOTO. 24:

—Text as for PHOTO. 19,

but reaction time

17 hours

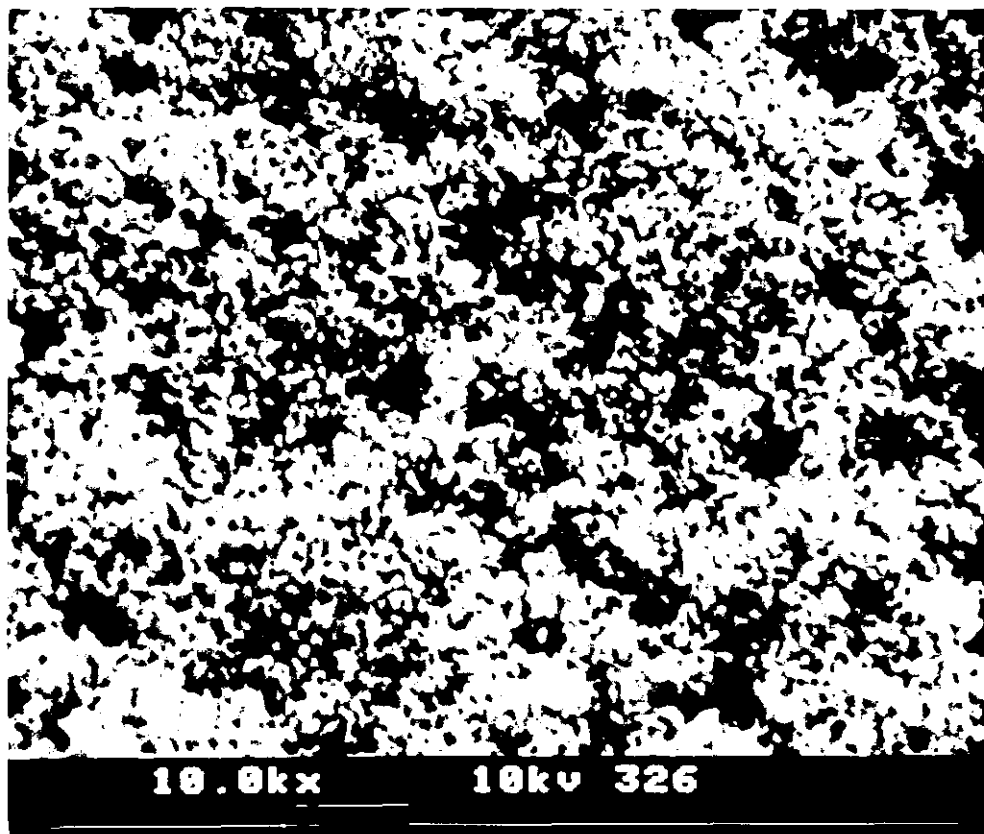
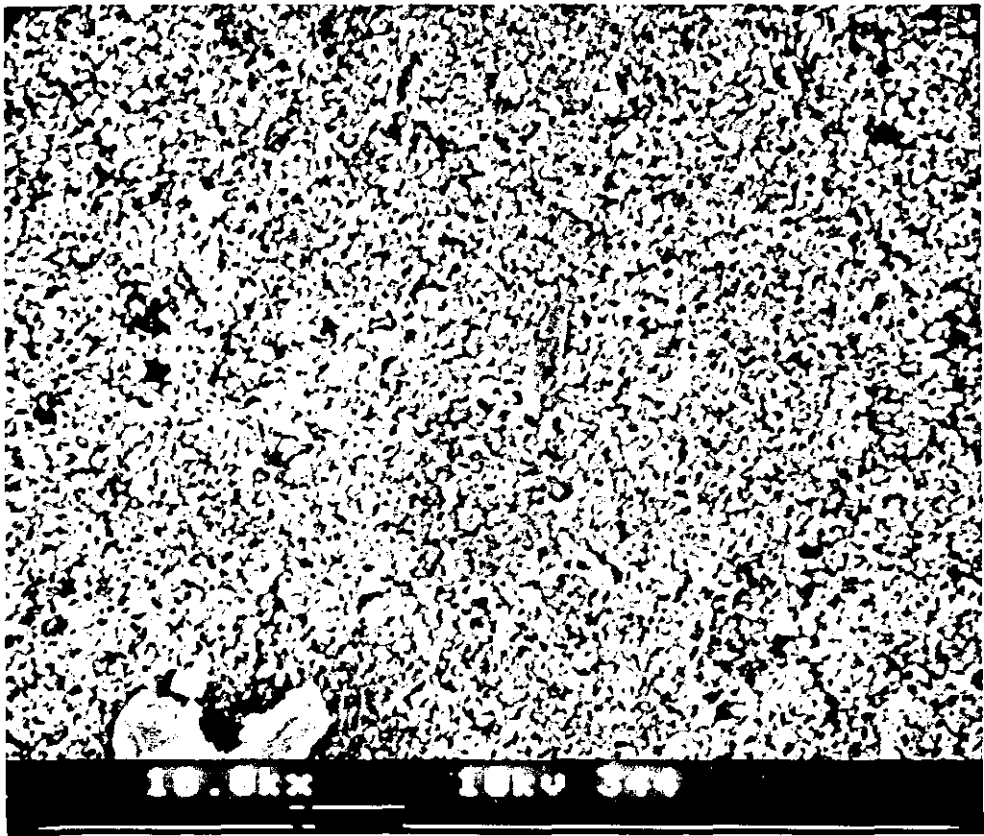




PHOTO. 25:

—Text as for PHOTO. 19

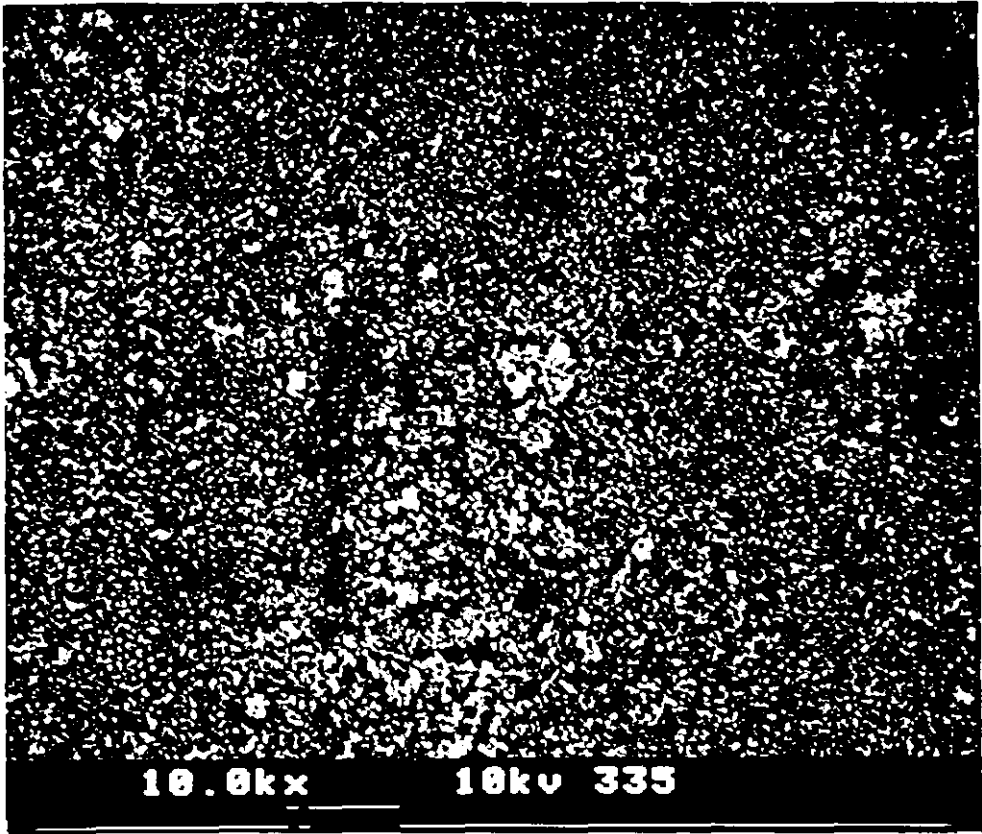
but reaction time

24 hours

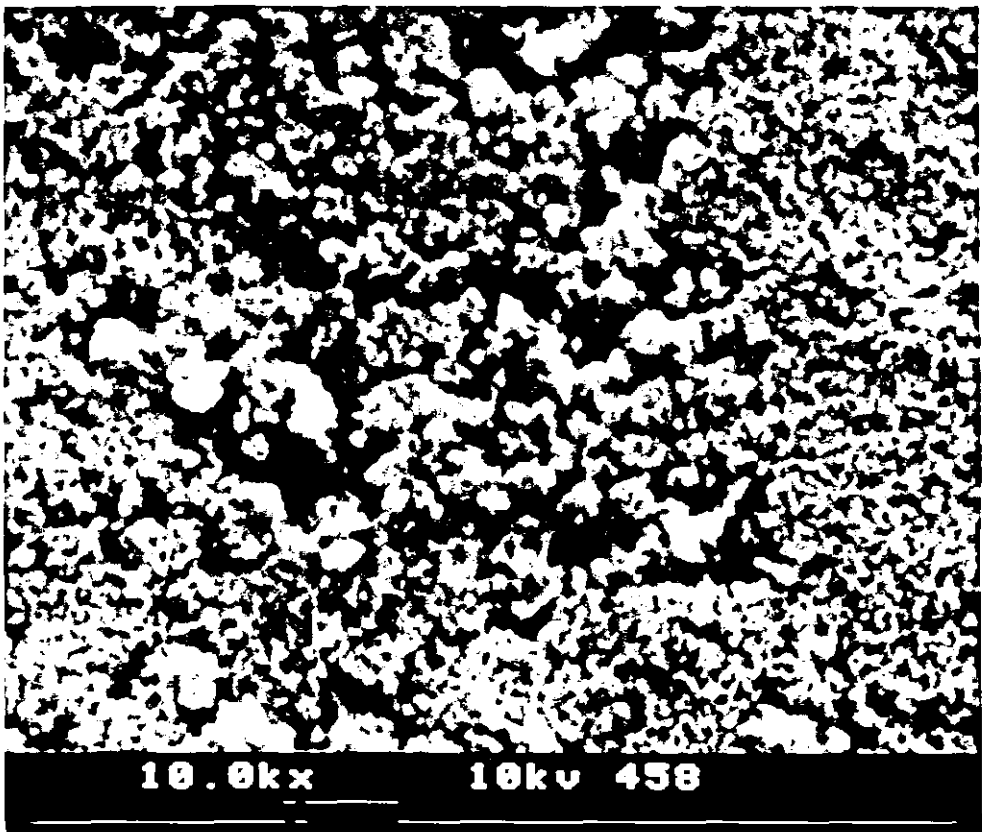
SEM's (Photos 26 to 28) showing the effect of increasing the temperature on the surface of a leady oxide disc [H_2SO_4 (10 mol dm^{-3}), 30 minute reaction time, then washed with *distilled water*].

PHOTO. 26:

—Temperature 25°C



10.0kx 10kV 335



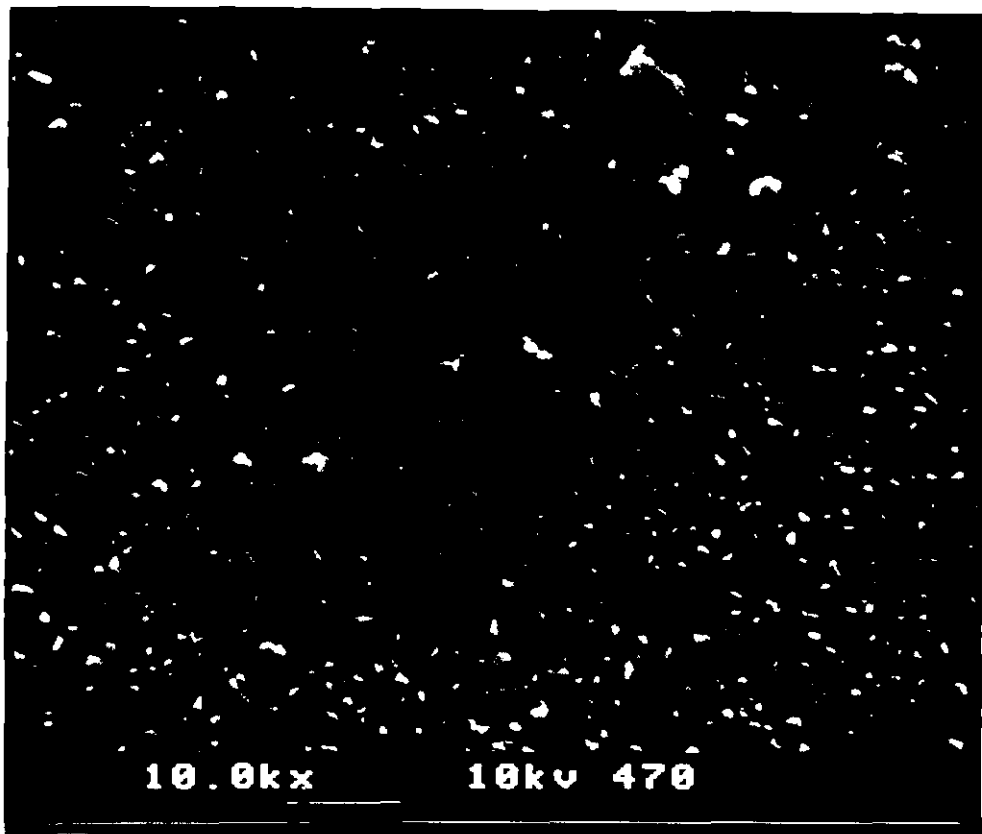
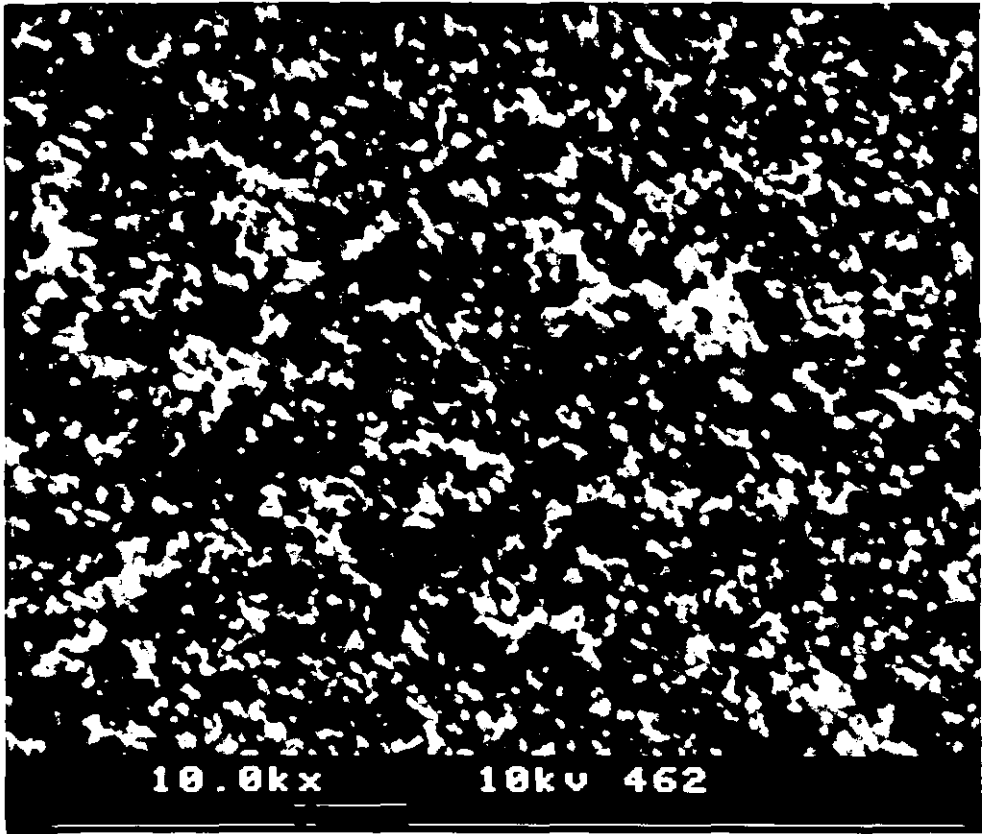
10.0kx 10kV 458

PHOTO. 27:

—Text as for PHOTO. 26,
but temperature 50°C

PHOTO. 28:

—Text as for PHOTO. 26,
but temperature 75°C



CHAPTER SIX.

FARADAIC IMPEDANCE MEASUREMENTS.

6.1 Introduction.

To continue the investigation into the properties of lead sulphate membranes impedance spectroscopy (IS) was employed. It was hoped that the diffusion limiting properties of a semi-permeable lead sulphate membrane would change the impedance spectroscopy's characteristics and provide an indication of its properties.

6.2 Electrical Circuits.

A microprocessor-based system coupled with a Solatron 1172 Frequency Response Analyzer (FRA) was employed to measure impedance data. This electrical engineers' instrument has become well established in electrochemistry and consists of a frequency generator and correlator able to output sine, square or triangular waveforms that can be used to excite the system under test. In the present work, sinusoidal perturbations, of ± 3 mV, were invariably used. The system's correlator is based on a Fourier analysis of the current response of the system on test, giving an in-phase and out-of-phase resultant, either as an *amplitude* and *phase angle*, a *log amplitude* and *phase angle*, or a *real* and *imaginary* component of the impedance (the latter being chosen for the work here). These two components, together with their respective frequency were, passed to a NEC Z80 microcomputer for storage on disc.

In conjunction with the Solatron 1172 FRA a Solatron 1186 'electrochemical interface' was used to provide potentiostatic control of the cell's characteristics. This instrument has special provision for use with a FRA, and allows the perturbation signal from the FRA to be superimposed on the internally generated polarisation voltage without affecting the potentiostatic control of the cell. The schematic diagram is illustrated in figure 28. Although the 1186 electrochemical interface has the ability to operate with *two* reference electrodes, in a four terminal mode, the work here was invariably done in the *three terminal mode*; with the working electrode (WE) externally shorted with the second reference electrode connection, while the secondary electrode (SE) and remaining reference electrode (RE) were connected to the electrochemical interface normally. Remote sensing (RS) was employed to remove all uncompensated resistances in the working electrode's lead.

The scan range was from 60 kHz to c.250 mHz, ten points per decade in a logarithmic sweep. Above 10 Hz the time period for a single measurement was equal to 60 times the period of the signal, below 10 Hz it was equal to the time period (100 s at 10^{-2} Hz, for example), the lower frequencies therefore became the major contributor to the total experiment time. Thus below 10 Hz the integration time was

Impedance Analysis Equipment

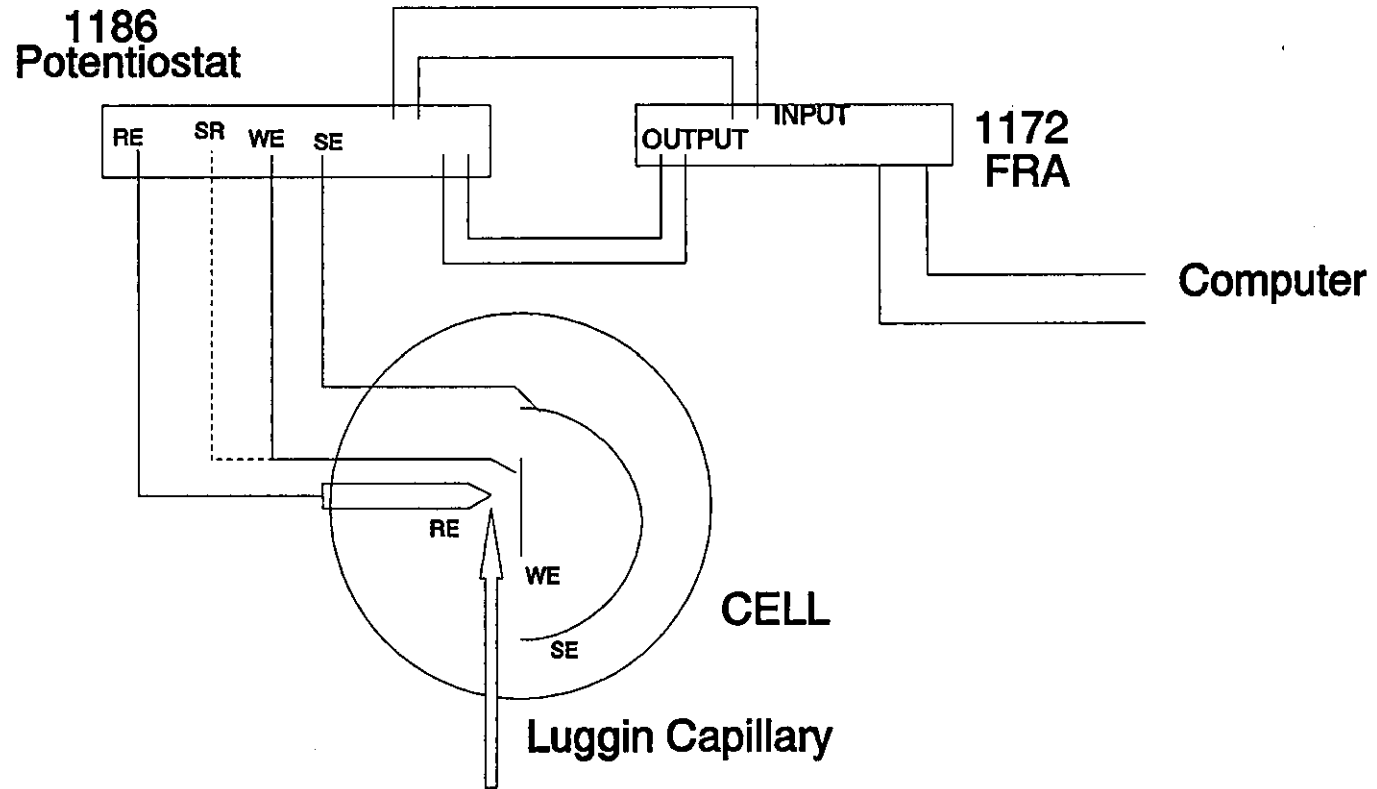


Figure 28

reduced from 100 to 10 and a *low pass filter* switched in. Each frequency spectrum normally taking 3 to 4 hours, after the initial formation and equilibrium periods.

6.3 Experimental Details.

Experiments were performed on planar lead electrodes in standard three limb cell (figure 23), which was immersed in a thermostatically controlled water bath. In this manner a temperature between 20 and 75°C, +/-0.5°C could be selected. Before the working electrode was immersed in the sulphuric acid the cell was connected and the Pb→PbSO₄ equilibrium potential set*. A lead sulphate layer was then formed by moving the lead electrode into the lead sulphate region (0 mV) for half an hour. The potential was then moved back to the Pb→PbSO₄ equilibrium potential and held for one hour before a frequency spectrum was run.

Several groups of experiments were then carried out by changing either the cell's temperature (between 25 and 60°C), or the acid concentration (between 1 and 10 mol dm⁻³). In subsequent experiments the rest potential (+/-10 mV), the formation times (from 0.5 to 16 hours) or the formation voltage (from 0 to +500 mV) were varied. Further experiments undertaken included the use of 'spongy carbon' (Schumacher Carbo 30G *high surface area*) secondary electrodes, 'porous' lead and PbO₂ (deposition onto Pt) working electrodes (the latter using a Pb/PbO₂ reference electrode).

6.4 Results and Discussion.

6.4.1 Impedance Measurements.

Tables 3 to 5** show the results of the impedance runs*** (voltages are quoted against the Hg/Hg₂SO₄ reference electrode, and are an average of at least three runs) with one set of typical impedance spectra shown in figures 29 to 37. Although the impedance spectra were of a complex nature some general characteristics have been resolved.

At low concentrations and temperatures— the spectra exhibit a high frequency semi-circle (although sometimes difficult to characterise) with a poorly defined Warburg tail— this can clearly be seen in the

* To protect any surface chemistry, the Pb→PbSO₄ equilibrium voltage was first determined by a linear sweep voltammogram at -972 mV Vs. Hg/Hg₂SO₄.

** In order to build a better picture of the impedance spectra the frequency, Z' and -Z'' co-ordinates for ω_{max} have also been included in the tables as: ω_{max}(freq.), ω_{max}(Z') and ω_{max}(-Z'') respectively.

*** Problems with electrical equipment has meant that it was not possible to obtain, or validate, some readings.

Conc /mol dm ⁻³	Temp °C	R _{ct} /Ω	C _{dl} /μF	ω _{max} (freq.) /Hz	ω _{max} (Z') /Ω	ω _{max} (-Z'') /Ω	roughness factor	Comments
5	25	920	13.8	12.6	420	346	0.88	Adsorption
	40	178	7.13	126	91	60.9	0.75	Warburg diffusion
10	25	2880	11.1	5.00	1591	1172	0.81	Adsorption
	40	528	9.57	31.5	273	234	0.90	In transition to diffusion control
	60	126	7.99	158	72	48	0.75	Rough Warburg diffusion

Table 3 IS Results for 3 mm lead disc at -970 mV (Vs. Hg/Hg₂SO₄).

Conc /mol dm ⁻³	Temp /°C	R _{ct} /ohms	C _{dl} /μF	ω _{max} (freq.) /Hz	ω _{max} (Z') /Ω	ω _{max} (-Z'') /Ω	roughness factor	Comments
1	25	2590	7.74	7.94	1535	1084	0.78	Adsorption
	40	612	26.1	9.96	360	165	0.55	Adsorption
	60	200	15.9	50.0	113	64	0.66	Rough Diffusion Control
5	25	1008	12.5	12.6	475	407	0.90	Adsorption
	40	568	11.2	25.1	334	229	0.77	Adsorption
	60	39	8.16	500	17	9.37	0.64	Rough Diffusion Control
10	25	2070	12.2	6.30	1063	1058	1.00	Adsorption
	40	512	6.22	50.0	225	182	0.87	Adsorption
	60	96	6.62	251	49.2	31.2	0.72	Rough Diffusion Control

Table 4 IS Results for 3 mm lead disc at -972 mV (Vs. Hg/Hg₂SO₄).

Conc /mol dm ⁻³	Temp /°C	R _{ct} /Ω	C _{dl} /μF	ω _{max} (freq.) /Hz	ω _{max} (Z') /Ω	ω _{max} (-Z'') /Ω	roughness factor	Comments
1	25	2600	6.14	9.97	1267	871	0.77	Adsorption
	40	1190	6.72	19.9	718	473	0.74	Adsorption-- Diffusion Control just starting
	50	480	13.2	25.1	259	133	0.60	Adsorption
5	25	1280	9.90	12.6	634	456	0.79	Adsorption
	40	135	7.46	158	64.3	54.9	0.90	Adsorption
	60	110	7.27	199	58.9	34.7	0.68	Diffusion Control just starting
10	25	2920	10.9	5.00	1532	1179	0.84	Adsorption
	40	240	8.36	79.4	115	81.2	0.78	Adsorption
	60	98	12.9	126	60.8	41.6	0.76	Adsorption still present

Table 5 IS Results for 3 mm lead disc at -974 mV (Vs. Hg/Hg₂SO₄).

Typical I.S. for $1 \text{ mol dm}^{-3} \text{H}_2\text{SO}_4$ at 25°C and -972 mV (Vs. $\text{Hg}/\text{Hg}_2\text{SO}_4$).

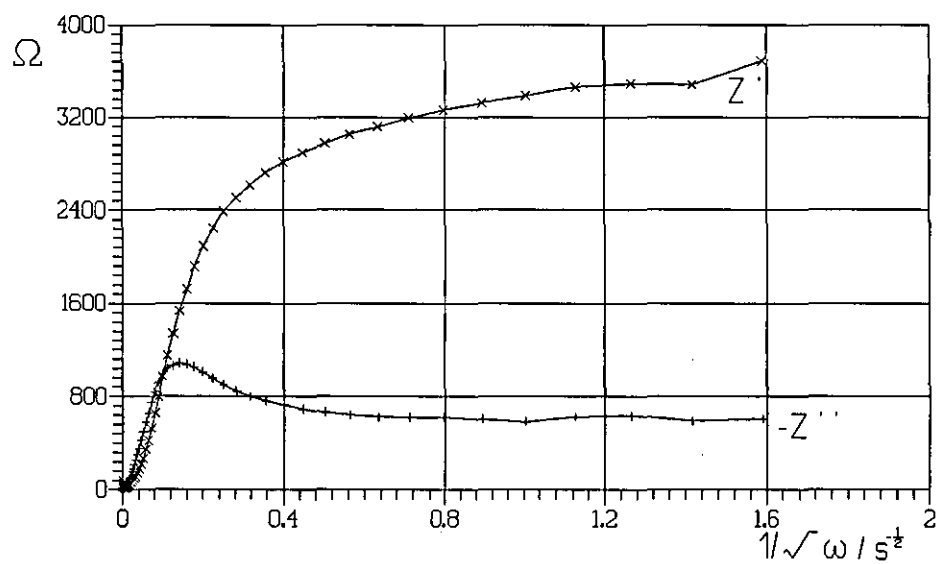
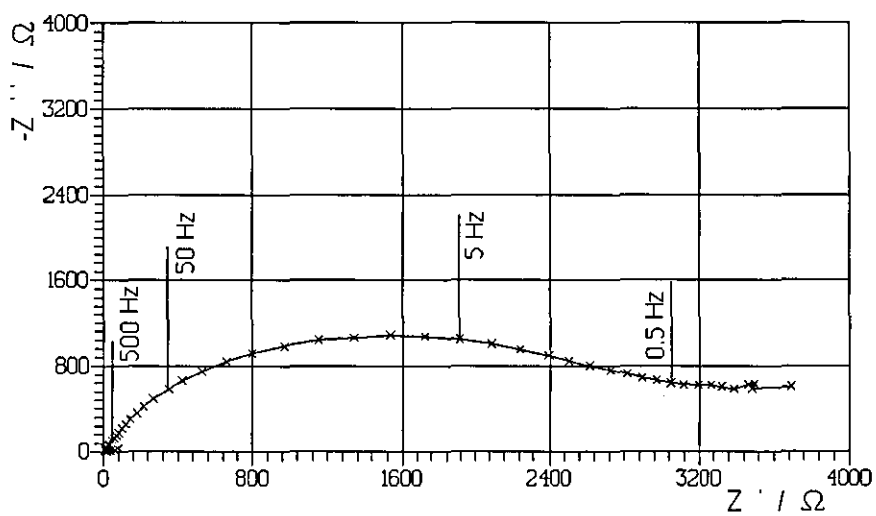


Figure 29

Typical I.S. for $1 \text{ mol dm}^{-3} \text{H}_2\text{SO}_4$ at 40°C and -972 mV (Vs. $\text{Hg}/\text{Hg}_2\text{SO}_4$).

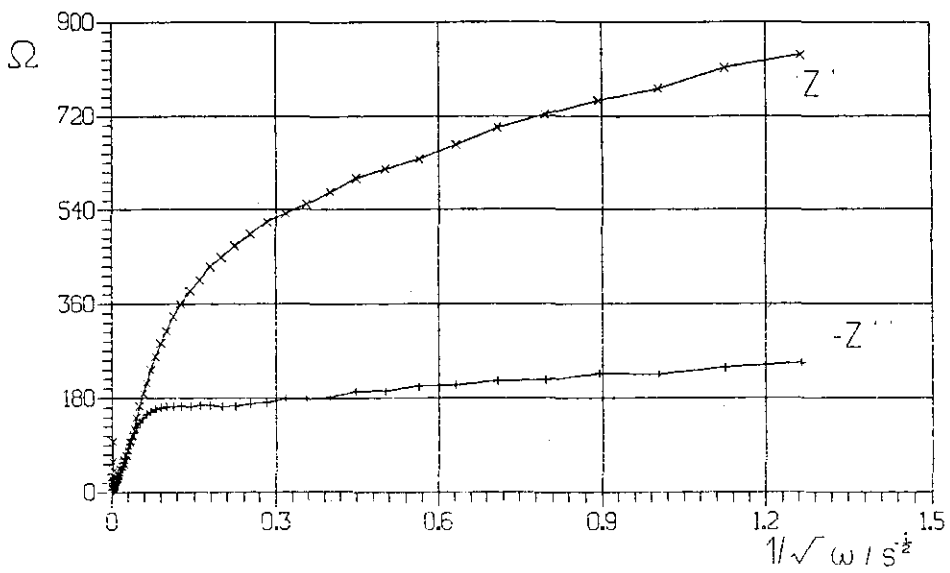
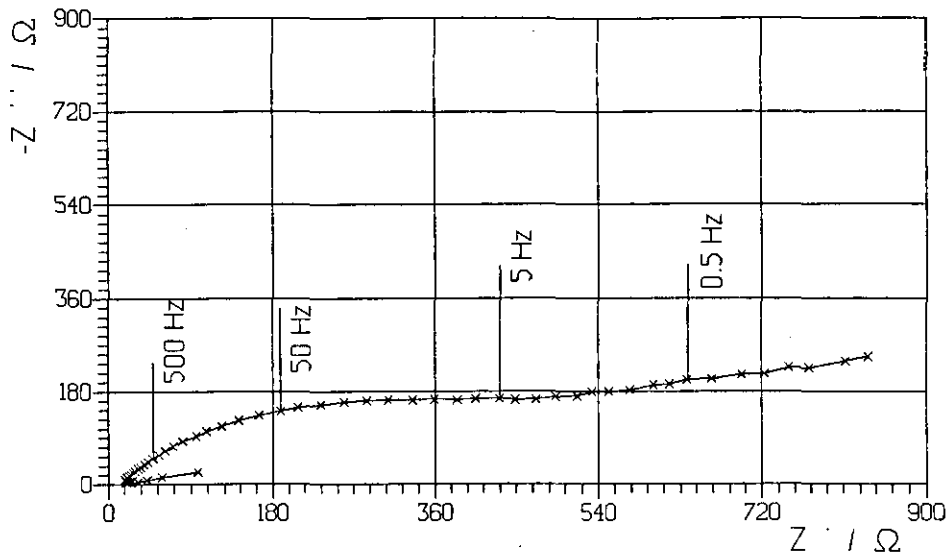


Figure 30

Typical I.S. for $1 \text{ mol dm}^{-3} \text{H}_2\text{SO}_4$ at 60°C and -972 mV (Vs. $\text{Hg}/\text{Hg}_2\text{SO}_4$).

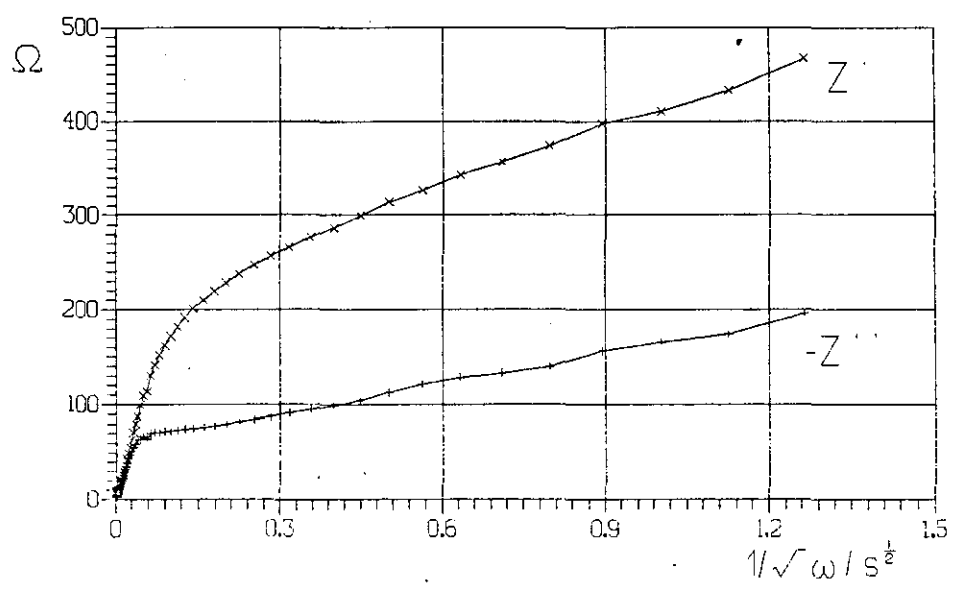
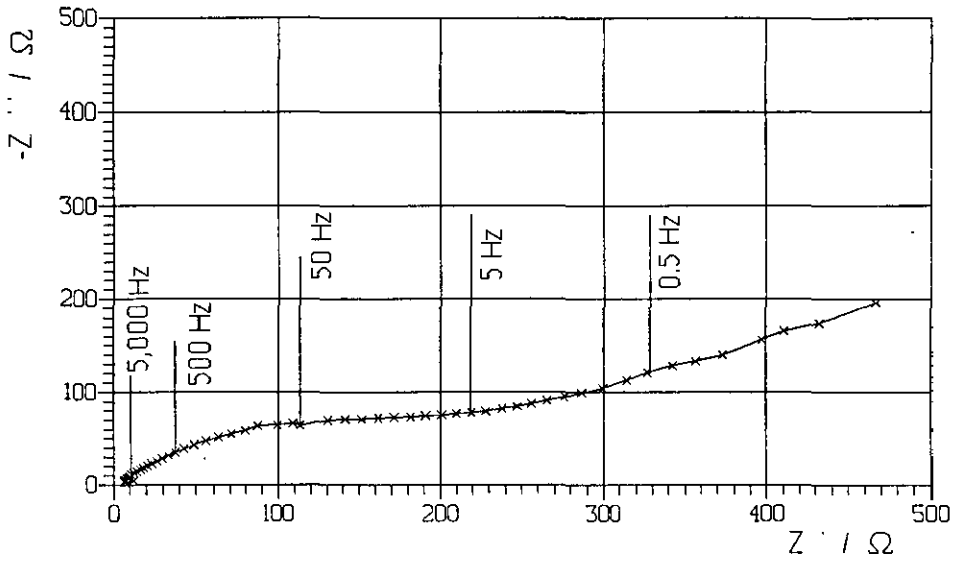


Figure 31

Typical I.S. for 5 mol dm³ H₂SO₄ at 25 °C and -972 mV (Vs. Hg/Hg₂SO₄).

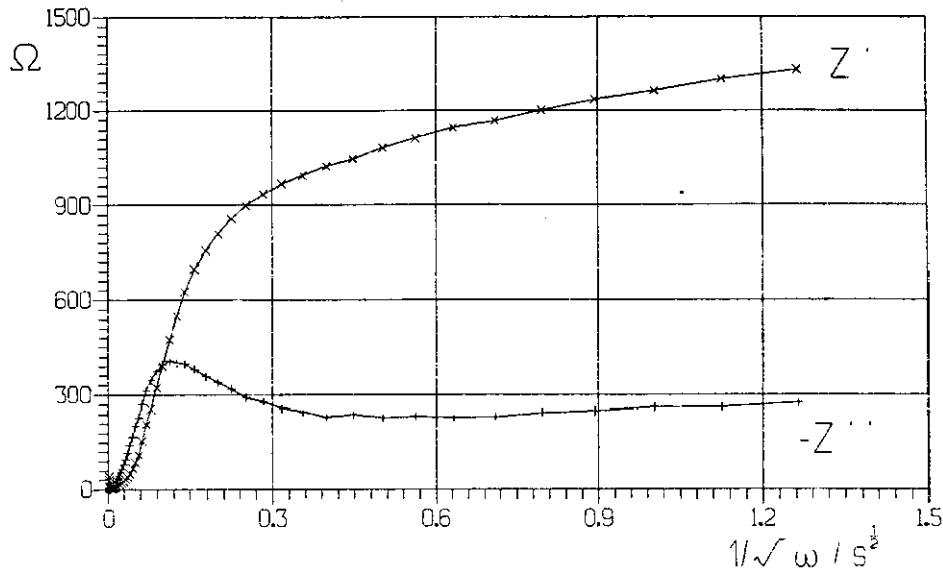
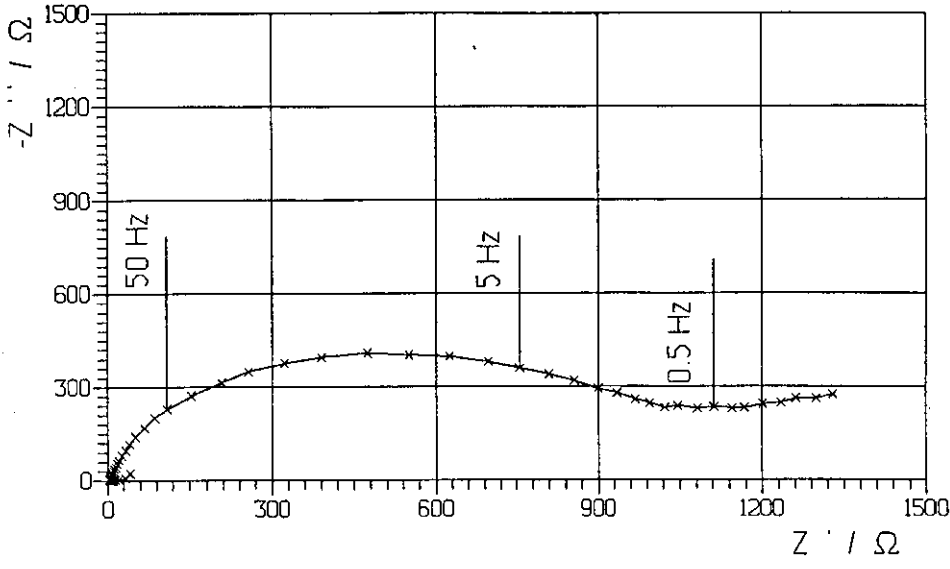


Figure 32

Typical I.S. for 5 mol dm³ H₂SO₄ at 40 °C and -972 mV (Vs. Hg/Hg₂SO₄).

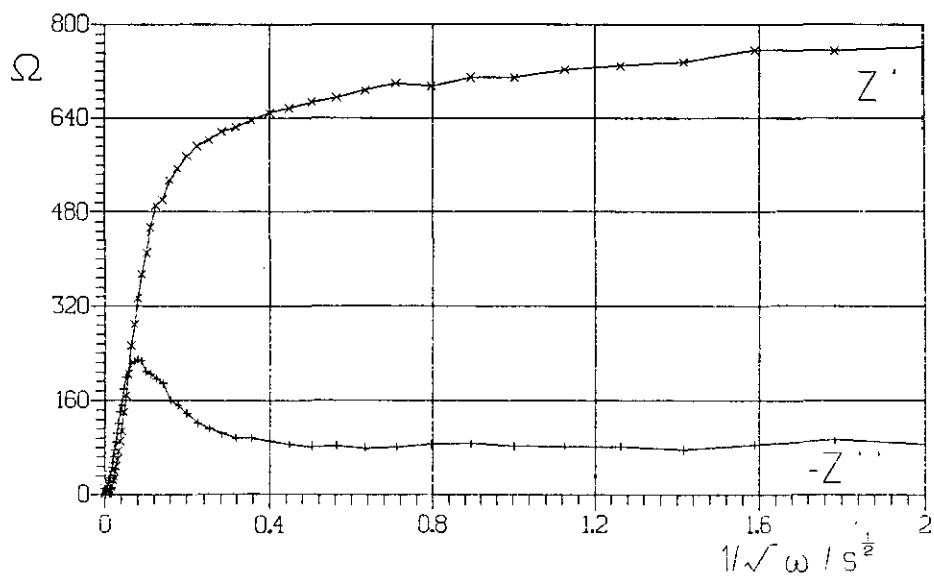
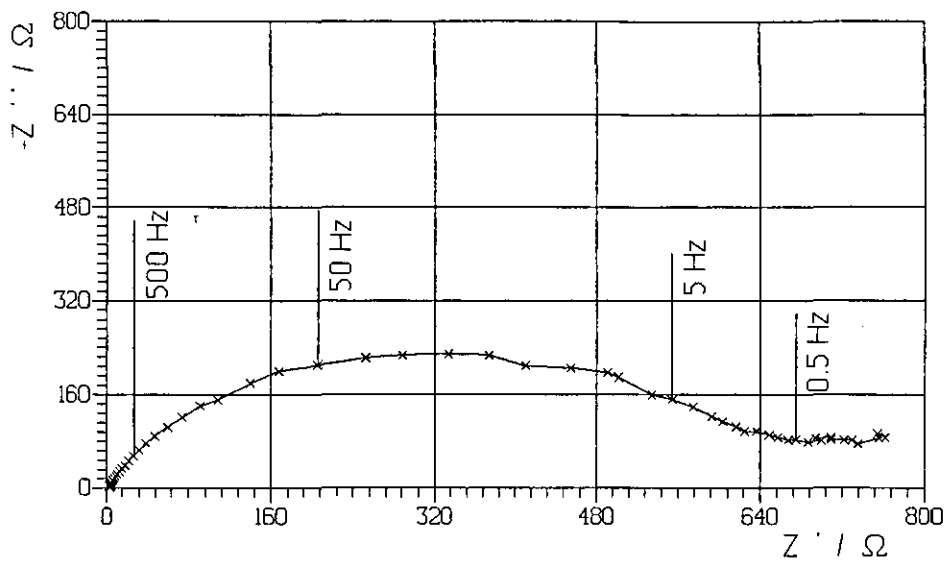


Figure 33

Typical I.S. for 5 mol dm³H₂SO₄ at 60 °C and -972 mV (Vs. Hg/Hg₂SO₄).

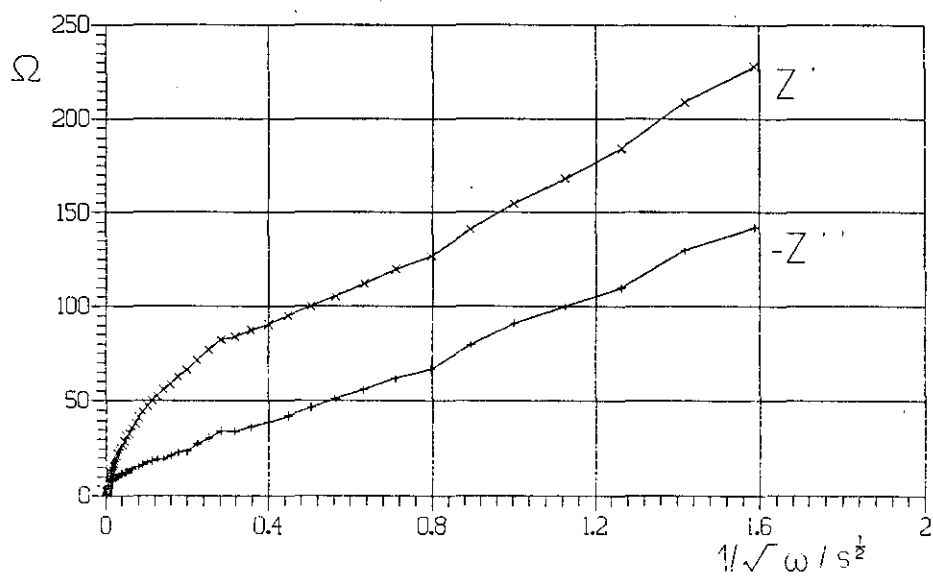
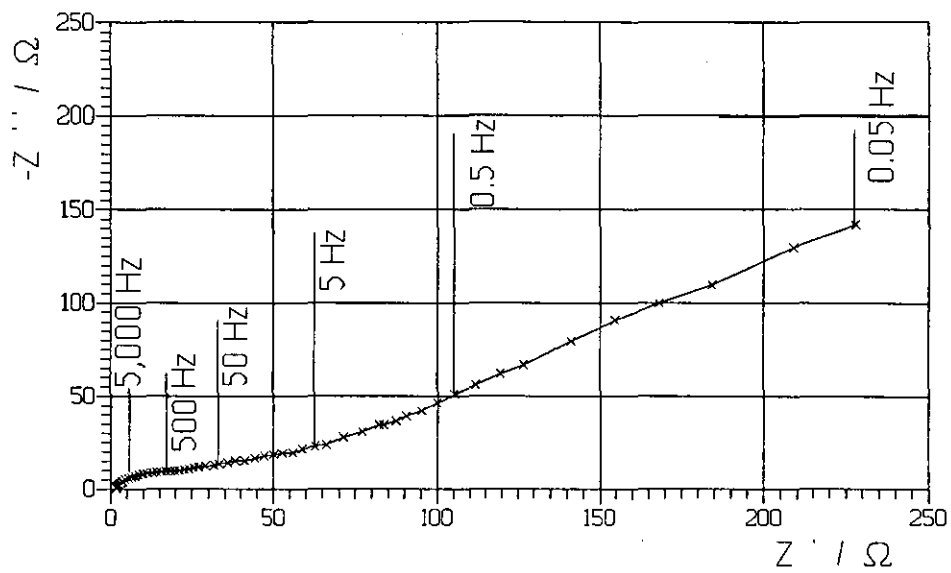


Figure 34

Typical I.S. for $10 \text{ mol dm}^{-3} \text{H}_2\text{SO}_4$ at 25°C and -972 mV (Vs. $\text{Hg}/\text{Hg}_2\text{SO}_4$).

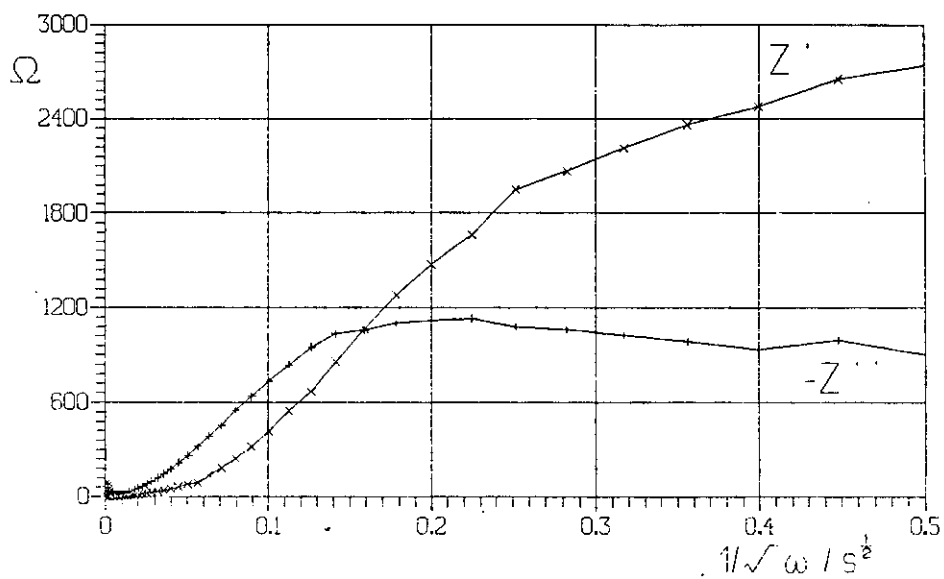
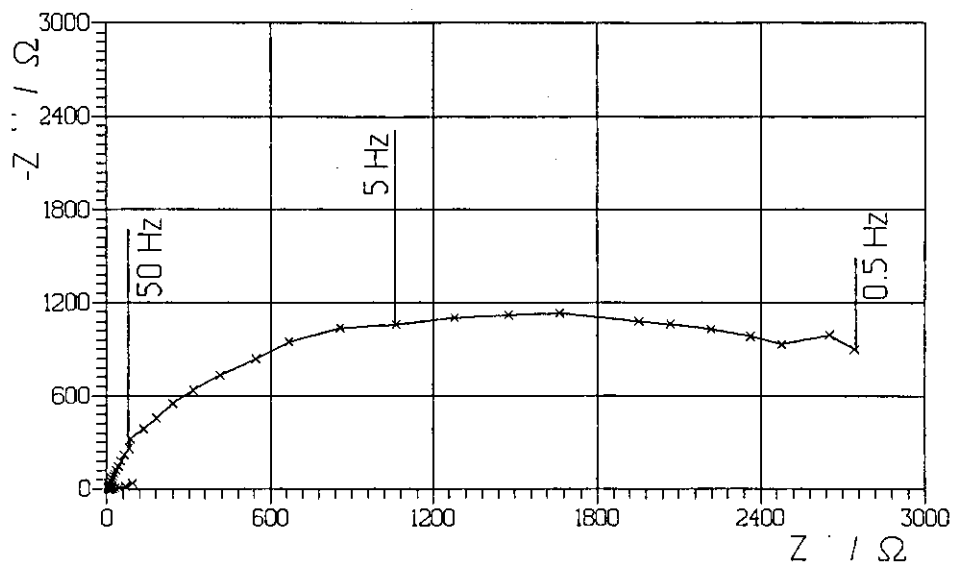


Figure 35

Typical I.S. for 10 mol dm³ H₂SO₄ at 40 °C and -972 mV (Vs. Hg/Hg₂SO₄).

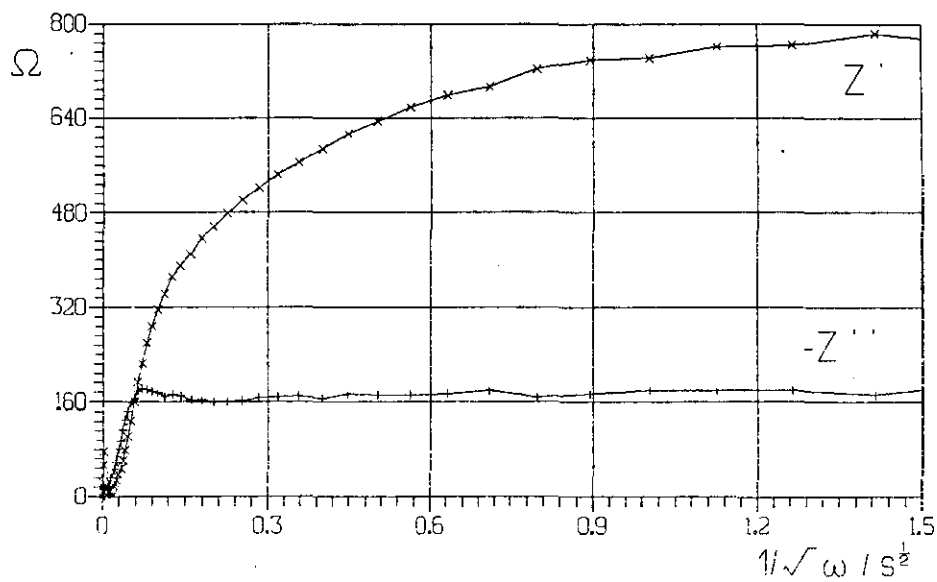
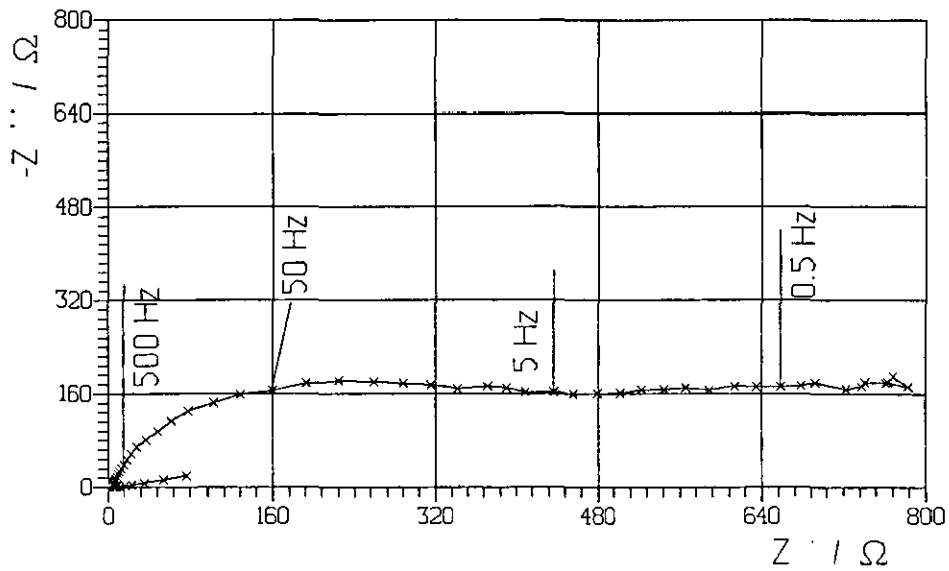


Figure 36

Typical I.S. for 10 mol dm³H₂SO₄ at 60 °C and -972 mV (Vs. Hg/Hg₂SO₄).

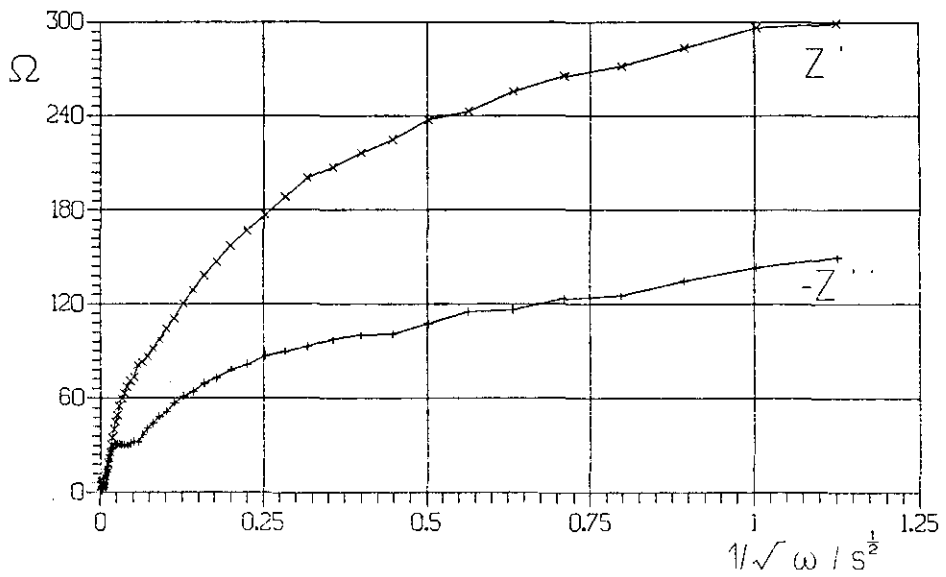
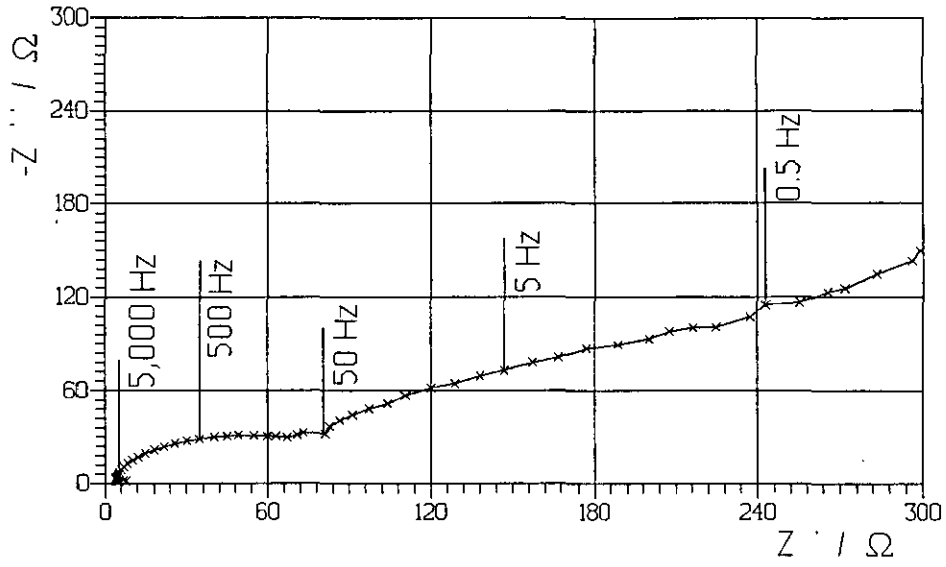


Figure 37

low temperature diagrams (particularly at 25°C) which shows the Warburg tail curving downwards towards the real axis. This behaviour is indicative of a *mixed* solid state and solution process, which can be confirmed by observing that the Randles' plot has a *positive intercept*— thus verifying the presence of an adsorbed species on the electrode surface¹⁰². Also, it can be seen, that a semi-porous electrode surface is indicated by the roughness factor and this was verified by an SEM analysis of the electrode surfaces which showed an irregular, porous layer of prismatic crystals.

One may therefore conclude that low concentrations and/or temperatures produce a poorly compacted, porous layer of lead sulphate crystals. Also from the results discussed in chapter five (page 48), one may conclude that such conditions *probably would not* produce any tightly compacted layer (membrane) and a porous electrode with adsorbed surface species *is* likely.

An increase in the Warburg tail is observed— from a low angle of nearly 25° to about 40°, as the formation temperature was increased. The change in the dihedral angle shows a decrease in the diffusion. If one considers the porous nature of the electrodes (as described above) then one may attribute the rise in the dihedral angle as a closing of the pores— presumably by a growth in the lead sulphate layer. Therefore, although there is a decrease in the diffusion rate (shown by the increasing dihedral angle) there is no evidence of a perm-selective membrane structure.

Increasing either the formation voltage (to +500 mV) or the formation time (to 16 hours), figure 38 for example, increased the sulphate layer thus producing an electrode with a more pronounced adsorption layer otherwise, no other effects were seen.

To illustrate the effect of moving away from the equilibrium potential— figure 39 shows a typical impedance spectrum for the system: 5 mol dm⁻³ H₂SO₄, at 25°C at -960 mV. Here the spectra show a high frequency semi-circle coupled with a low frequency Warburg diffusion dihedral demonstrating a higher rate of diffusion at this voltage— and probably indicating that the system has now moved away from equilibrium.

Porous lead discs (prepared by potentiodynamically cycling a planar lead electrode between lead sulphate and lead 4000 times) were used in a similar experiment to that described above, results from these experiments showed that a porous layer was still present; presumably because sulphation could not occur across the whole surface of the disc in the reaction time*.

* Due to electrical problems no reproducible results can be given.

I.S. for 5 mol dm⁻³ H₂SO₄ at 40°C and -974 mV, and
 Sulphate Layer formed at +500 mV (Vs Hg/Hg₂SO₄)

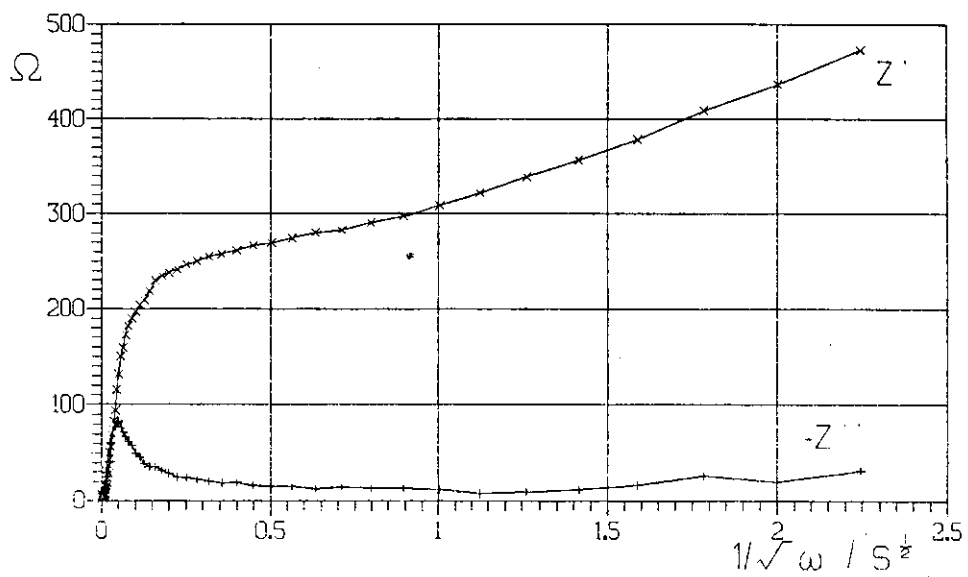
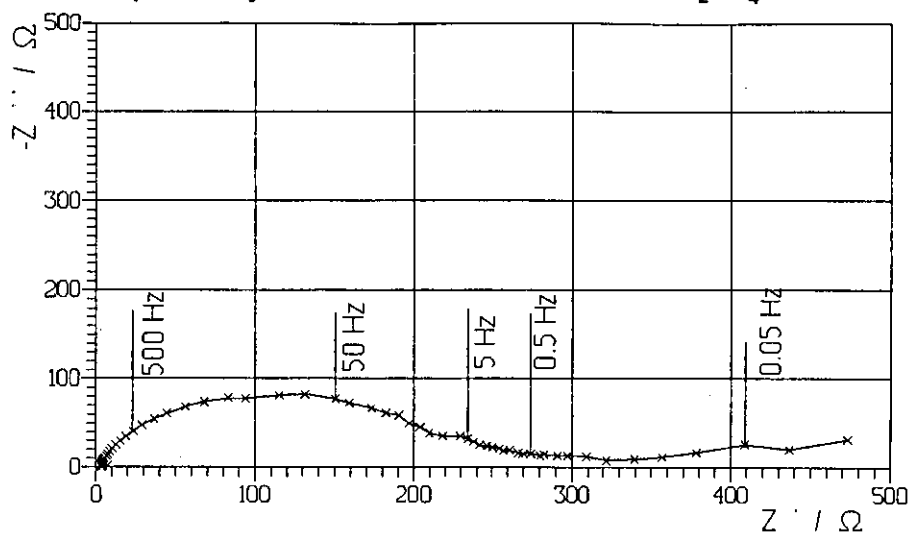


Figure 38

I.S. of 5 mol dm^{-3} at 25°C and -960 mV (Vs. $\text{Hg}/\text{Hg}_2\text{SO}_4$).

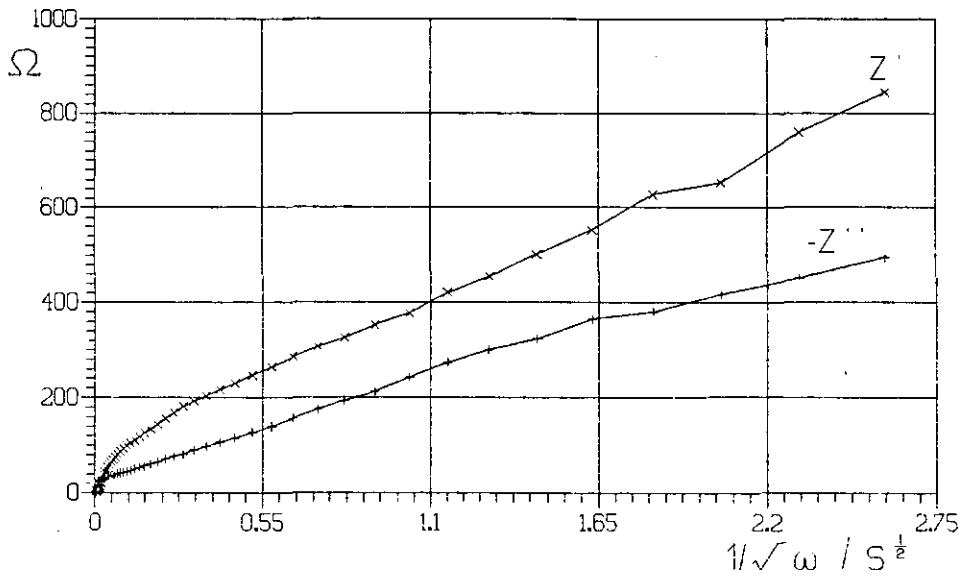
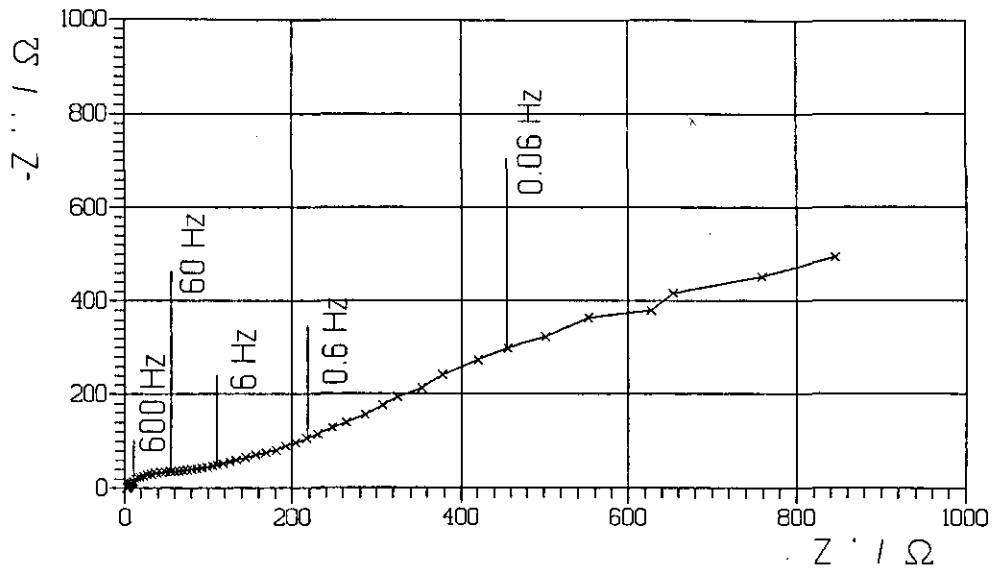


Figure 39

When working with a PbO_2 disc formed on to a Pt disc problems of adhesion and porosity were encountered. The PbO_2 disc would become detached from the electrode during the impedance measurement, probably because the a.c. impedance wave caused a change in the *surface layer* (of Pt— PbO_2), weakening the adhesion of the whole film.

Further Work.

Unfortunately because of time constraints insufficient data was collected to characterise the PbO_2 — PbSO_4 or porous lead systems. This would have been an important set of experiments to perform; first it would validate the Pb— PbSO_4 experiments and, secondly, would have provided important information on the positive plate in the lead acid battery.

Summary.

At lower temperatures (25°C) adsorption of SO_4^{2-} on to the Pb discs electrodes was observed.

When the temperature was raised to 60°C the impedance spectrum was changed to that of a rough, porous electrode.

It was concluded that no lead sulphate membranes were observed.

CHAPTER SEVEN.

X-RAY POWDER DIFFRACTION STUDIES.

7.1 Introduction.

Section 1.2 explained the industrial preparation of the SLI lead acid battery. These types of lead acid batteries employ a pasted plate design and offer good capacity at a relatively cheap price. Improvement in battery design has led, over the years, to changes—in the additives of the paste material, in the physical construction of the battery and in the composition of materials making up the battery plates. Many workers have researched into finding the ‘best’ compound a pre-formed lead acid battery plate should consist of⁶; ‘battery lore’ has stated that *tribasic lead sulphate* is (because of the subsequent formation of β -PbO₂) the preferred material. This section investigates the time of formation of basic lead sulphates from stoichiometric ratios of PbO:PbSO₄ starting materials and whether any change in material composition occurs because of polymeric (PVA, PAA) addition to the paste (used to form MDF-plates, chapter eight).

7.2 Experimental.

7.2.1 Preparation of n PbO·PbSO₄ mixtures.

Fisons’ ‘Analar’ grade yellow (‘massicot’) lead monoxide and lead sulphate (Koch-Light’s ‘Standard Laboratory’ grade) were accurately weighed on a 4 place decimal balance so that the PbO:PbSO₄ mixtures in the ratios: 1:1, 3:1 and 4:1 could be made. These mixtures (of about 1 g) were then finely ground and homogenised in a spectroscopical Ball Mill for 5 minutes.

The powders were then placed in a glass vial, enough distilled water added to fill the vials to about half full and then connected to a vacuum line. Once degassed, the vials were sealed, while still under vacuum, and placed in an oven, at 110°C (to equilibrate the contents to 100°C)**.

* Note: The terms ‘massicot’ and ‘litharge’ are used interchangeably by manufacturers of lead monoxide. This can cause a great deal of confusion as no specific phase is implied. In this work, however, the ‘Joint Committee on Powder Diffraction Standards’ (JCPDS) usage is maintained. That is:

- *litharge* is the orange-red, tetragonal phase of PbO (the α phase); while
- *massicot* is the yellow, orthorhombic phase of PbO (the β phase).

** As closed vials were used an estimate as to their equilibrated temperature when placed in an oven had to be made. It was decided that an oven at 110°C should equilibrate the vials to 100°C.

After 2, 3, 4, 5, 8, 16 hours and 1, 2, 3, 4 and 7 days the vials were opened, the contents filtered (using a Büchner flask) while still hot and freeze dried using liquid nitrogen. An X-ray Powder Diffraction (XPD) pattern was then run.

7.2.2 Materials Produced using PVA and PAA surfactants.

After curing and formation of the battery plates (chapter eight) a small slug from between one of the grids was removed— this being subsequently used for XPD analysis*.

7.3 Results and Discussions.

7.3.1 Lead Monoxide & Lead Sulphates Mixtures.

XPD patterns of the original pure PbO and PbSO₄ materials are given in figures 40 & 41**. Figures 40 & 41 patterns can be identified, within experimental error, by JCPDS cards 5-0570 (*massicot*) and 5-0577 (*anglesite*), respectively. The XPD patterns of 1:1, 3:1 and 4:1 PbO:PbSO₄ mixtures are shown in figures 42 to 44. By inspection of the originals (figures 40 & 41) these patterns can be identified as simple mixtures of lead monoxide and lead sulphate in the specified ratios***.

Results from the basic lead sulphate formation time experiments were all very similar; figures 45 to 47 show typical patterns obtained for the 1:1, 3:1 and 4:1 mixtures respectively. Comparison with JCPDS diffraction cards show that *mono-* (33-1486, Pb₂(SO₄)O), *tri-* (29-781, Pb₄O₃SO₄·H₂O) or *tetra-* (6-0283, PbSO₄·4PbO) basic lead sulphates, respectively, had been formed.

One may conclude from this that the reaction time kinetics to form basic lead sulphates from lead monoxide and lead sulphate is *less than 2 hours*. Recently work by Pavlov and Kapkov¹⁰³, using wet analysis and XPD techniques have shown that basic lead sulphates are produced within the first hour— initially being detected in the first 15 minutes. Therefore the preparation regime for the curing of the lead oxide pasted plates (using a three day curing period, chapter eight) should be sufficient to convert the material to tribasic lead sulphate.

* Part of the slug taken from the formed plate was used for BET and mercury porosimetry *first*, the remainder being used for XPD. This limited the amount of material which was available for XPD work.

** Only the *major* peaks in the XPD pattern are shown in the associated tables.

*** Due to *preferred orientation* (section 2.7.2.1) it is not possible to give quantitative percentages of components in mixtures using an XPD pattern.

XPD of Lead Monoxide

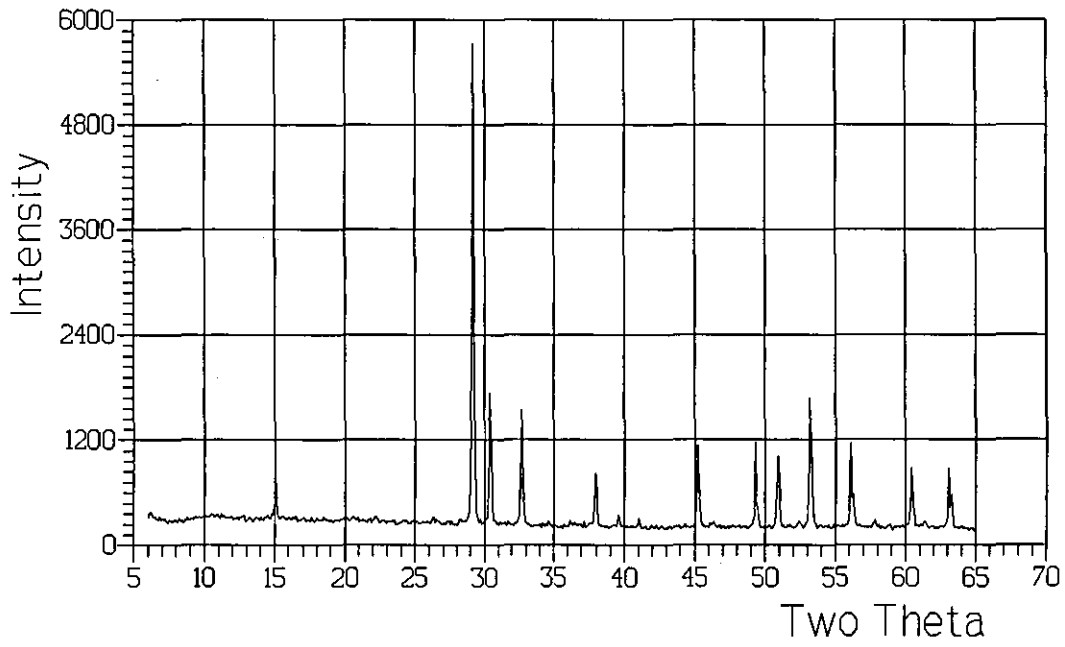


Figure 40

Two Theta:	D Value:	Intensity:
29.2	3.06	100
30.4	2.94	28
32.7	2.74	24
45.2	2.01	18
49.3	1.85	18
53.2	1.72	27
56.1	1.64	18

XPD of Lead Sulphate

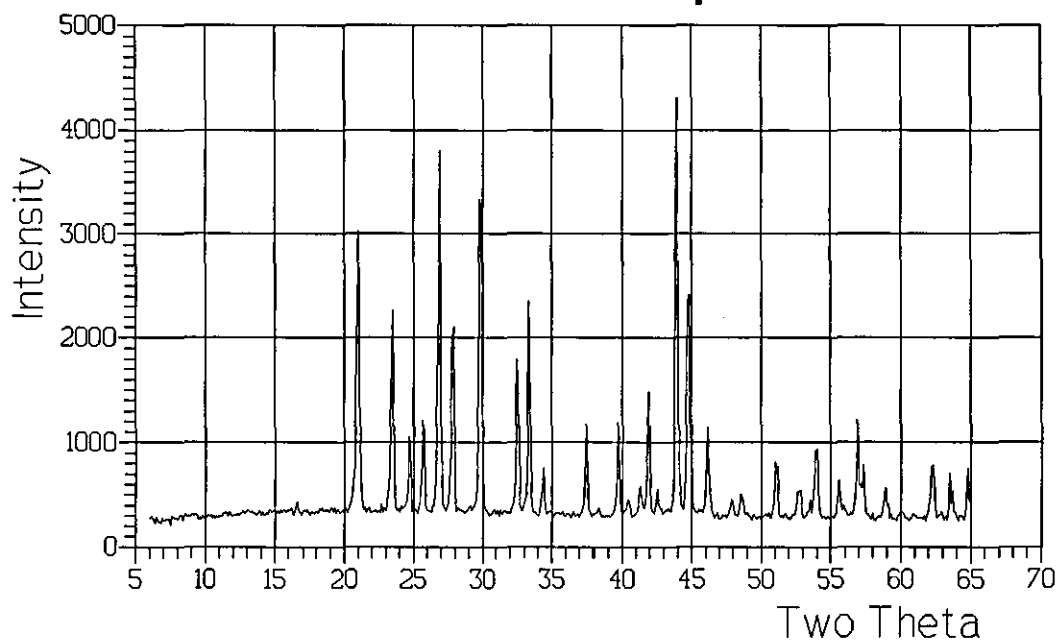


Figure 41

Two Theta:	D Value:	Intensity:
21.0	4.23	67
23.5	3.79	48
24.7	3.60	19
25.7	3.47	22
26.9	3.31	87
27.9	3.20	45
29.8	3.00	75
32.5	2.75	38
33.3	2.69	51
37.5	2.40	22
39.7	2.27	23
41.9	2.16	30
43.9	2.06	100
44.8	2.02	53
46.1	1.97	22
56.9	1.62	24

XPD of 1:1 Lead Monoxide - Lead Sulphate Mix

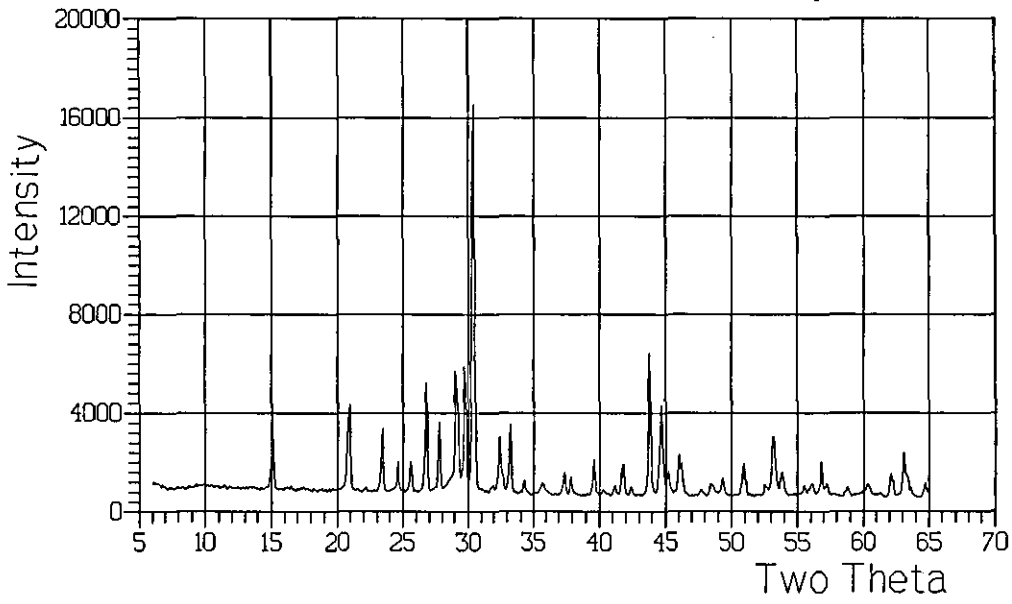


Figure 42

Two Theta:	D Value:	Intensity:
15.2	5.83	13
21.0	4.23	23
23.5	3.79	17
26.9	3.31	28
27.8	3.21	18
29.8	3.00	33
30.5	2.93	100
33.3	2.69	18
43.9	2.06	37
44.8	2.02	23
53.3	1.72	15

XPD of 3:1 Lead Monoxide - Lead Sulphate Mix

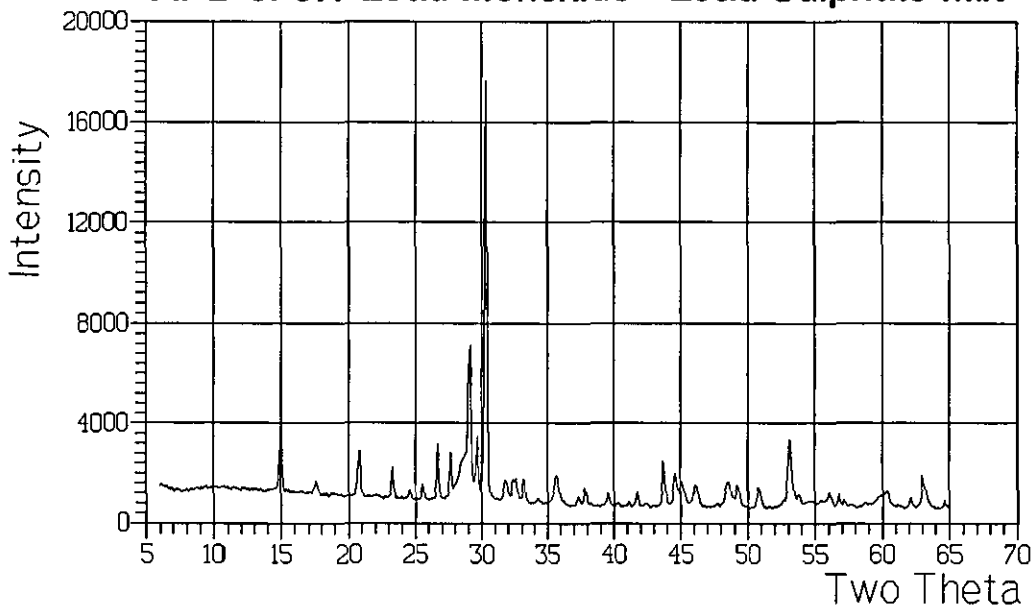


Figure 43

Two Theta:	D Value:	Intensity:
15.1	5.87	18
20.9	4.25	12
26.8	3.33	14
29.2	3.06	37
30.4	2.94	100
53.2	1.72	16

XPD of 4:1 Lead Monoxide - Lead Sulphate Mix

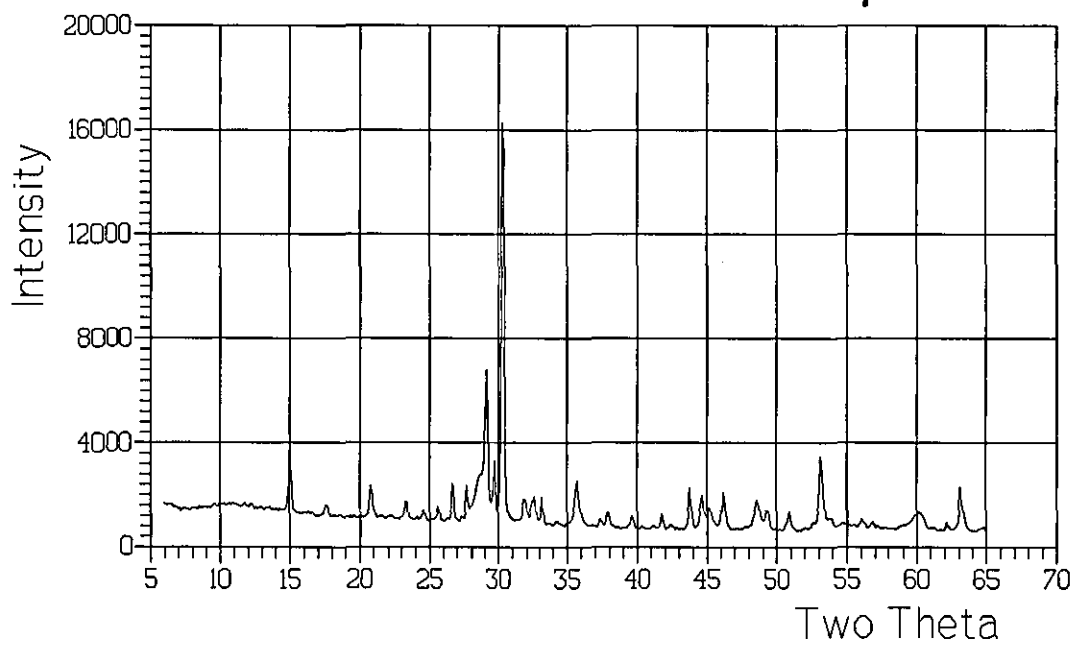


Figure 44

Two Theta:	D Value:	Intensity:
29.2	3.06	38
29.8	3.00	16
30.4	2.94	100
53.2	1.72	18

XPD of 1:1 Lead Monoxide - Lead Sulphate Mix After 3 Hours.

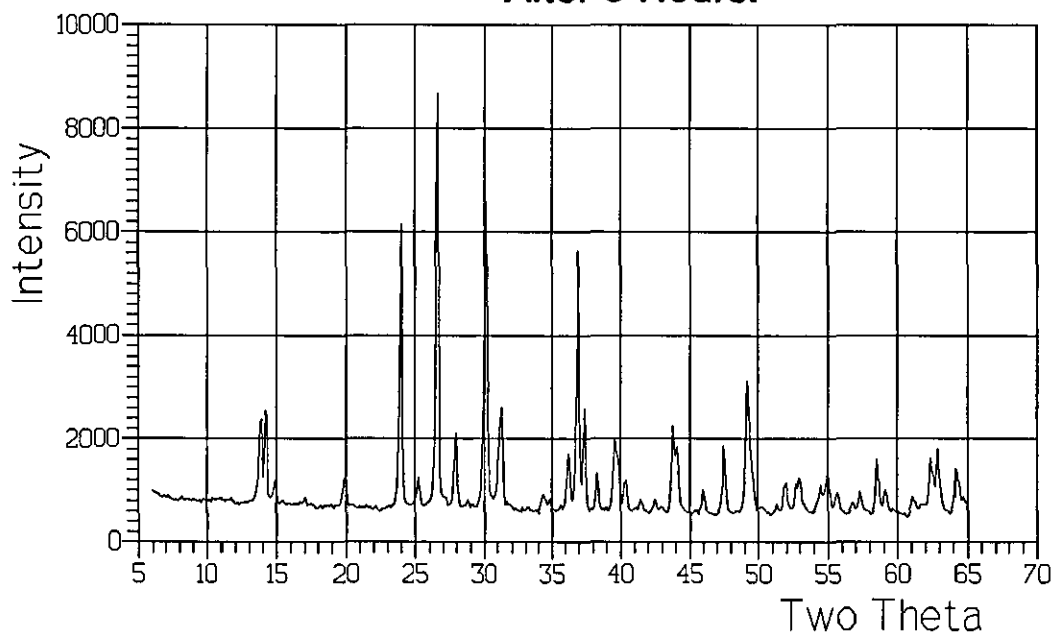


Figure 45

Two Theta:	D Value:	Intensity:
14.0	6.33	22
24.1	3.69	69
26.7	3.34	100
28.1	3.18	19
30.2	2.96	74
31.4	2.85	25
36.3	2.47	15
37.0	2.43	63
37.5	2.40	26
39.7	2.27	18
43.9	2.06	21
47.6	1.91	17
49.3	1.85	33
63.0	1.48	16

XPD of 3:1 Lead Monoxide - Lead Sulphate Mix After 3 Hours.

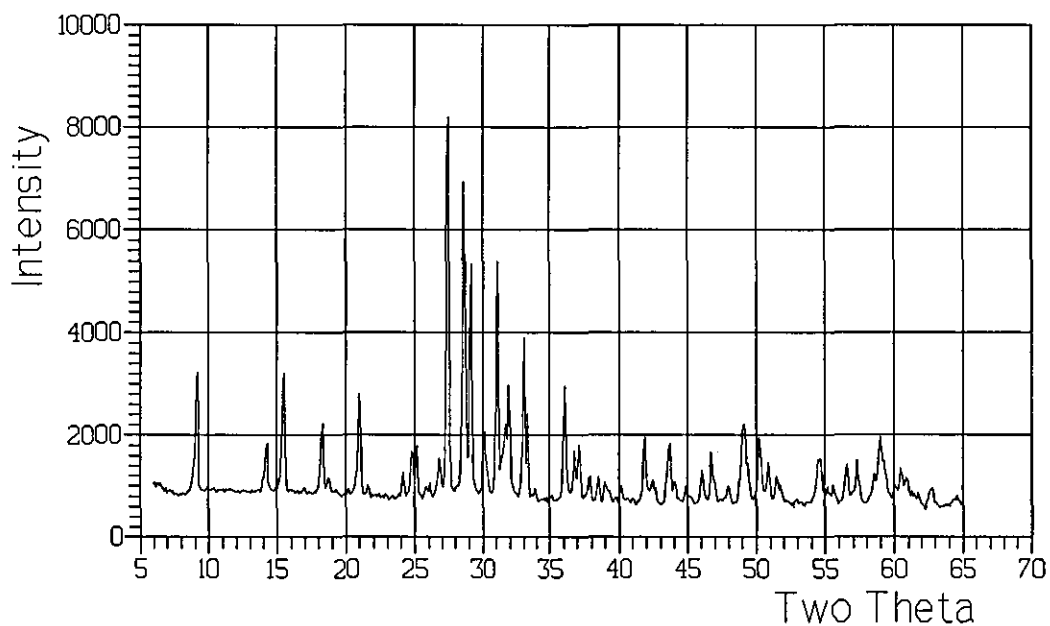


Figure 46

Two Theta:	D Value:	Intensity:
9.2	9.61	33
15.5	5.72	32
18.3	4.85	19
21.0	4.23	28
27.5	3.24	100
28.6	3.12	83
29.1	3.07	62
31.1	2.88	63
31.9	2.81	30
33.0	2.71	43
33.3	2.69	22
36.1	2.49	31
41.9	2.16	18
49.1	1.86	22
50.2	1.82	18
59.0	1.57	18

XPD of 4:1 Lead Monoxide - Lead Sulphate Mix After 3 Hours.

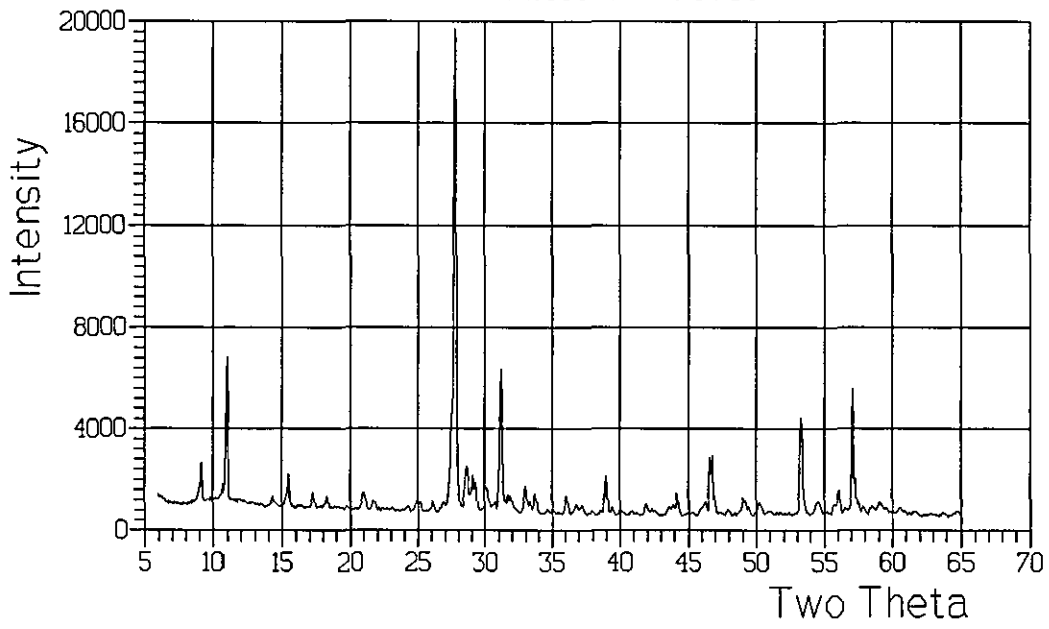


Figure 47

Two Theta:	D Value:	Intensity:
11.0	8.04	32
27.7	3.22	100
31.2	2.87	30
53.3	1.72	20
57.1	1.61	26

It is known that tetrabasic lead sulphate is produced above $70^{\circ}\text{C}^{28,103,104}$, whereas below this temperature tribasic lead sulphate is predominate. Pierson¹⁰⁵ found, at 83°C and 100% humidity that tribasic lead sulphate is converted to tetrabasic lead sulphate in 10 to 40 hours while Pavlov & Papazov¹⁰⁶ found that tetrabasic lead sulphate is formed from tribasic lead sulphate in the presence of PbO. The work here, however, shows that although high temperature and 100% humidity were used, only the stoichiometric material was produced in each case; no mixtures were observed— even in the presence of PbO. This implies that the effect of pressure also plays an important role in the formation of these compounds*.

Further Work.

A continuation of this work to include different temperature, pressure and starting material composition (excess amounts of PbO) would be invaluable in elucidating the stability of *mono-*, *tri-* and *tetra-* basic lead sulphates at various pressure. Whereas much work has been carried out in assessing the reaction of lead sulphates at various temperatures the fact that pressure builds up within the cured plates (due to unit cell changes) has not been considered.

7.3.2 MDF Cement Technique and XPD.

Figure 48 shows a typical XPD pattern of the cured, positive plate material. Although this pattern is of a complex nature, *tribasic lead sulphate* (card 29-781) can be seen to be the main constituent. These XPD patterns do not vary with type of polymer.

Figure 49 shows a typical pattern of a formed positive plate, again the pattern did not change when the polymer modified material was tested. This pattern is complex but $\beta\text{-PbO}_2$ (card 25-447, *patnerite*) can be identified. The remaining peaks in the pattern are probably of lead sulphate.

Summary.

Basic lead oxide sulphates were formed within 2 hours. Therefore the curing regime of the pasted plates for MDF investigations (chapter eight) would be expected to entirely convert the leady oxide paste to tribasic lead sulphate.

* The vapour pressure of water raises steeply with temperature and although 1 atmosphere pressure was attempted a higher pressure could have occurred.

Typical XPD Pattern of A Cured PVA, PAA or Water Treated Plate.

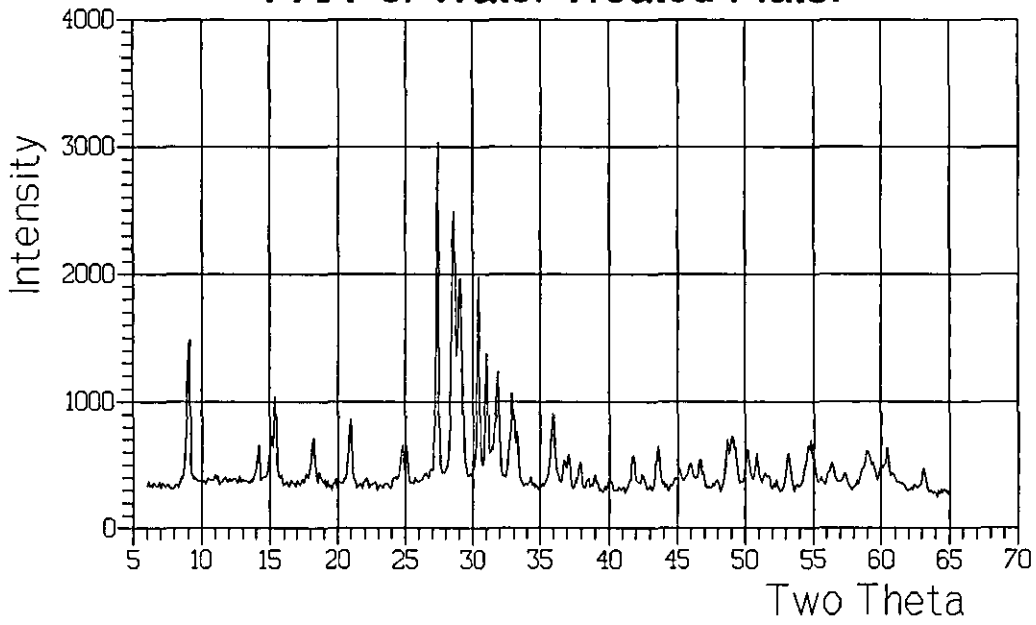


Figure 48

Two Theta:	D Value:	Intensity:
9.1	9.72	44
15.4	5.75	27
20.9	4.25	20
27.4	3.25	100
28.6	3.12	80
29.1	3.07	61
30.4	2.94	61
31.9	2.81	34
32.9	2.72	28
36.0	2.49	23

Typical XPD Pattern of A Formed PVA, PAA or Water Treated Plate.

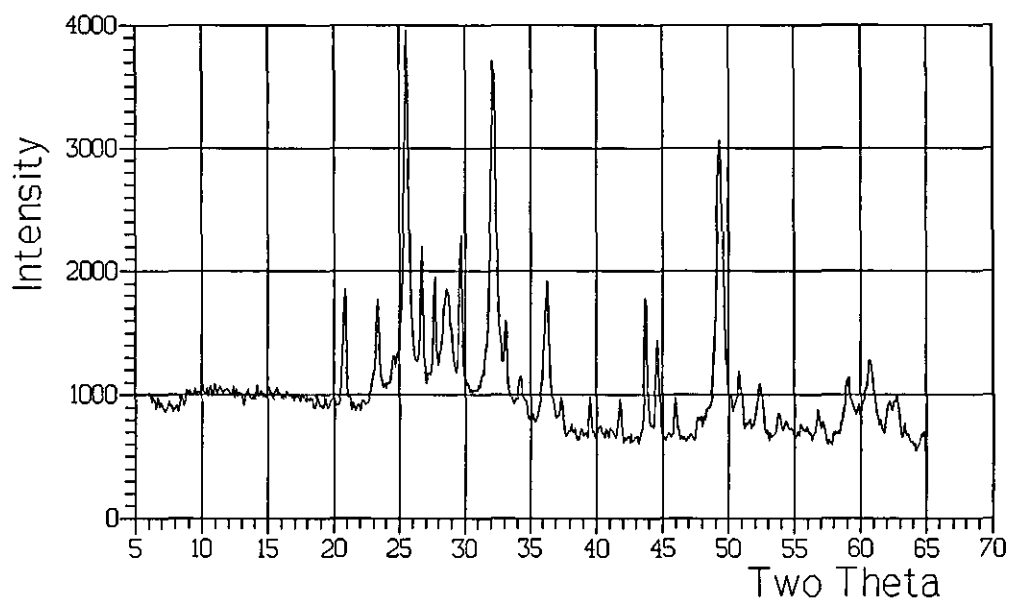


Figure 49

Two Theta:	D Value:	Intensity:
20.8	4.27	32
23.3	3.82	29
25.5	3.49	100
26.7	3.34	43
27.7	3.22	35
28.6	3.12	32
29.7	3.01	46
32.1	2.79	92
33.1	2.71	24
36.3	2.47	43
43.7	2.07	38
44.6	2.03	27
49.3	1.85	80
50.8	1.80	19
59.1	1.56	18
62.7	1.48	19

Pressure—as well as temperature, humidity, excess PbO and reaction time—should also be considered when analysing the formation of the basic lead sulphates.

Investigation of cured and formed 'MDF' plates showed no difference in the XPD pattern (compared with the control samples) and therefore it is concluded that the addition of PVA and PAA did not significantly affect the composition or phase of battery material produced.

CHAPTER EIGHT.

MACRO DEFECT FREE PASTE STUDIES: Electrochemical Cycling of Positive Pasted Plates.

8.1 Introduction.

Macro defect free cement technology (section 1.5.2) increased the strength of cement to approximately that of aluminium by the reduction of large pores in the structure. The reduction of these large pores was achieved by various means, but was essentially a conditioning process whereby a surfactant was added to prevent early agglomeration of material and the removal of any trapped air (the macro defects) could be achieved by working of the material.

In these experiments similar ideas were used to try to increase the *strength* of the battery paste, and thus prolong plate cycle life. Two surfactants, which are in widespread use in the cement industry, were selected for trial: polyvinyl alcohol (PVA) and polyacrylic acid (PAA).

8.2 Experimental.

8.2.1 Preparation of PVA and PAA solutions.

The preparation of PVA and PAA solutions is described in chapter 4, page 43.

8.2.2 Linear Sweep Voltammetry: Voltage Stability of PVA and PAA.

Linear sweep voltammetry of PVA and PAA in non-aqueous media was used to determine the stability of the polymers at high voltage. The circuit used for these experiments is shown in figure 26, and described section 4.2.1. The solvent chosen for these experiments was dimethylsulphoxide (DMSO), a support electrolyte of tetrabutylammonium tetrafluoroborate (TBTFB) was added to increase the conductivity of the DMSO-polymer solution.

Results showed: that both PVA and PAA were stable throughout the voltage range: -2 to +2 V. One may assume, therefore, that no break-down products were formed during the cycling experiments described in this chapter and changes which occurred to the pastes were because of PVA or PAA additives.

8.2.3 Preparation of Positive Plate Material Containing PVA or PAA.

Pastes were prepared by weighing out an amount of P10 (*Chloride plc*) sulphated lead oxide paste (200 g) to make up leady oxide:polymer wt/wt ratios of 0.23, 0.12, and 0.0% (i.e. plain paste). This was achieved by adding a slurry of the selected polymer and grey leady oxide powder, so that the final liquor content—and therefore the *paste density*—was comparable with that of the original P10 paste*.

The polymer and control pastes were placed inside a polythene bag and worked by hand in order to reduce the number of large air pockets trapped in the sample (i.e. *macro defects*). Finally a vacuum line was then attached to the bag containing the paste, and working of the material continued, for several minutes, prior to grid pasting.

Subsequent experiments showed that PAA was worthy of more detailed investigation and therefore additional pastes containing 0.63, 0.94 and 1.15% PAA were prepared.

8.2.4 Preparation of Positive Grids.

After the paste samples were thoroughly mixed they were pasted on to cut, accurately weighed, 9% Sb lead grids (from *Chloride plc*), of average dimensions 5.5 by 4.9 by 0.18 cm, using a plastic spatula. Before use all the grids had a long, 99.999% Pb lead carefully soldered on to one of the apexes of the grid. This contact was completely sealed with PTFE tape. The plates were then transferred to a beaker, positioned to remain upright and then this beaker was placed into a larger beaker which contained water. The larger beaker was covered and the plates cured at room temperature (20°C), in a humid atmosphere, for three days. After which time the beaker, containing the plates, was removed to an oven, at 90°C, for a further three days. This removed the moisture from the plates, and prevented 'flaking' during formation.

When the plates were removed from the oven they were immediately placed into a desiccator until required. Just before a plate was taken to be formed a small 'slug' of the plate was gently removed from between the grid wires for XPD investigations.

8.2.5 Formation Cycle.

The cured pasted plates were accurately weighed and then immersed in a 0.5 mol dm⁻³ H₂SO₄ forming solution held at 25°C using a thermostatically controlled water heater-stirrer. A forming current of C/15 was then passed (where C is the current required to completely discharge the plate in *one hour*—

* Experimental analysis of P10 paste previously established a liquor content of approximately 10% (wt/wt).

assuming that the active material is tribasic lead sulphate: i.e. $3\text{PbO}\cdot\text{PbSO}_4$). This rate was used to approximate the forming current in industry.

The schematic diagram for the forming (and cycling) apparatus is shown in figure 50. This used a Kemitron CP/M microcomputer to operate relays so that a plate could undergo either forming/charging, rest or discharge by switching between *one* galvanostat (a Thompson 'mini' potentiostat set galvanostatically) for charging, and the other for discharging. Two '8 bit' Digital-to-Analog Converters (DAC) were used to switch the relays of each galvanostat. This provided complete isolation of the equipment when a galvanostat was not in use. A separate '12 bit' Analog-to-Digital Converter (ADC) was permanently set between the reference electrode (RE) and plate, enabling voltage readings to be made by the computer (particularly important for cycling work, see section 8.2.6). The secondary electrodes (SE) were *two* SLI type negative plates (i.e. they contained a 'Spongy lead' active mass supported by a 9% Sb lead grid, supplied by *Chloride plc*) covered with a microporous grid separator (Porvic 1, see section 5.2.5) to prevent any 'shorting' with the working electrode (WE), while still providing a 'double sided', unimpeded current flow.

The following forming regime was followed: 16 hours charge, 2 hours rest, 4 hours charge, 2 hours rest and, finally, 4 hours charge. The timings were controlled by the computer programme (Appendix 3, page 80), and apart from replenishment of any evaporated water from the water bath or electrolyte, nothing further was required. This 'charge-and-standby' regime allowed any occluded gas to escape from the active material— thus reducing flaking and crumbling of the plates during the cycling experiments.

To remove any sulphuric acid (and so aid drying and prevent self discharge) the plate, once forming was complete, was soaked in distilled water for 2 minutes then washed under running, distilled water for 30 seconds and carefully dried between tissue paper before being stored in a desiccator (for 24-48 hours). The weight of the formed plate was then taken. Two small 'slugs' were removed from between two grids and the plate reweighed. These slugs were placed in a small sealed sample tube and stored in a desiccator, until required for porosity measurements (see 8.2.7). The thickness of the plate was then recorded using a micrometer at *nine* different places on the plate.

8.2.6 Cycling.

The same equipment as used in the forming process, figure 50, was used for the cycling experiments. In this case, however, 5 mol dm^{-3} sulphuric acid replaced the 0.5 mol dm^{-3} sulphuric acid used in the forming cycle and *two galvanostats* were required: one for controlling the charging process and the other for controlling the discharging process. A charge/discharge regime of C/5 was selected to match typical SLI battery current handling characteristics. The computer was used to record: the Top Of Charge voltage

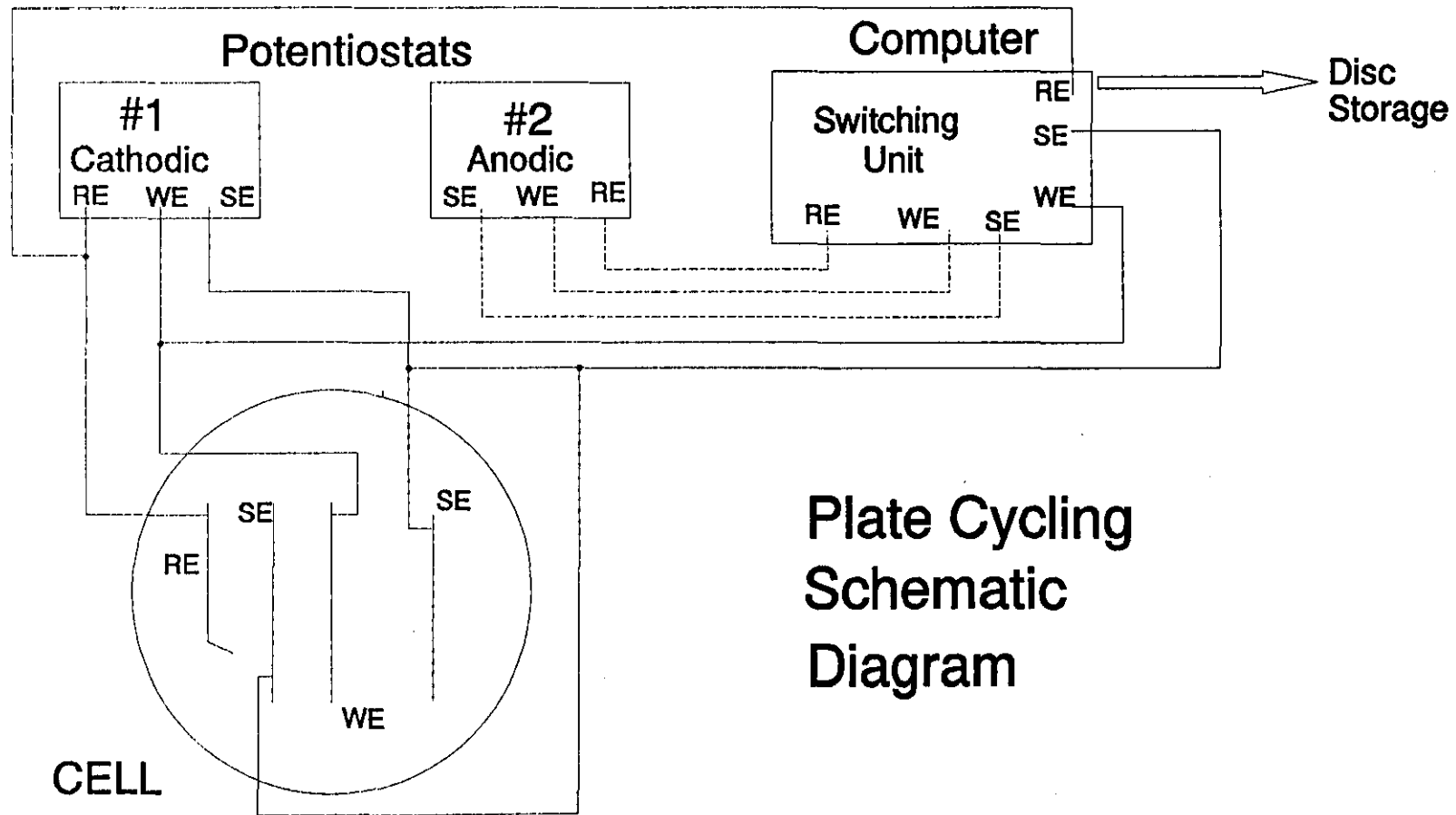


Plate Cycling Schematic Diagram

Figure 50

(TOC) (with respect to the Hg/Hg₂SO₄ reference electrode), the Time For Charge (TFC), Time For Discharge (TFD) of the plate and Total number of Cycles. This data was then stored on floppy disc.

The TOC voltage taken by the programme (Appendix 4, page 82) was determined by the following method: the plate voltage was continuously measured for the oxygen evolution plateau where there would be *little* rise in voltage with respect to time (taken to be not more than 2 mV in 4 minutes). To prevent any lower plateau region confusing the computer, the computer first ensured that the voltage was above +1500 mV before calculating dV/dt. Once a stable plateau region was found, the computer then performed a 20 minute overcharge to allow as much conversion to lead dioxide as possible. After this time the TOC voltage was recorded, the charging current turned off and the computer switched into a 'rest' cycle of 15 minutes, allowing most of the occluded gas to escape.

The plate then entered a discharge cycle, the TFD being determined when the plate voltage fell to +800 mV. This value was found, experimentally, to be just above the *cascade voltage* when complete reversal of the electrodes would occur if further galvanostatic discharge was allowed to continue. Immediately after this time was found, the plate was switched back to a charging regime, preventing as much sulphation of the heavily discharged plate as possible, and the process was repeated. Failure of a plate was taken to be when the TFD had been reduced to 80% of its highest value. In this way many more plates could be investigated in the time available.

When failure occurred, the plate was soaked in distilled water for 2 minutes, washed under running, distilled water for 30 seconds and carefully dried between tissue paper before being stored in a desiccator for 48 hours. The weight of the plate was taken and the surface thickness recorded (at the nine different places recorded during forming). Finally, two or three 'slugs' were removed from between the grids and stored in a small sealed sample tube then placed in a desiccator.

8.2.7 Surface Area/Porosity Measurements.

Macro defect free cement technology enabled large voids from cement pastes to be removed, which increased the strength of the cement. In these experiments PVA and PAA were added to the lead acid battery paste in an endeavour to increase its strength— and subsequently its cycle life/capacity. In order to observe what porosity changes may have occurred the following two surface area measurements were employed.

8.2.7.1. Mercury Porosimetry.

A Micromeritics pore-sizer 9305 was used. This machine allowed a semi-automated porosity measurement to be made by the intrusion of metallic mercury into evacuated pores present in the sample. The amount of intrusion was measured electronically as a change of capacitance between the outside of the sample container and the inside; a value which depends on the amount of mercury present between two contacts (an external silvered surface and the intruding mercury). Pore diameter sizes in the range 120 to 0.006 μm can be practically investigated; these values correspond to mercury intrusion pressures of 0.01 to 207 MPa. Calculation of pore size and distribution was readily determined by a microcomputer programme using standard cell constants supplied with the machine.

8.2.7.2. Brunauer, Emmett, Teller (BET) Measurements.

BET measurements, as pointed out in section 2.5.2, form a method of surface area analysis for smaller pores than those that can be determined by mercury porosimetry. A Micromeritics 2205 high speed surface area analyzer was used to determine the 'micro-pore' surface area. The instrument uses argon gas as the adsorbent and consists of a number of metallic tubes on to which special, long necked glass bulbs can be placed. A sample is carefully placed into the bulb which is then attached to one of the tubes, by means of an air tight seal. The sample is then heated for 2 hours while a vacuum is applied to remove sample moisture. Next, the sample is cooled using iced water for half an hour. After which time a set of internal bellows automatically measures the dead volume in the tube and bulb on a digital read-out. Argon is then introduced into the tube, while the sample is cooled with liquid nitrogen. The bellows are then switched in and a new reading is obtained. This directly measures the sample's surface area in cm^2 . The weight of the dried sample is then obtained and the surface area per gram calculated.

8.2.8 Atomic Absorption.

Atomic absorption spectroscopy (using a Shandon Southern A3400 atomic absorption spectrophotometer) was used to determine the levels of contaminants/impurities present in the cycling experiments— where small amounts of Cu, Sb or Fe could effectively 'poison' a plate*. Table 6* outlines conditions set so that the best sensitivity and precision were achieved. A stoichiometric air/acetylene flame was used (except for Cu, when a fuel lean mixture was used).

To determine whether *back titration* analysis was required, both back titration and standard addition methods were performed for each element and compared. It was found that results from the two

* Note: Although Pb is mentioned here, this refers to the Atomic Absorption settings used for measurements in section 8.3, page 69.

Detection element:	Detection wavelength / nm	Lamp Current /mA	Detection Limit /mg dm ⁻³
Cu	324.8	4.0	0.035
Sb	217.6	11.0	0.35
Fe	248.3	11.0	0.06
Pb	217.0	8.0	0.10

Table 6 Atomic Absorption Detection Limits.

methods were, within experimental error, the same and so the simpler method of standard solution was chosen as the normal analysis procedure.

Results showed: that levels of Cu, Sb and Fe were below experimental detection limits in all experiments.

8.3 Results and Discussion

Tables 7 to 9 show the results obtained from the cycling experiments for a variety of parameters.

The paste loss, plate thickness and weight of active material (before and after cycling) show the loss of material due to *mechanical stresses* built up by *volume changes* (associated with cycling between PbO₂ and PbSO₄)— a reduction in the paste loss per cycle being one possible benefit which MDF technology may have achieved.

Surface area (BET) and porosity (mercury porosimetry) measurements record the ability of the surfactants to reduce the macro pores (the macro defects) while keeping the micro pores available for the electrolyte.

The capacity per cycle and top of charge potential show the number of cycles required to reach the maximum *utilisation* of the active material and the overpotential required to recharge the paste, respectively. The time required to reach the maximum utilisation indicated that a restriction was imposed upon the sulphuric acid by smaller pores—and their distribution. While any change in the top of charge voltage (TOC) indicates the degree of isolation of active material.

If the dividing line between *micro* pores and *macro* pores is in the range 1 - 0.25 μm²⁹ and one combines the mercury porosimetry and BET results, the following conclusion can be drawn:

1. Neither surfactant affected the weight loss per cycle.

The ability of MDF cement strategy to increase battery paste strength— by eliminating macro pores— was limited by its water susceptibility; recurrence of macro pores, and the subsequent weakening of the cement structures, restricts the use of MDF cement technology to moisture free environments^{107,108}. If one considers the normal, aqueous-sulphuric acid systems used in the lead acid battery one sees that ideal conditions for the creation of macro pores are present. Moreover, because of *volume changes* associated with cycling between PbO₂ to PbSO₄ if removal of all macro pores (defects) is achieved, this could restrict the expansion of the paste, cause mechanical stresses to build up inside the active material and augment shedding or crumbling of the paste. The fact that there is no significant change in weight loss per cycle shows that weakening of the active material by either PVA or PAA is not a problem.

TYPE*:	Number of Cycles	Weight of Paste in Plate / g	TOC (max) / mV	TOC (min) / mV	Maximum TFD / minutes	Cumulative Total TFD / minutes	Maximum Capacity of Plate / mA hours g ⁻¹	Total Plate Capacity / A hours g ⁻¹
%Deviation:	12	12 [#]			11 [#]	16 [#]	18	16 [#]
PVA:								
0.12%	45	32.82	1639	1579	77.5	3044	57.0	2.24
0.23%	51	34.61	1695	1569	74.0	3353	51.5	2.35
PAA:								
0.13%	57	39.71	1690	1625	65.5	3302	48.1	2.43
0.23%	45	40.10	1682	1615	69.5	2757	51.1	2.03
0.63%	62	32.83	1635	1579	91.0	4909	66.9	3.61
0.94%	78	37.59	1638	1577	73.0	4909	53.6	3.61
1.15%	48	35.05	1655	1512	81.5	3517	59.9	2.59
Plain Paste:								
(0.0%)	50	38.85	1660	1589	77.6	3499	57.0	2.57

Table 7

* Notes:

- (1). TOC means the Top Of Charge (maximum or minimum) for the plate over its cycle life.
- (2). All readings are an average of two readings (five for plain paste).
- (3). [#] signifies %Deviation for 0.23% PVA has a reading 1.5 times that of the other column members.

TYPE:	mean-Thickness (start) / mm	mean-Thickness (finish) / mm	Change in Thickness: / mm	%weight Loss / %	%weight Loss per cycle / %
PVA:					
0.12%*	3.80	3.71	0.09	13.39 [#]	0.30 [#]
0.23%	3.87	3.69	0.18	23.23	0.44
PAA:					
0.13%	4.62	4.42	0.21	20.71	0.37
0.23%	4.65	4.51	0.15	15.95	0.36
0.63%	4.01	3.62	0.39	27.20	0.44
0.94%	3.89	3.43	0.46	28.19	0.38
1.15%	3.95	4.15	-0.20	23.74	0.49
Plain Paste:					
(0.0%)	4.52	4.41	0.11	19.55	0.39

Table 8

* Notes:

All readings are an average of two readings (five for plain paste), except for (#) items which were only one reading.

TYPE*:	Formed Sur Area (micro) / m ² g ⁻¹	Formed Sur Area (macro) / m ² g ⁻¹	Formed Sur Area (Total) / m ² g ⁻¹	Failed Sur Area (micro) / m ² g ⁻¹	Failed Sur Area (macro) / m ² g ⁻¹	Failed Sur Area (Total) / m ² g ⁻¹	Formed BET / m ² g ⁻¹	Failed BET / m ² g ⁻¹
PVA:								
0.12%	0.46	0.05	15.16	0.28	0.07	9.39	5.08	6.08
0.23%	0.29	0.03	20.62	0.33	0.07	10.54	4.94	7.39
PAA:								
0.13%	0.45	0.06	13.36	0.41	0.05	6.92	8.45	4.14
0.23%	0.57	0.07	28.99 [†]	0.40	0.06	5.46	5.21	4.29
1.15%	0.49	0.08	18.24	0.39	0.08	8.96	9.17	3.81
Plain Paste:								
(0.0%)	0.54	0.12	15.60	0.49	0.08	8.94	4.43	2.92

Table 9

• Notes:

- (1). Micro means pores, from mercury intrusion experiments, which are greater than 0.25 μm.
- (2). Macro means pores which are greater than 1 μm.
- (3). † contains a reading which was very high, probably due to moisture still remaining in the sample.
- (4). All values are an average of at least two readings (five for plain paste).

2. Both PVA and PAA reduce the proportion of macro porosity and increase the proportion of micro pores in the formed paste. (It should be noted that there were still some macro pores present in the formed paste— this was probably due to inadequate hand-pasting of the treated material on to the grids with the spatular— and any of these macro pores could limit the performance of the treated paste).

This supports the theory that MDF technology does not reduce the capacity significantly, as a reduction in the macro porosity must limit the discharge rate because the acid penetration into the paste is also reduced.

3. PVA probably does not affect cycle life, but it does decrease the overall ampere hour capacity per plate.

One possibility for this effect is that PVA's hydrophobic backbone is attaching itself to the paste substrate and causing an increased agglomeration of the PbO_2 .

4. There is a decrease between the formed and failed BET measurements for PAA and plain paste, but there is an increase for PVA plates (table 9).

The measurements appear, also, to show that there is some agglomeration of initial paste material by PVA which is removed, or reduced, during cycling.

5. The effect of PAA peaks between 0.6 and 0.9%. Between these two regions, cycle life and the overall ampere hour capacity per plate are increased. The macro porosity is reduced whilst, as previously mentioned, the weight loss per cycle is unchanged (compared with 'plain' paste)— therefore PAA must have provided a *second* beneficial effect.

Further linear sweep voltammetry experiments, on pure (99.999%) lead in $5 \text{ mol dm}^{-3} \text{ H}_2\text{SO}_4$, with and without the addition of PAA (to produce a 1% solution), showed that grid corrosion is not affected by this surfactant. The increased utilisation of the PbO_2 active material must therefore be *due to decreased sulphation* during cycling. Beneath the lead sulphate 'membrane'— investigated by Ruetschi *et al.*^{29,30}— the local pH approaches neutrality, carboxylate groups will be available which can increase the solubility of Pb^{2+} ions by forming a complex. Using atomic absorption spectroscopy it was found that the solubility of Pb^{2+} ions, in water, is increased 67 times by 1% PAA*. Previous experiments on the formation of PbSO_4 crystals in cellulose membranes showed that increasing the concentration of Pb^{2+} ions decreased the crystal size (chapter 5, page 51). *PAA is therefore inhibiting the onset of sulphation by*

* At pH 7, readings were 0.15 for water only and 10 for 1% PAA.

regulating the PbSO₄ crystal size, causing small PbSO₄ crystallites to form and increasing (or at least not reducing) the subsequent PbO₂ surface area on charge. The reduction in capacity, when the concentration of PAA is increased to 1.15%, is probably due to the acid decreasing the pH and therefore restricting the level of free carboxylate.

Another possibility is that PAA is increasing the acidity inside the plate's micropores and therefore making β -PbO₂ formation more favourable than the α polymorph and, subsequently, this leads to more capacity (as β -PbO₂ provides capacity). However, due to the large increase in Pb²⁺ ions by PAA it is more likely that the former conditions are predominant.

Further Work.

Further work with PAA modified plates should be repeated to confirm the results presented here. In particular prototype battery plates should be made to check if the same increases are observed when simulated industrial regimes are used.

The addition of higher amounts of PAA would provide further information as to the limiting effect noticed at the 1.15% modified PAA.

Summary.

The use of surfactants to reduce the *macro porosity* of the positive paste cannot be recommended commercially as no significant improvement is achieved for the extra work involved.

Further work on the addition of PAA is required, however, the initial results indicated that at least a 20 to 30% increase in ampere hour capacity per plate, or in cycle life occurs by the addition of, about, 0.9% wt/wt PAA.

There is an agglomeration of paste material when PVA is used as a surfactant. Further work on this might reveal a method of extending the capacity of a battery— particularly for tubular, and other crumbling/flaking protection, systems.

CHAPTER NINE.

FINAL DISCUSSION.

9.1 Introduction.

The investigations carried out in this work tried to answer some of the points raised by Julian²⁵ (chapter one)— *what properties lie behind a lead sulphate membrane? Does osmotic behaviour causes the amorphous structures seen in the lead acid battery? What is the possibility that improvements in lead acid battery design could be made by using macro defect free (MDF) technology?*

9.2 Lead Sulphate Membranes.

The first of these points relates to the neutral or *alkaline stable* α -PbO₂ and basic lead sulphates which have been observed in battery plates⁸⁸. Previous work⁸⁹ had suggested migration hinderance (due to small pores) or lead sulphate semi-permeable membranes²⁹. Ruetschi was the first to show that the movement away from the theoretical values could be accounted for by considering the Donnan equilibrium potential (table 2, chapter three). Lead sulphate membranes have since been (despite the problems raised in section 3.3) more or less accepted as an integral part of the lead acid battery system. Bullock & Butler¹⁰⁹, however, have raised the question of *PbO₂ membranes* where a Pb/(t-)PbO/PbO₂ is formed at the electrode surface, during charging. At present there is no clear evidence which is more accurate; the possibility exists that both membranes may form to some extent.

To examine these structures several techniques were attempted. In one set of experiments (chapter five) the surface of leady oxide discs— reacted at different sulphuric acid concentrations, at various reaction times or at a variety of temperatures— were examined using SEM. It was found that a change in the surface structure occurred around 7 mol dm⁻³. At the same time a deformation in the surface could be observed when water, rather than industrial alcohol, was used to wash the disc. This deformation was ascribed to water *buckling* a surface layer of PbSO₄, and provides good evidence that an integral, membrane type layer forms under certain conditions. Bialacki¹⁰¹, working with lead sulphate on lead dioxide, agrees that a change in the surface structure occurs around 7 mol dm⁻³. SEM's have also shown a tighter, more compact, film developing as the temperature or concentration is increased. In another set of experiments¹⁰⁰ an attempt was made to separate a lead sulphate corrosion film by the amalgamation of the (backing) lead sheet, after a suitable reaction time. However this section of work proved too complex to proceed and further experiments continued using impedance spectroscopy.

Impedance spectroscopy (IS) (chapter six) measurements using lead discs, porous lead discs (formed by potentiodynamically cycling between lead and lead sulphate 4000 times) or lead dioxide plated onto platinum attempted to discover more about lead sulphate membranes by observing changes in the impedance spectra as changes were made in concentration or temperature. However, due to problems with the electrical equipment and the lead dioxide disc detaching itself from the platinum substrate, only the lead - lead sulphate work provided reproducible results. These indicated that at low concentrations or temperatures an adsorbed surface layer was present, which broke down, as the temperature was raised. Finally separating into a charge transfer and Warburg (diffusion) processes. However, no surface film/membrane behaviour was established in these experiments.

9.3 MDF Technology and Positive Battery Paste.

Julian built on the idea of lead sulphate membrane, by considering the improvements being made in the cement industry— macro defect free (MDF) cement had yielded cement pastes which were ten times stronger than normal mixes²⁴. The development of this to the lead acid battery paste could lead to a reduction in the shedding, crumbling or flaking (and subsequent increase capacity/cycle life) of the battery's active mass. Two surfactants, polyvinyl alcohol (PVA) or polyacrylic acid (PAA), were added to commercially obtained battery paste. Results from this work showed that an improve plate capacity was observed for PAA treated pastes. This effect peaked between 0.6 to 0.9% (weight/weight). However, this improvement was not due to the MDF strategy but to PAA inhibiting the onset of sulphation by regulating the lead sulphate crystal size (chapter eight).

9.4 Discussion.

The cement industry was able to increase the strength of cement by the elimination of macro defects, however, in doing so the paste became water sensitive and subsequent wetting producing ingress, swelling, wetting, creeping and stress loss^{107,110}. The polymer is also known to leach out, causing dye shrinkage and these properties increases with %polymer addition¹⁰⁸. The polymer in MDF cement is known to play an active role in it construction¹¹¹. A gel like matrix is formed during the hydration which ~~strengbens~~ the mix and is known to be an important contribution¹¹² to the overall cement strength.

At the time of concept of MDF battery paste these problems were probably not known, Birchall²⁴ stated that re-hydration was not important! However, it can now be seen that the failure of MDF technology to provide the overall increase in paste strength is understandable. Moreover, during cycling of the lead

acid battery changes in unit cell size may cause cracks to develop, if space (voids) are not available to expand into. Therefore, MDF strategy is now not recommended for lead acid battery pastes.

The idea that silicate gardens theory could account for the amorphous structures in the lead acid battery has been refuted by Moseley¹¹³. Previously a difference in the hydrogen species between "active" and "inactive" PbO₂ was thought to exist. However a number of workers^{114,113} have shown that the inactivity of chemically prepared PbO₂ was a myth and particle size can account for the amorphous and inactivity observed in the lead acid battery. Ruetschi¹¹⁵ has proposed a detailed crystallographic picture for PbO₂; the oxygen lattice is complete, but cationic disorder means that vacancies are clustered together, in layers, and "acted as interfaces between ordered regions", he proposes the structure of PbO₂ to be:



where x is the cation vacancy fraction, y is the fraction of Pb²⁺ ions present (with respect to the total number of cation sites). α-PbO₂ was said to have a high x value, while β-PbO₂ varied depending upon whether it was chemically, or electrochemically, produced (the former having small, or zero, x).

APPENDIX ONE: Program to Control X Ray Diffractometer & Display Results.

```

20 REM STEPLIN MARK16 by Peter J MURRAY-JONES, with Dr Brown: LUT 7, 1985
30 ONERR GOTO 1900
40 HOME: PRINT: PRINT
50 D$ = CHR$(4): I$ = CHR$(9): REM THE COMPUTER MUST HAVE THE BLACKBOARD CARD
60 SO% = 6: DV% = 2: REM DEFAULT DRIVE
70 DIM C%(2000)
80 PRINT "DO YOU WISH TO ": INVERSE
90 PRINT "LOAD": NORMAL: PRINT "IN A FILE OF ": INVERSE
100 PRINT "DATA": NORMAL: INPUT " ? ": Z$
110 IF LEFT$(Z$,1) = "Y" THEN GOSUB 1270: IF LEFT$(PR$,1) = "N" THEN 540
120 PRINT: IF LEFT$(Z$,1) = "Y" THEN INPUT "DO YOU WANT A COPY OF THIS DATA WITH A BASEL
INE SHIFT (IF 'NO' YOU CAN HAVE ONE LATER)? ": H$: IF LEFT$(H$,1) = "N" THEN 400
130 IF LEFT$(Z$,1) = "Y" THEN 440
140 Z$ = "": HOME: PRINT: PRINT
150 INPUT "TYPE START ANGLE (2theta)? ": ST: PRINT: INPUT "TYPE IN FINAL ANGLE (2theta)? ": PF:
PRINT
160 IF PF = < ST THEN PRINT: PRINT: PRINT "Please make sure that the final angle is LARGE R than the start
angle. ": PRINT: PRINT: GOTO 150
170 INPUT "TYPE STEP SIZE (2theta)? ": S: IF S < .00125 OR S > 5 THEN PRINT: PRINT CHR$(7): " --
PLEASE INPUT A BETTER VALUE ": PRINT: GOTO 170
180 N = 800 * S: PRINT: INPUT "TYPE COUNT TIME (seconds)? ": T
190 IF T < .05 OR T > 200 THEN PRINT: PRINT CHR$(7): "TIME FACTOR INCORRECT. ": PRINT "PLEASE
INPUT A BETTER VALUE": PRINT: GOTO 180
200 PRINT: INPUT "DO YOU WANT TO SAVE THIS PATTERN TO DISC? ": Z$
210 IF LEFT$(Z$,1) = "Y" THEN GOSUB 1220
220 REM ALL LOGIC DEVIVES (PR$) REQUIRE NORMAL PRINTING, NOTE
230 GOSUB 1390: REMHARD COPY?
240 HOME: PRINT: PRINT: PRINT: INVERSE: PRINT " HIT A KEY TO START ... ": GET O$
250 HOME: FLASH: PRINT CHR$(7): "STANDBY": NORMAL: PRINT "..."
260 PRINT: T1 = 200: T2 = 0: GOSUB 730
270 IF C% < + 110 THEN INVERSE: PRINT: PRINT: PRINT: PRINT CHR$(7): "ARE YOU SURE THE X-
RAYS ARE ON" : NORMAL: INPUT SR$: IF LEFT$(SR$,1) = "N" THEN 240
280 HOME: PRINT: PRINT: PRINT "NB: YOU MAY STOP THE PROGRAMME EARLY BY PRESSING A
KEY. (THIS MAY TAKE SEVERAL SECONDS, HOWEVER)."
290 PRINT: INVERSE: PRINT "--STARTING TO RUN: ": NORMAL: NO = ABS((PF - ST) / S) + 1: D = 1: F =
20: T = T * 20: IF N < 256 THEN X = N: Y = 0: GOTO 310
300 Y = INT(N / 256): X = N - Y * 256
310 IF T < 256 THEN T1 = T: T2 = 0: GOTO 340
320 T2 = INT(T / 256): T1 = T - T2 * 256
330 POKE - 16368,0
340 FOR J = 1 TO NO: GOSUB 730
350 C%(J) = C%: IF PEEK(- 16384) > 127 THEN 1470: REM ROUTINE TO STOP PROGRAM EARLY
360 PRINT ST + S * (J - 1), C%(J): IF (J < NO) THEN GOSUB 780
370 NEXT
380 IF LEFT$(Z$,1) = "Y" THEN GOSUB 1150
390 IF LEFT$(H$,1) < > "Y" THEN 540
400 GOSUB 820: HOME
410 PRINT: PRINT: INPUT "DO YOU WANT ANOTHER COPY" : Q$: IF LEFT$(Q$,1) = "Y" THEN 400
420 HOME: PRINT: PRINT: INPUT "DO YOU WANT A COPY WITH THE BASELINE SET TO THE
BACKGROUND COUNT? ": W$
430 IF LEFT$(W$,1) < > "Y" THEN 540
440 CMIN = C%(1): FOR I = 2 TO NO: IF CMIN > C%(I) THEN CMIN = C%(I)
450 NEXT
460 PRINT: PRINT "RIGHT; INPUT THE BASELINE VALUE: IT SHOULD BE AROUND ",CMIN;" (EITHER
PRESS RETURN OR RETYPE A BETTER VALUE): ";
470 INPUT W$: IF W$ = "" THEN 510
480 IF (VAL(W$) > CMIN) THEN PRINT: PRINT: PRINT "PLEASE INPUT A SMALLER VALUE THAN ";
CMIN;" OR A 'CRASH' CAN RESULT!": PRINT: GOTO 460
490 IF (VAL(W$) < 0) THEN PRINT: PRINT: PRINT "PLEASE INPUT A NON-NEGATIVE NUMBER!": PRINT
: GOTO 460
500 CMIN = VAL(W$)
510 FOR I = 1 TO NO: C%(I) = C%(I) - CMIN: NEXT: CMIN$ = STR$(CMIN)
520 Y$ = Y$ + " with a subtracted baseline, (of " + CMIN$ + ")."

```

```

530 GOSUB 820: HOME : PRINT : PRINT : INPUT "DO YOU WANT ANOTHER COPY? "; QS: IF LEFT$(QS,1)
= "Y" THEN 530
540 HOME : PRINT : PRINT : PRINT "DO YOU WANT ANY "; : INVERSE : PRINT "CALCULATIONS" ;;
NORMAL: INPUT "? "; QS: IF LEFT$(QS,1) < > "Y" THEN 700
550 PRINT : INPUT "DO YOU WANT THIS PRINTED OUT? ";HCS: IF LEFT$(HCS,1) = "N" THEN HCS = "N"
560 RA = ST + (NO - 1) * S: REM GIVES MAXIMUM POINT ON SPECTRA
570 IF HCS = "N" THEN 590
580 PRINT D$; "PR£1": PRINT " CALCULATIONS ON: ";YS: PRINT " ===== ": PRINT : PRINT
D$; "PR£0"
590 HOME : PRINT : PRINT : INVERSE : PRINT "CALCULATION ROUTINE. " : NORMAL
600 PRINT : PRINT "ENTER THE OPTION YOU WOULD LIKE: ": PRINT : PRINT
610 PRINT "1. D-SPACING (GIVEN A TWO THETA VALUE). ": PRINT
620 PRINT "2. TWO THETA VALUE (GIVEN D-SPACING).": PRINT
630 PRINT "3. A PEAK AREA.": PRINT
640 PRINT "4. QUIT THE SECTION.": PRINT
650 INPUT B$: BO = VAL (B$): IF BO = 0 OR BO > 4 OR BO < 1 OR BO < > INT (BO) THEN PRINT CHR$(
7); "PLEASE TYPE 1-4.": PRINT : GOTO 650
660 IF BO = 4 AND HCS < > "N" THEN PRINT D$; "PR£1": PRINT CHR$( 12): PRINT D$; "PR£0": GOTO 700
670 IF BO = 4 THEN 700
680 ON BO GOSUB 940, 990, 1070
690 PRINT : PRINT : PRINT : PRINT : INVERSE : PRINT " PRESS A KEY TO CONTINUE. " : GET XG$: GOTO
590
700 HOME : PRINT : PRINT : INPUT "ANOTHER RUN? ";Z$: IF LEFT$(Z$,1) < > "N" THEN CLEAR RUN
710 HOME : PRINT : PRINT : PRINT "...Bye."
720 END : REM +++++**+++++
730 REM COUNT ROUTINE
740 PRINT D$; "PR£5": PRINT "OR";: POKE 770, T1: POKE 771, T2: PRINT "DG"
750 IF PEEK (768) < > 0 THEN 750
760 C% = PEEK (772) + (256 * (PEEK (773) + PEEK (774)) + (256 * 256 * (PEEK (775) + 776))) + (256 * 256 *
256 * (PEEK (777) + PEEK (778)))
770 PRINT D$; "PR£0": PRINT D$; "IN£0": RETURN
780 REM STEP SIZE ROUTINE
790 PRINT D$; "PR£5" : PRINT "OR";: POKE 768,D: POKE 770, X: POKE 771, Y: POKE 772, F: PRINT "SG"
800 IF PEEK (768) < > 0 THEN 800
810 PRINT D$; "PR£0": PRINT D$; "IN£0": RETURN
820 REM PLOT ROUTINE
830 CMAX = C%(1): FOR I = 2 TO NO: IF CMAX < C%(I) THEN CMAX = C%(I)
840 NEXT : IF CMAX = 0 THEN FLASH : PRINT "ERROR!": NORMAL : PRINT " -- X-RAYS ARE NOT ON .":
STOP
850 SCL = 55 / CMAX: IF HCS = "N" THEN 880
860 PRINT D$; "PR£1": PRINT "Title: ";YS: PRINT : PRINT "Time count (per step) /s: ";T / 20: PRINT : PRINT D$:
"PR£0"
870 IF LEFT$(HIS,1) = "2" THEN PRINT D$; "PR£1": GOTO 910
880 GOSUB 1580: TEXT : IF HCS = "N" THEN 930
890 IF LEFT$(HIS,1) < > "B" THEN PRINT D$; "PR31": GOTO 920
900 PRINT D$; "PR£1": PRINT : PRINT : PRINT : PRINT "Title: ";YS: PRINT: PRINT "Time count (per step)/s "; T/
20: PRINT
910 PRINT : PRINT : PRINT : FOR J = 1 TO NO: PRINT ST + S * (J -1), C%(J); TAB(20 + SCL * C% (J)); "":
NEXT
920 PRINT CHR$( 12): PRINT D$; "PR£0"
930 RETURN
940 REM D SPACING CALCULATION
950 INPUT "TYPE IN THE TWO THETA ANGLE: ";TT: TH = TT * 2 * 3.14159 / 720:DSP = 1.5418 / (2 * SIN
(TH)):DSP = (INT (1000 * DSP) + .5) /1000
960 PRINT "TwoTheta value: ";TT: PRINT "D-Spacing: ";DSP: IF HCS= "N" THEN 980
970 PRINT D$; "PR£1": PRINT "Two Theta value: ";TT: PRINT "D-Spacing: ";DSP: PRINT : PRINT D$; "PR£0"
980 RETURN
990 REM 2 THETA VALUING
1000 PRINT : INPUT "INPUT THE D-SPACING: ";DSP
1010 REM THIS MACHINE CAN'T DO ARCSIN THEREFORE THE FOLLOW DOES: TAN ^2=SIN ^2/(1-SIN ^2)
1020 D2 = 1.5418 / (2 * DSP): D2 = SQR (D2 ^ 2 / (1 - D2 ^ 2))
1040 PRINT : PRINT "D-spacing: ";DSP: PRINT " two theta value: "; TT:IF HCS = "N" THEN 1060
1050 PRINT D$; "PR£1": PRINT "D-spacing: ";DSP: PRINT "Two theta value: "; TT: PRINT : PRINT D$; "PR£0"
1060 RETURN
1070 REM PEAK AREA ROUTINE
1080 INPUT "TYPE START ANGLE: ";A1: PRINT : INPUT "TYPE FINAL ANGLE: ";A2

```

```

1090 IF A1 < = 0 OR (A1 < ST) OR A2 > RA OR A1 > = A2 THEN PRINT CHR$(7): PRINT "PLEASE TYPE
VALUES WHICH ARE WITHIN THE RANGE FOR THE SAMPLE ...": PRINT : GOTO 1080
1100 JS = (A1 - ST) / 8 + 1: JF = (A2 - ST) / S + 1
1110 B = (C%(JS) + C%(JF)) / 2: A = 0: FOR N = (JS + 1) TO (JF - 1): A = A + C%(N) - B: NEXT :A = A * S
1120 PRINT : PRINT "The Peak Area, between the points ";A1;" and ";A2;" , IS: ";A
1130 IF HC$ = "N" THEN 1150
1140 PRINT D$: "PR#1" : PRINT "The Peak Area, between the points ";A1;" and ";A2;" , is: ";A: PRINT D$: "PR#0"
1150 RETURN
1160 PRINT D$: "OPEN "; X$: " , S"; SO% ; " , D";DV%
1170 PRINT D$: "WRITE "; X $
1180 PRINT NO: PRINT T: PRINT ST: PRINT S
1190 FOR J = 1 TO NO: PRINT C%(J): NEXT
1200 PRINT D$: "CLOSE "; X$
1210 RETURN
1220 PRINT : PRINT "WHAT DO YOU WISH THE FILE TO BE CALLED" : INPUT X$
1230 IF X$ = " " THEN PRINT : PRINT : PRINT "PLEASE DO NOT USE A 'NULL' STRING AS A NAME ... ":
PRINT : PRINT : GOTO 1220
1240 LET X = VAL (X$): IF X < > 0 THEN PRINT : PRINT "PLEASE DO NOT USE A NUMBER FIRST.":
PRINT: PRINT : GOTO 1220
1250 GOSUB 1510
1260 RETURN
1270 INPUT "WHAT IS THE FILE CALLED? "; X$: LET X = VAL (X$): IF x < > 0 THEN PRINT : PRINT "
PLEASE DO NOT USE A NUMBER FIRST": GOTO 1270
1280 IF X$ = " " THEN PRINT : PRINT "PLEASE DO NOT USE A 'NULL' STRING AS A NAME!": PRINT :
PRINT : GOTO 1270
1290 GOSUB 1510
1300 PRINT D$: "OPEN"; X$;" , S"; SO% ; " , D";DV%
1310 PRINT D$: "READ ";X$
1320 INPUT NO, T, ST, S
1330 FOR J = 1 TO NO: INPUT C%(J): NEXT
1340 PRINT D$: "CLOSE "; X$
1350 HOME : PRINT : PRINT : INPUT "DO YOU WANT TO SEE THE SPECTRA? ";PR$: IF LEFT$: IF LEFT$(
PR$,1) = "N" THEN 1380
1360 PRINT : INPUT "--HARD COPY? ";HC$: IF LEFT$( HC$,1) = "N" THEN HC$ = "N": HI$ = "1": Y$ =X$:
PRINT : PRINT "--NB: REMEMBER TO HIT A KEY TO CONTINUE TO NEXT HI-GRAPHICS 'SHEET', ":
GOTO 1380
1370 HOME: PRINT : PRINT : INVERSE : PRINT "COPY ROUTINE" : NORMAL : GOSUB 1410
1380 RETURN
1390 HOME : PRINT : PRINT : INPUT "DO YOU WANT A HARD COPY? ";HS: PRINT
1400 IF LEFT$( H$,1) = "N" THEN 1460
1410 PRINT "WHAT DO YOU WANT TO CALL THE SPECTRA (IF YOU WISH TO CALL IT THE SAME NAME
AS THE DISC FILE THEN PRESS RETURN). "
1420 INPUT Y$: IF Y$ = "" THEN Y$ = X$
1430 PRINT : PRINT : PRINT "--A HI-RES GRAPHICS FORM "; INVERSE : PRINT "AND"; NORMAL : PRINT
"A '** -LINE FORM WILL BE PRINTED--"
1440 PRINT "UNLESS YOU TYPE": PRINT "1. FOR HI-GRAPHICS FORM ONLY." : PRINT "2. FOR '** -LINE
FORM ONLY. ": PRINT : PRINT : "(PRESS RETURN FOR BOTH)": INPUT HI$: IF HI$: = "" THEN HI$ =
"B": GOTO 1460
1450 CH = VAL (HI$): IF CH < > 1 AND CH < > 2 THEN 1430
1460 RETURN
1470 REM END THE RUN EARLY ROUTINE
1480 PRINT : INVERSE : PRINT "STOP THE PROGRAM (Y/N)? "; NORMAL : INPUT US
1490 IF LEFT$( U$,1) = "Y" THEN J = NO: GOTO 370
1500 U$ = "": POKE - 16368,0: GOTO 360
1510 REM CHECK WHICH DRIVE
1520 PRINT : PRINT "Which drive do you wish to use?": PRINT
1530 PRINT "NB, If the slot being used is NOT '6', then enter the correct slot AFTER the drive number -and PROCEED
it with an 'S': PRINT "(**PRESS 'RETURN' OR 'S6,D2')."
1540 INPUT DV$: IF DV$: IF DV$ = "" THEN 1570
1550 FOR GJ = 1 TO LEN (DV$) - 1: IF MID$( DV$,GJ,1) = "S" THEN SO% = VAL (MID$( DV$, GJ + 1 , LEN
(DV$)): DV% = VAL (MID$( DV$,1,GJ - 1)):K = LEN (DV$) - 1:DV$ = "DONE"
1560 NEXT : IF DV$ < > "DONE" THEN DV% = VAL (DV$)
1570 RETURN
1580 REM H PLOT ROUTINE: ALL GRAPHICS, BUT TO 180 (Y) ONLY (X:279)
1590 FIRST = 1
1600 GOSUB 1680:NV = 0
1610 DIV = CMAX / 180

```

```

1620   FOR J = 1 TO NO * 2 STEP 2
1630   IF (J + 1) = > NO * 2 THEN 1660: REM THIS STOPS AN OUT-OR-RANGE 'TAIL' OCCURRING DUE TO
      THE LAST POINT IN THE FOR-NEXT HITTING THE END OF THE DATA
1640   IF ((J - NV + 1)) > 279 THEN GOSUB 1780: GOSUB 1680: NV = NV + 280: GOTO 1660
1650   H PLOT (J - NV - 1), (180 - C%)(J + 1) / 2) / DIV) TO (J - NV + 1), (180 - C%)(J + 3) / 2) / DIV)
1660   NEXT : IF NO / 140 < > INT (NO / 140) THEN GOSUB 1780
1670   RETURN
1680   REM AXIS PLOT
1690   HGR2 : HCOLOR = 7: H PLOT 279,180 TO 0,180 TO 0,0
1700   FOR AX = 0 TO 279 STEP 5
1710   IF AX / 10 = INT (AX / 10) THEN H PLOT AX,180 TO AX,175: GOTO 1730
1720   H PLOT AX,180 TO AX,178
1730   NEXT
1740   FOR AX = 0 TO 170 STEP 5: IF AX / 10 = INT (AX / 10) THEN H PLOT 0,AX TO 5,AX: GOTO 1760
1750   H PLOT 0,AX TO 2,AX
1760   NEXT
1770   RETURN
1780   REM PRINT OUT FOR HI RES
1790   IF HC$ = "N" THEN GET X6$: GOTO 1880: REM NO HARD COPY
1800   PRINT D$; "PR£1"
1810   IF FIRST = 1 THEN FIRST = 0: GOTO 1830
1820   PRINT "..."; Y$
1830   PRINT : PRINT I$; "G2DER": PRINT : PRINT : PRINT
1840   PRINT : PRINT "Range (Two theta value) for x-axis: "
1850   PRINT ST + (NV / 2) * S; "to " : ST + ((NV + 279) / 2) * S
1860   PRINT CHR$ (12): REM FORM FEED
1870   PRINT D$; "PR£0"
1880   RETURN
1890   STOP
1900   REM ERROR ROUTINE; WILL ALLOW DATA SAVING AFTER SOME ERRORS
1910   PRINT : PRINT : FLASH : PRINT "ERROR" : NORMAL : PRINT "--NUMBER "; Y = PEEK (222): PRINT Y
1920   X = PEEK (218) + PEEK (219) + 256
1930   PRINT " --AT LINE: " : X
1940   PRINT : PRINT : PRINT "=="CONTINUE";: INPUT CN$ = "N" THEN STOP
1950   RESUME
1960   REM *****

```

APPENDIX TWO: Program to Find The Main Peaks in an XPD Pattern.

```

10    REM PEAK 65 - ANALYSIS OF PEAKS B, PJMJ, 6:1985
30    HOME : PRINT : PRINT : PRINT "Do you want "; INVERSE : PRINT "HELP" ;; NORMAL
40    INPUT F$: IF LEFT$(F$,1) = "Y" THEN 20000
50    PRINT : PRINT "DO YOU WANT TO CREATE A FILE FOR USE WITH THE "; INVERSE
60    PRINT "ANALYSIS PROGRAM";: NORMAL : INPUT SAS
70    IF LEFT$(SAS,1) < > "Y" AND LEFT$(SAS,1) < > "N" THEN 50
80    PRINT : PRINT "DO YOU WANT THE DATA PRINTED OUT": INPUT PQ$
90    DIM C% (2000), D%(1000), E% (1000)
100   LN = LOG (10):D$ = CHR$ (4):ED = 0:PER = 0:CI = 0:J = 0: N = 0: R = 0
110   CLIMBER = 0:FALLER = 0:CMA$ = 0:MAXC = 0:IN = 0:NV = 0: K% = 0
120   GOSUB 530
130   N = NO / 140: IF N < > INT (N) THEN N = INT (N) + 1:ED = 1
140   K% = 1: PRINT "Working ...": PRINT "baseline: "
150   NV = 1: FOR U = 1 TO N
160   PRINT "**";
170   CI = C%(NV): FOR J = 1 + NV TO 139 + NV
180   IF C%(J) = < 0 AND ED = 1 THEN 200
190   IF (C%(J) < CI) THEN CI = C%(J)
200   NEXT : FOR R =NV TO 139 + NV: C%(R) = C%(R) - CI: NEXT
210   NV = 140 + NV: NEXT
220   CMA$ = C%(10): FOR J = 2 TO NO: IF CMA$ < C%(J) THEN CMA$ = C%(J)
230   NEXT :PER = 11.99 * CMA$ / 100: REM 10% + 2 FOR BASELINE SET
240   PRINT : PRINT "peaks: ";
250   for J = 1 TO NO
260   GOSUB 600
270   NEXT
280   REM LISTING
290   PRINT : REM THIS REMOVES ANY HANG-UP '!' WHICH PREVENTS CONTROL SIGNALS OPERATING
300   IF LEFT$(SAS,1) < > "N" THEN GOSUB 5000
310   IF LEFT$(PQ$,1) = "N" THEN 510
320   PRINT D$; "PR£1"
330   PRINT CHR$ (27); "M"
340   PRINT "Maxima for ";X$;" "
350   PRINT : PRINT
360   REM TITLE
370   PRINT "No of Line: "; POKE 36,20
380   PRINT "Two Theta";: POKE 36,40
390   PRINT "D-Spacing";: POKE 36,60
400   PRINT "Intensity";: POKE 36,80
410   FOR J = 1 TO K% - 1
420   TT = ST + (E%(J) - 1) * S: REM ST STARTS AT C%(1)
430   DSP = INT (1.5418 / (2 * SIN (TT * 3.14159 / 360)) * 100 + .5) / 100
440   IN = INT (D%(J) / CMA$ * 10000 + .5) / 100
450   SP = INT (LOG (TT) / LN): POKE 36, (23 - SP): PRINT TT;
470   SP = INT (LOG (DSP) / LN): POKE 36, (43 - SP): PRINT DSP;
480   SP = INT (LOG (IN) / LN): POKE 36, (63 - SP) : PRINT IN
490   NEXT : PRINT CHR$ (12): PRINT D$; "PR£0"
492   HOME : PRINT : PRINT "RESETTING ..."
500   FOR R = 1 TO 1000: C%(R) = 0:D% (R) = 0:E%(R) = 0: NEXT : FOR R = 1001 TO 2000: C% (R) = 0:
510   NEXT
520   GOTO 100
520   END
525   REM ++++++
530   PRINT : READ X$: IF X$ = "-1" THEN STOP
540   PRINT "Reading ..."
550   PRINT D$; "OPEN";X$; ", S6, D1"
560   PRINT D$; "READ";X$
570   INPUT NO, T, ST, S
580   FOR J = 1 TO NO: INPUT C%(J):NEXT
590   PRINT D$; "CLOSE" ;X$: HOME : PRINT : PRINT : RETURN
600   REM PEAK FINDER
610   IF C%(J) < PER AND CLIMBER = 0 THEN FALLER = 0:LT = 0: GOTO 710
620   IF FALLER > 0 THEN 680
630   IF CLIMBER > 0 AND C%(J) < PER THEN 670

```

```

640 IF C%(J) < CLIMBER THEN MAXC = CLIMBER: CLIMBER = 0:FALLER = C%(J): GOSUB 720: GOTO
710
650 CLIMBER = C%(J): LJ = J: GOTO 710
660 REM ***
670 MAXC = CLIMBER : CLIMBER = 0:FALLER = 0: GOSUB 720: GOTO 710
680 IF FALLER < (C%(J) - CMAX / 100) THEN CLIMBER = C%(J):FALLER = 0:LJ = J: GOTO 710
682 REM ***
690 FALLER = C%(J): GOTO 710
700 REM ***
710 RETURN
720 REM STORE DATA OF A PEAK
730 PRINT " ";
740 E%(K%) = LJ: D%(K%) = MAXC: K% = K% + 1: MAXC = 0: LJ = 0: RETURN
4999 REM ++++++
5000 PRINT "Writing ...."
5002 IF LEN (X$) > 24 THEN X$ = LEFT$ (X$, LEN (X$) - 1)
5004 X$ = X$ + "!"
5010 PRINT D$; "OPEN"; X$; ", S6, D2": PRINT D$; "WRITE" ;X$
5020 PRINT K% - 1,S,ST
5021 FOR J = 1 TO K% - 1:TT = ST + (E%(J) - 1) * S
5023 IN = INT (D%(J) / CMAX * 10000 +.5) / 100
5025 PRINT TT: PRINT IN
5027 NEXT J
5030 PRINT D$; "CLOSE" ;X$: HOME : PRINT : PRINT : RETURN
10000 REM *****
10010 REM
10020 REM ***DATA HERE***
10090 REM ***DATA STOPS***
20000 SPEED = 100: REM ++++++
20005 PRINT
20010 PRINT "TO RUN THIS PROGRAMME ONE MUST USE DATA STATEMENTS WITH THE CATALOGUE
NAME OF THE FILE TO BE ANALYSED ... THIS ALLOWS THE COMPUTER TO RUN AT ITS FASTEST
RATE."
20020 PRINT
20030 PRINT "PLEASE REMOVE ANY DATA STATEMENTS AT 10000 OR ABOVE AND SUBSTITUE YOUR
OWN. -END THE DATA WITH '-1'."
20040 PRINT : PRINT "THE DATA WILL BE SAVED ON DRIVE 2, AND TAKEN FROM DRIVE 1. TO
DESCRIMINATE BETWEEN THE TWO FILES: THE NEW FILE WILL HAVE AN '!; AS THE LAST
CHARACTER; EITHER BY INSERTION, OR DELETION (OF THE LAST CHARACTER)."
20041 PRINT "-PLEASE MAKE SURE THIS WILL BE 'OK'."
20050 PRINT : PRINT "THIS CHARACTER (OR DELETION) CAN BE CHANGED VIA LINES 5002 AND 5004."
20060 PRINT: PRINT "--NOTE:": PRINT "THE NEW FILES(S) CREATED ON DRIVE 2 ARE FOR THE ";
INVERSE
20070 PRINT "ANALYSIS PROGRAMME";: NORMAL : PRINT ". SO, IF YOU WISH TO RE-RUN THIS
TABULATION OF PEAKS PROGRAMME THEN YOU ";: INVERSE
20080 PRINT "MUST";: NORMAL : PRINT "USE THE ORIGINAL DATA FILE. ": PRINT : PRINT "ALSO NOTE,
THIS PROGRAMME CHECKS PEAKS GREATER THAN ~10%; THIS MAY BE CHANGED BY ALTERING
'PER' ON LINE 230.": SPEED = 255
20090 STOP

```

APPENDIX THREE: Program to Form a Cured Plate.

```

10   REM (C) PJMJ, LUT 7/1987
20   DIM T%(16)
30   T%(1)=0:T%(2)=0:T%(3)=0:REM SET TIMER DEFAULTS
40   PRINT CHR$(26) "          AUTOMATIC FORMATION OF PLATES":PRINT "(c) Peter Murray-Jones,
LUT for AAS: VERSION 1.2 13/7/87":PRINT "NB/ ALL OTHER VERSIONS ARE COPIES!"
50   PRINT:PRINT"Please input all timings in DECIMAL MINUTES; ie.":PRINT "1 hour 37 minutes is 162 (161.67)
decimal minutes (inputs are rounded up)."
```

60 PRINT:INPUT "WHAT FIRST CHARING PERIOD DO YOU WISH (<CR>=DEFAULT)", CP1\$: IF
LEN(CP1\$)=0 THEN CP1=1600 ELSE CP1=VAL(CP1\$)

70 INPUT "WHAT IS THE TIME FOR THE FIRST WAIT PERIOD ((CR)=DEFAULT)", WP1\$: IF
LEN(WP1\$)=0 THEN WP1=200 ELSE WP1=VAL(WP1\$)

80 INPUT "WHAT IS THE TIME FOR THE SECOND CHARING PERIOD (<CR>=DEFAULT)", CP2\$:IF
LEN(CP2\$)=0 THEN CP2=400 ELSE CP2=VAL(CP2\$)

90 INPUT "WHAT IS THE TIME FOR THE SECOND WAIT PERIOD (<CR>=DEFAULT)", WP2\$:IF
LEN(WP2\$)=0 THEN WP2=200 ELSE WP2=VAL(WP2\$)

100 INPUT "WHAT IS THE TIME FOR THE LAST CHARGING PERIOD ((CR)=DEFAULT)", CP3\$: IF
LEN(CP3\$)=0 THEN CP3=400 ELSE CP3=VAL(CP3\$)

110 INPUT "WHAT IS THE TIME FOR THE LAST WAIT PERIOD (<CR>=DEFAULT)", WP3\$: IF LEN
(WP3\$)=0 THEN WP3=200 ELSE WP3= VAL(WP3\$)

120 CYCLE%=1:INPUT "READY TO START "; AS\$:IF LEFT\$(AS,1)<>"Y" THEN 120

130 PRINT:PRINT "NB/ 'Q' can be pressed at anytime to stop the program-- enter the password in 30 seconds, or
repeat."

140 TIME%=CP1

150 WHILE CYCLE%<4:REM TURN ON RELAY

160 GOSUB 610:DY%=TD1%:PRINT "SETTING TO CHARGE CYCLE NUMBER ";CYCLE%;" AT "; TH1%;"
HRS. "; TM1%;" MINS.":T1%=TH1%:T2%=TM1%

170 P=64:E=2500:GOSUB 550

180 GOSUB 610:LFT%=0:WHILE LFT% <TIME%:GOSUB 730

190 AZ\$=INKEY\$:IF AZ\$="Q" THEN GOSUB 330

200 GOSUB 610:IF DY%(>TD1% THEN TH1%=TH1%+24

210 LFT%=(TH1%-T1%)*100+(TM1%-T2%)*10/6:WEND:PRINT

220 P=64:E=-2500:GOSUB 550:PRINT "CHARGING CYCLE FINISHED...": GOSUB 610:
DY%=TD1%:T1%= TH1%:T2%=TM1%:PRINT:PRINT "NOW ON WAIT PERIOD AT ";T1%;" HRS. ";T2%;"
MINS."

230 ON CYCLE% GOSUB 780,820,860

240 LFT%=0:WHILE LFT%<TIME%:GOSUB 730

250 AZ\$=INKEY\$:IF AZ\$="Q" THEN GOSUB 330

260 GOSUB 610: IF DY%<>TD1% THEN TH1%=TH1%+24

270 LFT%=(TH1%-T1%)*100+(TM1%-T2%)*10/6:WEND:PRINT

280 PRINT "WAIT PERIOD FINISHED. ":CYCLE%=CYCLE%+1:ON CYCLE%-1 GOSUB 760, 800, 840

290 WEND

300 PRINT "FORMING OF PLATE IS OVER!":P=64:E=-2500:GOSUB 550 PRINT

310 PRINT "BYE..."

320 END

330 REM PASSWORD STOP Routine

340 A%=TH1%:B%=TM1%:C%=TD1%:D%=TW1%:E%=TS1%:REM STORE VALUES TO RE-SET LATER

350 PRINT

360 GOSUB 610:REM FIND OUT THE TIME

370 HR%=TH1%:MN%=TM1%:SC%=TS1%

380 PRINT "TYPE PASSWORD":GOSUB 510

390 FLAG=0:CK\$="1":GOSUB 460:REM CHECK INPUT

400 IF FLAG=1 THEN 430

410 PRINT "NOW SECOND NUMBER":CK\$="2":GOSUB 460

420 IF FLAG<>1 THEN GOSUB 680:REM PROC STOP...

430 TH1%=A%:TM1%=B%:TD1%=C%:TW1%=D%:TS1%=E%

440 GOSUB 510:RETURN

450 REM

460 AZ\$=INKEY\$:IF LEN(AZ\$)=0 THEN GOSUB 610 ELSE IF AZ\$<>CK\$ THEN FLAG=1:GOTO 490 ELSE
490

470 IF TH1%=0 AND HR%=23 THEN TH1%=24

480 IF ((TH1%*100+TM1%*10/6+TS1%/36)-(HR%*100+MN%*10/6+SC%/36))<30/36 THEN 460 ELSE PRINT
"TIME UP": FLAG=1

490 RETURN

500 REM

510 REM CLEAR BUFFER

```

520 FOR K%=1 TO 60:AZ$=INKEY$:NEXT:PRINT
530 RETURN
540 REM
550 REM DA SETTING-- P IS THE PORT FOR OUTPUT AND E IS THE VALUE; BOTH ARE LEFT
    UNCHANGED AFTER.
560 IF ABS(E)>2500 THEN E1=2500*SGN(E) ELSE E1=E
570 E1=(E1+2500)/19.6078 :REM ROUNDING UP OCCURS AT THE PORT
580 OUT P, E1
590 RETURN
600 REM
610 REM TIMER
620 REM 4=SEC; 5=MIN; 6=HOURS; 7=DAY; 8=MONTH; 9=YEAR; 10=WEEK
630 T%(0)=&HCF:TIM%=VARPTR(T%(0))-1
640 CALL TIM%
650 TH1%= VAL(HEX%(T%(6))):TM1%= VAL(HEX$(T%(5))): TD1%= VAL(HEX$(T%(7))):TW1%=
    VAL(HEX$(T%(10))): TS1%= VAL(HEX$(T%(4)))
660 RETURN
670 REM
680 REM STOP PROCEDURE.
690 PRINT "STOP OCCURRED AT CYCLE NUMBER: ",CYCLE%
700 PRINT :PRINT "RELAYS HAVE BEEN RESET.":E=-2500-P=64:GOSUB 550
710 PRINT:INPUT "READY TO CONTINUE ", A$:IF LEFT$(A$,1)="N" THEN STOP
720 RETURN
730 REM PRINT OUT TIME LEFT
740 Z%=(TIME%-LFT%):Z1%=INT(Z%/100)*100: Z2%=(Z%-Z1%)*6/10: Z$=STR$(Z1%/100)+" : "+STR$(Z2%)
750 PRINT " ";CHR$(13);"TIME REMAINING: ";Z$:CHR$(13);:RETURN
760 REM CHARGE PERIOD 2.
770 TIME%=CP2:RETURN
780 REM WAIT PERIOD ONE.
790 TIME%=WP1:RETURN
800 REM CHARGE PERIOD 3.
810 TIME%=CP3:RETURN
820 REM WAIT PERIOD TWO.
830 TIME%=WPZ:RETURN
840 REM DUMMY; LAST WAIT PERIOD ALREADY COMPLETED.
850 RETURN
860 REM 3RD WAIT PERIOD
870 TIME%=WP3:RETURN
880 STOP

```

APPENDIX FOUR: Program to Cycle & Record Readings from a Plate.

```

10   ON ERROR GOTO 1310:REM OFF PROCEDURE.
20   REM PJMJ, LUT 9/1987
30   DIM A%(1000,3), T%(16):REM SET FOR 1000 CYCLES WHERE: (? ,1)=TIME FOR TOC, (? ,2)=TIME FOR
    DISCHARGE AND (? ,3) IS TFC
40   T%(1)=0:T%(2)=0:T%(3)=0:REM SET TIMER DEFAULTS
50   TP%=0:E=-2500:P=64:GOSUB 1180:P=65:GOSUB 1180 :REM RESET RELAYS
60   VFALL%=0:REM CHECK FOR HOW MANY TIMES THE VOLTAGE FALLS BELOW PREVIOUS IN
    TOTAL (AT LINE 280)
70   PRINT CHR$(26):PRINT "          RUN/RESTRICTED RUN CYCLING: VERSION 01.50":PRINT "
    (last revised: 17/9/1987. (C) Peter Murray-Jones, LUT for AAS)."
```

80 PRINT:PRINT "(NB/ ALL OTHER VERSIONS ARE COPIES!)"

90 INPUT "Do you want to run a RESTRICTED CYCLE program (CR>=N)";RC\$:IF LEN(RC\$)=0 THEN
RC\$="N"

100 IF LEFT\$(RC\$,1)="Y" THEN INPUT "Input the WEIGHT of the paste of this WATER treated
plate";WPT:WPT=119*WPT/34.5:PRINT "RUN-TIME IS THEREFORE SET TO: ",WPT," DEC. MINUTES
(MAXIMUM)"

110 INPUT "DO YOU WANT TO CHANGE ANY OF THE DEFAULTS (<CR>=N)";F\$:IF LEN(F\$)=0 THEN
F\$="N"

120 IF LEFT\$(F\$,1)="N" THEN CHECK%=1500: DELTIME%=4:DELVOLT5%=2:FALLOFF%=800:
TC%=1:REST%=10:MAX%=0:OVER%=20:L2%=0 ELSE GOSUB 1650

130 PRINT "DO YOU WISH TO GO STRAIGHT TO THE WAIT PERIOD FOR THIS RUN (<CR>=N)?": INPUT
WT\$: IF LEN(WT\$)=0 THEN WT\$="N"

140 IF LEFT\$(RC\$,1)="Y" THEN PRINT:PRINT"THIS IS A RESTRICTED CYCLE RUN."

150 DOT%=0:PRINT: PRINT "PLEASE INPUT NAME OF THE OUTPUT DATA FILE (IF '.' SPECIFIED, THEN
FILE TYPE ASSUMED TO FOLLOW)":INPUT FILES: IF LEN(FILES\$)=0 THEN PRINT:GOTO 150

160 IF LEN(FILES\$)>12 THEN PRINT:PRINT "TOO BIG, TRY AGAIN":GOTO 150

170 IF RIGHT\$(FILES\$,1)=". " THEN PRINT "PLEASE DO NOT END WITH A '.'": GOTO 150 ELSE GOSUB
1820:IF CNT>1 THEN 150: REM FILE DOT CHECKS

180 FOR J%=1 TO LEN(FILES\$):IF (MID\$(FILES\$,J%,1)=". " AND J%<10 AND LEN(FILES\$)>J%) THEN
FILES\$=LEFT\$(FILES\$,J%+3):DOT%=1:J%=LEN(FILES\$)-J%+1: IF LEN(FILES\$)<7 THEN
F\$=LEFT\$(FILES\$,LEN(FILES\$)-J%)+". TMP": J%=LEN(FILES\$) ELSE
F\$=LEFT\$(FILES\$,3)+".TMP":J%=LEN(FILES\$)

190 NEXT:IF DOT%<>1 THEN IF LEN(FILES\$)>8 THEN PRINT:PRINT "NAME TOO BIG, TRY
AGAIN.":GOTO 150 ELSE FILES\$=FILES\$+".DAT": IF LEN(FILES\$)<7 THEN
F\$=LEFT\$(FILES\$,LEN(FILES\$)-4)+".TMP" ELSE F\$=LEFT\$(FILES\$,3)+".TMP"

200 PRINT "DISC FILES ASSIGNED. MAIN FILE IS "; FILES\$:PRINT "TEMPORARY FILE IS "; F\$

210 PRINT:PRINT "INPUT: 1. TO CONTINUE FROM A DISC FILE ('LOAD A DISC').":PRINT " 2. TO RUN
THE PROGRAM":INPUT AZ:IF AZ=1 THEN GOSUB 1440 ELSE IF AZ<>2 THEN 210

220 PRINT:PRINT:PRINT "Ok, hit 'Q' to stop program-- enter password in time limit of 30 seconds; else repeat
operation.... Hitting 'Q' may TAKE a few seconds to work."

230 REM CHARGING CYCLE.

240 BL%=0:PRINT "-.SETTING TO CHARGE. ":P=64: E=2500: GOSUB 1180: VC%=0:GOSUB
1240:H1%=TH%:M1%=TM1%:D1%=TD1%

250 IF LEFT\$(WT\$,1)="Y" THEN WT\$="N":GOTO 480

260 WHILE VC%<CHECK%:GOSUB 1090:AZ\$=INKEY\$:IF AZ\$="Q" THEN GOSUB 910

270 WEND:PRINT"VOLTAGE ABOVE LOWER VOLTAGE LIMITS, DIFFERENTIATING TO FIND TOC..."

280 REM CONTINUE TO CHECK NOW WITH TIMER

290 GOSUB 1090: VC1%=VC%:GOSUB 1240:T1%=TH1%:T2%=TM1%:DY%=TD1%:REM SET TIMER

300 AZ\$=INKEY\$:IF AZ\$="Q" THEN GOSUB 910

310 GOSUB 1240:IF TD1%<>DY% THEN TH1%=TH1%+24

320 IF (TH1%*100+TM1%*10/6)-(T1%*100+T2%*10/6)<(DELTIME%*10/6) THEN 300

330 GOSUB 1090:GOSUB 1240:IF (VC%-VC1%)>=0 THEN 380

340 REM VOLTAGE DROP TRAP

350 BL%=BL%+1:PRINT "VOLTAGE HAS FALLEN BELOW PREVIOUS READING, WHILST ON
CHARGE";BL%," TIME(S)":PRINT"AT ";TH1%," HRS. ";TM1%," MINS.":PRINT "(PRESENT VOLTAGE IS
";VC%," mV, PREVIOUS VOLTAGE WAS ";VC1%,"mV."

360 VFALL%=VFALL%+1:PRINT "TOTAL NUMBER OF TIMES (VFALL%) IS NOW: "; VFALL%:PRINT
"REPEATING PREVIOUS CHARGE PERIOD.":GOTO 290

370 REM TRAP ENDS

380 IF VC%-VC1%>DELVOLTS% THEN 290: REM CHECKS THAT THE CHANGE IS LESS THAN 2MV

390 REM OVERCHARGE PERIOD

400 PRINT"TOC FOUND. PRINT"NOW ON OVER CHARGE PERIOD";:GOSUB 1240: T1%=TH1%:
T2%=TM1%:DY%=TD1%:PRINT "AT: ";TH1%,"HRS. ";TM1%,"MINS."

410 AZ\$=INKEY\$:IF AZ\$="Q" THEN GOSUB 910

420 GOSUB 1240:IF TD1%<>DY% THEN TH1%=TH1%+24

```

430 IF (TH1%*100+TM1%*10/6)-(T1%*100+T2%*10/6)<(OVER%*10/6) THEN 410
440 GOSUB 1090:PRINT "OVERCHARGE PERIOD FINISHED. TOC NUMBER ";TC%:"
STORED":A%(TC%,1)=VC%:REM STORE TOC
450 GOSUB 1240:PRINT "TOC ("; VC%:"mV) OCCURRED AT ";TH1%;" HRS. ";TM1%;" MINS."
460 IF TD1%<>D1% THEN TH1%=TH1%+24
470 A%(TC%,3)= ((TH1%-H1%)*100+(TM1%-M1%)*10/6):PRINT "TIME TAKEN IS: "; A%(TC%,3);"DEC.
MINUTES"
480 PRINT "NOW ON WAIT PERIOD.":P=64:E=-2500:GOSUB 1180:REM SWITCH PD OFF
490 GOSUB 1240:T1%=TH1%:T2%=TM1%:DY%=TD1%:REM SET TIMER
500 FOR J%=1 TO 10:PRINT CHR$(7):NEXT:GOSUB 1730
510 AZ$=INKEY$:IF AZ$="Q" THEN GOSUB 910
520 GOSUB 1240:IF TD1%<>DY% THEN TH1%=TH1%+24
530 IF (TH1%*100+TM1%*10/6)-(T1%*100+T2%*10/6)<(REST%*10/6) THEN 510
540 REM START OF DISCHARGE CYCLE.
550 GOSUB 1240:T1%=TH1%:T2%=TM1%:DY%=TD1%: PRINT: PRINT "DISCHARGE CYCLE STARTING AT
"; TH1%;"HRS ";TM1%;"MINS."
560 P=65:E=2500:GOSUB 1180:REM SWITCH ON RELAY
570 VC%=10000:WHILE VC%>FALLOFF%:GOSUB 1090
580 AZ$=INKEY$:IF AZ$="Q" THEN GOSUB 910
590 REM TIMER 120 DEC MINS. FOR CHECKING FOR RESTRICTED RUN PLATES.
600 GOSUB 1240:IF TD1%<>DY% THEN TH1%=TH1%+24
610 IF LEFT$(RC$,1)="Y" THEN IF (TH1%*100+TM1%*10/6)-(T1%*100+T2%*10/6) >WPT THEN PRINT
"TIMER UP AT: ";TH1%;"HRS. ";TM1%;"MINS.:VC%=123: REM STOP WHILE LOOPING
620 WEND:P=65:E=-2500:GOSUB 1180:REM DISCHARGE CYCLE ENDS.
630 GOSUB 1240:PRINT"DISCHARGE PERIOD FINISHED AT";TH1%;" HRS. ";TM1%;" MINS."
640 GOSUB 1240:IF TD1%<>DY% THEN TH1%=TH1%+24
650 A%(TC%,2)=((TH1%-T1%)*100+(TM1%-T2%)*10/6):PP%=INT(A%(TC%,2)/100): PRINT "DISCHARGE ";
TC%;" FINISHED TIME TAKEN= "; PP%;" HRS. ; INT((A%(TC%,2)-PP%*100)*60/100); " MINS."
660 IF A%(TC%,2)>MAX% THEN MAX%=A%(TC%,2)
670 GOSUB 880:REM SAVE INTERMEDIATE DATA ON DISC.
680 GH=MAX%:GOSUB 1620:PRINT "THE MAX. DISCHARGE TIME NOW IS: ";GHH%;"HRS. AND "
GHM%;"MINS.":PRINT "THIS MEANS THE POINT OF FAILURE WOULD BE REACHED
AT";GH=MAX%*.8:GOSUB 1620:PRINT GHH%;"HRS. AND ";GHM%;"MINS."
690 IF A%(TC%,2)>=.8*MAX% THEN TC%=TC%+1:IF TC%<=1000 THEN 230 ELSE PRINT "MORE THAN
1000 CYCLES COMPLETED!!!":GOSUB 800: GOTO 230:REM START RECHARGE
700 REM FAILURE HAS OCCURRED (LESS THAN 80% OF MAX. CHARGE REMAINING).
710 PRINT:PRINT:PRINT "FAILURE HAS OCCURRED AT CYCLE NUMBER ";TC%;
720 PRINT "TOP OF CHARGE VOLTAGE FOR THIS WAS ";A%(TC%,1);"."
730 GOSUB 1390:REM PUT DATA DISC
740 REM TRY AND LEAVE PLATE IN A CHARGED STATE:
750 GOSUB 1240:T1%=TH1%:T2%=TH2%:P=64:E=2500:GOSUB 1180: PRINT"CHARGING PLATES FOR HALF
AN HOUR BEFORE ENDING JOB.":WHILE (TH1%-T1%)*100+ (TM1%-T2%)*10/6 < 30*10/6:GOSUB
1240:AZ$=INKEY$:IF IAZ$="Q" THEN GOSUB 910
760 WEND:P=64:E=-2500:GOSUB 1180
770 PRINT :PRINT :PRINT "OK FINISHED CYCLING... DO YOU WISH TO DELETE YOUR TEMPORARY
FILE?":INPUT A$:IF LEFT$(A$,1)="Y" THEN KILL F$
780 PRINT:PRINT "The voltage fell below the previous one (VFALL%); VFALL%;" times in total.": PRINT :PRINT
"BYE..."
790 STOP
800 REM CREATE NEW FILES WHEN MORE THAN 1000 CYCLES COMPLETED
810 GOSUB 1400:L1%=LEN(FILES):IF (L1%-4)<5 THEN L2%=L1%-4 ELSE L2%=5
820 KILL F$
830 FILES="EXT"+LEFT$(FILES,L2%)+".DAT":F$=LEFT$(FILES,6)+".TMP":PRINT
840 PRINT "MORE THAN 1000 CYCLES COMPLETED !!!!! (WOW)."
850 PRINT "NEW DATA FILES CREATED: MAIN FILE-- "; FILES:PRINT "TEMPORARY FILE --"; F$
860 TC%=1:RETURN
870 REM
880 REM DISC INTERMEDIATE SAVING
890 OPEN "O", £1, F$
900 PRINT £1, TC%: FOR J%=1 TO TC%: PRINT £1,A%(J%,1), A%(J%,2),A%(J%,3): NEXT:CLOSE £1:RETURN

910 REM PASSWORD STOP ROUTINE
920 A%=TH1%:B%=TM1%:C%=TD1%:D%=TW1%:E%=TS1%:REM STORE VALUES TO RE-SET LATER
930 PRINT
940 GOSUB 1240:REM FIND OUT THE TIME
950 HR%=TH1%:MN%=TM1%:SC%=TS1%:DA%=TD1%
960 PRINT "TYPE PASSWORD":GOSUB 1140

```

```

970 FLAG=0:CK$="1":GOSUB 1040:REM CHECK INPUT
980 IF FLAG=1 THEN 1010
990 PRINT "NOW SECOND NUMBER":CK$="2":GOSUB 1040
1000 IF FLAG<>1 THEN GOSUB 1310:REM PROC STOP...
1010 TH1%=A%:TM1%=B%:TD1%=C%:TW1%=D%:TS1%=E%
1020 GOSUB 1140:RETURN
1030 REM
1040 AZ$=INKEY$:IF LEN(AZ$)=0 THEN GOSUB 1240 ELSE IF AZ$<>CK$ THEN FLAG=1:GOTO 1070
ELSE 1070
1050 IF DA%<>TD1% THEN TH1%=TH1%+24
1060 IF ((TH1%*100+TM1%*10/6+TS1%/36)-(HR%*100+MN%*10/6+SC%/36)) <30/36 THEN 1040 ELSE PRINT
"TIME UP":FLAG=1
1070 RETURN
1080 REM 1090 REM AD CONVERT; VC% IS OUTPUT
1100 Z1=INP(83):FOR X=1 TO 200:NEXT X
1110 Z2=INP(81):Z3=INP(80):VC%=(256*(Z2 AND 15)+Z3)/1.6125:IF Z2 AND 128 THEN 120 ELSE
VC%=VC%*-1
1120 PRINT "                                ",CHR$(13);"Latest voltage is:
";VC%;"mV";CHR$(13);:RETURN
1130 REM
1140 REM CLEAR BUFFER
1150 FOR K%=1 TO 60:AZ$=INKEY$:NEXT:PRINT
1160 RETURN
1170 REM
1180 REM DA SETTING-- P IS THE PORT FOR OUTPUT AND E IS THE VALUE; BOTH ARE LEFT
UNCHANGED AFTER.
1190 IF ABS(E)>2500 THEN E1=2500*SGN(E) ELSE E1=E
1200 E1=(E1+2500)/19.6078 :REM ROUNDING UP OCCURS AT THE PORT
1210 OUT P, E1
1220 RETURN
1230 REM
1240 REM TIMER
1250 REM 4=SEC; 5=MIN; 6=HOURS; 7=DAY; 8=MONTH; 9=YEAR; 10=WEEK
1260 T%(0)=&HCF:TIM%=VARPTR(T%(0))-1
1270 CALL TIM%
1280 TH1%=VAL(HEX$(T%(6))):(TM1%=VAL(HEX$(T%(5))): TD1%=VAL(HEX$(T%(7))):
TW1%=VAL(HEX$(T%(10))):TS1%=VAL(HEX$(T%(4)))
1290 RETURN
1300 REM
1310 REM STOP PROCEDURE.
1320 PRINT "STOP OCCURRED AT CYCLE NUMBER:", TC%;"."
1330 PRINT :PRINT "RELAYS HAVE BEEN RESET":E=-2500:P=64: GOSUB 1180: P=65:GOSUB 1180:PRINT
"The voltage has fallen below the previous voltage (VFALL%);VFALL%," times in total."
1340 IF TC%<1 THEN 1360 ELSE PRINT "SAVE MAIN FILE TO DISC":INPUT A$:IF LEFT$(A$,1)="N" THEN
1360
1350 GOSUB 1390:PRINT"RESULTS HAVE BEEN SAVED TO DISC (MAY BE RELOADED LATER FROM THE
.DAT FILE)":PRINT "NB/ TEMPORARY FILE NOT DELETED. "
1360 ON ERROR GOTO 0
1370 STOP
1380 REM
1390 REM PUT DATA TO MAIN DISC FILE
1400 IF TC%>1000 THEN TP%=TC%:TC%=1000:OPEN "O", £1, FILE$:PRINT £1, TC%: FOR J%= 1 TO
TC%:PRINT £1, A%(J%,1), A%(J%,2), A%(J%,3):NEXT :CLOSE £1: TC%=TP%: TP%=0
1410 IF TC%<=1000 THEN OPEN "O",£1,FILE$:PRINT £1,TC%:FOR J%=1 TO TC%:PRINT £1,A%(J%,1),
A%(J%,2),A%(J%,3):CLOSE £1
1440 REM INPUT DATA FILE FOR EXTENSION
1450 PRINT :PRINT:PRINT "INPUT DATA FILE NAME (INCLUDE EXTENSION), ELSE HIT (RETURN) FOR ";
FILE$: INPUT FILE1$:IF LEN(FILE1$)=0 THEN FILE1$=FILE$
1460 PRINT:PRINT "READING PREVIOUS DATA FILE..."
1470 OPEN "I", £1, FILE1$:INPUT £1, TC%:FOR J%=1 TO TC%:INPUT £1, A%(J%,1), A%(J%,2),
A%(J%,3):NEXT:CLOSE £1
1480 MIN%=10000:MIN1%=10000:MAX%=0:MAX1%=0:MIN2%=1000:MAX2%=0:FOR J%=1 TO TC%:IF
A%(J%,1)>MAX1% THEN MAX1%=A%(J%,1)
1490 IF (A%(J%,1)<MIN1% AND A%(J%,1)<>0) THEN MIN1%=A%(J%,1)
1500 IF (A%(J%,3)<MIN2% AND A%(J%,3)<>0) THEN MIN2%=A%(J%,3)
1510 IF A%(J%,2)>MAX% THEN MAX%=A%(J%,2)
1520 IF A%(J%,3)>MAX2% THEN MAX2%=A%(J%,3)

```

```

1530 IF (A%(J%,2)<MIN% AND A%(J%,2)<>0) THEN MIN%=A%(J%,2)
1540 NEXT:PRINT:PRINT "DATA READ. THERE WERE ";TC%;" PREVIOUS INPUTS.": PRINT:PRINT
"MINIMUM TOC VOLTAGE WAS ";MIN1%;"mV, AND MAXIMUM TOC VOLTAGE WAS ";MAX1%;
"mV.":PRINT
1550 PP%=INT(MAX%/100):PRINT "MAXIMUM TIME FOR DISCHARGE WAS ";PP%;" HRS. ";
INT((MAX%-PP%*100)*6/10);" MINS.":PRINT
1560 PP%=INT(MIN%/100):PRINT "MINIMUM TIME FOR DISCHARGE WAS ";PP%;" HRS.
";INT((MIN%-PP%*100)*6/10);" MINS.":PRINT
1570 PRINT"DO YOU WISH TO ALTER THE MAXIMUM TIME FOR DISCHARGE (THIS WILL NOT EFFECT
THE STORED VALUES)?"
1580 IF (A%(TC%,1)=0 OR A%(TC%,2)=0 OR A%(TC%,3)=0) THEN 1590 ELSE TC%=TC%+1
1590 INPUT AS:IF LEFT$(A$,1)="Y" THEN INPUT "TYPE IN THE NEW MAXIMUM TIME FOR DISCHARGE ";
MAX%
1600 PRINT:PRINT "READY TO CONTINUE?":INPUT AS:IF LEFT$(A$,1)<> "Y~ THEN 1600
1610 RETURN
1620 REM WORK OUT HRS/MINS, GHH RETURNS THE HOURS, GHM RETURN THE MINUTES, GH IS THE
INPUT IN DEC. MINUTES.
1630 GHH=INT(GH/100):GHM=INT((GH-GHH*100)*6/10+.5)
1650 REM CHANGE DEFAULTS SECTION
1660 PRINT "Type in the VOLTAGE (in mV) you want to start":INPUT "differentiation checking at (<CR>=Default) ";
Z$:IF LEN(Z$)=0 THEN CHECK%=1400 ELSE CHECK%=VAL(Z$)
1670 PRINT "Type in the DELAY TIME (in minutes) you want between":INPUT "differentials checks (<CR>=Default)
"; Z$:IF LEN(Z$)=0 THEN DELTIME%=4 ELSE DELAYTIME%=VAL(Z$)
1680 PRINT "Type in the VOLTAGE DIFFERENCE (in mV) you want between":INPUT "differentials
(<CR>=Default) "; Z$:IF LEN(Z$)=0 THEN DELVOLTS%=2 ELSE DELVOLTS%=VAL(Z$)
1690 PRINT "Type in the VOLTAGE (in mV) where you wish the discharge":INPUT "to cycle to end (<CR>=Default)
";Z$:IF LEN(Z$)=0 THEN FALLOFF%=800 ELSE FALLOFF%=VAL(Z$)
1700 PRINT "Type in the time required (in minutes) for OVERCHARGE (<CR>=Default) ":INPUT Z$:IF
LEN(Z$)=0 THEN OVER%=20 ELSE OVER%=VAL(Z$)
1710 PRINT "Type in the time require for REST (in minutes), after":INPUT "the overcharge period (<CR>=Default)
";Z$:IF LEN(Z$)=0 THEN REST%=10 ELSE REST%=VAL(Z$)
1720 RETURN
1730 REM PRINT OUT FILE SO FAR
1740 PRINT " No. ";SPACES$(10);"TOC/mV"; SPACES$(10);"TFC/HRS:MINS"; SPACES$(11); "TFD/ HRS:MINS"
1750 IF TC%=0 THEN 1810
1750 FOR J%=1 TO TC%:PRINT J%,A%(J%,1),GH=A%(J%,3): GOSUB 1620: PRINT
SPACES$(8);GHH;" ";GHM;"GHM$=STR$(GHM)
1770 REM GHM MADE A STRING TO HELP FORMAT LAYOUT; +3 BECAUSE BASIC ADDS ONE FOR THE
SIGN OF THE NUMBER:
1780 GH=A%(J%,2):GOSUB 1620:PRINT SPACES$(16-LEN(GHM$)+3);GHH;" ";GHM
1790 IF J%/20=INT(J%/20) THEN PRINT " No. ";SPACES$(10); "TOC/mV"; SPACES$(10); "TFC/
HRS:MINS";SPACES$(11);"TFD/ HRS:MINS"
1800 NEXT
1810 RETURN
1820 REM FILE CHECKING
1830 CNT=0:FOR J%=1 TO LEN(FILE$)
1840 IF (MID$(FILE$,J%,1)=".") THEN CNT=CNT+1
1850 NEXT:IF CNT>1 THEN PRINT "PLEASE DO NOT USE MORE THAN ONE '.'"
1860 RETURN

```

1. Schallenberg R.H., "*Bottled Energy*", 1st Ed., American Philosophical Society, 148, (1982).
2. British Patent No.:3926, (10th September 1881).
3. Bode H., "*Lead-Acid Batteries*", 1st Ed., J. Wiley, London, (1977).
4. "*Basic Battery Technology*.", Internal Publication, Chloride Technology Ltd., England, (1984).
5. Brown O.N., Shelley R.L. & Kanning E.W., *Trans. Electrochem. Soc.*, **64**, 335, (1933).
6. Torre A., Torralba M., Garcia A. & Adeva P., *J. Power Sources*, **15**, 77, (1985).
7. Lander J.J., *Trans Electrochem. Soc.*, **95**, 174, (1949).
8. Vinal G.W., "*Storage Batteries*.", 4th Ed., J. Wiley, London, (1955).
9. Lynes T. C., Hovorka F. & Wells L. E., *Ind. Eng. Chem.*, **37**, 776, (1945).
10. Hatfield J. E. & Brown O. W., *Trans. Electrochem. Soc.*, **72**, 361, (1937).
11. Greenburg R.H. & Caldwell B.P., *Trans Electrochem. Soc.*, **80**, 71, (1941).
12. Gladstone J. H. & Tribe A., *Nature*, **27**, 583, (1883).
13. Beck W.H. & Wynne-Jones W.F.K., *Trans. Faraday Soc.*, **50**, 136, (1954).
14. Covington A.K., Dobson J.V. & Wynne-Jones W.F.K., *Trans. Faraday Soc.*, **61**, 2050, (1965).
15. Vincent C. A. *et al.*, "*Modern Batteries*", 1st Ed., Edward Arnold, London, (1984).
16. Maha M., Panazzi N., Spinelli P., Ginatta M.V. Ginatia N. & Orsello G., in "*Electrochemical Engineering (EFCE Pub. series 51)*", Symposium series **98**, 173, 1st Ed., Pergamon Press, London, (1986).
17. Birchall J.D., Howard A.J. & Bailey J.E., *Proc. R. Soc. Lond. A*, **360**, 445, (1978).
18. Double D.D., Hellowell A. and Perry S.J., *Proc R. Soc. Lond. A*, **359**, 435, (1978).
19. Birchall J.D., Howard A.J. & Double D.D., *Cement and Concrete Research*, **10**, 145, (1980).
20. Hazlehurst T H., *J Chem Ed.*, **18**, 286, (1941).
21. Birchall D., *Chemistry & Industry*, 403, (3rd July 1989).
22. Feret R., *Bull. Soc. Encor. Ind. Nat. Paris*, **II**, 1604, (1897).
23. Birchall J. D., Howard A. J. & Kendall K., *Nature*, **289**, 388, (1981)
24. Birchall J.D., *Phil. Trans. R. Soc. Lond. A*, **310**, 31, (1983).
25. Julian K., *J. Power Sources*, **11**, 47, (1984).
26. Caulder S.M., Murday J. S. & Simon A.C., *J. Electrochem. Soc.*, **129**, 876, (1982).
27. Hill R.J., *Mater. Res. Bull.*, **17**, 769, (1982).
28. Rand D.A., "*The ILZRO project LE-290*" (private communication), (1987).

29. Ruetschi P., J. Electrochem. Soc., **120**, 331, (1973).
30. Ruetschi P. & Angstadt R.P., J. Electrochem. Soc., **111**, 1323, (1964).
31. Helmholtz H., Wied. Ann., **7**, 377, (1879).
32. Gouy A., J. Phys., **9**, 457, (1910).
33. Chapman D.L., Phil. Mag., **25**, 475, (1913).
34. Stern O., Z. Elektrochem., **30**, 508, (1924).
35. Grahame D.C., Chem. Rev., **41**, 441, (1947).
36. Frumkin A.N., J. Electrochem. Soc., **107**, 461, (1960).
37. Devanathan M.A.V., Bockris J.O'M. & Müller K., Proc. Roy. Soc., London, **A274**, 55, (1963).
38. Cooper I.L. and Harrison J.A., Electrochim. Acta, **22**, 519 & 1361 & 1365, (1977).
39. Caspari W.A., Z. Physik. Chem., **30**, 89, (1899).
40. Erdey-Gruz T. & Volmer M., Z. Physik. Chem., **105A**, 203, (1930).
41. Bulter J.A.V., Proc. Roy. Soc., **157A**, 423, (1936).
42. Berzins T. & Delahay P., J. Amer. Chem. Soc., **77**, 6448, (1955).
43. Randles J.E.B., Trans. Farad. Soc., **48**, 828, (1952).
44. Vetter K.J., Z. Physik. Chem., **194**, 284, (1950).
45. Tafel J., Z. Physik. Chem., **50**, 641, (1905).
46. Losev V.V., "Modern Aspects of Electrochemistry", (Eds. B.E.Conway & J. O'M.Bockris), **7**, 314, Butterworths, London, (1972).
47. Levich V.G., Advan. Electrochem. Eng., **4**, 249, (1966).
48. Marcus R.A., Electrochim. Acta, **13**, 995, (1968).
49. Dogonadse R.R., in "Reactions of Molecules at Electrodes", (Ed.: Hush, N.S), Wiley, New York, (1971).
50. Randles J.E.B., Trans. Farad. Soc., **44**, 327, (1948).
51. Sevcik A., Coll. Czech. Chem. Commun., **13**, 349, (1948).
52. Langmuir, J. Amer. Chem. Soc., **38**, 2221, (1916).
53. Brunauer S., Emmett P.H. & Teller E., J. Amer. Chem. Soc., **60**, 309, (1938).
54. McClellan A.L. & Harnsberger H.F., J. Colloid Interface Sci., **23**, 577, (1967).
55. Ritter H. L. & Drake L. C., Ind Eng. Chem., Anal. Ed., **17**, 782, (1945).

56. Drake L.C., Ind. Eng.Chem., 41, 780, (1949).
57. Washburn E.W., Proc. Nat. Acad. Sci. USA, 7, 115, (1921).
58. Young T., "Miscellaneous works", (Ed.:Peacock G.), 1, 418, J. Murray, London, (1855).
59. Laplace P.S., "Mécanique Céleste", Suppl. Book 10, (1806).
60. Ershler B.V., Discussions Faraday Soc., 1, 269, (1947).
61. MacDonald J.R., "Impedance Spectroscopy", 1st Ed., Wiley & Sons, New York, (1987).
62. Hampson N.A., Karunathilaka S.A.G.R., Leek R., J. Appl. Electrochem., 10, 3, (1980)
63. Warburg E., Ann. Physik., 67, 493, (1899).
64. Warburg E., Ann. Physik., 6, 125, (1901).
65. Randles J.E.B., Discussion Faraday Soc., 1, 11, (1947).
66. Sluyters-Rehbach M. and Sluyters J.H., "Electroanalytical Chemistry", (Ed. A.J. Bard), 4, 3, Dekker, New York, (1970).
67. Sluyters-Rehbach M., Koojāam D.J. and Sluyters J.H., in "Polarography (Proceedings of the 3rd Int. Congress)", (Ed. Hills, G.J.), 1, 135, Macmillan Press, Southampton, (1964).
68. De Levie R., Adv. in Electrochem & Electrochem Eng., (Eds.: Delahay,P & Tobias,C.W.), 6, 329, Interscience, New York, (1967).
69. De Levie R, Electrochim Acta, 9, 1231, (1964).
70. Grahame D.C., J. Electrochem. Soc., 99, 370C, (1952).
71. Laitinen H.A. & Randles J.E.B., Trans. Faraday Soc., 51, 54, (1955).
72. Doblhoff K. & Armstrong R.D., Electrochim. Acta, 33, 453, (1988).
73. Mathias M.F. & Haas O., J. Physical Chemistry, 96, (7), 3175, (1992).
74. Glasser L.S.Dent, "Crystallography and its Applications", 1st Ed., Van Nostrand Reinhold Ltd., London, (1977).
75. Hirsch-Ayalon P., Rec. Trav. Chim., 75, 1065, (1956).
76. Overbeek J. Th. G., in "Colloid Science Vol. I: Irreversible Systems", Chapter 4, (Ed. H. R. Kruyt), 1st Edition, Elsevier Pub. Comp., Amsterdam, (1952).
77. Overbeek J. Th. G., J. Colloid Sci., 8, 593, (1953).
78. Hirsch-Ayalon P., J. Poly. Sci., 23, 679, (1957).
79. Hirsch-Ayalon P., Rec. Trav. Chim., 79, 382, (1960).
80. Hirsch-Ayalon P., Rec. Trav. Chim., 80, 376, (1961).
81. Hirsch-Ayalon P., J. Membrane Biol., 12, 349, (1973).

82. Honig E. P., Hengst J. H. Th. & Hirsch-Ayalon P., Ber. Bunsenges Physikal Chem., **72**, 1231, (1968).
83. Honig E. P. & Hengst J. H. Th., Electrochim. Acta, **15**, 491, (1970).
84. Honig E. P. & Hengst J. H. Th., Electrochim. Acta, **17**, 75, (1972).
85. Lakashminarayanaiah N., Chem. Revs., **65**, (5), 491, (1965).
86. Bode H. & Voss E., Z. Elektrochem., **60**, 1053, (1953).
87. Ruetschi P. & Cahan B. D., J. Electrochem Soc., **104**, 406, (1957).
88. Burbank J., J. Electrochem. Soc., **104**, 693, (1957).
89. Pavlov D., Electrochim. Acta, **13**, 2051, (1968).
90. Pavlov D., Poulieff C. N., Klaja E. & Iordanov N., J. Electrochem. Soc., **116**, 316, (1969).
91. Pavlov D. & Papova R., Electrochim. Acta, **15**, 1483, (1970).
92. Pavlov D. & Iordanov N., J. Electrochem. Soc., **117**, 1103, (1970).
93. Pavlov D., Ber. Bunsenges Physikal Chem., **71**, 398, (1966).
94. Guo Y., J. Electrochem. Soc., **139**, (8), 2114, (1992).
95. Hirsch-Ayalon P., Rec. Trav. Chim., **80**, 365, (1961).
96. Valeriotte E. M. L. & Gallop L. D., J. Electrochem. Soc., **124**, 370, (1977).
97. Aguf I. A., Khim. Istockikam (USSR), **10**, 34, (1975).
98. Sakashita M., Fujita S. & Sato N., J. Electroanal. Chem., **154**, 273, (1980).
99. Hampson N.A., in "The Electrochemistry of Lead", (Ed. A.T. Kuhn), 1st Ed., Academic Press, London, (1979).
100. Huber K., Z. Elektrochem., **59**, 693, (1955).
101. Bialacki J.A., *PhD. Thesis*, Loughborough University of Technology, (1984).
102. Canagaratha S.G & Hampson N.A., J. Electroanal. Chem., **86**, 361, (1978).
103. Pavlov D. & Kapkov N., J. Electrochem. Soc., **137**, (1), 16 & 21, (1990).
104. Bode H. & Voss E., Electrochim Acta, **1**, 318, (1959).
105. Pierson J.R., in "Power Sources", (Ed.: Collins, D.H.), **2**, 1stEd., Pergamon Press, Oxford, (1970).
106. Pavlov D. & Papazov G., J. Appl. Electrochem., **6**, 339, (1976).
107. Poon C.S. L.E. Wessell & Groves G.W., Materials Science & Technology, **3**, 993, (1987).
108. Cannon C.M. & Groves, G.W., J. Materials Science, **21**, 4009, (1986).
109. Bullock K.R. & Butler M.A., J. Electrochem. Soc., **133**, 1085, (1986).

110. Poon C.S. & Groves G.W., J. Materials Science, **23**, 657, (1988).
111. Sinclair W. & Grooves G.W., J. Material Science, **20**, 2846, (1985).
112. Eden N.B. & Bailey J.E., J. Material Science, **19**, 2677, (1984).
113. Moseley, P.T. & Bridger, N. J., J. Electrochem. Soc., **131**, 608, (1984).
114. Hill J., J. Electrochem. Soc., **134**, 1326, (1987).
115. Ruetschi P. & Giovanoli R., in "*Power Sources*"; **13**, (Ed. T Kelly & B W Baxter), page 81, International Power Sources Committee, Leatherhead (England), (1991).
116. Sluyter J.H., Rec. Trav. Chin. pas-bas, **79**, 1092, (1960).

